

A hetero-Diels-Alder Strategy Towards The Rubromycins

Nicky John Willis



Thesis submitted in partial fulfilment of the requirements for the degree of
Doctor of Philosophy, at the University of London



© Nicky John Willis, 2014. The copyright of this thesis, unless otherwise stated, rests with the author and no quotation or information derived from it may be published without the prior consent of the author.

Statement of Originality

I, Nicky John Willis, confirm that the research included within this thesis is my own work or that where it has been carried out in collaboration with, or supported by others, that this is duly acknowledged below and my contribution indicated. Previously published material is also acknowledged below.

I attest that I have exercised reasonable care to ensure that the work is original, and does not to the best of my knowledge break any UK law, infringe any third party's copyright or other Intellectual Property Right, or contain any confidential material.

I accept that the College has the right to use plagiarism detection software to check the electronic version of the thesis. I confirm that this thesis has not been previously submitted for the award of a degree by this or any other university.

The copyright of this thesis rests with the author and no quotation from it or information derived from it may be published without the prior written consent of the author.

Signature: Date:

Details of collaboration and publications:

1. "***ortho-Quinone Methides in Natural Product Synthesis***" N. J. Willis, C. D. Bray, *Chemistry a European Journal*, 2012, **18**, 9160-9173.
2. "***Single-molecule in vivo imaging of bacterial respiratory complexes indicates delocalized oxidative phosphorylation***" I. Llorente-Garcia, T. Lenn, H. Erhardt, O. Harriman, L. Liu, A. Robson, S. Chiu, S. Matthews, N. J. Willis, C. D. Bray, S. Lee, J. Y. Shin, C. Bustamante, J. Liphardt, T. Friedrich, C. Mullineaux, M. C. Leake, *Biochimica et Biophysica Acta*, 2014, **1837**, 811-824.
3. "***An operationally simple, palladium catalysed dehydrogenative cross-coupling reaction of pyridine N-oxides and thiazoles "on water"***" N. J. Willis and J. M. Smith, *RSC Advances*, 2014, **4**, 11059-11063.

Dedicated to my amazing family.
For all their kindness and unwavering support,
My gratitude cannot be put into words.

Acknowledgements

First and foremost, I would like to thank Dr. Christopher D. Bray for his guidance, support and patience over the course of this project. He has been a continual source of motivation and inspiration, for which I am incredibly grateful.

I'd also like to thank members of the Bray group, both past and present. I couldn't have asked for better colleagues to work alongside. A special mention must go to Siobhán Hackett for the constant inspiration generated from her excellent baking skills!!

I'd also wish to thank Dr. Martin Swarbrick, Dr. James M. Smith and the rest of the team at Cancer Research Technology Ltd, Cambridge, for all their advice and support in addition to agreeing to host my impactQM work placement.

I am also extremely grateful to Dr. Luning Liu and the rest of the OXPPOS team for working so hard to progress this project to a successful outcome.

I also wish to express thanks to Prof. Mike Watkinson and the members of my advisory panel, Dr. Peter Wyatt and Dr. Adrian Dobbs who have also been a great source of motivation and information. I'd like to thank them for their time, informative conversations and useful suggestions.

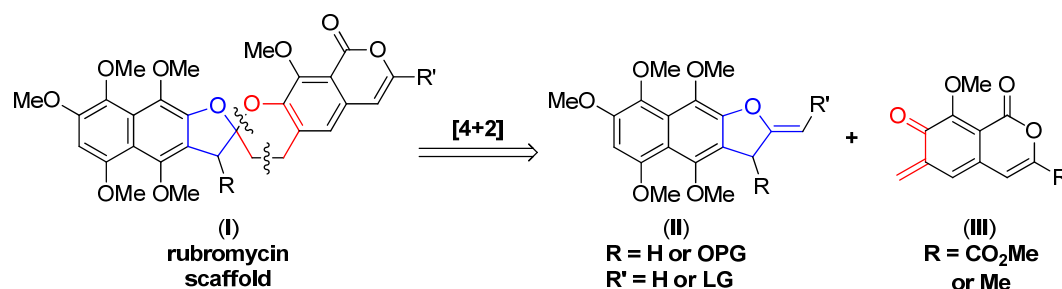
I'm also extremely grateful to members of the technical staff at Queen Mary for their tireless enthusiasm and support and the EPSRC for funding this project.

All crystallographic data data was gratefully received from Majid Motevalli, Queen Mary and high resolutionmass spectrometry data was generated at the NMSSC, University of Swansea respectfully.

Over the past few years, I have had the great fortune to be surrounded by a number of exceptionally kind and talented people. I couldn't begin to name every person, nor adequately express my gratitude, but I hope that they each understand how much their support and friendship is appreciated.

Abstract

Due to their interesting biological properties and complex molecular architectures, the rubromycin family of natural products, have attracted the attention of a number research groups over the last sixty years. Despite this significant interest, there is still a requirement for a short, robust, and modular synthetic route towards these intriguing secondary metabolites. This thesis presents an investigation into the application and development of Bray's recent [4+2] cycloaddition methodology, towards achieving this goal (**Scheme I**).



Scheme I. Retrosynthetic analysis of the rubromycin scaffold

The initial introductory chapter outlines the structural relationships and biological properties of the rubromycins, in addition to providing details of the current understanding of their biochemical synthesis. This is followed by a comprehensive review of the five synthetic strategies used to construct the challenging [5,6]-*bis*-benzannulated spiroketal rubromycin core outlined in turn. In the third and final introductory chapter, the application and relative merits of these strategies towards the synthesis of fully elaborated rubromycin scaffolds is discussed.

The results of this investigation towards a flexible and modular synthesis of γ -rubromycin are then presented and discussed in chapter four. The three main topics covered are; exploration of synthetic routes towards the naphthazarin (**II**), exploration of synthetic routes towards the *ortho*-quinone methide (**III**), and utility of the *ortho*-quinone methide in 'inverse' electron-demand [4+2] cycloaddition reactions. The experimental details of this investigation and selected ¹H and ¹³C are also reported in chapters 5 and 6 respectively.

Abbreviations List

ACP	Acyl carrier protein
Ar	Aryl
AT	Acyl transferase
Bn	Benzyl
BuLi	Butyl lithium
CAN	Cerium ammonium nitrate
CoA	Co-enzyme A
CYC	Cylcases
DCE	1,2-Dichloroethane
DDQ	2,3-Dichloro-5,6-dicyano-1,4-benzoquinone
DH	Dehydratase
DHF	Dihydrofuran
DMA	<i>N,N</i> -Dimethylacetamide
DMAP	Dimethylamino pyridine
DMF	<i>N,N</i> -Dimethylformamide
DMPU	1,3-Dimethyl-3,4,5,6-tetrahydro-2(1 <i>H</i>)-pyrimidinone
DMSO	Dimethylsulfoxide
DNA	Deoxyribonucleic acid
dppf	1,1'-Bis(diphenylphosphino)ferrocene
E ⁺	Electrophile
EDCI	<i>N</i> -(3-Dimethylaminopropyl)- <i>N'</i> -ethylcarbodiimide hydrochloride
EDG	Electron-donating group
equiv.	Equivalent
EOM	Methyl ethyl ether
ER	Enoylreductase
ESI	Electro-spray ionisation
EWG	Electron-withdrawing group
FAD	Flavin adenine dinucleotide
<i>h</i> DA	<i>hetero</i> -Diels-Alder
HIV-RT	Human immunodeficiency virus reverse transcriptase
HMDS	Hexamethyldisilazane
HOMO	Highest occupied molecular orbital
HRMS	High resolution mass spectrometry
<i>h</i> -telomerase	Human telomerase
<i>hν</i>	Electromagnetic radiation
IBX	2-Iodoxybenzoic acid
IC ₅₀	Half maximal inhibitory concentration
IR	Infrared radiation
KR	Ketoreductase
KS	Ketoacylsynthase
LUMO	Lowest unoccupied molecular orbital
M	Molarity

MCoA	Malonyl co-enzyme A
<i>m</i> CPBA	<i>meta</i> -Chloroperoxybenzoic acid
MMPP	Magnesium bis(monoperoxyphthalate) hexahydrate
MOM	Methyl methyl ether
Ms	Methanesulfonyl
MS	Molecular sieves
μw	Microwave
<i>m/z</i>	Mass-to-charge ratio
NBS	<i>N</i> -Bromosuccinimide
NIS	<i>N</i> -Iodosuccinimide
NMO	<i>N</i> -methylmorpholine <i>N</i> -oxide
NMR	Nuclear magnetic resonance
Nu ⁻	Nucleophile
<i>o</i> -QM	<i>ortho</i> -Quinone Methide
OTf	Trifluoromethanesulfonate
PKS	Polyketide synthase
R	Generic substituent
<i>R_f</i>	Retardation factor
RNA	Ribonucleic acid
r.t.	Room temperature
RT	Reverse transcriptase
salen	2,2'-Ethylenebis(nitrilomethylidene)diphenol <i>N,N'</i> -Ethylenebis(salicylimine)
SAR	Structure activity relationship
SET	Single electron transfer
S _N 1	Nucleophilic substitution (uni-molecular)
S _N 2	Nucleophilic substitution (bii-molecular)
SNAr	Nucleophilic aromatic substitution
sp.	Species
TBAB	Tetrabutylammonium chloride
TBACl	Tetrabutylammonium bromide
TBAF	Tetrabutylammonium fluoride
TBAI	Tetrabutylammonium iodide
TBS	Tertbutyldimethylsilyl
TERT	Telomerase reverse transcriptase
TES	Triethyl silyl
TFA	Trifluoroacetic acid
Tf	Trifluoromethanesulfonate
TFAA	Trifluoroacetic anhydride
THF	Tetrahydrofuran
TMEDA	<i>N,N,N',N'</i> -Tetramethylethylenediamine
TMS	Trimethyl silyl
TPAP	Tetrapropylammonium perruthenate
Ts	Tosyl
Ts-A	Telomerase substrate primer
<i>t</i> -telomerase	Human telomerase

Contents

Chapter 1: Introduction		
1.1	Introduction to Rubromycins	11
1.2	Biological and Pharmacological Activity of the Rubromycins	13
1.3	Pharmaceutical Importance of HIV1-RT	14
1.4	Pharmaceutical Importance of Telomerase	15
1.5	Rubromycin Biosynthesis	18
Chapter 2: Rubromycin Model Systems		
2.1	[5,6]- <i>bis</i> -Benzannulated Spiroketal Synthesis	23
Chapter 2a: Previous Model Studies		
2.2	Greul and Brockmann Approach (Strategies A and B)	25
2.3	de Koning Spiroketalisation Approach	26
2.4	Brimble's Sonogashira Coupling/Spiroketalisation Approach	27
2.5	Brimble's Radical Spirocyclisation Approach	28
2.6	Reißig's Spiroketalisation	29
2.7	Li and Xue's Gold-Catalysed Spiroketalisation	30
2.8	Danishefsky's 6- <i>exo</i> -trig Spirocyclisation Approach	31
2.9	Kita's Pummerer Approach (Strategy C)	32
2.10	Pettus' [3+2] Cycloaddition Strategy (Strategy D)	34
2.11	<i>hetero</i> -Diels-Alder Approaches (Strategy E)	35
2.12	<i>ortho</i> -Quinone Methides	36
2.13	Serendipitous Synthesis of Spiroketals <i>via</i> a [4+2] cycloaddition	38
2.14	Thermally Initiated <i>hetero</i> -Diels-Alder Approach to Spiroketals	39
2.15	Base Initiated <i>hetero</i> -Diels-Alder Approach to Spiroketals	42
Chapter 2b: Contemporaneous Model Studies		
2.16	Brimble's Radical Spirocyclisation Approach	46
2.17	Li and Xue's Dual Pd(II)/Cu(II)-Catalyzed Spiroketalisation	46
2.18	Li and Xue's Fluoride Promoted 6- <i>exo</i> -trig Spirocyclisation	48
2.19	Li and Xue's <i>hetero</i> -Diels Alder Approach	49

Chapter 3:	Total Synthesis Studies	
3.1	Introduction	51
Chapter 3a:	Previous Total Synthesis Studies	
3.2	Danishefsky's Total Syntheses of Heliquinomycin Aglycone	53
3.3	Reißig's Cyclisation Approach	55
3.4	Kozlowski's Attempted Synthesis of Pupuromycin	56
3.5	Kita Total Synthesis of γ -Rubromycin	58
3.6	Project Aim	60
Chapter 3a:	Contemporaneous Total Synthesis Studies	
3.7	Brimble's Formal Synthesis of γ -Rubromycin	62
3.8	Pettus' Total Synthesis of γ -Rubromycin	64
3.9	Li and Xue's Formal Synthesis of γ -Rubromycin	66
3.10	Li and Xue's Total Synthesis of δ -Rubromycin	67
Chapter 4:	Results and Discussion	
4.1	Retrosynthetic Analysis	71
4.2	Danishefsky's Naphthazarin Synthesis	73
4.3	Alternative Naphthazarin Synthesis	77
4.4	Methylene Installation Strategies	78
4.5	Isocoumarin Moiety	82
4.6	Kozlowski's Isocoumarin	82
4.7	Behar's Isocoumarin	83
4.8	Chatterjea's Isocoumarin	85
4.9	Reißig's Isocoumarin	87
4.10	Acetate Installation Strategies	97
4.11	Claisen Strategy	98
4.12	Direct Formylation Strategy	101
4.13	Cross-Coupling Strategy	107
4.14	Morpholine <i>hetero</i> -Diels-Alder Strategy	114
4.15	Summary and Conclusions	123
Chapter 5 :	Experimental	128
Chapter 6:	NMR Spectra	178

Chapter 1:

Introduction

“Few scientists acquainted with the chemistry of biological systems at the molecular level can avoid being inspired.”

Donald James Cram (1919 –2001)
American Chemist & Nobel Laureate

1.1 Introduction to the Rubromycins

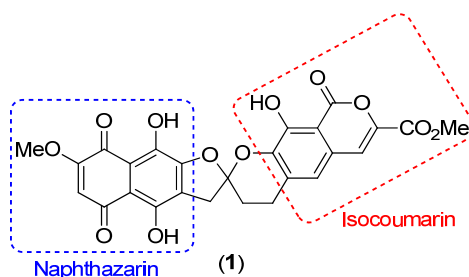
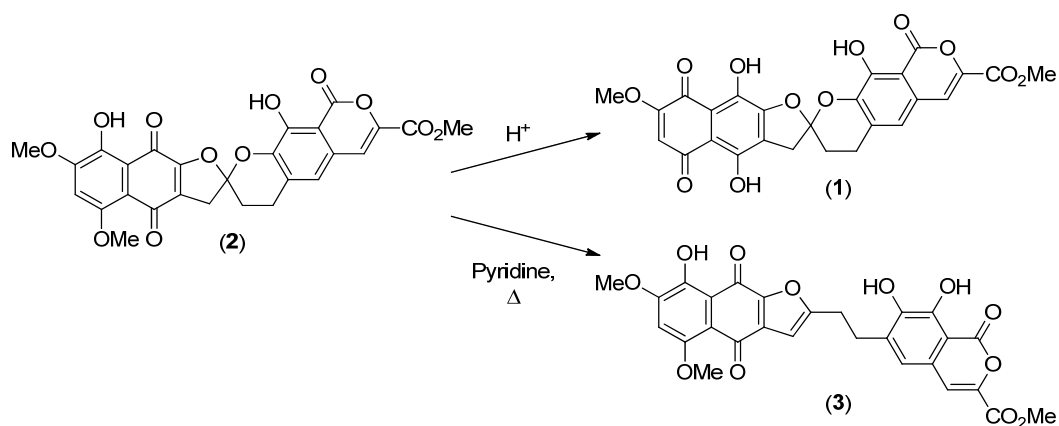


Fig. 1. γ -Rubromycin

Since the initial isolation and discovery of “rubromycin” (2) from *Streptomyces collinus* in 1953 by Brockmann and Renneberg,¹ the rubromycin family initially proved to be of interest to the scientific community due to their intriguing biological properties. However their complex hexacyclic [5,6]-bis-benzannulated spiroketal core, connecting the naphthazarin and isocoumarin moieties (**Fig. 1**), that are difficult to access *via* chemical synthesis has attracted the attention of several natural products research groups.



Scheme 1. Structural relationship between α -, β - and γ -rubromycin

Brockmann and Renneberg subsequently found that treatment of “rubromycin” (2) with pyridine at reflux afforded “collinomycin” (3), which they had also isolated previously from *Streptomyces collinus*.² Conversely treatment of “rubromycin” (2) with dilute hydrochloric acid afforded a novel red pigment (1) (**Scheme 1**). Due to the evident structural relationship of these three molecules they were subsequently renamed α (3), β (2) and γ -rubromycin (1) in accordance with their respective R_f values.³

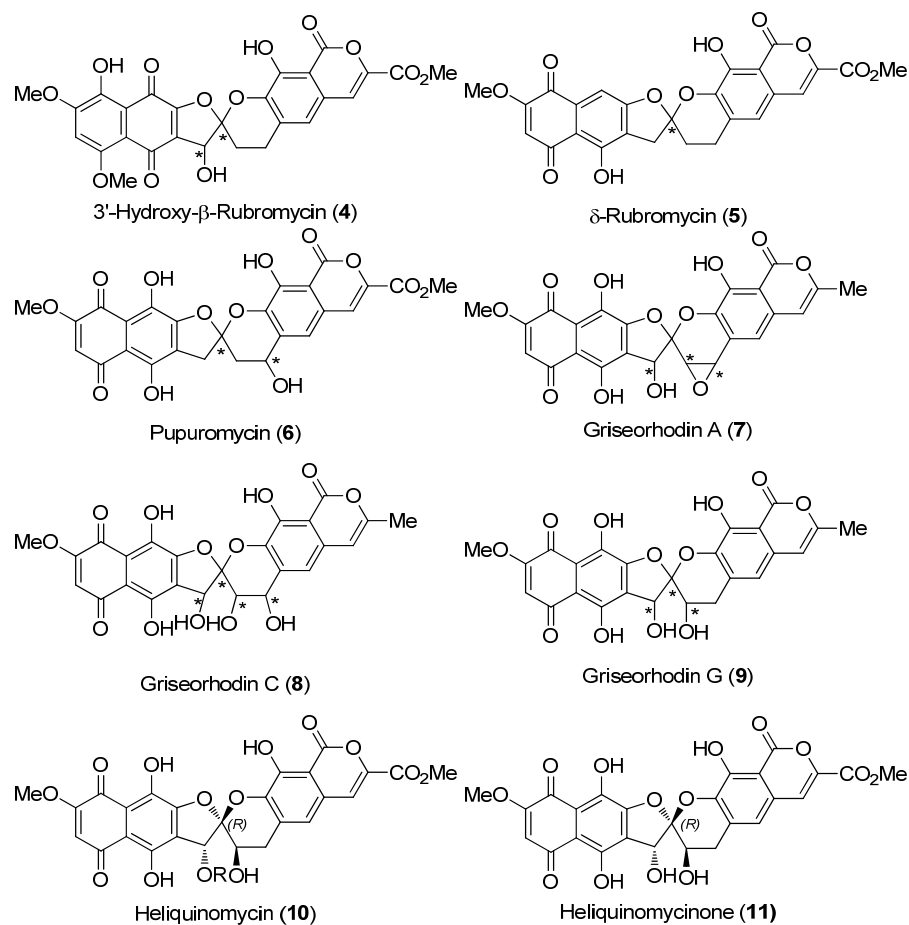


Fig. 2. Rubromycin structures

Since these early works a number of other “rubromycin” type natural products have been isolated. These include 3'-hydroxy-β-rubromycin (4) and δ-rubromycin (5) (from *Streptomyces*)⁴; pupuromycin (6) (from *Actinoplanes ianthinogenes*)^{5,6}; griseorhodin A (7), C (8) and G (9) (from *Streptomyces californicus and griseus*)^{7,8,9} and heliquinomycin (10) (from *Streptomyces* sp. MJ 929-SF2).¹⁰

1.2 Biological and Pharmacological Activity of the Rubromycins

Since their initial isolation, the rubromycins have been known to be potent antimicrobial agents capable of inhibiting the growth of various bacteria and fungi at micro to nanomolar concentrations.¹¹ The biological properties of rubromycins and their analogues were further examined in 2000 by Hayashi and co-workers. Interestingly their results showed micromolar levels of inhibition of human immunodeficiency virus type 1 reverse transcriptase (HIV-1 RT) and telomerase (**Table 1**) both high profile pharmaceutical targets, sparking a renewal of interest.¹²

Compound	IC ₅₀ (μM) of TS-A ^a concentration of		IC ₅₀ (μM) of HIV-1 RT
	0.2 μM	2.0 μM	
α-Rubromycin (3)	>200	>200	>200
β-Rubromycin (2)	3.06 ± 0.85	8.64 ± 2.3	33.3 ± 2.4
γ-Rubromycin (1)	2.64 ± 0.09	17.8 ± 2.0	19.9 ± 1.6
Purpomycin (6)	3.19 ± 0.45	15.9 ± 2.1	22.9 ± 0.45
Griseorhodin A (7)	12.2 ± 3.1	41.6 ± 9.8	10.5 ± 1.2
Griseorhodin C (8)	5.87 ± 0.44	2.58 ± 1.7	11.4 ± 1.8

Table 1. Comparison of the biological activity of the rubromycins

From the results of Hayashi's study it appears that the benzannulated spiroketal moiety of the rubromycins is the essential pharmacophore for both telomerase and HIV1-RT activity as α-rubromycin (**3**), an open-chain member of the rubromycin family exhibits dramatically reduced levels of inhibition (IC₅₀ >200 μM) (**Fig. 3**).¹³

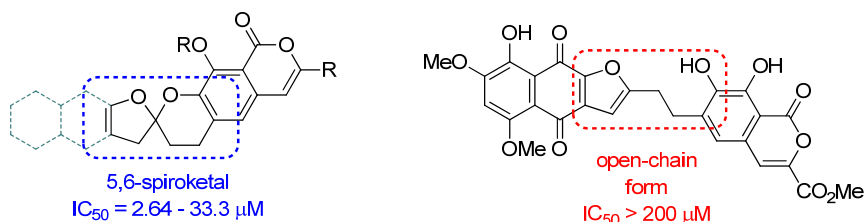


Fig. 3. Pharmaceutical importance of the 5,6-spiroketal

^a Telomerase Substrate Primer.

1.3 Pharmaceutical Importance of HIV1-RT

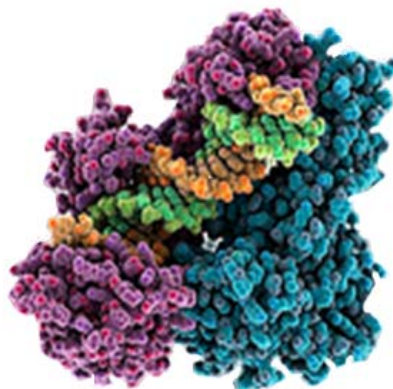


Fig. 4. Computer generated image of HIV-1 RT (blue/pink) DNA (green/orange) complex ¹⁴

HIV1-RT is a retroviral enzyme that facilitates transcription of retroviral RNA into retroviral DNA inside a host cell. This is the reverse process of regular cellular transcription processes and is central to the infectious nature of retroviruses, several of which cause disease in human hosts, such as acquired immune deficiency syndrome (AIDS) and human T-cell lymphotropic virus 1 (HTLV-1), which can subsequently lead to leukaemia.

Currently, non-nucleoside based small molecule type reverse transcriptase inhibitors (NNRTIs) are believed to bind to a hydrophobic pocket of the enzyme near the polymerase active site (see **Fig. 4**, polymerase active site occupied by DNA).¹⁵ It appears that this allosterically distorts the enzyme sufficiently that polymerase cannot occur despite binding of both the required nucleic acid and reverse transcription (RT) substrates. This mechanism of inhibition is however still somewhat unclear and therefore greater understanding of the RT mechanism of action is currently required for more targeted drug discovery processes.^{16,17}

1.4 Pharmaceutical Importance of Telomerase

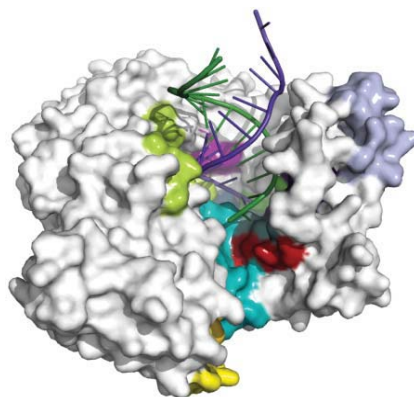


Fig. 5. Surface representation of TERT with modelled RNA (green) and DNA (purple).¹⁷

Telomerase is a unique ribonucleoprotein complex,¹⁸ comprised of two major components, a catalytic subunit (TERT, Telomerase Reverse Transcriptase) and an integral RNA component (TER, Telomerase RNA) that require stable association to form the functional holoenzyme (**Fig. 5**). It is this complex that is responsible for maintaining length and integrity of linear chromosome termini known as telomeres [Greek; *telos* (end) *meros* (part)] during cellular replication processes.^{19,20,21,22} It is believed that as telomeres are shortened due to replication processes such as mitosis, cells age and can therefore only replicate a finite number of times until reaching critical length (Hayflick limit),²³ at which point cell-replication cannot continue.

It is therefore essential that telomere length is maintained. Telomerase is over-expressed in most tumour cells from virtually all types of cancer (80-90%). As telomerase is essential for long term telomere maintenance, it is therefore crucial for long-term survival of tumour cells and tumour progression. Due to this high telomerase activity, cancer cells can almost be considered as immortal (not limited by Hayflick limit) thus avoiding apoptosis.^{24,25} Conversely 'normal' cells express little or no telomerase and generally have longer telomeres than tumour cells, making telomerase a relatively specific and pharmaceutically attractive anti-cancer target.²⁶

Despite intense academic and industrial efforts and innumerable *in vitro* and cell studies, no small-molecule telomerase inhibitors have to date emerged as fully approved pharmaceutical agents, although a number of vaccines and oligonucleosides are currently under investigation in clinical trials.²⁷ This attrition has been largely attributed to insufficient understanding of human telomerase (*h*-telomerase) structure and mechanisms of interdiction in addition to further complexities presented by the enzymes dimeric composition.²⁸ One significant obstacle has been the lack of sufficient quantities of stable and purified TERT, which has thwarted access to a functionally relevant X-ray crystal structure.

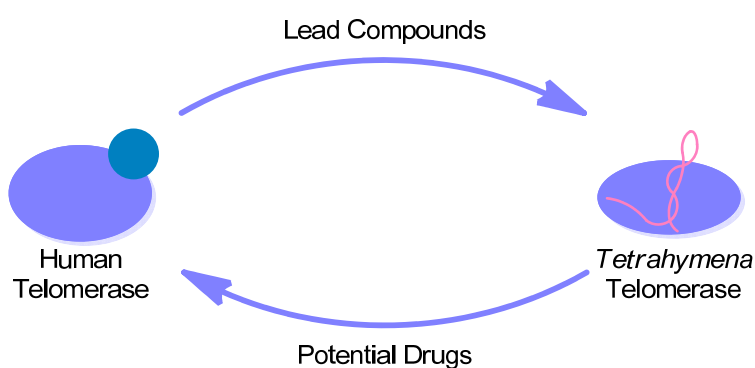
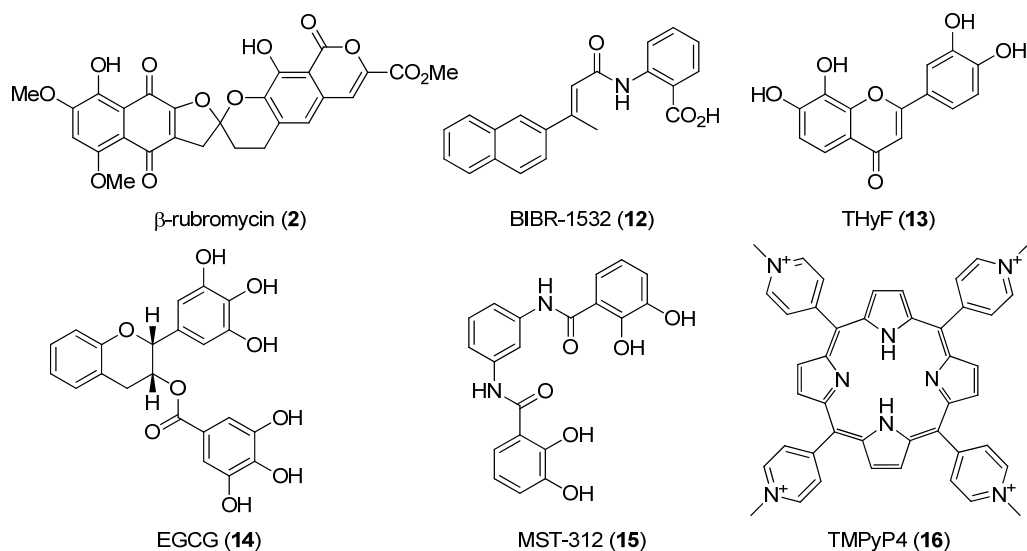


Fig. 6. Pettus' telomerase inhibitor development strategy

Due to this purification problem, it was recently proposed jointly by the groups of Pettus and Reich that monomeric *Tetrahymena* telomerase (*t*-telomerase) may provide the most useful platform for inhibitor development.²⁹ Said investigation screened spectrum representative telomerase inhibitors against both *h*-telomerase and *t*-telomerase to ascertain if inhibitor structure activity relationship (SAR) is conserved between enzymes. If successful, potential inhibitors could then be screened during early development against *t*-telomerase for practical reasons. Second generation lead compounds could then be screened against *h*-telomerase, reducing the amount of biological labour involved in generating SAR data (**Fig. 6**).



Entry	Inhibitor	<i>h</i> -TRAP IC ₅₀ (μM)	Maximal Inhibition	<i>t</i> -TRAP IC ₅₀ (μM)	Maximal Inhibition
1	β -Rubromycin	1.53 ± 0.21	90%	0.81 ± 0.08	100%
2	BIBR-1532	4.6 ± 0.48	100%	> 200	NA
3	THyF	0.25 ± 0.06	100%	0.62 ± 0.17	100%
4	EGCG	1.18 ± 0.16	80%	0.37 ± 0.12	85%
5	MST-312	12.8 ± 2.9	100%	> 200	NA
6	TMPyP	0.15 ± 0.01	100%	0.14 ± 0.014	100%

Table 2. Pettus and Reich's SAR comparison study data

Interestingly this hypothesis was quite effective for four of the six series of compounds tested and appears to show that *t*-TRAP assays (polymerase chain reaction based telomeric repeat amplification protocol) may allow for reasonable SAR predictions for telomerase inhibitors based upon a rubromycin scaffold (**Entry 1, Table 2**). This study also reported that β -rubromycin did not exhibit any G-quadruplex stabilising effect during thermal melt analysis. It therefore appears that the rubromycins do not inhibit telomerase through a G-quadruplex stabilization mechanism.

1.5 Rubromycin Biosynthesis

Polyketides constitute a large, structurally diverse range of biologically active natural products. The origin of this diversity is particularly intriguing as they are essentially polymeric structures of repeating acetate and propionate subunits. In bacteria (i.e. rubromycin producing *Streptomyces*) the synthesis of secondary metabolites is usually controlled by remarkably versatile and amenable enzymatic clusters, known as type-II polyketide synthases (PKSs). These clusters consist of several repeating domains, each with a role in either the functionalisation and/or chain elongation.

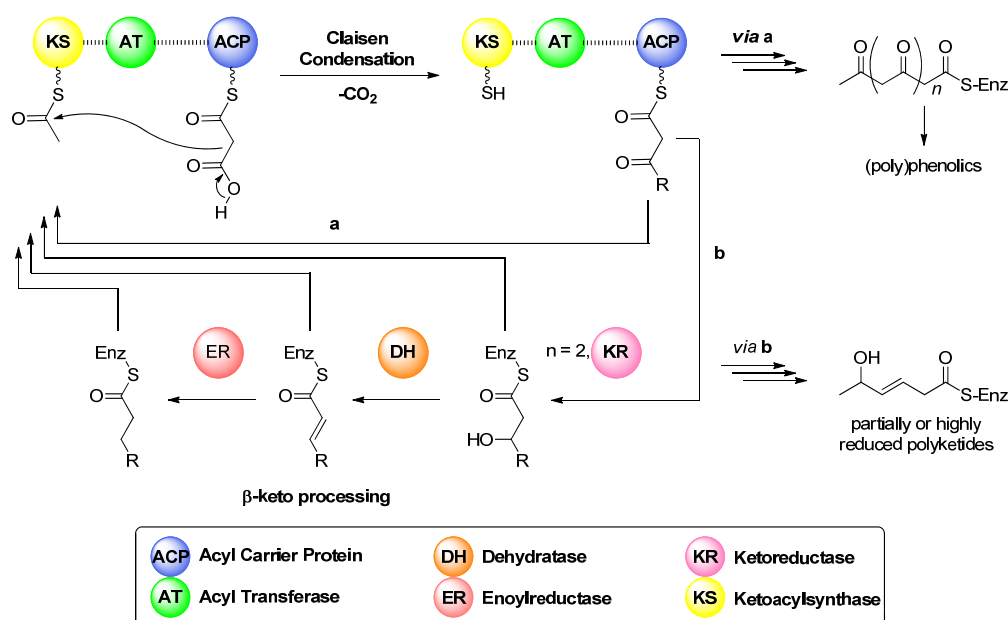


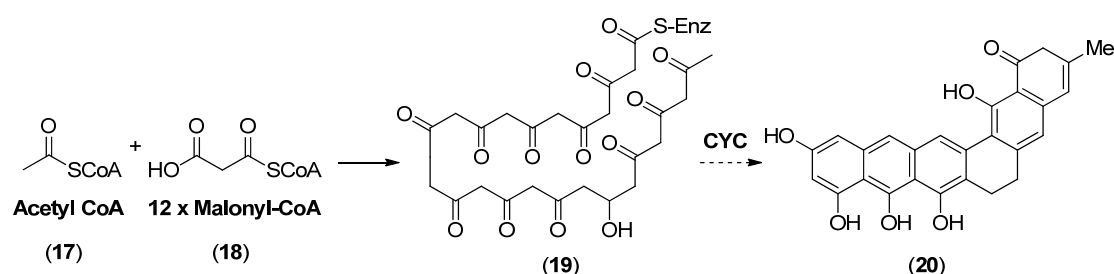
Fig 7. Overall view of polyketide biosynthesis³⁰

This massive biological assembly line can essentially be considered as a two-stage process. The initial biosynthetic sequence involves enzymes that are generally highly conserved between all type-II PKS systems. The acetate-type molecular building blocks consumed by these massive polyenzymatic systems are generally in the form of acetyl-coenzyme A (CoA) and malonyl-coenzyme A (MCoA) respectively.

These subunits undergo chain elongation by repetitive decarboxylative Claisen thioester condensations between an activated acyl starter unit and a defined number of MCoA

derived extender units (**pathway a, Fig. 7**). The resulting poly- β -oxoacyl-CoA chain, after optional β -keto processing (**pathway b, Fig. 7**) can then undergo regiospecific cyclisation by cyclases (CYC) to furnish the bare aromatic molecular polyketide skeleton.

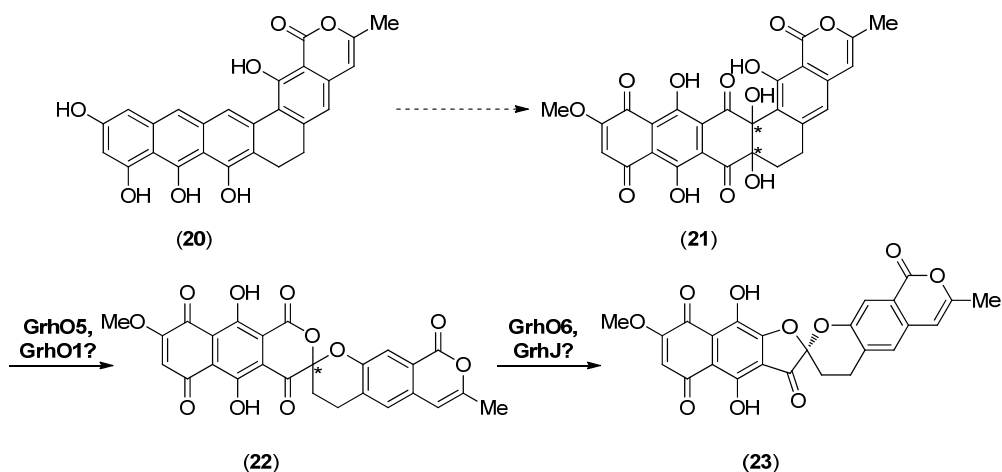
The biodiversity of these initial structures is surprisingly limited, which is a stark comparison to the plethora of intermediates that results from the subsequent tailoring stage carried out by a significantly larger and more diverse enzymatic family. These are commonly referred to as tailoring enzymes and often responsible for pharmacophore installation.



Scheme 2. Inferred PKS route from ^{13}C labelling study

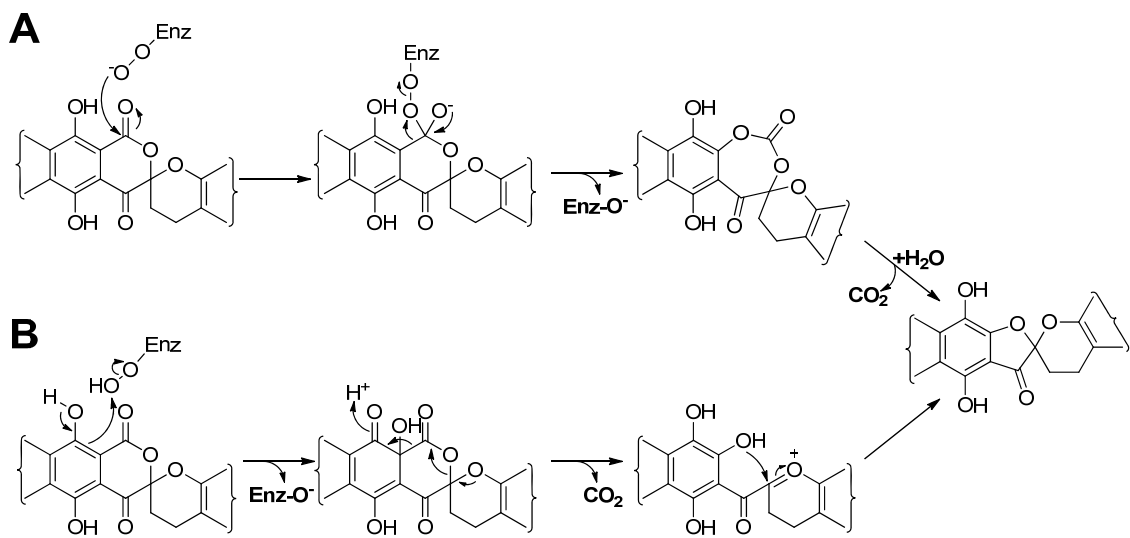
Independent biosynthetic labelling studies using 1,2- ^{13}C acetic acid, have implied that both β -rubromycin (**2**) (from *Streptomyces* sp. A1)³¹ and the heliquinomycin aglycon (from *Streptomyces* sp. MJ929-SF2)³² incorporated 13 acetate units during polyketide biosynthesis, giving identical labelling patterns, inferring an unusually lengthy tridecaketide origin. Upon further inspection of the gene cluster, the most likely PKS product appears to be a pradimicin-type intermediate (**20**).

The precise post-PKS tailoring of (**20**) to afford the desired rubromycin skeletons is still a subject of discussion. However, recent study by Li and Piel³³ identified the type-II PKS gene cluster (*grh* cluster) that encodes for the biosynthesis of griseorhodin A (**7**) (from *Streptomyces* sp. JP95). Further investigation of this unusually large oxidoreductase rich and diverse gene cluster shed further light on this pathway.³⁴



Scheme 3. Inferred post-PKS biosynthetic tailoring

One key enzyme identified was the flavin adenine dinucleotide (FAD) dependant oxidoreductase GrhO5, which upon removal generates the ‘unnatural’ antibiotic collione (21). This enzyme was attributed to facilitate [6,6]-bis-benzannulated spiroketal formation, although the product of the immediate downstream GrhO1 enzyme could not be fully characterized.



Scheme 4. Possible enzymatic installation of the spiroketal

The close protein homology of GrhO6 to oxidative enzymes, which may facilitate inferred Baeyer-Villiger type processes suggested related chemical functionality to this enzymatic class, inferring a possible enzymatic mechanism involving the monooxygenase unusually acting on the ester functionality over the ketone (**Scheme 4, Route A**). Conversely, carbon-bond cleavage could also be rationalized by enzymatic hydroxylation, promoting subsequent fragmentation before rearomatisation to the [5,6]-*bis*-benzannulated spiroketal (**Scheme 4, Route B**).

Chapter 2:
Rubromycin Model
Systems

2.1 [5,6]-bis-Benzannulated Spiroketal Synthesis

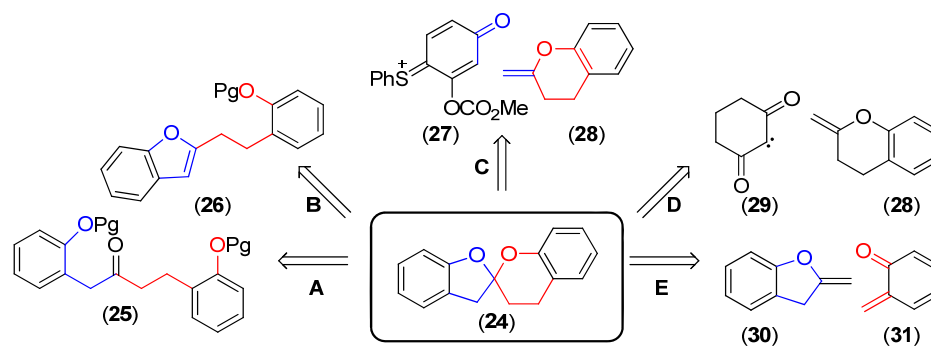


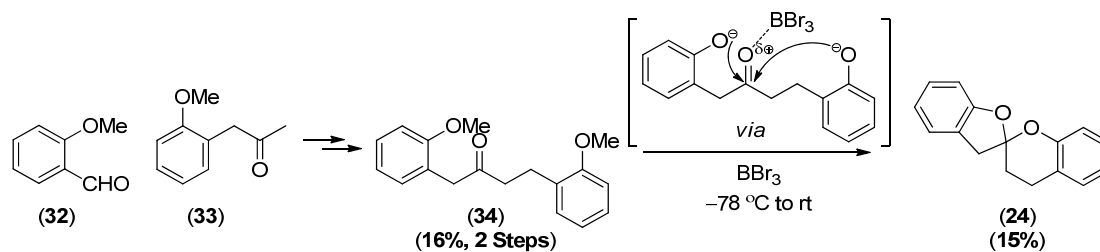
Fig. 8. Retrosynthetic analysis of [5,6]-bis-benzannulated spiroketals

The key structural motif conserved throughout the natural rubromycins is the [5,6]-bis-benzannulated spiroketal, which forms the central scaffold. Said spirocyclic core links the benzofuran and the benzopyran moieties *via* a central sp^3 carbon atom (spiro carbon) such that the two cyclic ethereal oxygen atoms are orientated orthogonal to each other.

Despite the attractive pharmacological potential of [5,6]-bis-benzannulated spiroketal (**24**), a general modular, robust and scalable methodology with broad substrate scope has to date proved elusive. There have however been considerable and heroic efforts made by a number of research groups. The main approaches considered (**Strategies A-E, Fig. 8**) have however yielded some interesting results and useful synthetic tools. It is the aim of this chapter to describe each of these five strategies in turn, including their development and synthetic scope. It is the author's intention to make a clear distinction between literature reports described both before the start (**Chapter 2a**), and during the course of this investigation (**Chapter 2b**).

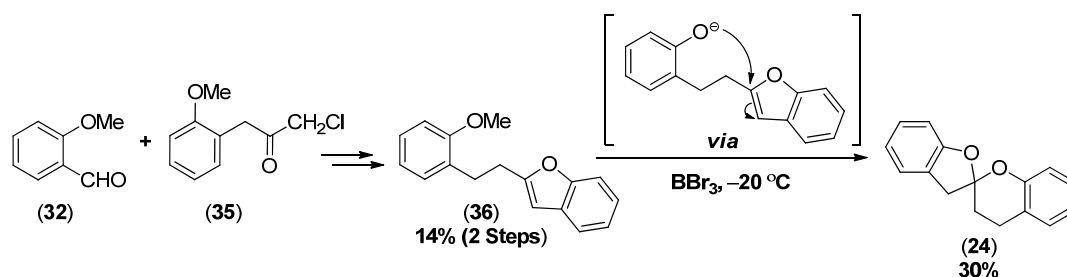
Chapter 2a:
Previous Model
Studies

2.2 Greul and Brockmann Approaches (Strategies A and B)



Scheme 5. Greul and Brockmann spiroketal synthesis

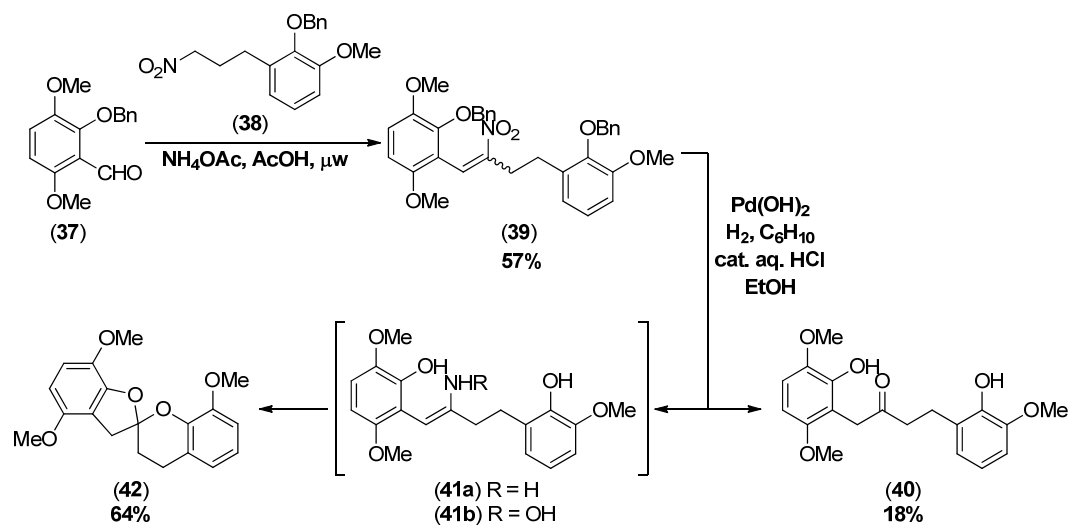
The seminal publication in this field by Greul and Brockmann in 1971,³⁵ outlined the first two strategies (**Strategies A-B, Fig. 8**) to the simple non-substituted [5,6]-*bis*-benzannulated spiroketal (**24**). The first of these, “strategy A” (**Scheme 5**) involves Lewis-acid promoted demethylation, of a *bis*-(*o*-methoxyphenyl)-substituted ketone (**34**) (prepared by aldol condensation followed by hydrogenation). The naked phenoxide then undergoes Lewis-acid catalysed spirocyclization to form (**24**) in an extremely modest yield (2.4% over 3 steps). This strategy shall from herein be referred to as spiroketalisation.



Scheme 6. Greul and Brockmann spiroketal synthesis

The alternative route “strategy B”, (**Scheme 6**) involves condensation of the *o*-methylated salicyl aldehyde (**32**) with a chloromethyl ketone (**35**), followed by subsequent Clemmensen reduction³⁶ to give the 2-(2-aryl)ethylbenzofuran precursor (**36**). This subsequently undergoes Lewis-acid promoted demethylation and cyclization to give the desired compound (**24**) in a slightly improved yield (4.2% over 3 steps). This strategy shall herein be referred to as the 6-*exo*-trig spirocyclisation approach and shall be discussed later (**Section 2.8**).

2.3 de Koning Spiroketalisation Approach



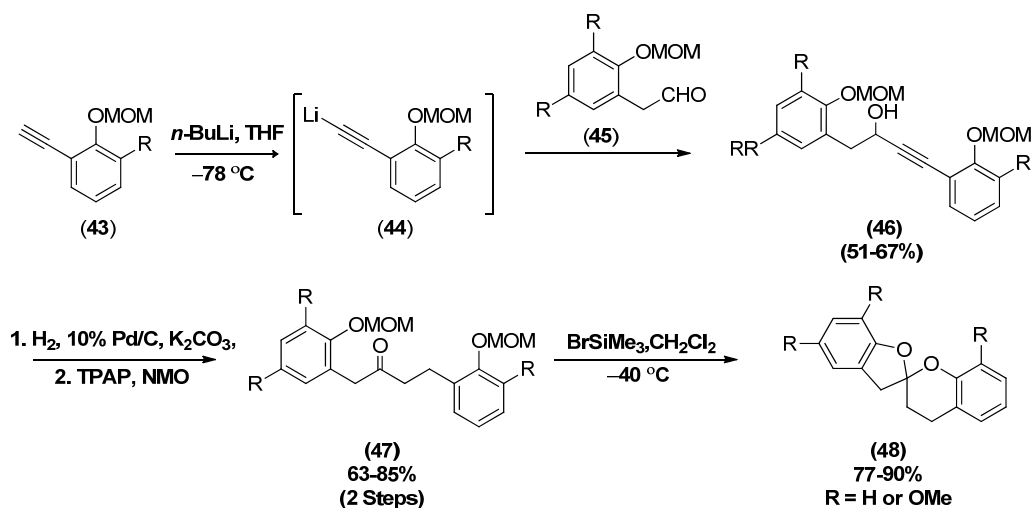
Scheme 7. de Koning spiroketal model system

Surprisingly, no further synthetic efforts were observed in the literature until 1998 when de Koning and co-workers described a modification to Greul and Brockmann's spiroketalisation procedure (Scheme 7).^{37,38} Their approach nicely showcased Varma and co-workers procedure for the solventless, microwave-assisted synthesis of nitroalkenes *via* a Henry reaction to couple the two fragments, providing (39) in 57% yield.³⁹

Subsequent exposure of (39) to Pearlman's catalyst and catalytic HCl, under an atmosphere of hydrogen promoted spiroketal formation *via* a "Nef-type" process in a markedly improved 64% yield. The authors initially suggested that the nitro group is reduced to afford enamine (41a), which under aqueous acidic conditions would hydrolyse to (40) and then cyclise to (42).^b Alternatively, it was suggested that the nitro group may be reduced to the unsaturated hydroxylamine (41b), which then tautomerises to an unsaturated oxime that again hydrolyses to (40) and cyclises under the acidic conditions.

^b It was of note that in acidic solution sideproduct (40) slowly cyclised to (42).

2.4 Brimble's Sonogashira Coupling/Spiroketalisation Approach



Scheme 8. Brimble's rubromycin model study

In 2003 Brimble and co-workers further improved the efficiency of the spiroketalisation approach (**Scheme 7**).⁴⁰ Said methodology combines the effective use of a Sonogashira type coupling⁴¹ to prepare various aryl acetylene fragments (**46**). These were converted to the cyclisation precursors (**47**) in two steps, namely full hydrogenation of the alkyne before subsequent oxidation of the resultant alcohol species using catalytic tetrapropylammonium perruthenate (TPAP) and *N*-methylmorpholine-*N*-oxide (NMO). Subsequent MOM-deprotection of both the γ - and δ -phenolic groups using bromotrimethylsilane facilitated spirocyclization to give (**48**) in overall yields of 77-90%, a significant improvement on Greul and Brockmann's pioneering efforts.

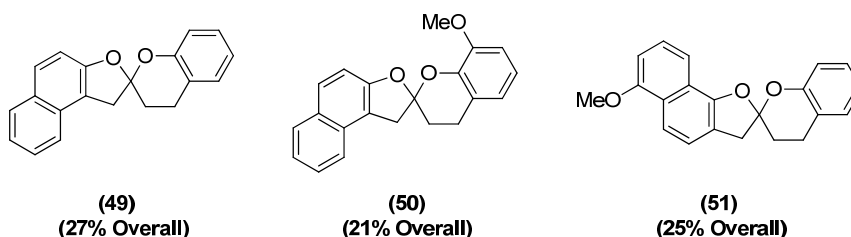
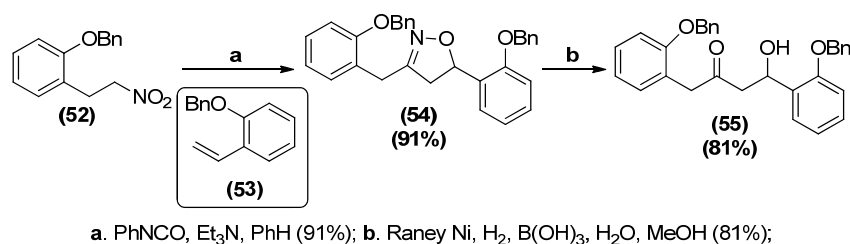


Fig. 9. Additional spiroketal motifs generated by Brimble

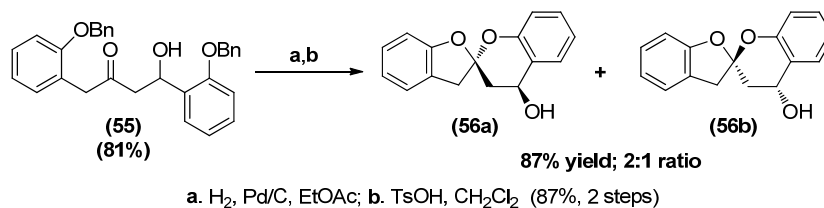
In a subsequent 2007 communication,⁴² Brimble *et al.* demonstrated that this methodology also has additional scope in synthetic chemistry by generating a small number of simple *bis*-benzannulated spiroketals with alternative aromatic motifs (**Fig. 9**).

2.5 Kozlowski's Spiroketalisation



Scheme 9. Synthesis of Kozlowski's model precursor

In 2006 the Kozlowski group demonstrated that a Brønsted-acid spiroketalisation could be used to construct a [5,6]-*bis*-benzannulated spiroketal with the desired oxidation pattern exhibited in pupuromycin (**6**). This strategy featured a novel approach to precursor (**55**) generated *via* hydrogenation of the isoxazoline [3+2] cycloaddition product (**54**) formed between styrene (**53**) and nitroalkane (**52**) (**Scheme 9**).



Scheme 10. Kozlowski's model spiroketalization

The key finding of this study, was however that exposing spiroketalisation precursor (**55**) to stepwise hydrogenation and Brønstead acid promoted spirocyclisation conditions facilitated the diastereo-enriched synthesis of spiroketal (**56**) (2:1 mixture). This preference was rationalised by Kozlowski due to both the anomeric effect and a proposed hydrogen bond interaction in (**56a**) (**Fig. 10**).

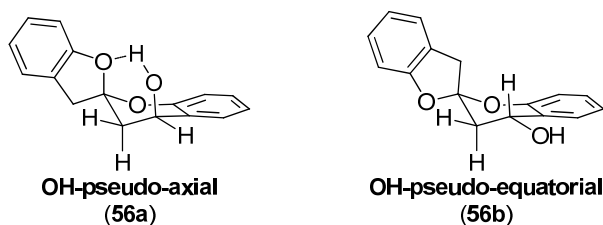
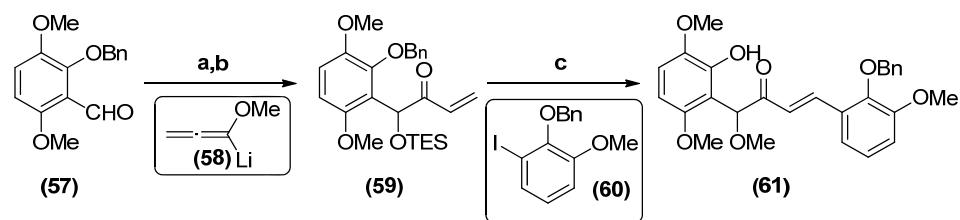


Fig. 10. Kozlowski's rationalisation for diastereo-enrichment

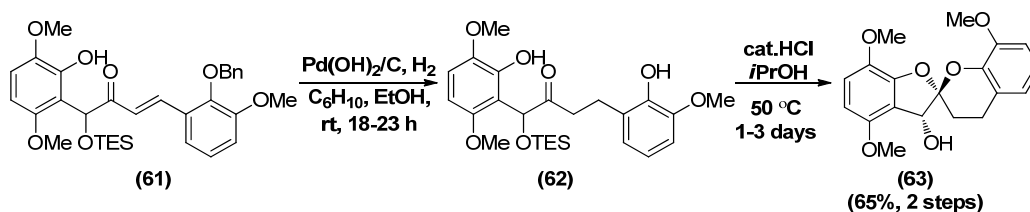
2.6 Reißig's Spiroketalisation



ai. (58), THF, $-40\text{ }^\circ\text{C}$, 1 h; ii. then $-78\text{ }^\circ\text{C}$, (57), 3 h; iii. then H_2SO_4 (5%), $0\text{ }^\circ\text{C}$, 2 h, (98%); b. TESCl, Pr_2NEt , DMF, rt, 2 h, (78%); c. $\text{Pd}(\text{OAc})_2$, NaHCO_3 , TBACl, MS 4 Å, DMF, $60\text{ }^\circ\text{C}$, 24 h, (82%);

Scheme 11. Synthesis of the prerequisite α,β -unsaturated ketone

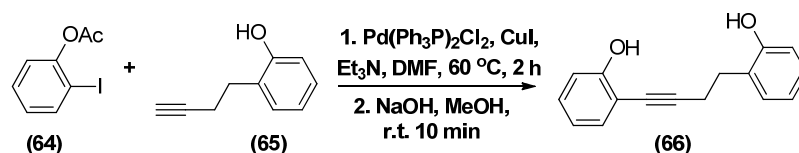
Contemporaneously to Kozłowski's finding, Reißig and co-workers also reported [5,6]-bis-benzannulated spiroketal synthesis based around a similar Brønstead-acid promoted spiroketalisation.⁴³ This approach differed from those outlined previously by employment of an α,β -unsaturated ketone spiroketalisation precursor (61). Said species was generated from a Heck reaction between aryl iodide (60) and TES-protected α -hydroxy enone (59) (prepared in 3 steps from nucleophilic addition of lithiated methoxyallene (58) to benzaldehyde (57), followed by subsequent acid hydrolysis and silylation) (Scheme 11).



Scheme 12. Thermodynamically controlled *trans*-selective spiroketalisation

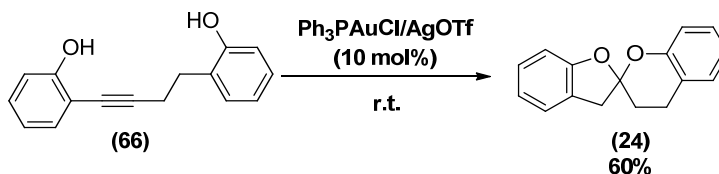
Upon subjection of (61) to hydrogenation conditions and subsequent exposure to catalytic amounts of acid promoted a diastereoselective spiroketalisation to afford *trans*-spiroketal (63) exclusively (Scheme 12).

2.7 Li and Xue's Gold-Catalysed Spiroketalisation



Scheme 13. Gold-catalysed route to spirocyclization precursor

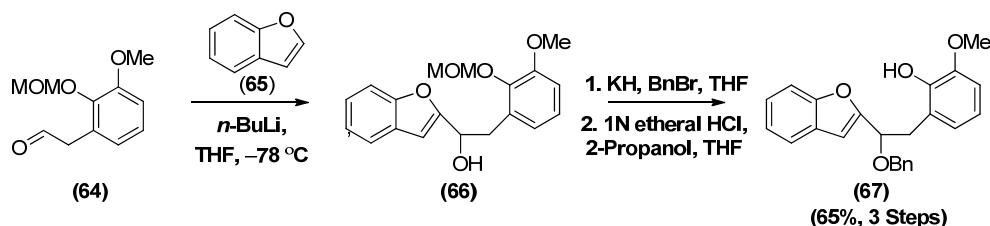
Shortly afterwards in 2007, Li and Zue demonstrated that a simple [5,6]-*bis*-benzannulated spiroketal (**24**) could be generated from alkyne (**65**) and aryl iodides e.g. (**64**) (**Scheme 13**).⁴⁴ These fragments were initially coupled using Sonogashira type methodology before basic acyl cleavage revealed the phenolic *bis*-aromatic alkyne spirocyclization precursor (**66**) similar to those employed by Brimble *et al.* (**46**). The subsequent one-pot metal catalysed spiroketalization procedure is however a significantly more elegant model than Brimble's avoiding atom inefficient multi-step preparation of a prerequisite sp² hybridised ketone. The gold (I) catalyst in question [Ph₃PAuCl/AgOTf (10 mol%)] was successfully employed at room temperature affording (**24**) in 62% yield after 48 hours (**Scheme 14**).



Scheme 14. Gold-Catalysed Spirocyclization

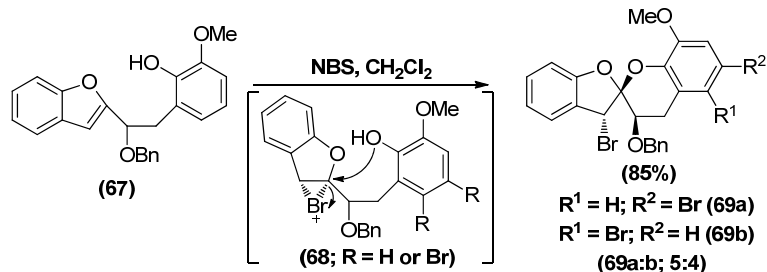
The proposed mechanism for this reaction involves co-ordination of the gold species to the alkyne and the *ortho*-phenol, which enhances the electrophilicity of the alkyne (**66**). The furan moiety is then believed to form first during a double intramolecular phenolic attack, generating the model spiroketal (**24**). The active gold species is then believed to be simultaneously liberated however further mechanistic details are at the time of writing unknown and were only speculated upon by the authors.

2.8 Danishefsky's 6-*exo*-trig Spirocyclisation Approach



Scheme 15. Danishefsky's synthesis of the spirocyclisation precursor

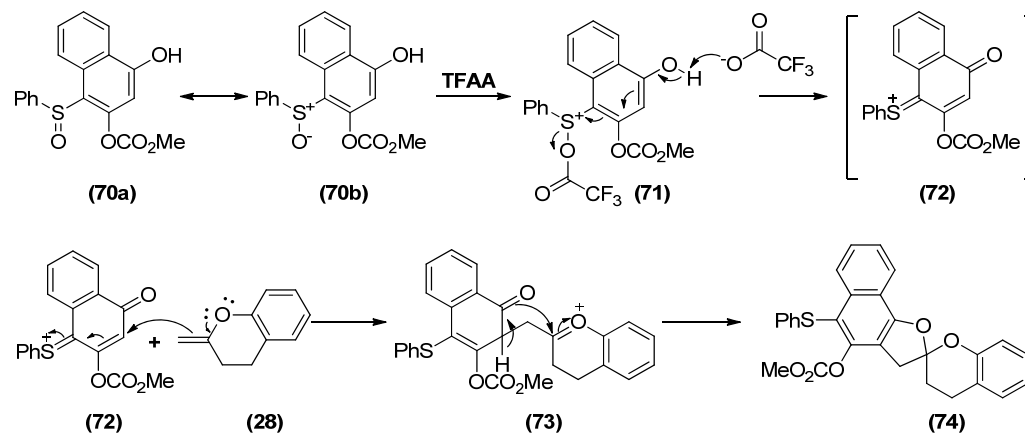
Building on the findings of Greul and Brockmann, Danishefsky and co-workers were, at the start of this investigation, the only group to optimise the 6-*exo*-trig spirocyclisation strategy towards [5,6]-*bis*-benzannulated spiroketals (**Strategy B, Fig 8**). This methodology was very effectively employed during the synthesis of their heliquinomycin (**10**) model system in 2001.⁴⁵ In their approach the cyclisation precursor (**67**) was prepared by coupling of aldehyde (**64**) with 2-lithio-2,3-benzofuran, followed by benzyl protection of the free alcohol (**66**), before Brønsted acid-promoted deprotection of the methoxy methyl ester to furnish the prerequisite phenol (**67**) (**Scheme 15**).



Scheme 16. Danishefsky's model stereoselective spirocyclization

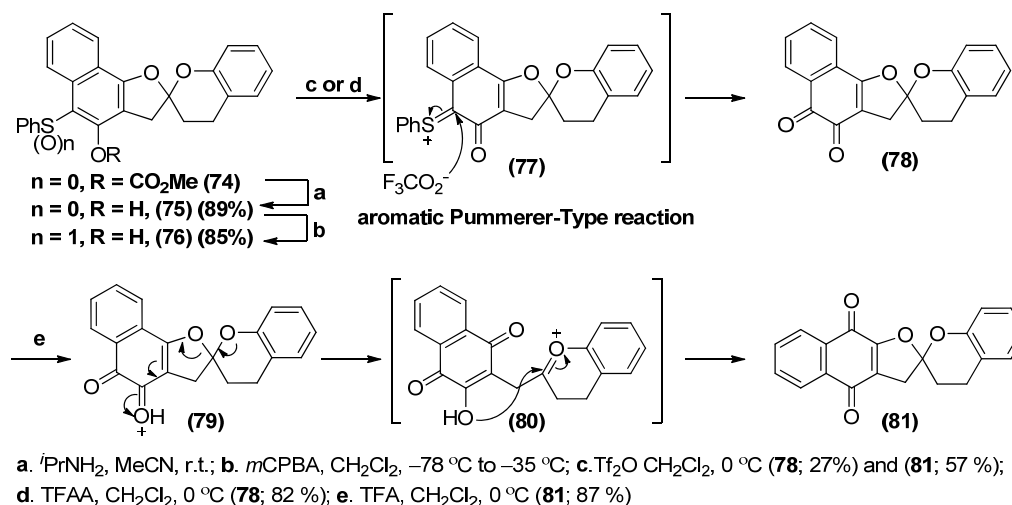
Various unsuccessful attempts were made to cyclise (**67**) *via* face selective epoxidation of the furan, with the aim of promoting intramolecular nucleophilic attack from the phenol. After screening a variety of reagents to activate the benzofuran (Hg(II) salts, Pd, HCl, PhSeCl and I₂) it was found that treatment with NBS generated bromonium ion (**68**) (**Scheme 16**). Concomitant intramolecular nucleophilic attack of the phenol afforded the desired [5,6]-*bis*-benzannulated spiroketal (**69**) in good overall yield (85%). This process was however somewhat complicated by non-regiospecific bromination of the benzopyran leading to a mixture of regioisomers (**69a:69b**; 5:4).

2.9 Kita's Pummerer Approach (Strategy C)



Scheme 17. Kita's Pummerer reaction

The third disconnection approach (**Strategy C, Fig.8**), was first made in 2007 by Kita and co-workers and was shown to be an effective, route to the [5,6]-bis-benzannulated spiroketal (**81**).⁴⁶ The initial spiroketal (**74**) was prepared in one pot by a previously unknown aromatic Pummerer-type reaction between sulfoxide (**70a**) and 2-methylenechroman (**28**) (Scheme 17) in the presence of trifluoroacetic anhydride (TFAA), before spiroketalization of the resultant oxonium ion proceeded with re-aromatization of the nathalene to furnish (**74**) in 73% yield (10 mg isolated).

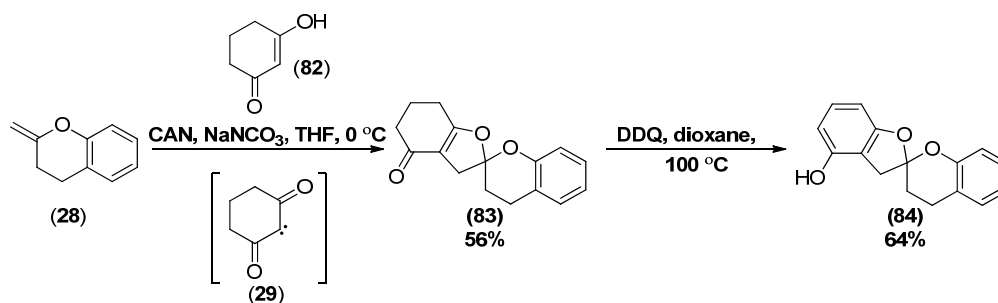


Scheme 18. Kita's construction of rubromycin model system

Serendipitously, whilst trying to derivatise (**76**) to the *ortho*-quinone species (**78**) by a second aromatic Pummer-type reaction using triflic anhydride, unexpected direct formation of the pentacyclic rubromycin model (**81**) was observed in 57% yield, in addition to (**78**; 27 %yield).

During mechanistic investigation it was shown that treatment of (**76**) with trifluoroacetic anhydride (TFAA) afforded *ortho*-quinone (**78**) as a single product in 82% yield. Subsequent treatment of the *ortho*-quinone (**78**) with trifluoroacetic acid (TFA) afforded (**81**) *via* an unprecedented rearrangement in 87% yield (**Scheme 18**). Kita and co-workers proposed that electron donation of the β -oxygen assists carbonyl protonation, thus promoting formal cleavage of the ketal, forming oxonium intermediate (**80**). This then undergoes intramolecular cyclisation to form the pentacyclic model rubromycin core (**81**). This strategy from herein shall be referred to as the Pummerer approach.

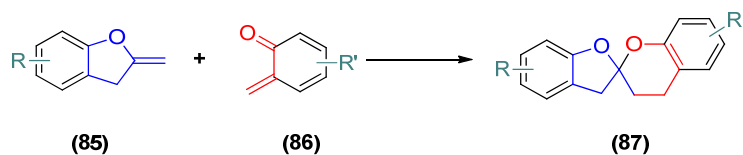
2.10 Pettus' [3+2] Cycloaddition Strategy (Strategy D)



Scheme 19. Pettus [3+2] model study

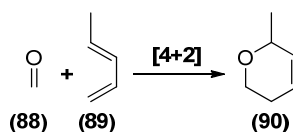
A further novel approach was developed by Pettus and co-workers (Strategy D, Fig. 8) in 2006 based around construction of a dihydrofuran *via* a [3+2] cycloaddition.⁴⁷ Using Roy's cerium ammonium nitrate (CAN) mediated conditions,⁴⁸ they were able to promote a [3+2] cycloaddition between *exo*-enol ether (28) and 1,3-dicarbonyl carbene (29) oxidatively generated *in situ* (Scheme 19) from (82) in moderate yield (56%). The resultant [5,6]-*mono*-benzannulated spiroketal (83) was then further aromatized using 2,3-dichloro-5,6-dicyanobenzoquinone (DDQ) to furnish the desired [5,6]-*bis*-benzannulated spiroketal (84) (64%). This strategy from herein shall be referred to as the [3+2] cycloaddition approach.

2.11 *hetero*-Diels-Alder Approaches (Strategy E)



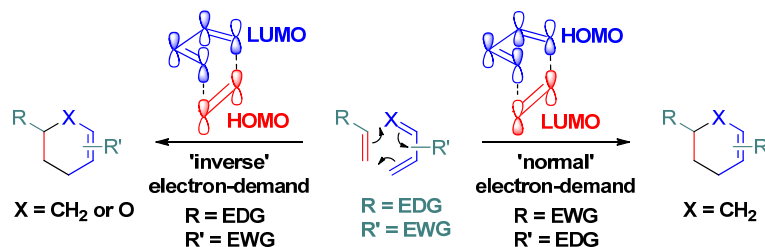
Scheme 20. *hDA* approach to [5,6]-bis-benzannulated spiroketals

The final strategy (**Strategy E, Fig.8**) towards [5,6]-bis-benzannulated spiroketals, that had been reported at the start of this investigation was to generate this interesting scaffold via a *hetero*-Diels-Alder (*hDA*) reaction (**Scheme 20**) between an *exo*-enol ether and an *ortho*-quinone methide (*o*-QM) such as **(85)** and **(86)** respectively.



Scheme 21. Seminal *hetero*-Diels-Alder reaction

Since the first report by Otto Diels and Kurt Alder's of their famous [4+2] cycloaddition reaction first carried out over 80 years ago, this cycloaddition has proved to be an extremely popular⁴⁹ and useful reaction in organic synthesis.^{50,51} An account of the incorporation of a oxygen atom in a [4+2] cycloaddition was reported two decades later by Gresham and Steadman (**Scheme 21**).⁵² Since then the scope of this reaction has been expanded to work effectively with both nitrogen⁵³ and phosphorus.⁵⁴

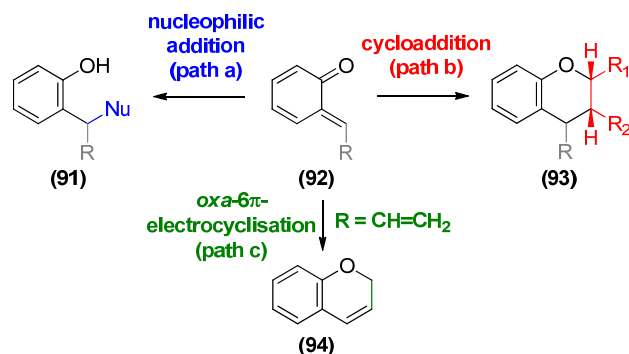


Scheme 22. Frontier molecular orbital description of Diels-Alder cycloadditions

Importantly, the reactivity of *o*-QMs **(86)** in [4+2] cycloadditions are somewhat different in terms of frontier molecular orbital theory to the simple diene's employed in Diels and Alder's early work and can be best described as 'inverse' electron-demand *hetero*-Diels-Alder reactions. This is because it is the alkene component, which contributes an electron

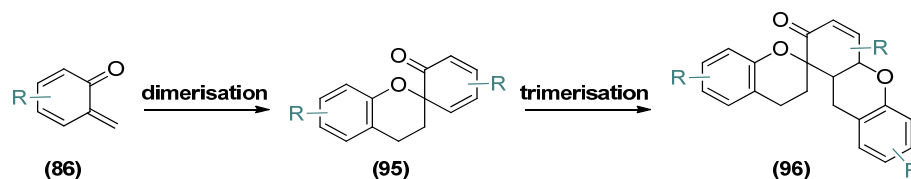
pair from its HOMO to the LUMO of the electron rich 4π component to generate a new molecular orbital, which is the opposite to that observed during ‘normal’ Diels-Alder reactions (**Scheme 26**).

2.12 *ortho*-Quinone Methides



Scheme 23. Primary reaction modes of *o*-QMs

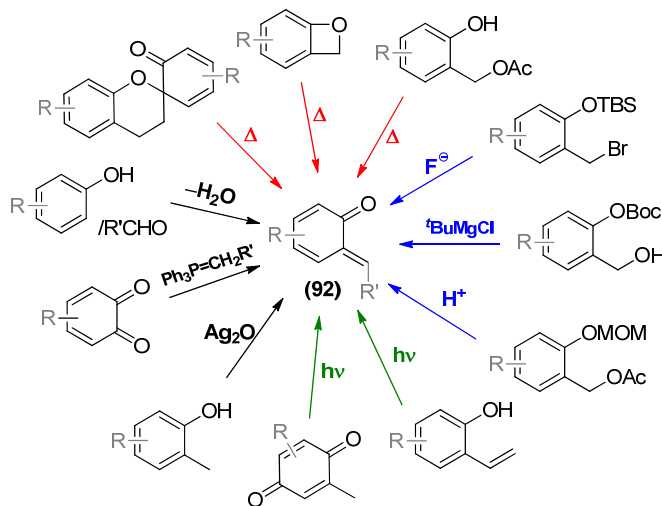
ortho-Quinone methides (*o*-QMs) e.g. (**86** and **92**) are highly reactive, ephemeral intermediates that were first alluded to in 1907 by Fries.⁵⁵ More recently in 2002, Amouri provided crystallographic evidence of *o*-QMs isolated as η^4 π -complexes of Os, Rh and Ir.⁵⁶ Despite their transient nature, there is an abundance of evidence for their function in a variety of biological systems and their use in organic synthesis is ever increasing, with a multitude of recent natural product syntheses being based on the formation of an *o*-QM.^{57,58} The transient nature of *o*-QMs is due to their propensity to undergo rapid rearomatisation either by Micheal addition of nucleophiles (**Scheme 23**, **path a**) or, often more usefully, by cycloaddition with 2π partners (**path b**) or *via oxa-6 π -electrocyclisation* to give benzopyrans (**path c**).^{57,58}



Scheme 24. Dimer and trimer formation

Surprisingly this rapid reactivity is often seen as a deterrent to synthetic development in the field with the potential for dimer- and trimerisation a major stumbling block

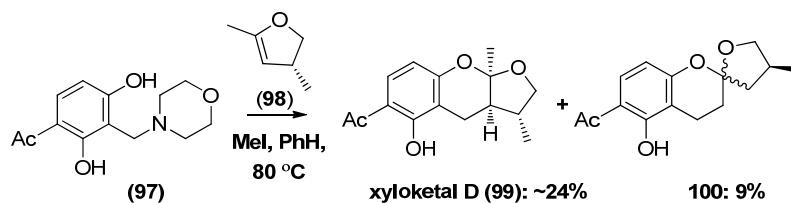
(Scheme 24).⁵⁹ To counteract this, the localized *o*-QM concentration is generally kept low to avoid dimerisation and/or it is common to employ an excess of the nucleophilic or dieneophilic components. *o*-QMs can be generated *via* a broad range of chemically diverse methodologies (Scheme 25).



Scheme 25. Overview of methods for forming *o*-QMs

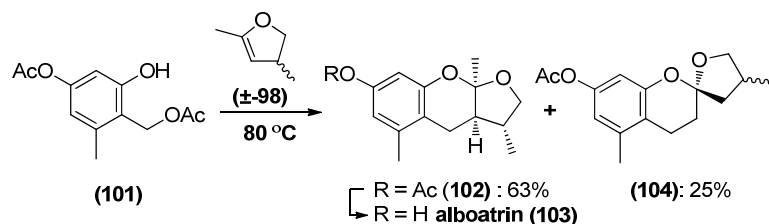
Typically, this process involves an elimination event of either a benzylic or phenolic substituent to generate a methylene or carbonyl functionality with concomitant dearomatisation. Perhaps the most commonly encountered of these methods for *o*-QM generation is the elimination of a stable molecule (Scheme 25), typically a benzylic substituent to generate the methylene and α -carbonyl functionalities with concomitant dearomatisation. This process may be induced thermally (red pathways) including retro-dimerisation⁶⁰; by addition of a nucleophile⁶¹, base⁶² or acid⁶³ (blue pathways); tautomerisation, which may be induced thermally⁶⁴ or photolytically⁶⁵ (green pathways); via benzylic oxidation or oxidative Pd-catalysis⁶⁶; Wittig methylenation⁶⁷ of an *ortho*-quinone or by aldol condensation.⁶⁸ Many of these initiation methods have been applied in the synthesis of a variety of structurally challenging natural products.⁵⁷

2.13 Serendipitous Synthesis of Spiroketal *via* a [4+2] Cycloaddition



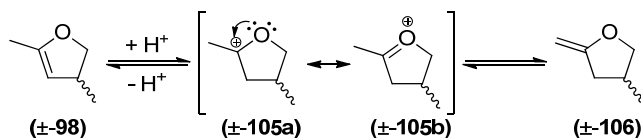
Scheme 26. Wilson's total synthesis of xyloketal D

To the best of the author's knowledge the first reported example of [5,6]-*mono*-benzannulated spiroketal generation occurring *via* an *o*-QM intermediate was published in 2004 by Wilson and co-workers during efforts towards the xyloketal family of natural products (**Scheme 26**).⁶⁹ The *o*-QM was generated *via* thermolytic extrusion of *N*-methylmorpholine from (**97**), before *in situ* [4+2] cycloaddition with (*R*)-4,5-dihydro-2,3-dimethylfuran (**98**) furnished xyloketal D (**99**). An intriguing observation in this reaction was the accompaniment of the [5,6]-*mono*-benzannulated spiroketal (**100**) as an unanticipated side product.



Scheme 27. Baldwin's total synthesis of alboatrin

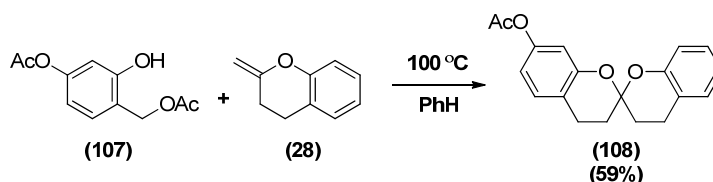
Contemporaneously to Wilson's initial efforts Baldwin and co-workers reported a similar observation during the total synthesis of the phytotoxic natural product alboatrin (**Scheme 27**).⁷⁰ *o*-QM generation was achieved upon heating acetate (**101**) in the presence of (±)-4,5-dihydro-2,4-dimethylfuran (±-**98**), which afforded the key alboatrin precursor (**102**) as the major product (63% yield) in addition to spiroketals (**104**) (25%), generated as a 3:2 mixture of diastereomers.



Scheme 28. Acid promoted *exo*-enol isomerism

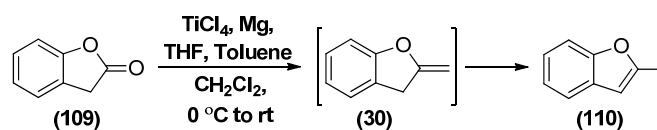
It is proposed that spiroketals (**100** and **104**) observed by the groups of Baldwin and Wilson both result from the cycloaddition of an intermediate *o*-QM with an exocyclic enol ether (**106**), which is generated *via* thermally reversible *endo*-enol isomerisation of dihydrofuran (**98**) (Scheme 28).

2.14 Thermally Initiated *hetero*-Diels-Alder Approach to Spiroketal



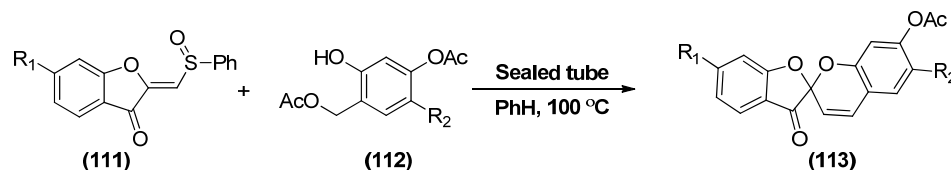
Scheme 29. Li and Xie's synthesis of a [6,6]-*bis*-benzannulated spiroketal

In 2006 Li and Xie demonstrated that the procedure developed by Baldwin and co-workers for *o*-QM generation could accommodate the use of 2-methylenebenzopyrans (Scheme 29).^{60b} Cycloaddition to generate a handful of [6,6]-*bis*-benzannulated spiroketals such as (**108**) was achievable in reasonable yields (47-60%), though it was noted that this process could be improved by the addition of a Lewis acid such as TiCl₄ to 70-73%.



Scheme 30. Formation of *endo*-enol ether

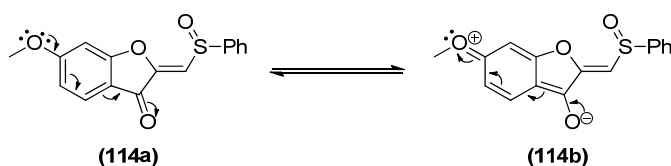
Unfortunately, attempts to synthesise aromatic [5,6]-spiroketals using this procedure failed due to isomerisation of *exo*-enol ether (**30**) to the *endo*-form (**110**) (Scheme 30). This led them to investigate milder conditions to avoid this detrimental rearrangement.



Scheme 31. Li and Xie's spiroketal synthesis model

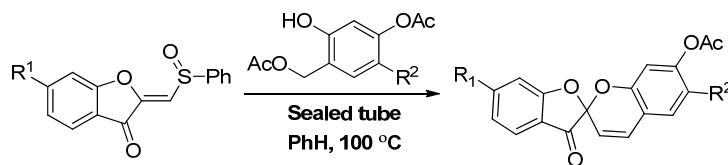
In 2008, Li and Xie successfully adapted their previous [4+2] cycloaddition reaction^{60b} of *o*-QMs generated from (**112**) as 4π components, towards use with stabilised vinyl

sulfoxides as 2π partners (**111**) to generate spiroketal motifs (**Scheme 31**).^{60c} As these 2π partners are far less susceptible to irreversible isomerisation to benzofurans, they were found to be stable enough to tolerate the high temperatures required for thermal extrusion of the acetate. To the best of this author's knowledge this is the first reported example of the intentional employment of *h*DA reaction to afford a [5,6]-*bis*-benzannulated spiroketal. Their results (**Table 3**) show an increased yield when the *o*-QM is brominated, (**entry 5 vs. 2**) presumably due to removal of electron-density from the LUMO by the inductive effect thus reducing the energy gap between the HOMO and LUMO. This may be more apparent due to the inverse electron demand type nature of said [4+2] cycloaddition.



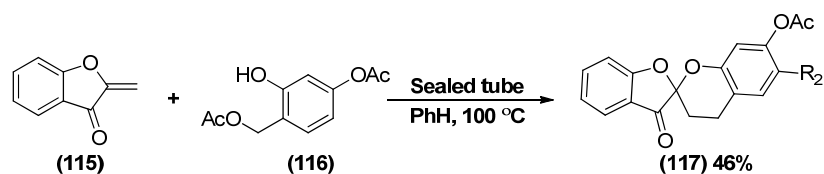
Scheme 32. Resonance stabilisation exhibited in Li and Xie's vinyl sulfoxide

The opposite effect (addition of an electron donating methoxy group) however appears to be less significant (**entry 2 vs. 3**). This is presumably due to resonance-stabilisation of the carbonyl (**Scheme 32**), significantly decreasing the electron donating effect of the methyl ether with respect to delocalisation of electron density on the LUMO of the methylene functionality.



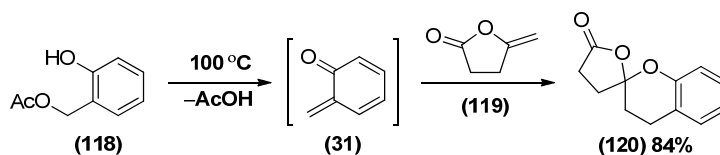
Entry	R ¹	R ²	Yield (%)
1	Me	H	55
2	H	H	58
3	MeO	H	62
4	Me	Br	76
5	H	Br	90
6	MeO	Br	86

Table 3. Thermal [4+2] cycloaddition scope



Scheme 33. Further scope for Li and Xie's [4+2] cycloaddition

Following from the success of this strategy towards unsaturated pyrans, Li and Xie also showed that this strategy could be used to generate saturated [5,6]-bis-benzannulated spiroketals, however with a noticeable reduction in yield (**Scheme 33**).



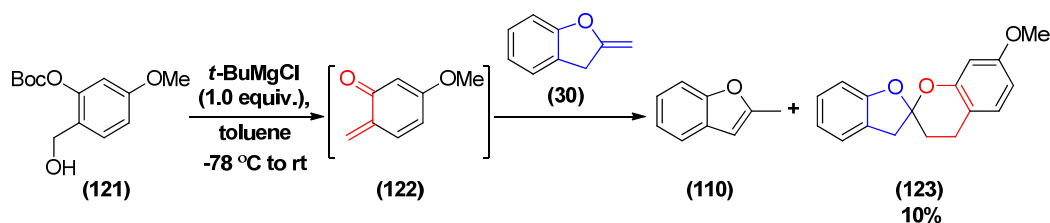
Scheme 34. Further uses of Bray's *h*DA reaction

In the same year, Bray has also demonstrated that [4+2] cycloaddition between an *o*-QM (**31**) generated *in situ* from 2-hydroxybenzyl acetate (**118**) (**Scheme 34**) in neat γ -methylene- γ -butyrolactone (**119**) (which notably did not exhibit *exo-enol* isomerism under the acidic conditions at 100 °C) affording spiroketal (**120**).^{60d} Subsequent screening showed the reaction could also tolerate a range of both electron-rich and electron-deficient *o*-QM species (**Table 4**).

<i>o</i> -QM Precursor		<i>h</i> DA Product		Yield (%)
R ¹	R ²	R ¹	R ²	
H	H	H	H	84
OAc	H	OAc	H	76
CO ₂ Me	H	CO ₂ Me	H	79
H	Br	H	Br	80
H	OMe	H	OMe	75
H	NO ₂	H	NO ₂	82

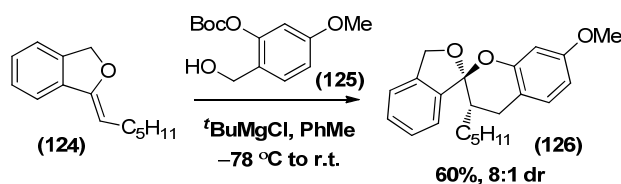
Table 4. Bray's [4+2] thermal cycloaddition products

2.15 Base Initiated *hetero*-Diels-Alder Approach to Spiroketal



Scheme 35. Pettus' base mediated [4+2] cycloaddition approach

Building on these findings, Pettus and co-workers described a mild, base initiated [4+2] cycloaddition reaction in which *o*-QM (122) was generated using 1.0 equiv of *t*-BuMgCl at -78 °C.⁷¹ Unfortunately *exo*-enol isomerism was also a significant even under these milder kinetic conditions, affording (123) in only 10% yield due to significant *exo*-enol isomerism (**Scheme 35**).



Scheme 36. Pettus' paecilospirone model system

This effect was however significantly reduced when the using an *exo*-enol ether that cannot re-aromatise (**Scheme 36**). This was achieved by functionalising the olefin with a *n*-pentyl moiety, which perhaps assists facial selectivity and ultimately furnished the diastereomerically enriched (8:1) paecilospirone model compound (126).

Benzyl alcohol		Chroman spiroketal		Yield (%)	dr ^a
R	R'	R	R'		
H	Bn	H	OBn	61	3:1
H	Boc	H	Boc	77 ^b	3.5:1
Br	Boc	Br	Boc	72	4.5:1

^b The combined yield of the two isomers

Table 5. Pettus' diastereoselective [4+2] cycloaddition substrate scope

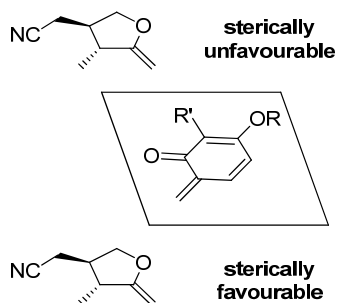
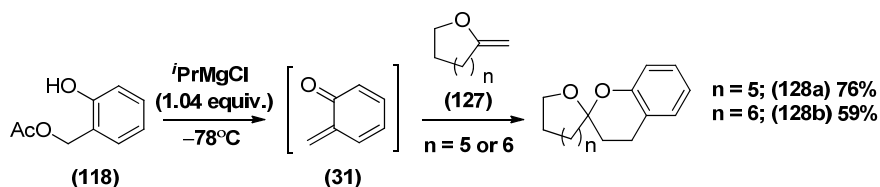


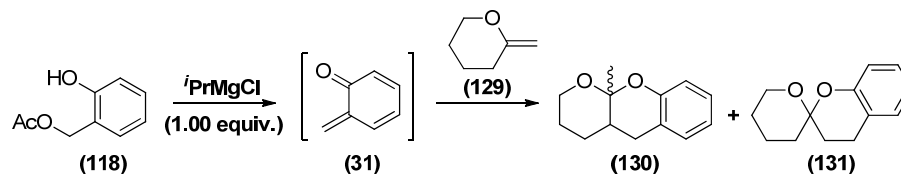
Fig. 11. Sterically driven face selectivity

It is also of note that this methodology was developed alongside a diastereoselective [4+2] cycloaddition to generate a model system for the asymmetric synthesis of berkeleyic acid (**Table 5**).^{72,73} This strategy was successful by introduction of a diastereomerically pure *exo*-enol ether thus biasing the cycloaddition to favour one face preferentially (**Fig. 11**). Unfortunately however an approach of this nature is inherently impossible with a benzofuran as required for a rubromycin approach.



Scheme 37. Bray's mild *hDA* procedure

Contemporaneously to Pettus's findings, Bray also demonstrated a base initiated, [5,6]-benzannulated spiroketal forming *hDA* reaction (**Scheme 37**).^{62d} This transformation was achieved by deprotonating *o*-methylene-acetoxy-phenols such as (**118**) with a slight excess (1.04 equiv.) of *i*PrMgCl base at -78°C to generate *o*-QM (**31**). Pre-formed *exo*-enols such as (**127**) were then added before warming the reaction mixture slowly to room temperature over 16 hours, which promoted a [4+2] cycloaddition to furnish the desired spiroketal (**128a**) in 76% overall yield.

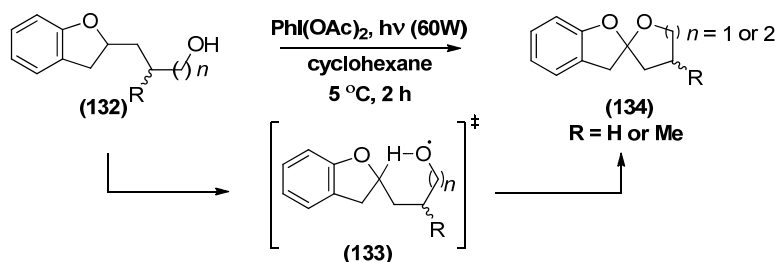


Scheme 38. Bray's *hDA* procedure using 1.00 equiv. of *i*PrMgCl

Intriguingly, when 1.00 equivalent of $t\text{PrMgCl}$ was used to initiate a *h*DA reaction between **(118)** and **(129)** a 6:1 product ratio of **(130)**:**(131)** was obtained (**Scheme 38**). This is presumably from the *h*DA reaction of the *endo*-isomer, thus demonstrating the importance of 100% phenolic deprotonation before addition of the enol ether (See **Scheme 37, 128b** for comparison).

Chapter 2b:
Contemporaneous
Model Studies

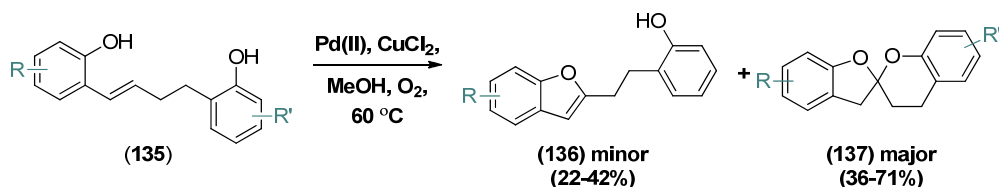
2.16 Brimble's Radical Spirocyclisation Approach



Scheme 39. Brimble's radical approach

During the course of this investigation, there were also a number of reports from the aforementioned research groups, working towards a definitive, robust methodology suitable for the generation of all of these intriguing natural products and synthetic analogues. The first of these was published in 2011 by Brimble and co-workers, in which they demonstrated that spiroketal formation can be facilitated using a photochemically initiated oxidative radical cyclisation (**Scheme 39**).⁷⁴ Higher yields were generally observed for the formation of the 5,5-spiroketal ($n = 1$; 42-92%) relative to 5,6-spiroketal ($n = 2$; 40-73%), which was attributed to intramolecular hydrogen abstraction proceeding through an unfavored seven-membered transition state (**133**, **Scheme 39**, $n = 2$), when forming six-membered rings.

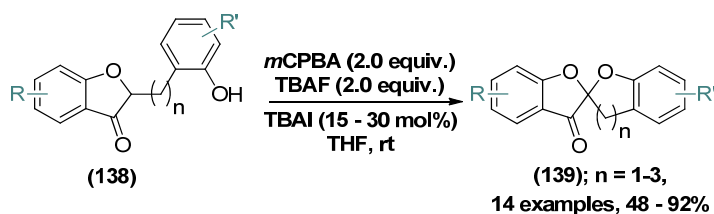
2.17 Li and Xue's Dual Pd(II)/Cu(II)-Catalyzed Spiroketalisation



Scheme 40. Li and Xue's Wacker spiroketalisation

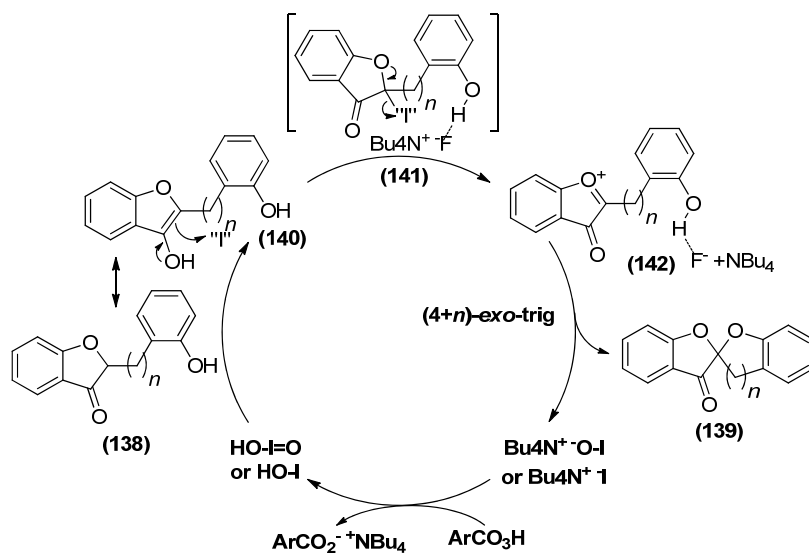
Shortly afterwards Li and Xue also published an adaptation of their previous gold-catalysed spiroketalisation of alkynes (**Scheme 14**), this process however differed in that spiroketalisation was promoted *via* a Pd(II)/Cu(II)-catalyzed chemoselective tandem aerobic cyclisation from phenolic olefins (**Scheme 40**).⁷⁵

2.18 Li and Xue's Fluoride Promoted 6-*exo*-trig Spirocyclisation



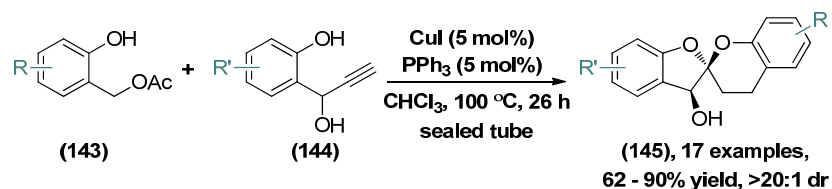
Scheme 42. Li and Xue's spiroketalization conditions

The following year, Li and Xue also reported a 6-*exo*-trig spirocyclisation approach that occurs *via* an apparent dual fluoride/hypoiodite promoted pathway (**Scheme 42**).⁷⁶ Their hypothesis was to generate a hypoiodite reagent *in situ* from *m*CPBA and TBAI to activate the benzofuranone enol tautomer (**140**) towards an unusual S_N1 spiroketalisation. After screening the reaction conditions for additives to increase phenolic nucleophilicity it was observed that TBAF (2.0 equiv.) provides a remarkable increase in isolated yields (42 to 89%; R and R' = H; n = 1). From control experiments it is proposed that the fluoride component enhances nucleophilicity, *via* a proposed H-bonding interaction (**141**). The iodide then eliminates to give an oxonium ion (**142**), which undergoes contemporaneous intramolecular nucleophilic attack, ultimately forming the spiroketal (**Scheme 43**). The reaction was reported to synthesise [5,5],[5,6] and [5,7]-motifs.



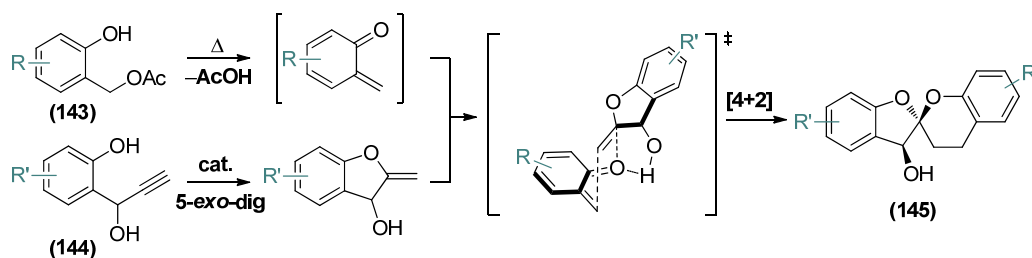
Scheme 43. Proposed catalytic cycle

2.19 Li and Xue's *hetero*-Diels-Alder Approach



Scheme 44a. Xue's copper catalysed cycloaddition cascade

Later that year, Li and Xue also published a diastereoselective cycloaddition route to these moieties *via* a unique cascade process (**Scheme 44a**).⁷⁷ This strategy revolves around the ability to convert an *ortho*-propenyl phenol into an *exo*-cyclic enol ether *via* a copper catalysed 5-*exo*-dig cyclisation and simultaneously form an *o*-QM thermally in one pot. These reactive intermediates then combine *via* a *h*DA reaction with remarkable diastereoselectivity. This selectivity appears to arise from a proposed transition state involving a hydrogen-bonding interaction between 3'-hydroxy group and the carbonyl of the *o*-QM (**Scheme 44b**). The scope of this reaction was also very good, tolerating a range of electron withdrawing and donating groups in generally good yields (62-90%) and excellent diastereoselectivities (>20:1).



Scheme 44b. Proposed reaction mechanism

Chapter 3:
Total Synthesis
Studies

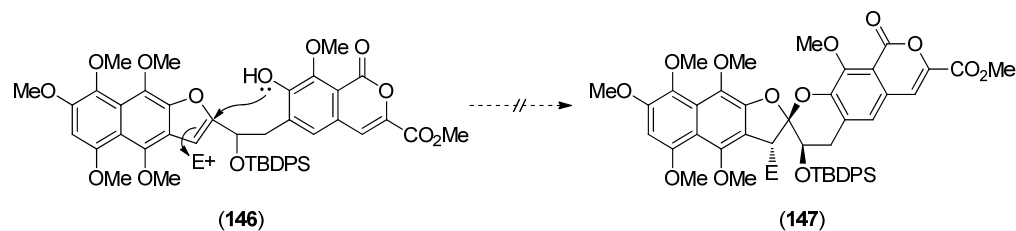
3.1 Introduction

When it comes to Nature's molecular architecture, the secondary metabolites with their eclectic myriad of designs, have perhaps been the most admired and sought-after targets for synthetic chemists.⁷⁸ Although structural beauty and novelty are important reasons to synthesise natural products, biological activity is often the key driving force behind these projects. This is of particular importance for biologically active compounds that can only be isolated in minute quantities. An ideal strategy in this field would be convergent, employ mild conditions and minimal use of cumbersome and atom inefficient protecting group chemistry.

As the rubromycins have both structurally and biologically intriguing properties, it is of little surprise that a number of research groups have endeavoured to synthesize them in recent years.⁷⁹ Although the five strategies outlined in chapter two had been reported at the start of this investigation, there was still very little known in terms of their robustness. This chapter will therefore outline the collective synthetic efforts from these research teams in applying their methodologies, to the synthetic challenge of the rubromycins and their analogues. Again this chapter shall be divided into reports published before the outset of this investigation (**Chapter 3a**), and those reported during this study (**Chapter 3b**).

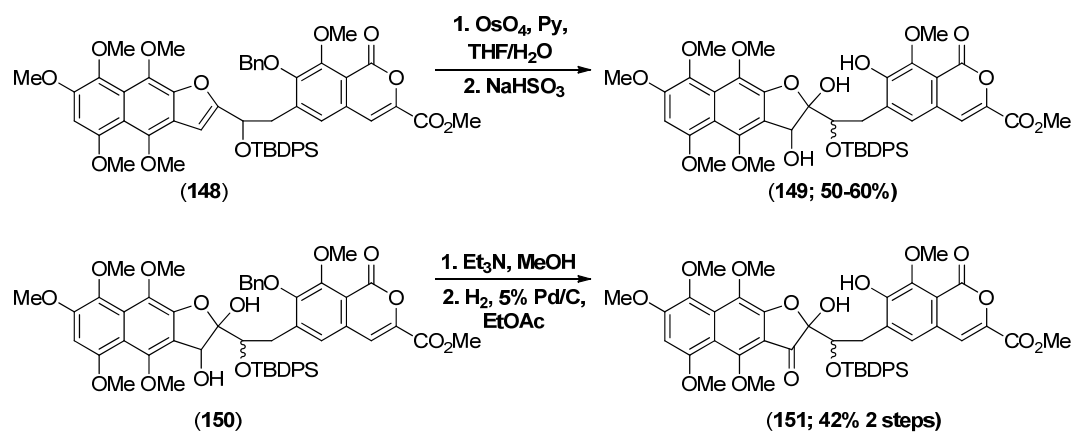
Chapter 3a:
Previous Total
Synthesis Studies

3.2 Danishefsky's Total Syntheses of Heliquinomycin Aglycone



Scheme 45. Danishefsky's failed spirocyclisation

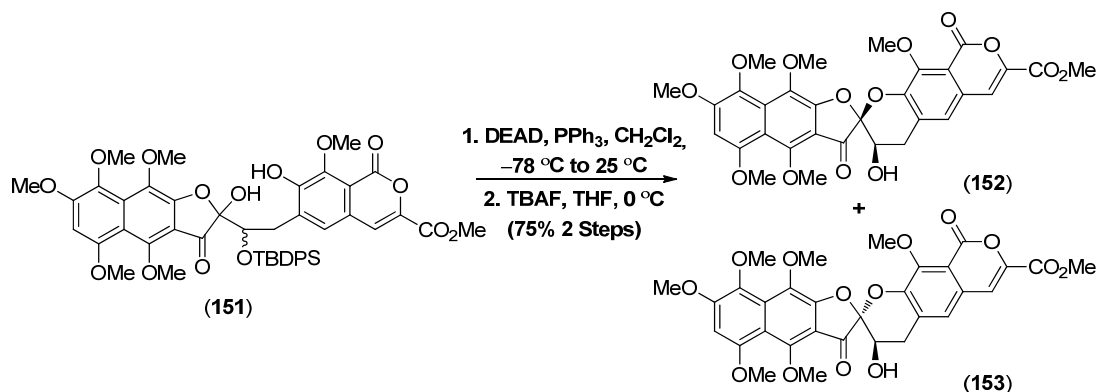
In 2001 Danishefsky and co-workers reported the total synthesis of the heliquinomycin aglycone (heliquinomycinone) (**10**).⁸⁰ Building on their diastereoselective model system (**Scheme 12**), naphthofuran (**146**) was prepared as they envisaged that upon treatment with NBS, diastereoselective intramolecular cyclization could be achieved in the same fashion (**Scheme 45**). Unfortunately, due to the electron-rich nature of the pentamethoxy-naphthalene ring, (**147**) could not be generated using NBS, or upon subjection of the material to a variety of other halogenating, epoxidising and bond-activating metal-based reagents.



Scheme 46. Danishefsky's serendipitous generation of spirocyclisation precursor (**151**)

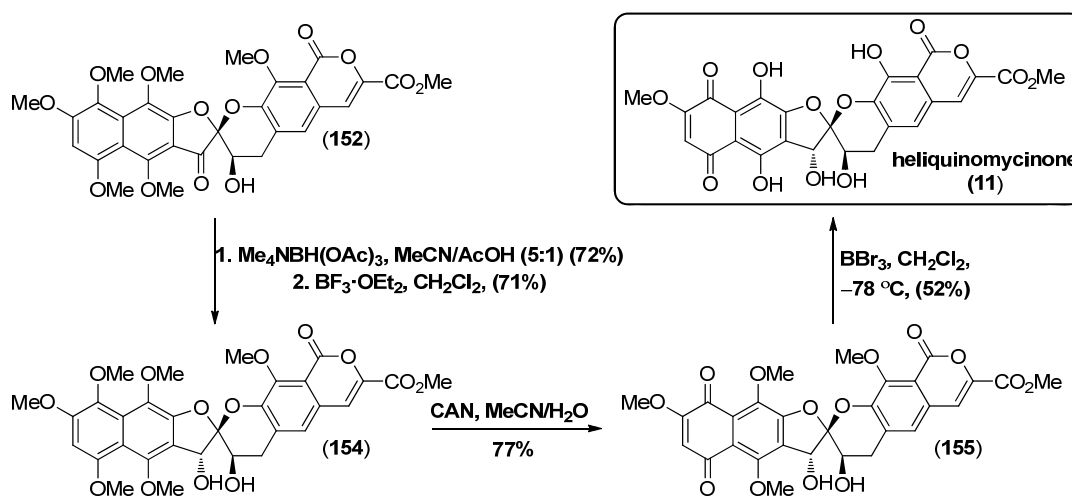
Successful oxidation of the targeted furan was however achieved using osmium tetroxide (**Scheme 46**) without compromising structural integrity, giving rise to a 1:1 mixture of inseparable diastereomers (**149**). Serendipitous exposure of the benzylated diastereomeric products (**150**) to air in the presence of triethylamine/methanol (the author presumes during chromatography) lead to selective oxidation of the hydroxyl group on

the furan moiety. Removal of the benzyl ether was subsequently achieved by hydrogenolysis to furnish the modified anomeric cyclisation precursor (**151**).



Scheme 47. Danishefsky's Mitsunobu spirocyclisation

The desired cyclization could then finally be achieved under optimised Mitsunobu conditions (**Scheme 47**),⁸¹ affording a 1.2:1 mixture of spiroketals (**152**) and (**153**) (after desilylation) that could be separated cleanly.

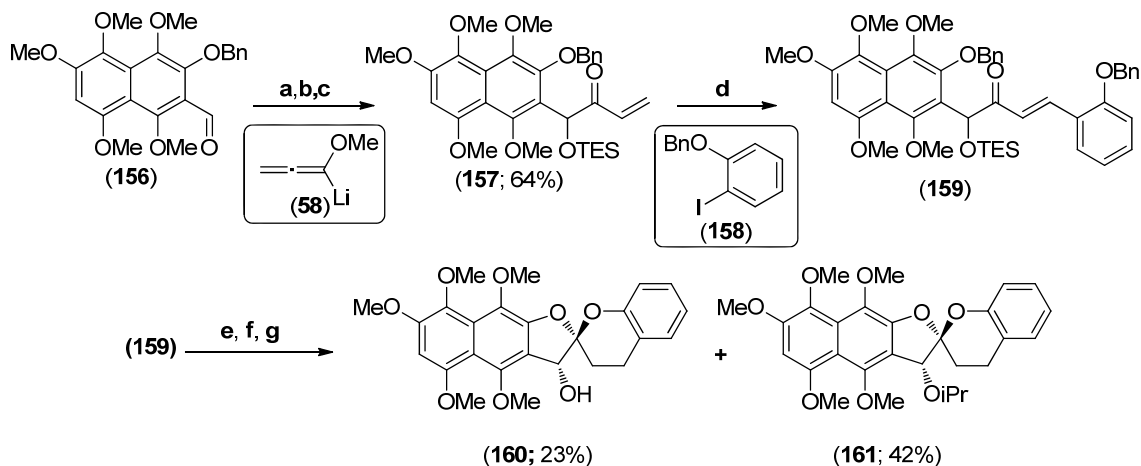


Scheme 48. Danishefsky's completion of heliquinomycinone (**11**)

Ketone (**152**) was then stereoselectively reduced using tetramethylammonium triacetoxyborohydride before subsequent treatment with BF₃·OEt₂ promoted inversion of the dihydrofuran alcohol, required to furnish the correct stereochemistry of heliquinomycin-[5,6]-spiroketal core (**Scheme 48**). The naphthyl aglycone precursor (**154**) was then selectively oxidised to the desired methylated precursor (**155**) upon treatment with CAN. The unnatural rubromycin analogue heliquinomycinone (**11**) was then furnished *via* regiospecific demethylation of the aryl-methoxy substituents of (**155**) using

the comparatively mild $\text{BBr}_3 \cdot \text{Me}_2\text{S}$ complex at -78°C in 52% yield. Unfortunately, after several attempts this material could not be glycosylated with a cymarose moiety to give the desired natural product (**10**).

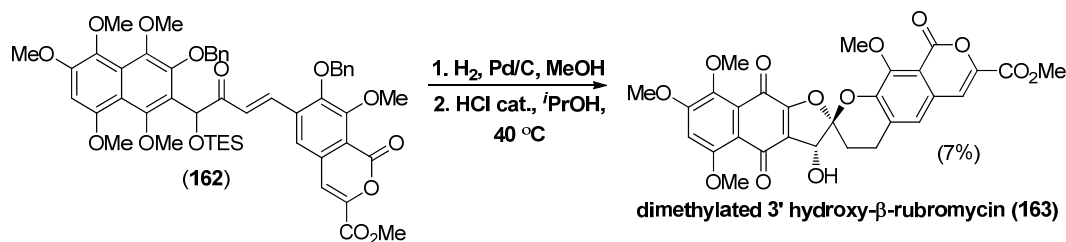
3.3 Reißig's Cyclisation Approach



a. **(58)**, THF, -78°C ; b. H_2SO_4 , THF, 0°C ; c. TESCl, *i*PrNEt, DMF; d. $\text{Pd}(\text{OAc})_2$, NaHCO_3 , TBACl, mol. sieves, DMF, 60°C ; e. Pd/C, H_2 , MeOH, 2d; f. cat. HCl 21 h; g. cat. conc. HCl, *i*PrOH, 50°C , 2 d

Scheme 49. Generation of Reißig's advanced model

Building on their previous findings (**Section 2.6**) Reißig and co-workers subsequently demonstrated in 2006 that their methodology could tolerate functionalised naphthazarin precursor (**156**) in an advanced model study to generate spiroketalisation precursor (**159**). Exposure of (**159**) to spiroketalisation conditions afforded a clean mixture of hydroxyl (**160**) and alkoxy (**161**) spiroketals^c as single diastereomers (**Scheme 49**).⁴³



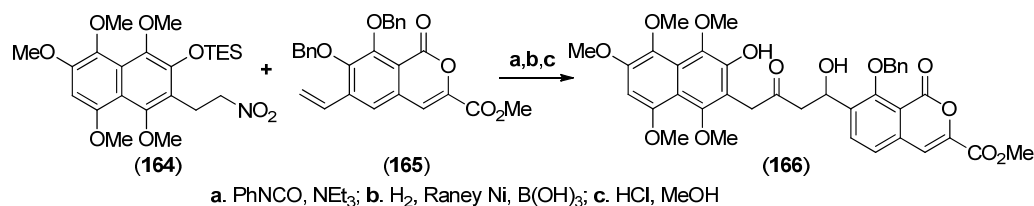
Scheme 50. Reißig's synthesis of dimethylated 3'-hydroxy- β -rubromycin (**163**)

Surprisingly when advanced intermediate (**162**) was exposed to the identical conditions, a complex product mixture was produced, leading to isolation of the *trans*-dimethylated

^c Generated from solvolytic displacement of the benzylic alcohol

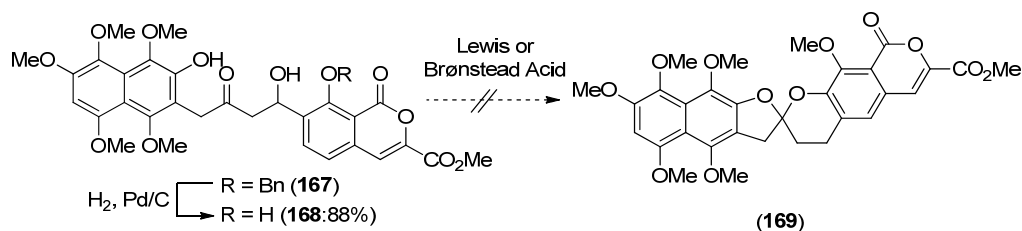
3'-hydroxy- β -rubromycin (**163**) in markedly reduced yields (7%) (**Scheme 50**).⁸² Due to this markedly reduced level of product formation, it appears that electronic complications of the electron-rich naphthalene and the electron-deficient isocoumarin moieties are detrimental to rubromycin synthesis *via* an intramolecular cyclisation pathway. Reißig and co-workers hypothesised that electronically well-balanced aromatics would therefore be required to facilitate a successful Brønsted-acid promoted spiroketalisation.

3.4 Kozłowski's Attempted Synthesis of Pupuromycin



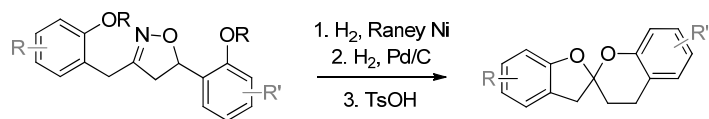
Scheme 51. Kozłowski's synthesis of advanced spirocyclization precursor (**166**)

Also in 2006, Kozłowski and co-workers demonstrated that their elegant [3+2]-cycoaddition procedure (see section 2.5) could be employed to generate the desired pupuromycin spirocyclization precursor (**166**) in a relatively convergent manner (3 steps from naphthalene (**164**) and isocoumarin (**165**) precursors), (**Scheme 51**).



Scheme 52. Kozłowski's failed acid mediated spiroketalization

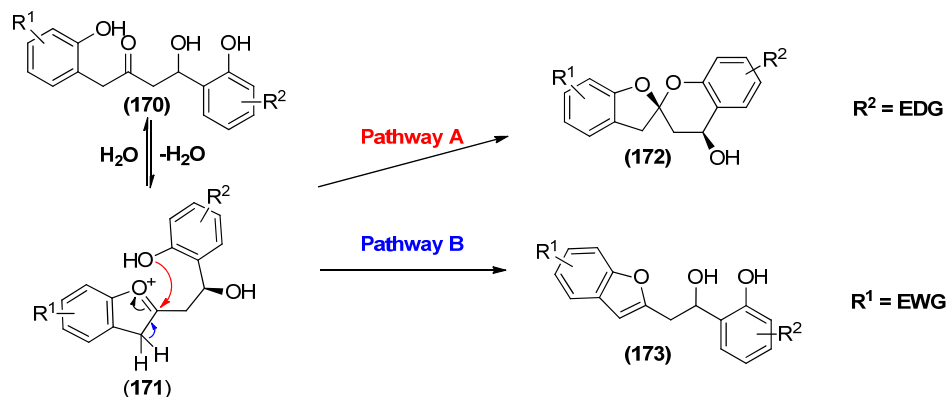
Similar to Reißig's findings, a Brønsted acid-promoted spiroketalisation reaction could not be achieved (**Scheme 52**). To try and develop a more precise understanding of this chemistry they carried out a combinatorial screening study of isoxazoline spirocyclisation precursors using conditions from their model study (**Table 6**).



Entry	Isoxazoline	Product	Yield (%)
1			72
2			66
3			46

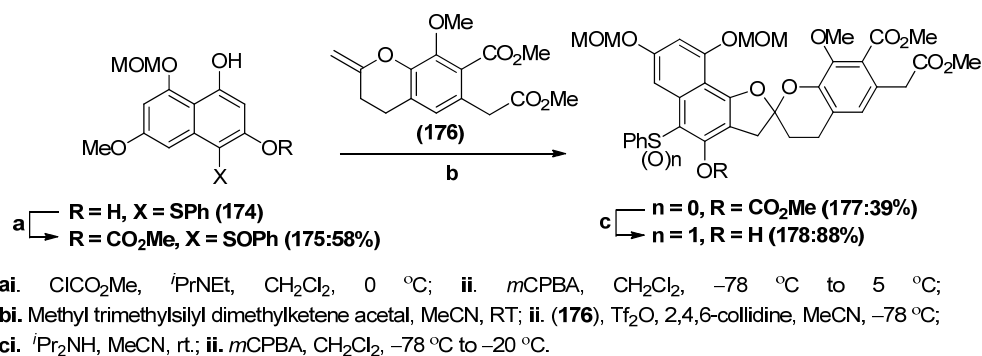
Table 7. Kozolwski's combinatorial screening results

Their results (**Table 7**) suggest that the nucleophilicity of the isocoumarin alcohol can be a critical hinderance to the desired approach (**Scheme 53, Pathway A**). This appears to be due to the inductive effects of the two carbonyl substituents of the isocoumarin diminishing this phenolic nucleophilicity, such that the irreversible formation of the stable aromatic furan becomes the dominant pathway (**Pathway B**).



Scheme 53. Electronic effects on spirocyclization

3.5 Kita Total Synthesis of γ -Rubromycin

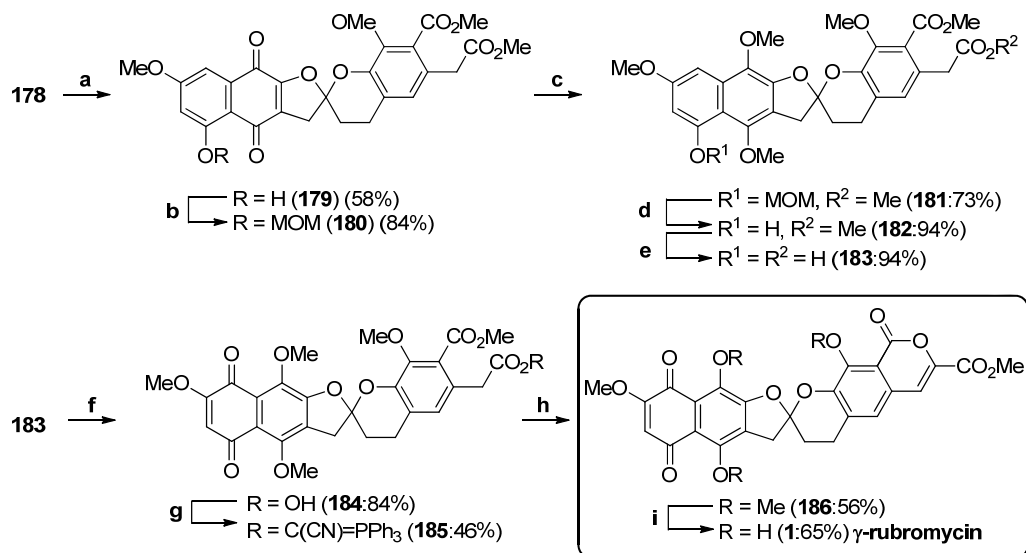


Scheme 54. Kita's Pummerer key spiroketal formation step

Having demonstrated a convergent methodology to furnish the model pentacyclic ketal (**81**) (Section 2.9), Kita *et al.* then began efforts towards the synthesis of γ -rubromycin (**1**) in 2007.⁸³ Upon subjection of the advanced isocoumarin (**176**) and naphthalene (**175**) precursors to the Tf_2O promoted aromatic Pummerer-type reaction conditions, spiroketal product (**178**) was furnished as expected, in 39% yield (Scheme 54).^d

Subjection of the resultant spiroketal (**177**) to $t\text{Pr}_2\text{NH}$ afforded the naked phenol, followed by oxidation using *m*-CPBA to furnish the pre-requisite sulfoxide reagent (**178**). Treatment with TFAA, promoted a second aromatic Pummerer-type reaction to form an *ortho*-quinone intermediate [analogous to (**78**) in the mechanism outlined in (Scheme 19)]. This in turn, linearly converted to the paraquinone species (**179**) with concomitant removal of the methoxymethyl (MOM) protecting group (Scheme 55).

^d It should also be noted that based on Reißig and Kozłowski's earlier reports, Kita had postponed installation of the isocoumarin motif until after formation of the spiroketal.



ai. TFAA, CH_2Cl_2 , 0°C ; ii. TFA, CH_2Cl_2 , 0°C ; **b.** MOMCl, $i\text{Pr}_2\text{NEt}_3$, CH_2Cl_2 , 0°C ; **c.** $\text{Na}_2\text{S}_2\text{O}_4$, Me_2SO_4 , K_2CO_3 , acetone, reflux; **d.** TFA, CH_2Cl_2 , 0°C ; **e.** 10% KOH, MeOH, RT; **f.** $[\text{Co}(\text{salen})_2]$, O_2 , DMF, RT; **g.** (triphenylphosphonylidine)acetonitrile, EDCI, DMAP, CH_2Cl_2 , RT; **h.** dimethyldioxirane, MeOH, 0°C ; **i.** BBr_3 , CH_2Cl_2 , -78°C to 0°C .

Scheme 55. Kita's total synthesis of γ -rubromycin (**1**)

After MOM reprotection, quinone reduction and methylation the corresponding dihydroxyquinone dimethyl ether (**181**) could be generated before selective MOM deprotection and base-catalysed hydrolysis afforded the phenolic carboxylic acid (**183**) in good yield (88% over 2 steps). $[\text{Co}(\text{salen})_2]$ catalysed oxidation of the naphtholene afforded the desired paraquinone species (**184**) (84%), which upon subjection to Wong's conditions⁸⁴ facilitated conversion of the carboxylic acid moiety to the α -keto ester intermediate (**185**) before immediately cyclising to furnish the desired lactone (**186**). Regiospecific BBr_3 deprotection of the methoxy substituents afforded the desired γ -rubromycin species (**1**) in <1% overall yield and marked the first reported chemical synthesis.

3.6 Project Aim

At the start of this investigation into the rubromycins, the author (like many of the aforementioned research groups) was motivated by both the synthetic challenge of constructing the rubromycin scaffold, as well as the prospect of synthesising unnatural analogues possessing more “drug-like” physiochemical properties, to be employed as “tool” compounds for target validation of telomerase in the field of oncology.

To explore either of these areas, development of a robust synthetic route towards these secondary metabolites was clearly of paramount importance. To accomplish this, our approach embraced the philosophy that a synthetic route is of most use when it is convergent.⁸⁵

As the field of total synthesis is arguably the toughest test for newly developed synthetic methodology, this investigation hoped to explore both the strengths and limitations of Bray’s *h*DA methodology^{62d} (**Section 2.14**) and further develop this chemistry towards the syntheses of the rubromycins. It was anticipated that this procedure would have the major advantage, over strategies “A” and “B” (**Fig. 5**), of generating two C–C bonds in modular process. It was also hoped that milder conditions than those used in strategies “C” and “D” (**Fig.5**) could also be employed, allowing for greater functional group tolerance.

As developing the [4+2] cycloaddition step was the main objective central to these goals, γ -rubromycin (**1**) was chosen as the primary synthetic target, as a number of potentially useful late stage functional group modifications had already been described in the prior art by Kita (**Scheme 55**).⁸³

Chapter 3b:
Contemporaneous
Total Synthesis
Studies

3.7 Brimble's Formal Synthesis of γ -Rubromycin

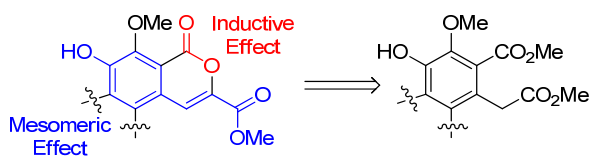


Fig. 12. Retrosynthetic analysis of isocoumarin precursor

From the very outset of this investigation it was however very clear that we were not the only research group keen to improve on Kita's procedure towards the rubromycins (**Section 3.5**).⁸⁶ The first of these reports by Brimble, appeared in the literature almost immediately after this projects inception in 2009. Drawing from the previous hypotheses generated by Reißig and Kozłowski that delicate electronic balancing of aromatic units should permit Brønsted acid-promoted spiroketalization, Brimble and co-workers, were convinced that spirocyclization would be possible only by paying deserved attention to the use of an appropriate isocoumarin ring precursor, due to its dual inductive and mesomeric properties (**Fig. 12**).

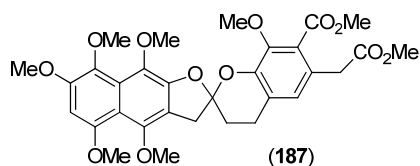
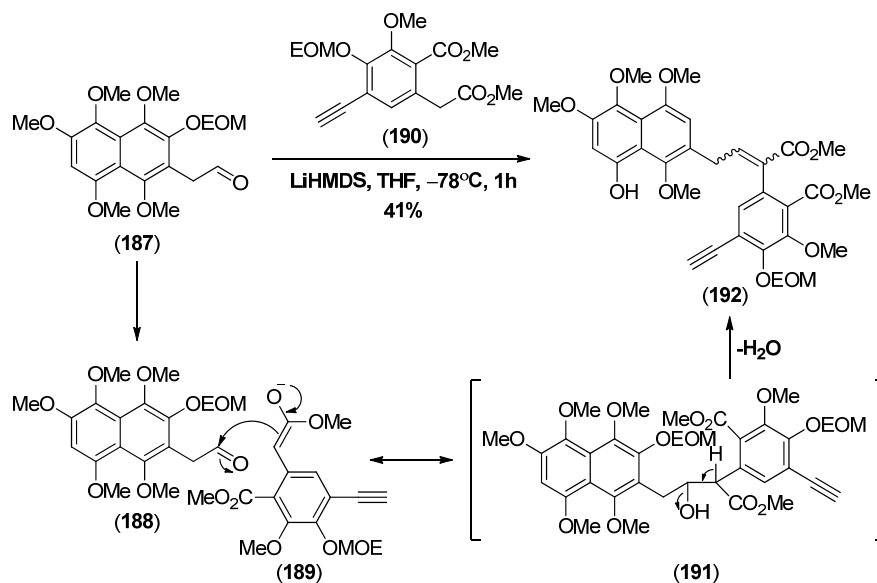


Fig. 13. Brimble's key intermediate

In an attempt to overcome this significant hurdle in the synthesis of pentacyclic spiroketals, isocoumarin ring formation was as in Kita's investigation noticeably postponed until after the key spiroketalisation step. Their hypothesis was that this would significantly reduce the electron-withdrawing mesomeric effect of the eastern fragment and consequently increase the nucleophilicity of the phenol, thus encouraging the key acid-promoted spiroketalisation as previously demonstrated (**Section 2.4**) to give the key intermediate [5,6]-bis-benzannulated spiroketal (**187**) (**Fig. 13**).

Having synthesised key advanced intermediates (**188**) and (**190**) Brimble and co-workers anticipated utilisation of the Sonogashira-acetylide methodology developed during their model study (**Scheme 8**) would facilitate a suitable spirocyclization precursor.

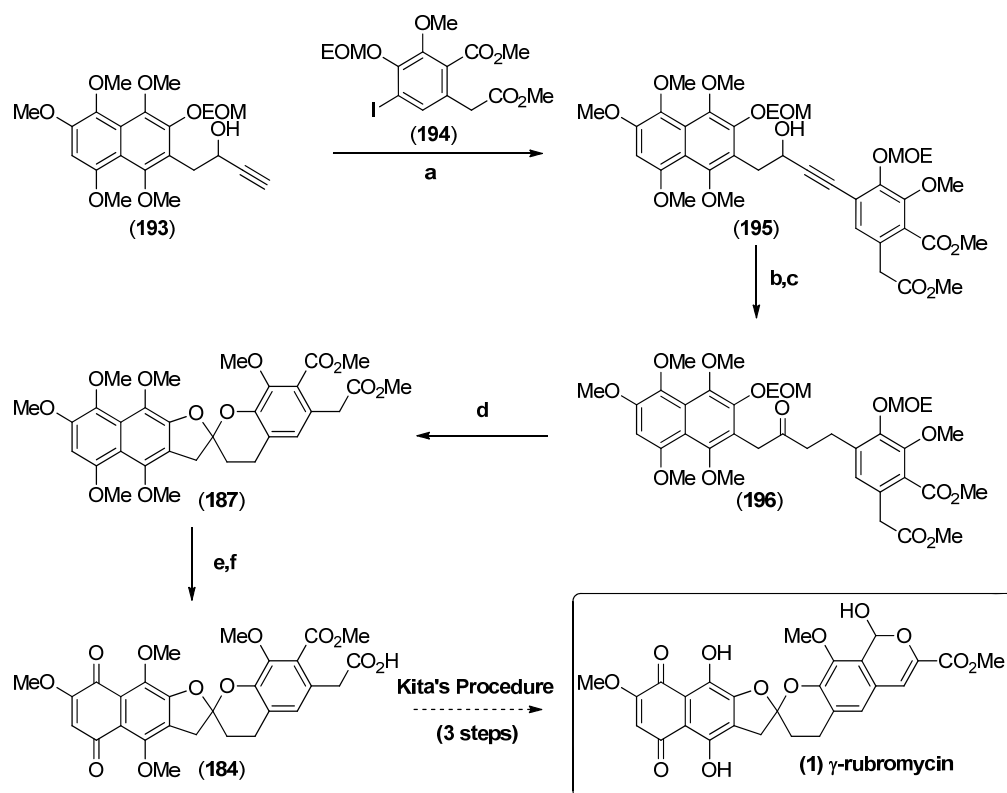
Unfortunately attempts to promote the lithium-mediated process were unsuccessful due to the formation of adduct (**192**) *via* aldol condensation of the methyl ether enolate (**189**) with aldehyde (**188**).



Scheme 56. Adduct (**192**) formation by aldol condensation

Due to this setback, Brimble consequently adjusted this strategy to avoid the lithium-mediated process by using the acetylene (**193**) and iodide species (**194**) as Sonogashira coupling partners (**Scheme 57**). The coupling was successful yielding the desired tricyclic acetylene (**195**) in 91% yield.^e Subsequent hydrogenation of the alkyne followed by oxidation of the alcohol using 2-iodoxybenzoic acid (IBX) afforded the desired spirocyclisation precursor (**196**) in 95% yield (over 2 steps). Spirocyclization was then successfully achieved using the conditions developed during previous model studies furnishing the desired 5,6-*bis*-benzannulated spiroketal (**187**) in 80% yield. Kita's advanced intermediate (**186**) was finally achieved by selective hydrolysis of the aliphatic ester to the carboxylic acid thus completing a formal synthesis of γ -rubromycin (**1**) in 17 steps (equivalent to 1.4% yield of natural product **1**).

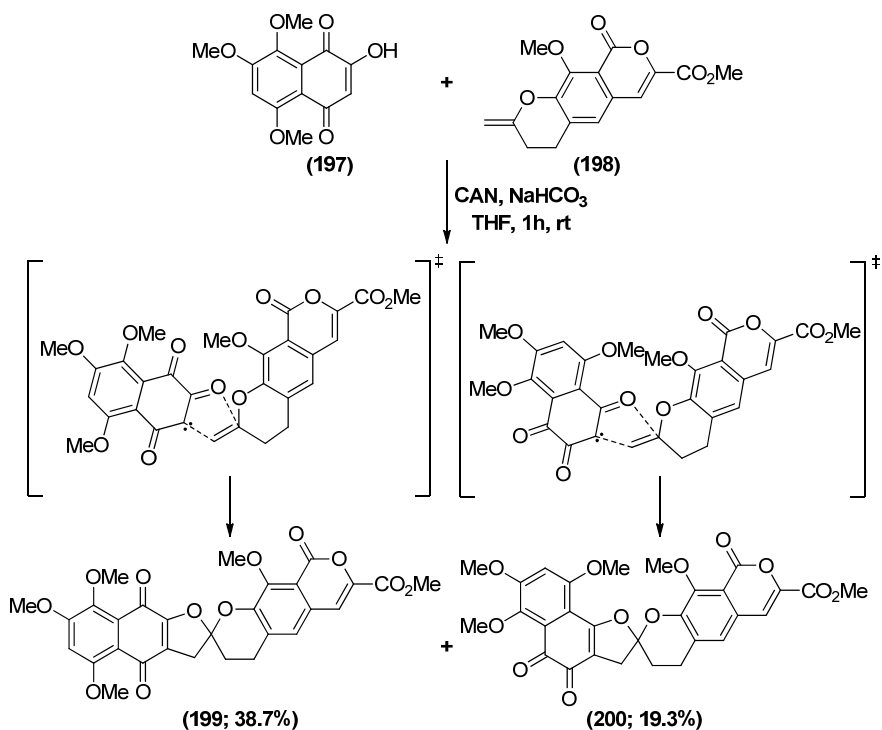
^e Non amine base (Cs₂CO₃) was used to minimise homo-coupling.



Scheme 57. Brimble's synthesis of Kita's Advanced intermediate (**184**)

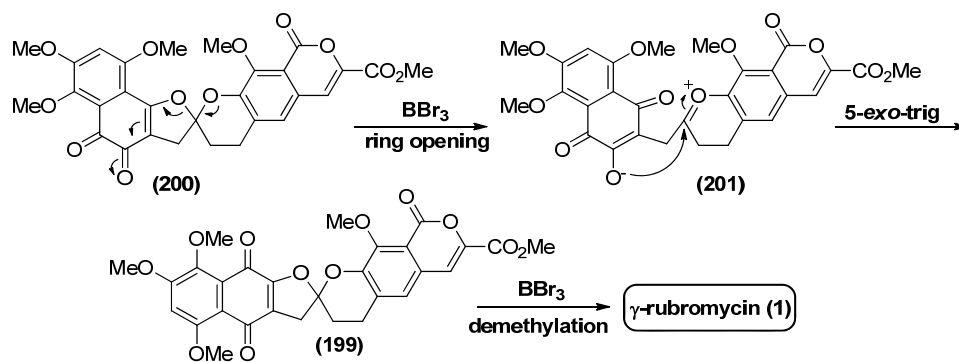
3.8 Pettus' Total Synthesis of γ -Rubromycin

Subsequently in 2010, during our ongoing synthetic efforts towards a modular approach to the rubromycins, Pettus and co-workers reported the first successful cycloaddition approach based around their previous model studies (**section 2.10**). Having successfully generated reasonable quantities of both the desired quinone (**197**) and *exo*-enol ether (**198**), they demonstrated that these intermediates could indeed be coupled in the presence of CAN to give a 1:2 mixture of *para*- and *ortho*-quinones (**199**) and (**200**) respectively (**Scheme 58**).



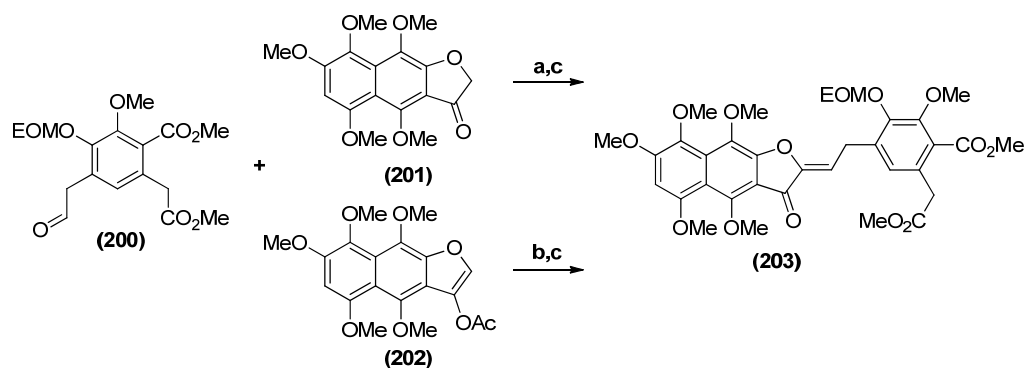
Scheme 58. Pettus [3+2] key cycloaddition step

Fortuitously, deprotection and concomitant tautomerization of both individual isomers with BBr₃ converged to the desired title compound (**Scheme 59**) in a total yield of 31.1% (over two steps) *via* a similar rearrangement described previously by Kita (**Scheme 18**), thus furnishing the title compound in 4.4% overall yield.



Scheme 59. Pettus' BBr₃ promoted quinone tautomerization to γ -rubromycin (**1**)

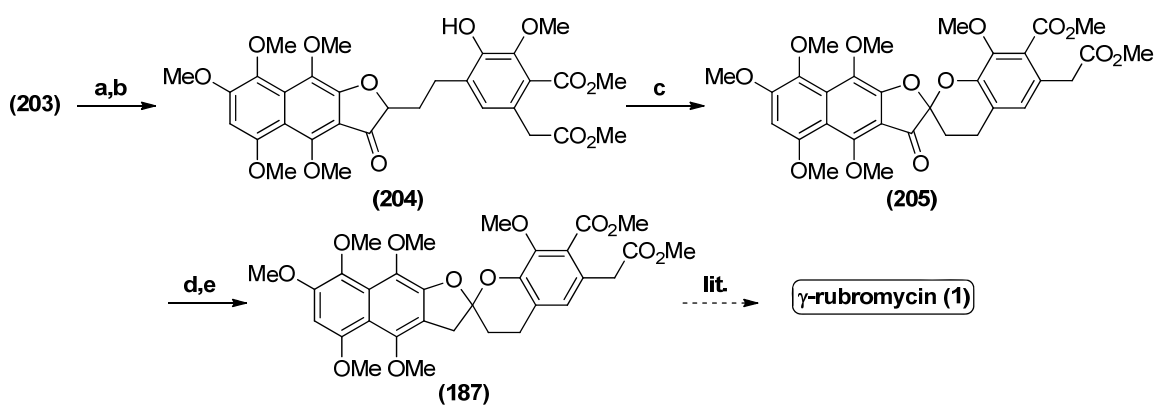
3.9 Li and Xue's Formal Synthesis of γ -Rubromycin



a. LiHMDS, THF, $-78\text{ }^{\circ}\text{C}$ to $-40\text{ }^{\circ}\text{C}$, 4 h, (82%); b. LDA, THF, $-78\text{ }^{\circ}\text{C}$ to $-40\text{ }^{\circ}\text{C}$ (85%);
 c. MsCl, Et₃N, $-78\text{ }^{\circ}\text{C}$ to $-40\text{ }^{\circ}\text{C}$, 1 h, (86%)

Scheme 60. Xue and Li's fragment γ -rubromycin coupling reactions

In 2012, Li and Xue also managed to achieve a formal synthesis of γ -rubromycin (**1**) *via* their aforementioned fluoride promoted 6-*exo*-trig spirocyclisation approach (section 2.18). This procedure was however less elegant than Pettus' approach due to a lack of convergence, requiring five steps post fragment coupling to generate (**187**). A further drawback was the rather protracted synthesis of the pre-requisite naphofuran ketone (**201**) or naphofuran (**202**) species. Union of the fragments could then be achieved *via* aldol condensation to furnish the key cyclisation precursor (**203**) (Scheme 60).

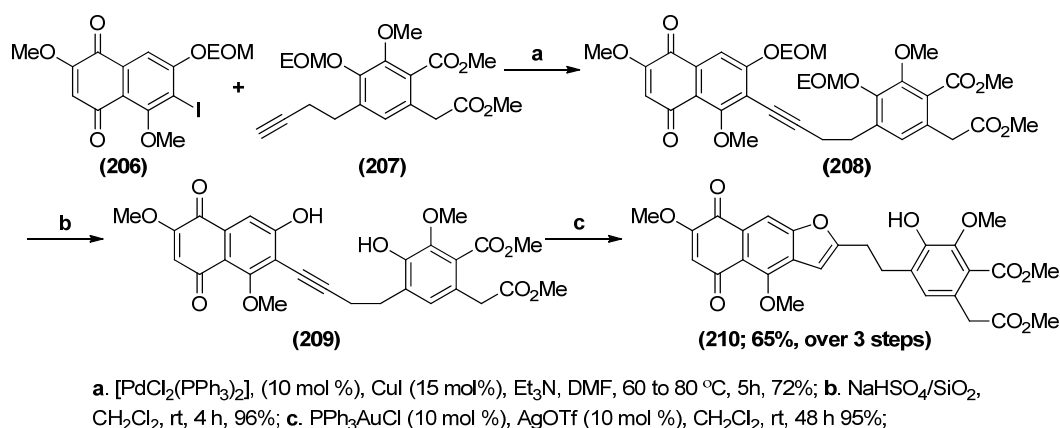


a. H₂, Pd/C, MeOH, dioxane, 2h, (98%); b. TFA, 0 $^{\circ}\text{C}$ (98%); mCPBA, TBAF, TBAI, THF, rt, 1h (88%);
 d. NaBH₄, MeOH, 0 $^{\circ}\text{C}$, 10 min (95%); e. Et₃SiH, TFA, 50 $^{\circ}\text{C}$, 5 min, (81%).

Scheme 61. Xue and Li's possible fragment coupling reactions

Subsequent hydrogenation and phenolic deprotection furnished naked phenol (**204**), before treatment with *m*-CPBA, TBAF and TBAI promoted the desired hypiodide species facilitating spiroketalization in an impressive 88% yield at room temperature (**Scheme 61**). The naphofuran ketone was then removed selectively in a stepwise reduction using NaBH₄, then Et₃SiH/TFA to afford Brimble's key intermediate (**187**), thus completing a formal synthesis of γ -rubromycin (**1**) in a yield equivalent to 0.9-1.2% for (**1**)^f.

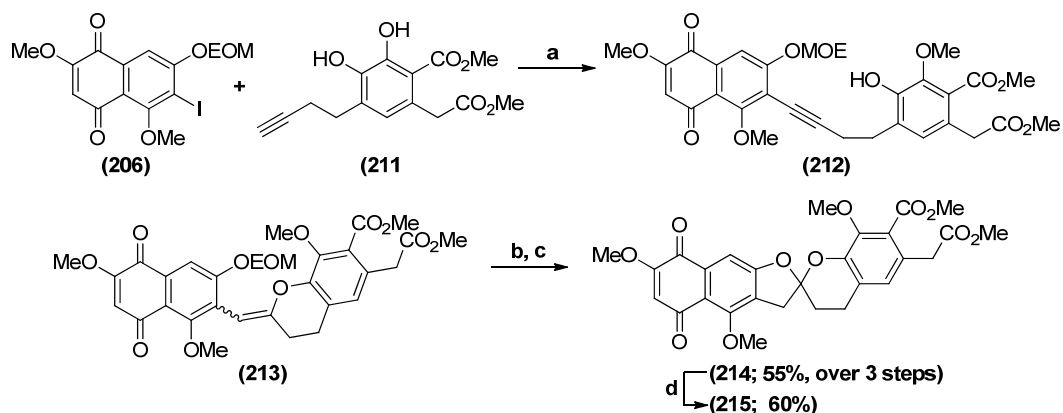
3.10 Li and Xue's Total Synthesis of δ -Rubromycin



Scheme 62. Xue and Li's δ -rubromycin fragment coupling reactions

Shortly afterwards, Li and Xue also successfully synthesised δ -rubromycin using a modified version of a transition-metal-catalysed cascade spiroketalization (**Section 2.7**). Advanced model alkyne was generated *via* a Sonogashira coupling between (**206**) and (**207**), before blanket EOM-deprotection furnished the prerequisite diol (**209**) (69% over 2 steps). However upon subjection of the intermediate, to the previously optimised conditions (**Scheme 14**) benzofuran formation was exclusively observed (95%) (**Scheme 62**), which could only be further cyclised to the spiroketal in trace amounts upon treatment with AuCl, K₂CO₃ and CH₃CN at 70 °C for 24 h.

^f Yield calculated for (**1**) using literature yields for the final steps.

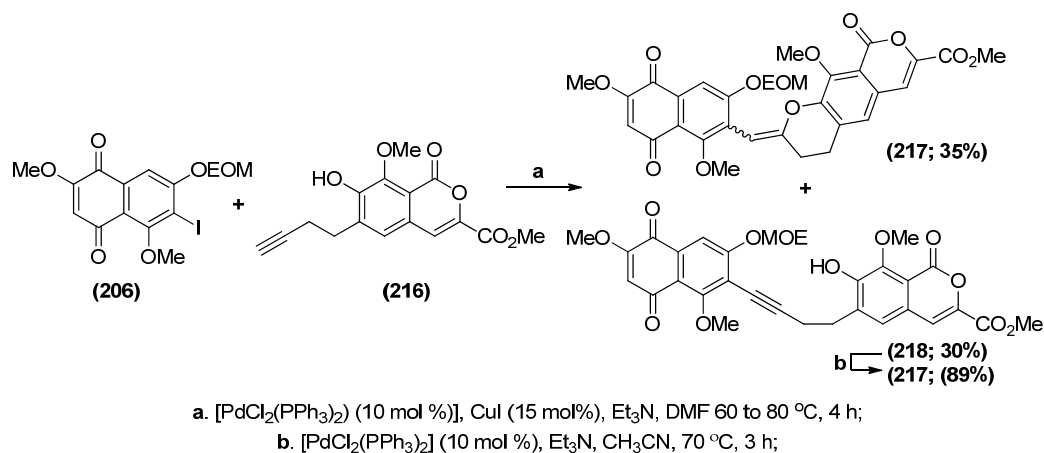


a. $[\text{PdCl}_2(\text{PPh}_3)_2]$, (10 mol %), CuI (15 mol%), Et_3N , DMF, 60 to 80 °C, 5h, 70%; **b.** AuCl (10 mol%), K_2CO_3 (10 mol%), CH_3CN , 70 °C, 6 h, 90%; **c.** AgOTf (10 mol %), CH_2Cl_2 , rt, 8 h 87%; **d.** BBr_3 , CH_2Cl_2 , -78 to -20 °C, 0.5 h, 60%.

Scheme 63. Xue and Li's transition metal catalysed spiroketalization, towards δ -rubromycin

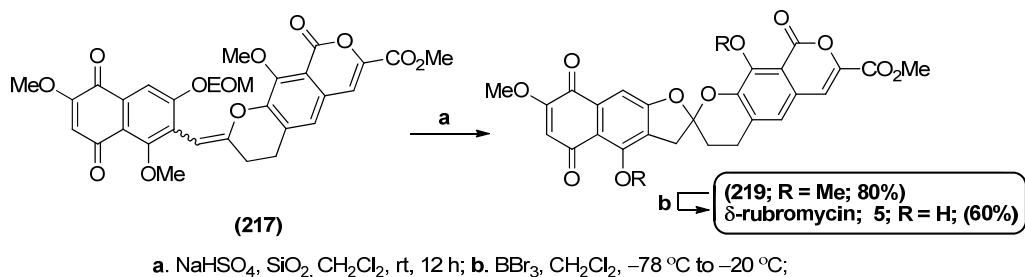
With the aim of circumventing benzofuran formation prior to nucleophilic attack of the isocoumarin phenolic oxygen atom, Xue and Li repeated the Sonogashira coupling with the unprotected phenol (**211**). When the corresponding alkyne product (**212**) was exposed to a catalytic amount of AuCl and K_2CO_3 , benzopyran (**213**) was generated in excellent yield (90%). Exposure to AgOTf afforded the desired spiroketal (**214**) *via* a transition-metal-catalysed spiroketalisation in 87% yield. Although one, could envisage completion of δ -rubromycin from the resultant product *via* Kita's protocol (Section 3.5, Scheme 55), attempts were then made towards a fully convergent approach using the fully elaborated isocoumarin.

Unfortunately, upon repeating the Sonogashira coupling reaction with a fully elaborated isocoumarin a mixture of alkyne (**218**) and pyran (**217**) were observed. Interestingly the alkyne could not be cyclised using $\text{AuCl}/\text{K}_2\text{CO}_3$ as described previously (Scheme 64). However upon subsection of the alkyne to $[\text{PdCl}_2(\text{PPh}_3)_2]$, the pyran could be generated in 89% yield.



Scheme 64. Xue and Li's palladium catalysed Sonagashira/pyran formation procedure

Subsequent removal of the MOM ether revealed the naked phenol, which underwent concomitant spiroketalization *via* a 5-*endo*-trig ring closure to furnish the desired spiroketal (219). Gratifyingly upon treatment of the resultant spiroketal with BBr_3 regioselective demethylation could be achieved to furnish δ -rubromycin (5) in an impressive 8.7% overall yield (**Scheme 65**).



Scheme 65. Xue and Li's synthesis of δ -rubromycin (5)

Chapter 4:
Results & Discussion

4.1 - Retrosynthetic Analysis

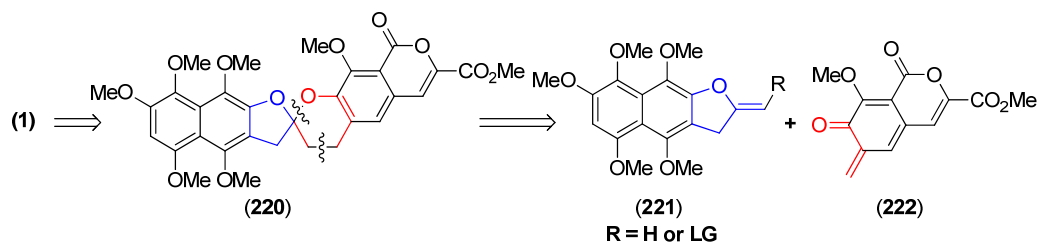


Fig. 14. Retrosynthetic analysis of key intermediate (220)

Retrosynthetic disconnection of two carbon-carbon bonds of γ -rubromycin (**1**), proposed for a [4+2] cycloaddition reaction affords *exo*-enol ether (**221**) and *o*-QM (**222**). It was therefore anticipated that if the mild inverse electron-demand *h*DA conditions could tolerate the electronics of these moieties, then a convergent synthesis amenable to analogue development may be possible.

It was however, clear from the outset that due to the formation of the spiroketal at a very late stage, this strategy was to carry a certain degree of risk. An additional concern for this strategy was that a [4+2] cycloaddition, had never, to the author's knowledge, been achieved with such an electron-deficient *o*-QM.

Fortunately, due to the great volume of work previously undertaken in this key research area, several routes to various isocoumarin and naphthazarin subunits of the rubromycin family had been previously reported (see Section 3). This information was extremely valuable as an efficient and reproducible route to these subunits was thought to be an essential requirement for this strategy to be effective.

Naphthazarin Synthesis

“Architecture starts when you carefully put two bricks together. There it begins”

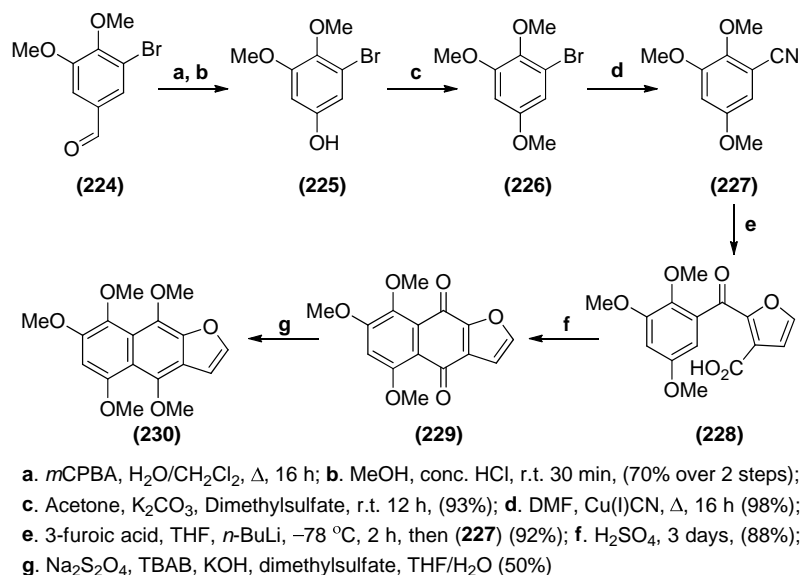
Ludwig “Mies” van der Rohe (1886 –1969),

German Architect

4.2 Danishefsky's Naphthazarin Synthesis

As the benzofuran moiety, is also a fundamental pre-requisite in the 6-*exo*-trig spirocyclisation approach, Danishefsky's synthesis of heliquinomycinone (Section 3.2) offered by far the most suitable shortcut to the carbon skeleton of the 2 π partner (221). This approach is based around a modification of Perry's strategy towards the synthesis of 2-ethylfurananthoquinones.^{45,80,87}

In addition to the strong homology with the anticipated 2 π hDA component (221), the synthesis of this moiety was also reportedly achieved in a very respectable overall yield of 30%, with reasonable accessibility from commercially available bromo-veratraldehyde (224) making it a logical starting point (Scheme 66).

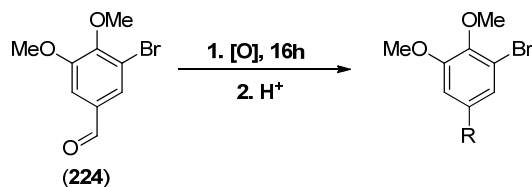


Scheme 66. Danishefsky's synthesis of the naphthazarin⁸

In this strategy, key nitrile⁸⁸ (227) was provided using Rizzacasa's synthesis, from benzaldehyde (224) *via* Daykin oxidation, followed by methylation of the resultant phenol using Me₂SO₄ to give trimethoxy-protected aryl bromide (226). This was ultimately converted to (227) using the Rosenmund-van Baun cyanation in 65% yield over three steps. Subsequent nucleophilic addition of the dianion of 3-furoic acid to

⁸ Yields quoted in brackets represent reported literature values.

nitrile⁸⁸ followed by aqueous work-up afforded furoic acid (**228**), which when subjected to strong acidic conditions underwent an intramolecular Friedel Crafts type cyclisation to afford quinone (**229**). This was subsequently reduced and methylated in a one pot procedure to furnish the desired naphofuran (**230**) as a pale yellow solid.



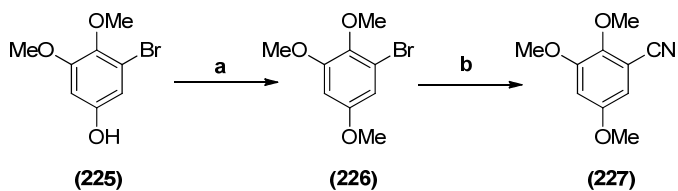
Entry	Oxidant	Solvent	Temp (°C)	Yield (%)		
				R = CHO (224)	R = OH (225)	R = CO ₂ H (224a)
1	<i>m</i> CPBA (1.49 equiv)	CH ₂ Cl ₂	40	76-99	0-19	0
2	<i>m</i> CPBA (1.49 equiv)	CHCl ₃	62	66-88	5-34	0
3	H ₂ O ₂ (20 equiv.)	1 M NaOH	100	95	3	0
4	H ₂ O ₂ (20 equiv.)	5 M NaOH	100	86	12	0
5	MMPP (1.0 equiv) ⁸⁹	MeOH	rt	0	0	99.5
6	<i>m</i> CPBA ⁱ (1.49 equiv)	CHCl ₃	62	5-19	65-88	0

ⁱ Commercial bromovetraldehyde (**225**) further purified by silica gel chromatography prior to use

Table 8. Optimisation of the Dakin reaction

In the author's hands the first step, the Baeyer-Villiger reaction initially proved low-yielding and unreliable (**entries 1 and 2; Table 8**) relative to literature reports (70-82%).^{90,91} Clearly this was undesirable for the initial step of a natural product synthesis, therefore an short optimisation study was carried out using common, readily available per-acids. Upon purification of the reaction mixtures by silica gel chromatography of the crude reaction mixtures the author was surprised to observe that the recovered starting material was isolated as a "brilliant white" solid rather than luminous canary yellow as supplied. The origin of this extreme colour was not detectable by ¹H NMR or GC/MS nor was there any available data from known contaminants listed by the supplier. Even more surprising was that subjection of "brilliant white" aldehyde (**224**) to the original reaction

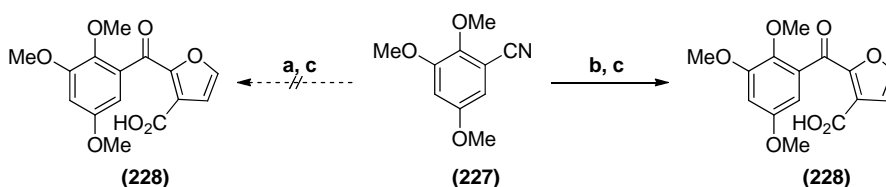
conditions, yields increased up to and in excess of those reported in the literature on a 4.5 g scale (**entry 6, Table 8**).



a. Acetone, K_2CO_3 , Dimethylsulfate, r.t. 12 h, (99.2%); **b.** DMF, $Cu(I)CN$, Δ , 16 h (98%)

Scheme 67. Scale-up of key nitrile

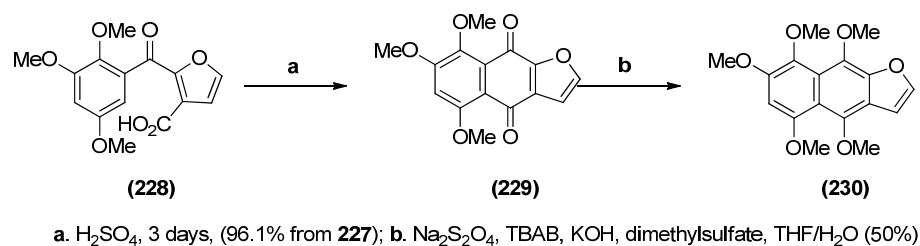
Thankfully, methylation of the resultant phenol and subsequent S_NAr with $CuCN$ in DMF proceeded without incident on 9.5 g scale (**Scheme 67**) to give the nitrile (**227**) in slightly improved yield (97%, over 2 steps). Unfortunately, further problems were encountered with regard to the nucleophilic addition of dianion of 3-furoic acid to nitrile (**227**).



ai. 3-furoic acid, THF, $-78^\circ C$; **ii.** $n-BuLi$ (2.2 equiv.), $-78^\circ C$, 2 h; **iii.** (**227**) $-78^\circ C$ to r.t., 16 h;
bi. 3-furoic acid, THF, $-78^\circ C$; **ii.** $t-BuLi$ (2.2 equiv.), $-78^\circ C$, 2 h; **iii.** (**227**) $-78^\circ C$ to r.t., 16 h;
c. 1M HCl, 2 h, r.t.;

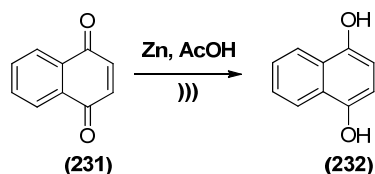
Scheme 68. Nucleophilic addition of dianion of 3-furoic acid to nitrile (**227**)

In the author's hands, the initial reaction conditions delivered no conversion to the expected ketone (**228**). A small aliquot of the $n-BuLi$ and 3-furoic acid mixture was therefore removed under nitrogen and injected directly into CD_3OD and the resultant mixture was subsequently analysed by 1H NMR. This experiment indicated that there was no detectable deuteration at the 2-position of the furan at $-78^\circ C$ in the author's hands. This problem was therefore overcome by increasing the strength of the base from $n-BuLi$ ($pK_a \approx 50$) to $t-BuLi$ ($pK_a \approx 55$), which after acidic work-up furnished the desired carboxylic acid (**228**) in ca 99% yield.



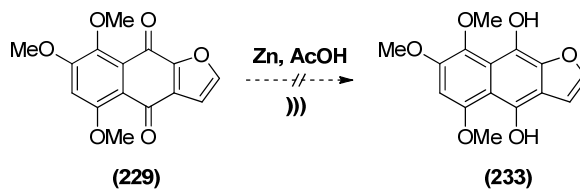
Scheme 69. Completion of Danishefsky's naphthofuran

Gratifyingly, treatment of the resultant carboxylic acid with neat H₂SO₄ for 3 days facilitated the desired intramolecular Friedel-Crafts cyclisation as described by Danishefsky affording quinone (**229**) in 96 % yield (lit. 88%).³ Upon subjection of the quinone (**229**) to the one pot reduction/methylation conditions we found that our initial product recovery to be very poor (5-20%). However by thoroughly deoxygenating the solution with argon for 1 h prior to addition of the Na₂S₂O₄ appeared to help stabilise the reactive radical species, furnishing (**231**) in yields of (40-55%) as a pale yellow solid on a 100 mg scale, however in the author's hands these yields could not be achieved on a larger scale.



Scheme 70. Reichwagen's Zn SET quinone reduction.

Having established that Danishefsky's route to quinone (**229**) was reproducible and scalable in the author's hands, the low yields and unpredictable nature of the existing one-pot quinone reduction/methylation procedure made it rather unattractive. Upon inspection of the literature, the procedure that initially appeared most attractive was the seemingly underutilised Reichwagen's Zn SET quinone reduction (**Scheme 70**).⁹²

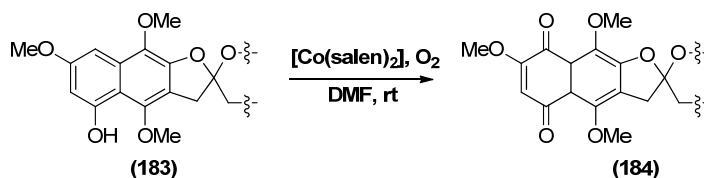


Scheme 71. Attempted Reichwagen's procedure.

Unfortunately in the author's hands, when this protocol was applied to the more electron-rich trimethoxy-naphthoquinone (**229**), only unreacted starting material was recovered. No reaction could be initiated by heating the ultrasonic bath to 80 °C, activating the Zn with acid, thoroughly degassing the solution or any combination of these.

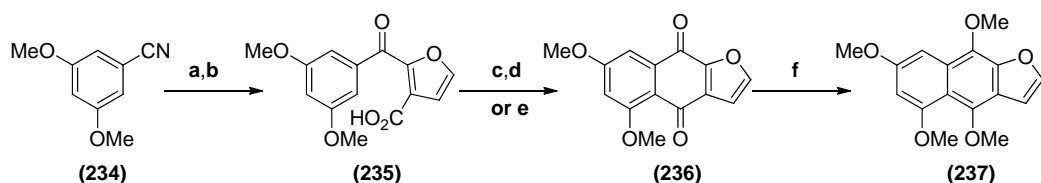
4.3 Alternative Naphthazarin Synthesis

Due to erratic yields in the late stage reduction strategy, combined with the high cost of the bromovetraldehyde starting material and alternative shorter and more scalable synthesis of a suitable 2π partner was investigated. Key areas identified for optimisation were cost/synthesis of the aryl-nitrile, usefulness of the intermediates in model cycloadditions and improving the naphthoquinone reduction.



Scheme 72. Kita's late stage oxidation

Interestingly, upon re-examination of the literature it was noticed that a late stage oxidation of advanced intermediate (**183**) by Kita had been achieved in 84% yield (**Scheme 72**). It was therefore anticipated that the commercially available and more affordable 3,5-dimethoxybenzonitrile (£917.10 mol⁻¹ vs £6151.26 mol⁻¹)^h could be employed in a similar approach, thus removing a net 3 synthetic steps, significant material costs and the risks involved in handling CuCN in DMF.



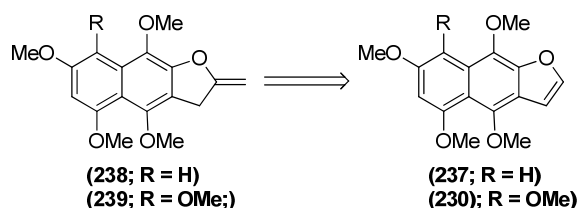
a. 3-furoic acid, *t*-BuLi, -78°C; b. HCl_(aq.) (90% over 2 steps); c. (COCl)₂, cat. DMF; d. AlCl₃, CH₂Cl₂ (88% over 2 steps); e. H₂SO₄, rt, 3 days (86%); fi. NaS₂O₄, TBAF, HF/H₂O; ii. KOH/H₂O (slurry); iii. Me₂SO₄ (64%).

Scheme 73. Synthesis of tetramethoxy-naphthazarin (**237**)

^h Prices based on 25g and 5g bottles from www.sigmaaldrich.com on 26/01/2014

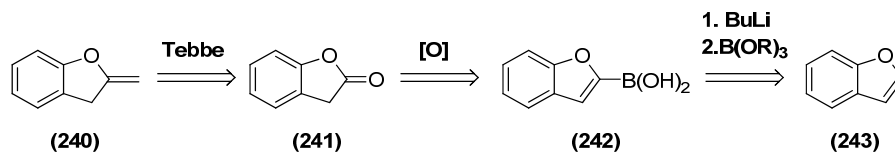
Gratifyingly applying Danishefskys' quinone synthesis protocol to **(234)** was remarkably straightforward and **(236)** could be generated in 77% over 3 steps (**a,b,e Scheme 73**). The Friedel-Crafts reaction could also be facilitated in comparable yield by derivatising **(235)** to the corresponding acid chloride before promoting cyclisation upon addition of AlCl_3 (**c,d, Scheme 73**). Subjection of **(236)** to the aforementioned one pot reduction/methylation proceeded in an increased yield (relative to **Scheme 69**) of 64%, presumably due to the decreased electron density of the aromatic moiety.

4.4 Methylene Installation Strategies



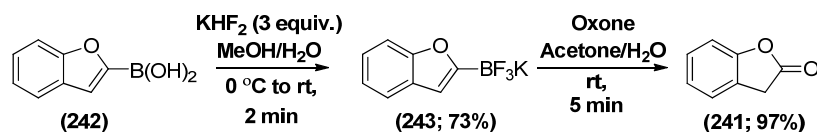
Scheme 74. Retrosynthetic analysis of the 2π component

Having established two potential naphthazarin syntheses, synthetic efforts were then directed towards installation of the essential benzofuryl-methylene to generate the key 2π component (**Scheme 74**). As little work had been conducted into this area, it was difficult to assess the ease of this transformation and thus methylene installation was modelled using benzofuran (**243**).



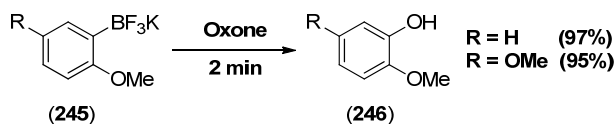
Scheme 75. Proposed methylene installation strategies

As the 2-position of benzofurans is known to be the most acidic site ($\text{p}K_{\text{a}} = 33.2$; THF)⁹³ a deprotonation/electrophilic trapping methodology was envisaged. The most promising route selected was based around Molander and co-workers extremely rapid and high yielding procedure for the oxidation of organotrifluoroborates using Oxone.^{94,95} This was of particular interest as they were able to convert functionalised benzofuran (**243**) to benzofuranones in 71% overall yield without the requirement of silica gel chromatography (**Scheme 76**).



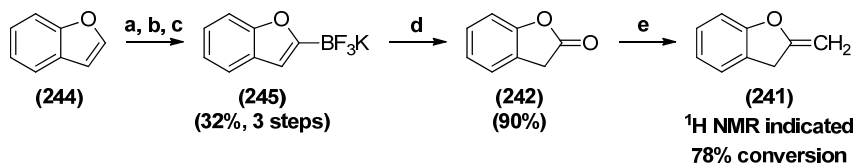
Scheme 76. Molander's oxidative lactone formation

The reaction conditions reported also appeared to tolerate aryl methyl ethers when used to convert aryltrifluoroborates to phenols (**Scheme 77**). This was reported to occur without any side reactions and thus presented itself to be the ideal oxidation protocol to generate the fully functionalised benzofuranone.



Scheme 77. Methyl ether functional group tolerance of Molander's oxidation

Gratifyingly, the author found Molander's reports to be very easily reproduced on the first attempt, furnishing (**242**) in 29% overall yield from benzofuran. With this material in hand, the lactone was exposed to the Tebbe reagent, before treatment with aqueous NaOH generated a green solution, as described by Grubbs. Analysis of the solution by ^1H NMR in 0.1 M NaOD, in D_2O indicated 78% conversion to (**241**) based on integration of the methylene signals 3.97 ppm (2H, 78 %, **241**): 3.69 ppm (2H, 22 %, **242**) and the presence of two new broad CH signals at 4.92-4.81 ppm (1H, 78%) and 4.40-4.26 ppm (1H, 78%).⁹⁶



ai. *n*-BuLi (1.05 equiv.), THF (−78 °C to 0 °C, 2 h); **ii.** (*i*PrO)B (1.20 equiv., −78 °C to r.t., 16 h); **b.** 2M aq. HCl (10 equiv.); **c.** KHF_2 (3.00 equiv.), MeOH/ H_2O (0 °C to r.t., 32%, 3 steps); **d.** Oxone (1.00 equiv.), Acetone/ H_2O , r.t., 5 min (90%); **ei.** Toluene:THF (3:1), cat. pyridine, −40 °C; **ei.** Tebbe reagent, (−40 °C, 30 min then −40 °C to r.t. over 90 min); **ei.** 15% aq. NaOH (−10 °C, 78% conversion by ^1H NMR).

Scheme 78. In house synthesis of *exo*-enol ether (**241**)

Having replicated the protocols of Molander and Grubbs, it was anticipated that this olefin installation strategy could be applied to generate either olefin (**238**) or (**239**) from naphthazarin (**237**) or (**230**). However as conditions to generate *ortho*-quinone methide (**222**) had not yet been established, the author believed that it would be prudent not to commit samples of (**237**) or (**230**) towards this strategy until this challenge had been overcome. It was hoped that this cautious approach would maximise the probability of developing practical conditions that would be compatible with both the generation and coupling of these two reactive subunits.

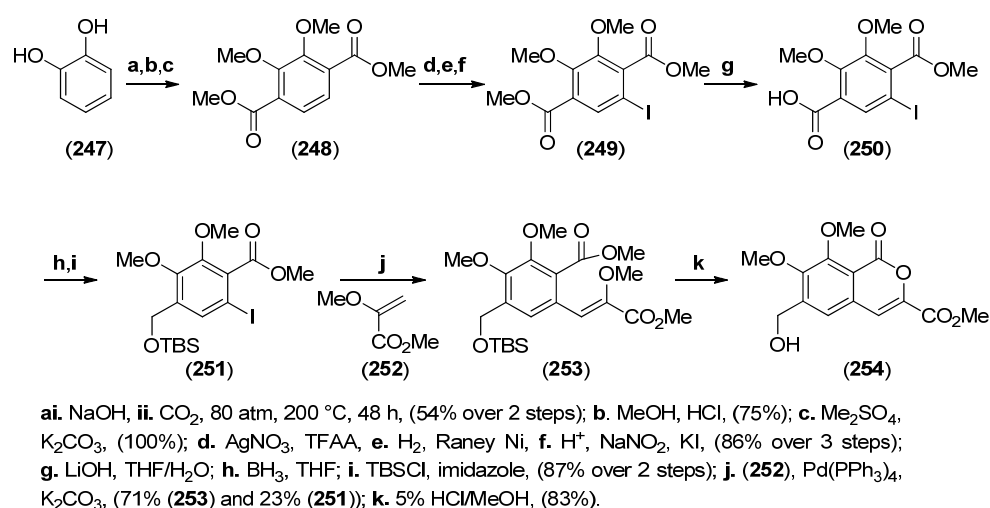
Isocoumarin

Synthesis

4.5 Isocoumarin Moiety

Unlike the naphthazarin, with one clear starting point, there have been several routes to the isocoumarin moieties of the rubromycin family similar to our requirements. Of these methodologies many have been surprisingly lengthy for a planar, bicyclic moiety. This has mostly been due to the various oxidation states within this structure. At the outset of our investigation, there appeared to be a handful of literature preparations amenable to synthesis of the 4π component (**222**).

4.6 Kozłowski's Isocoumarin



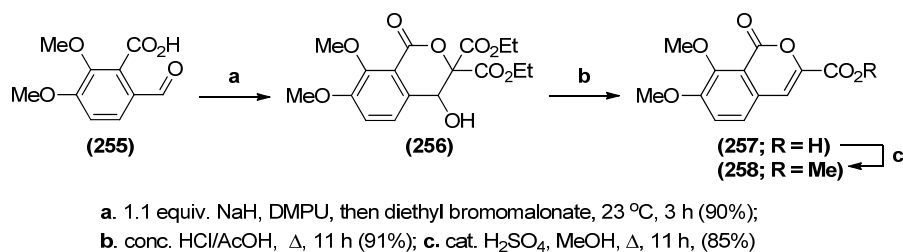
Scheme 80. Kozłowski's isocoumarin synthesis

During a large body of work in this field Kozłowski's reported the most unique isocoumarin preparation in 2001, as it is the only method not based around a vanillin-like starting material.⁹⁷ This methodology initially employs high-pressure *bis*-carboxylation of catchecol (**247**) and the resultant dicarboxylated product subsequently underwent two step methylation to afford dimethyl 2,3-dimethoxyterephthalate (**248**). As direct electrophilic iodination of the electron deficient arene was not viable, mono-iodination was accomplished *via* a three-step procedure. This was accomplished *via* sequential nitration of the aromatic, which was subsequently regiospecifically reduced to the corresponding aniline, before eventual iodination under Sandmeyer conditions to furnish (**249**) in 86 % yield over 3 steps.

Regiospecific saponification of the least hindered methyl ester was achieved using LiOH in THF:H₂O before chemoselective reduction of the resultant carboxylic acid and subsequent protection of the corresponding alcohol as a silyl ether (**251**). Once sufficiently protected, Heck coupling could be achieved with methyl enol ether (**252**) giving (**252**) in 21.5% yieldⁱ (over 10 steps), thus setting up for acid-promoted intramolecular condensation to afford benzyl alcohol (**254**) in 17.9% overall yield (17.9%).

While this route appears to have the advantage that conversion of the silyl protected carboxylic acid to the corresponding acetyl ester type *o*-QM precursor, this route is however long-winded and requires high pressure apparatus not available to the author. The Heck coupling was also later described as “not reproducible” by the same research group in 2010,⁹⁸ citing dehalogenation as a significant problem and was thus discounted by the author as a suitable starting point.

4.7 Behar’s Isocoumarin



Scheme 81. Behar’s isocoumarin synthesis

A more concise isocoumarin synthesis was outlined by the Behar group.⁹⁹ The main advantage of this route is that opianic acid starting material (**255**) is commercially available, allowing a significant reduction in the number of steps towards the isocoumarin scaffold. Unfortunately progress on the isocoumarin moiety (**258**) initially proved problematic due to the author’s inability to reproduce these results (**Scheme 81**).

ⁱThere was a notable recovery of (**251**) (23%) for this step.

They reported a route to condensate (**256**), using what would appear a rather facile reaction, proceeding simply by deprotonation of opianic acid using NaH at 23 °C, followed by nucleophilic addition to diethyl bromomalonate, before intramolecular cyclisation. However in the author's hands, it was not possible to isolate the corresponding cyclised condensate (**256**) but it is believed based upon ¹H NMR evidence (shift in malonate ¹H signal from 4.83 to 5.81 ppm indicative of a deshielding effect) that an open-chain form (**259**) was the major product generated.

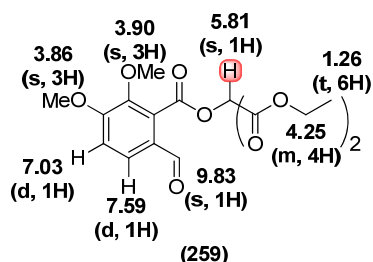


Fig. 15. Proposed open-chain form of the condensate

The reaction was extensively screened against a variety of temperatures (−78 °C to 130 °C), bases (NaH, K₂CO₃, Na₂CO₃, DBU, Et₃N) and solvents (THF, DMPU, DMF, Et₃N,) however the desired cyclic species could not be generated efficiently *via* this method. Unfortunately this species could not be cyclized thermally and/or upon subjection to acid (various mixtures of H₂SO₄, HCl, AcOH, H₂O, PTSA, NH₄Cl).

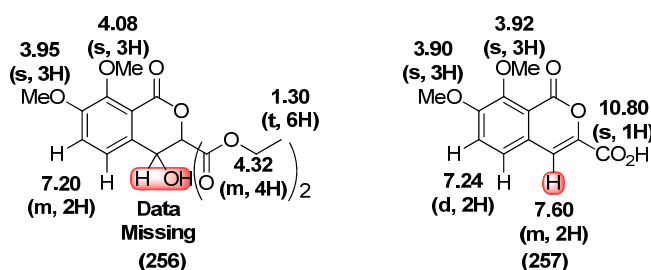
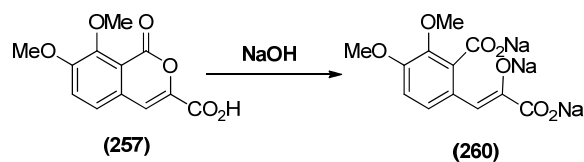


Fig. 16. Behar's ¹H NMR assignments

Upon further scrutiny of Behar's experimental procedure it was noticed that the ¹H NMR data^j generated for the intermediates (**256**) and (**257**) did not appear to correspond to the structures proposed (Fig. 16) casting further doubt in the author's mind, regarding the synthetic utility of this protocol.

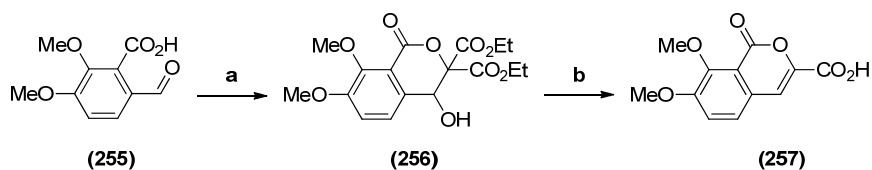
^j No spectra available in Behar's publication for comparison



Scheme 82. Anticipated metal coumarinate formation

Metal alkoxide or hydroxide type base cyclisation of the condensate was considered, however this was not attempted due the known instability of isocoumarin lactones towards ring opening to form metal coumarinates in the presence of dilute hydroxide (**Scheme 82**), which can be difficult to eliminate entirely from alkoxide reagents, even when freshly prepared.¹⁰⁰

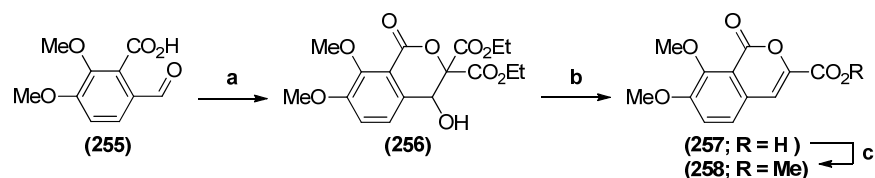
4.8 Chatterjea's Isocoumarin



a. K_2CO_3 , but-2-one, then diethoxybromomalonate, Δ , 3 h; b. HCl/AcOH , Δ , 1 h (70% over 2 steps);

Scheme 83. Chatterjea's synthesis of the isocoumarin moiety

When delving deeper into the Behar groups report, it was found that the carboxylic acid (**257**) had been synthesised in 1965 by Chatterjea *et al.*¹⁰¹ using conditions outlined above (**Scheme 83**). In the author's hand's formation of (**257**) initially proved elusive after several attempts. This initial failure to replicate these results was attributed to the possible presence of trace amounts of NaOH in solution (caused by trace amounts of water in equilibrium with Na_2CO_3) causing a ring opening effect as described previously (**Scheme 82**). This problem was overcome partially by thorough distillation and purification of the reagents, in combination with addition of activated molecular 3Å sieves to the reaction mixture, facilitating product formation but in erratic yields (10 to 65%).



a. K_2CO_3 , but-2-one, then diethoxybromomalonate, Δ , 3 h; b. HCl/AcOH, Δ , 1 h (0-65% over 2 steps); c. TMSCHN₂ (2M in EtO₂), CH₂Cl₂, r.t., 30 min, then AcOH (99%) or cat. H₂SO₄, MeOH, Δ , 12 h (97%)

Scheme 84. Revised synthesis of the isocoumarin moiety

Gratifyingly, the methyl ester could also be synthesised in an excellent yield (97%) by performing a Fisher-Speir esterification, refluxing the carboxylic acid in methanol in the presence of catalytic sulphuric acid. It was also found that this transformation could also be accomplished upon treatment of carboxylic acid (257) with diazo(trimethylsilyl)methane afforded the corresponding methylester (258) cleanly and in excellent yield (99%).

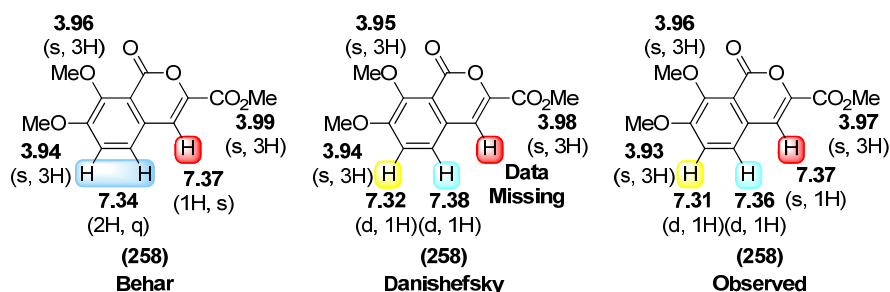


Fig. 17. ¹H NMR data for Chattejea's methylated isocoumarin (250)

It was however found that the literature ¹H NMR data for (258) given in the two known preparations (by the Danishefsky and Behar research groups) to be somewhat unusual as neither appeared to correspond with our findings (Fig. 17). The key differences are that Danishefsky's data does not provide evidence to suggest the presence of the styrenyl ¹H signal (7.37 ppm) and that Behar's assignment of the aromatic ¹H signal as a quartet and therefore two chemically equivalent nuclei would appear erroneous to the author. An X-ray crystal structure (Fig. 18) for the author's sample was therefore obtained so as to confirm it to be the desired methyl ester (258).

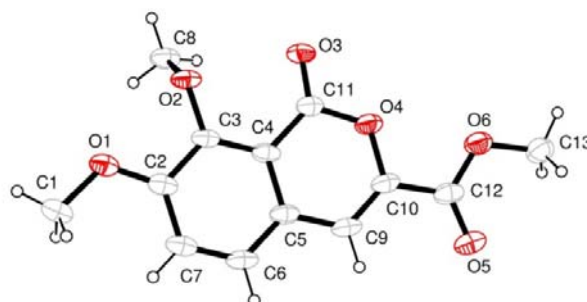
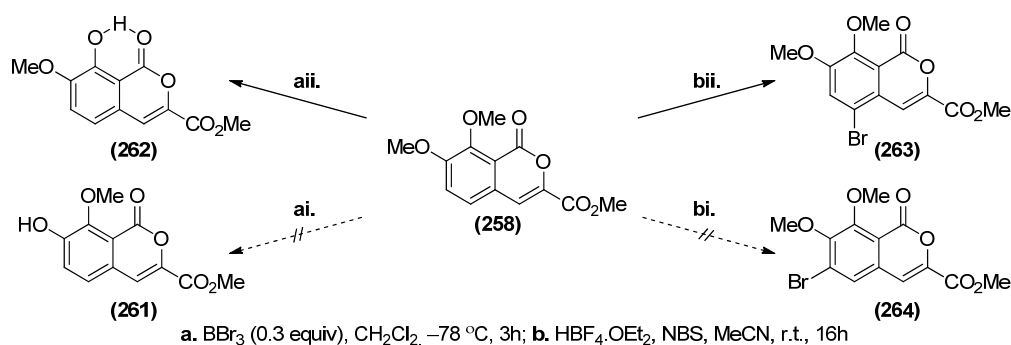


Fig. 18. X-Ray crystal structure of methylated isocoumarin (**258**)

4.9 Reißig's Isocoumarin



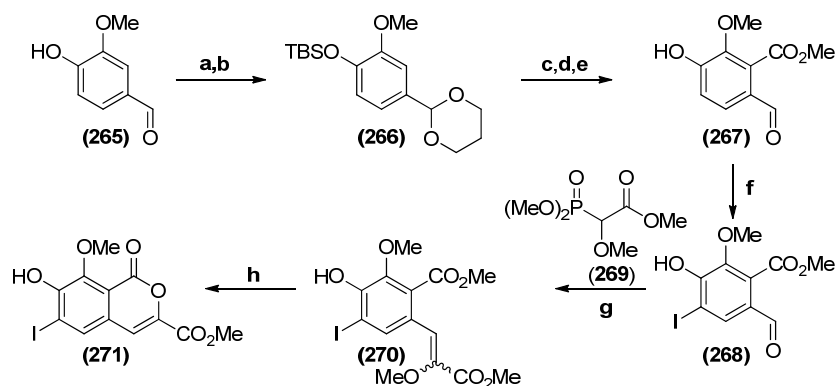
Scheme 85. Reißig's attempted halogenations

The fourth and ultimately more flexible, and reliable synthetic route explored was that reported by Reißig and co-workers, during their synthetic efforts towards the rubromycins.^{102,103} Their initial approach aimed to selectively deprotect (**258**) with 0.3 equiv of BBr_3 (i.e. 0.9 equiv. of bromide) at $-78\text{ }^\circ\text{C}$ (pathway ai., Scheme 85). They had then envisaged that allylation of the phenol (**261**), followed by a Claisen rearrangement to permit functionalisation at the 6-position. Unfortunately for the advancement of this methodology it was found by both the Reißig group and in the author's hands^k that the 8-methoxy group was selectively attacked, presumably due to complexation between the Lewis acid and the neighbouring carbonyl functionality (pathway aii., Scheme 85).

Their second approach to functionalise the 6-position was *via* bromination with NBS (pathway bi., Scheme 85). Unfortunately for the advancement of this methodology it

^k Reaction was repeated due to lack of previous supporting information available

was found by both the Reißig group and in the author's hands that bromination occurred exclusively at the 5-position (**pathway bii., Scheme 85**). In light of this evidence and in the absence of a selective enzymatic operation to facilitate this transformation, they developed a novel concise method more amenable to encompassing chemical diversity (**Scheme 86**).

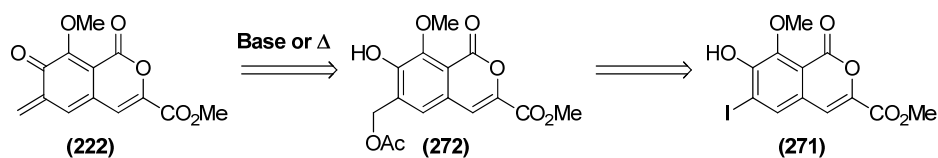


a. TBSCl, Et₃N, DMAP, CH₂Cl₂, r.t., 24 h (97%); **b.** 1,3-Propanediol, *n*-Bu₄NBr₃, HC(OMe)₃, CH₂Cl₂, r.t., 2.5 h (82%); **c.** *n*-BuLi, cyclohexane, r.t., 3 h; **d.** ClCO₂Me, 0 °C to r.t., 16 h; **e.** HCl (37%, aq), KF, THF, r.t., 6-24 h (58% over 3 steps); **f.** Me₄NiCl₂, NaHCO₃, CH₂Cl₂, r.t., 4 h (91%); **g.** (**269**), NaHMDS, THF, -78 °C to r.t. (82%); **h.** HBr (47%, aq):MeOH (1:1), Δ, 12 h (55-68%).

Scheme 86. Reißig revised synthesis of the isocoumarin moiety

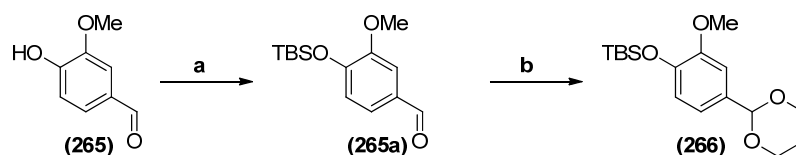
This was accomplished by *ortho*-lithiation of protected vanillin derivative (**266**) before treating with excess methyl chloroformate, prior to one-pot double deprotection using KF under acidic, aqueous conditions to furnish esterified vanillin (**267**) in 46% yield over 5 steps. Regiospecific iodination was then achieved using the slightly unusual tetramethylammonium dichloroiodate reagent as a extremely mild and synthetically useful source of electrophilic iodine. The resultant halobenzaldehyde (**268**) was then olefinated using a Horner-Wadsworth-Emmons reaction using methyl (dimethylphosphono)methoxyacetate (**269**)¹ affording (**270**). Cyclisation was subsequently achieved *via* Brønstead acid-promoted lactone formation in a mixture of refluxing aqueous HBr and methanol, furnishing the desired iodoisocoumarin (**271**) as a precipitate in 19-23% yield over 8 steps.

¹ Literature appears to indicate phosphonate production to be the limiting scalability factor.



Scheme 87. Envisaged functionalisation of ReBigs iodo-isocoumarin (**271**)

Despite the increased number of synthetic steps, this route therefore appeared to offer significant advantages over those previously outlined, with regard to a scalable and effective rubromycin synthesis. Firstly, vanillin (**265**) is a significantly more economical starting material (£7.02 mol⁻¹)^m than the more specialist opianic acid (**255**) reagent (£2240.63 mol⁻¹).ⁿ Secondly, the iodinated product (**271**) has greater homology with the required *o*-QM precursor (**272**), as the desired and synthetically difficult 7-hydroxy-8-methoxy oxidation pattern (**Scheme 87**) is already ‘pre-installed’ in the starting material (**265**), which is also available in bulk quantities.



- a. TBSCl, Et₃N, DMAP, CH₂Cl₂, r.t., 24 h (96-98%);
 b. 1,3-Propanediol, *n*-Bu₄NBr₃, HC(OMe)₃, CH₂Cl₂, r.t., 2.5 h (85-91%);

Scheme 88. Scale-up of acetal synthesis

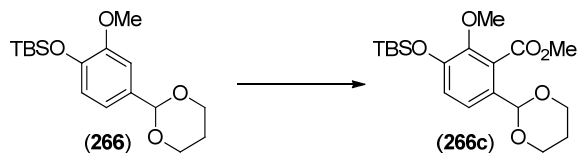
This route was explored to assess its reproducibility, scalability ease of use and scope for derivatisation. Initial results (**Scheme 88**) were very promising, in the author’s hands Reibig’s route to (**266**) was found to be a high yielding (96-98% observed, 97% reported) and highly scalable (carried out on 1 to 50 g scale, 7.56 g reported). The acetal protection, again proved to be very effective and scalable (from 926 mg reported to 80 g in 91% overall yield).^o The 3-step conversion of (**266**) to the corresponding ester (**267**) also proved to be highly reproducible in the author’s hands. However the undesirable yields reported (58%) and observed (55-60%) in the author’s hand appears to be the result

^m Price based upon 2kg bottle from www.sigmaaldrich.com on 03/07/2010

ⁿ Price based upon 5g bottle from www.alfa.com on 03/07/2010

^o Dry loading sample onto SiO₂ must be done below 30 °C to afford degradation.

of poor conversion (ca 55-63% calculated by ^1H NMR of the crude reaction mixture) to the corresponding TBS/acetal protected methyl ester (**266c**) rather than the harsh deprotection conditions as one may have anticipated. It was therefore proposed that poor lithiation of (**266**) may be limiting product formation.

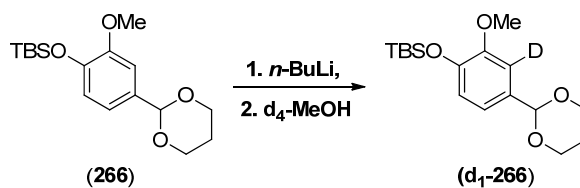


Entry	RLi	Equiv.	Solvent	Conditions	Yield
1	<i>n</i> -BuLi, TMEDA	2.3	Et ₂ O	0 °C, 2 h	16%
2	<i>n</i> -BuLi,	1.2	C ₆ H ₁₂	r.t., 3 h	40%
3	<i>n</i> -BuLi,	3.0	C ₆ H ₁₂	r.t., 3 h	29%
4	<i>t</i> -BuLi,	1.2	C ₆ H ₁₂	r.t., 3 h	20%
5	<i>n</i> -BuLi,	1.2	C ₆ H ₁₂	0 °C, 5.5 h	56%

Table 9. Reißig's optimization study

When looking at previous results (**Table 9**) by Reißig and co-workers it appears, rather unsurprisingly, that lithiation is inversely proportional to temperature over longer reaction times. Interestingly the use of cyclohexane as a non-coordinating solvent appears to significantly improve yields relative to Et₂O. The author assumes that as the acetal is only weakly *ortho*-directing that cyclohexane is an ideal solvent to enhance selective *ortho*-lithiation.

The main drawback of using this solvent however is that it has a melting point of 4-7 °C. In an attempt to decrease the freezing point of the solvent, without making the reaction mixture more polar, a reverse addition protocol (ie adding the arene to a solution of pre-cooled *n*-BuLi in hexanes/C₆H₁₀) was investigated (**Table 10**). It was found that using this protocol, maintaining the external cooling bath at -1 °C was the lowest temperature the reaction mixture would stir easily and would not be susceptible to freezing due to the standard error in the cooling unit apparatus. This temperature could however be decreased to -6 °C after addition of (**266**) to the reaction mixture.

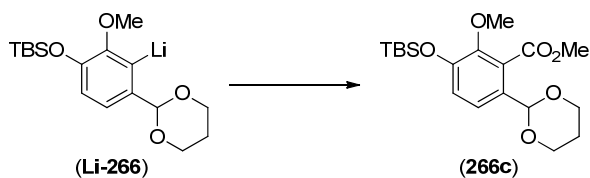


Entry	Temp (°C)	Time (h)	<i>n</i> -BuLi (equiv.)	Solvent	Conversion (%)
1	-1	2	1.2	C ₆ H ₁₂	56
2	-1	20	1.2	C ₆ H ₁₂	61
3	-1	20	2.0	C ₆ H ₁₂	58
4	-6 ⁱ	10	1.2	C ₆ H ₁₂	84
5	-6 ⁱ	20	1.2	C ₆ H ₁₂	80
6	-6 ⁱ	20	2.0	C ₆ H ₁₂	79

ⁱ External cooling bath was reduced from -1 to -6 °C after addition of (266)

Table 10. Deuteriation study of (266)

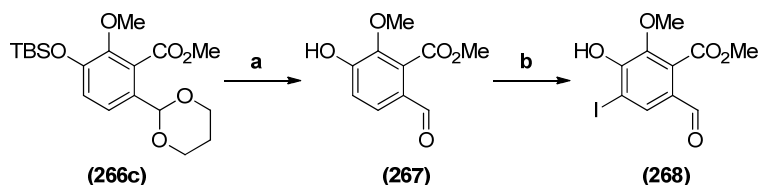
Interestingly decreasing the temperature to -6 °C facilitated a significant increase in lithiation (**entries 2 vs entry 5, Table 10**). It also appeared that increasing the amount of *n*-BuLi had little effect on the overall conversion and that leaving the reaction mixture for longer than 10 hours had no appreciable effect upon the yield. These optimised conditions for lithiation (**entry 4, Table 10**) were then applied to (266) using Reißig's conditions for the electrophilic quench (**entry 4, Table 11**). Unfortunately, the author was surprised to find that the reaction actually occurred in a slightly reduced yield (50% vs 56%) than described in the literature. As this electrophilic quench with ClCO₂Me was achieved in a significantly lower level of conversion to that previously described using D₂O (**entry 4, Table 10**), this step required further optimisation. Thankfully, after a short optimisation study, it was found that increasing the amount of ClCO₂Me and maintaining the reaction temperature at 10 °C, yields could be improved to 72% overall (**entry 7, Table 11**).



Entry	Temp (°C)	Time (h) ⁱ	ClCO ₂ Me (equiv.)	Solvent	Conversion (%)
1	-6	24	1.94	C ₆ H ₁₂	36
2	-6 to 0	24	1.94	C ₆ H ₁₂	48
3	-6 to 10	24	1.94	C ₆ H ₁₂	56
4	-6 to 25	24	1.94	C ₆ H ₁₂	50
5	-6 to 10	24	1.0	C ₆ H ₁₂	32
6	-6 to 10	24	2.0	C ₆ H ₁₂	57
7	-6 to 10	24	3.0	C ₆ H ₁₂	72
8	-6 to 10	24	4.0	C ₆ H ₁₂	64

ⁱ Reaction mixture was allowed to warm passively from -6 °C to the defined reaction temperature (over ca 30 min) and held at the that temperature for the time stated below.

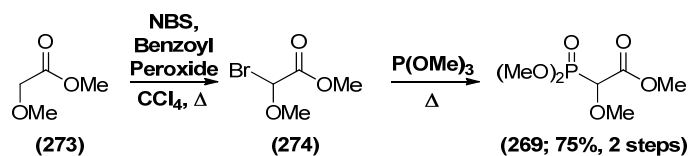
Table 11. Esterification of (257)



a. HCl (37%, aq), KF, THF, r.t., 6-24 h (65-70%); b. Me₄NiCl₂, NaHCO₃, CH₂Cl₂, r.t., 4 h (99.9%);

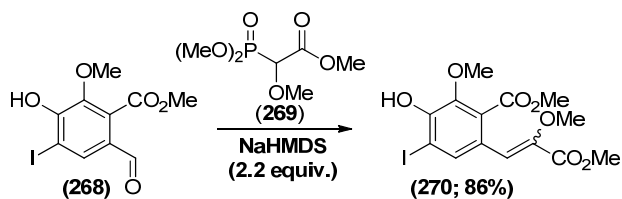
Scheme 89. Synthesis of Iodophenol (259)

The author was pleased to find that dual deprotection proceeded as described (**Scheme 89**), however yields initially appeared variable (45-50%) between reactions, however with close monitoring of the reaction by TLC analysis, yields were increased and more consistent (65-70%). The author was also pleased to observe that iodination to (268) could be carried out quantitatively, without any side reaction at the C-5 positions upon using an excess of Me₄NiCl₂.



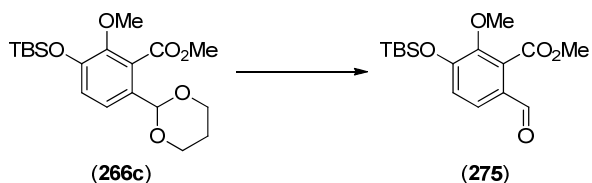
Scheme 90. Synthesis of phosphonate (266)

Synthesis of phosphonate (**269**) also proceed without incident on 20 g scale.^p This was achieved by radical bromination of methyl methoxyacetate (**273**) to give the corresponding bromide (**274**). This was then purified by distillation under reduced pressure before dropwise addition of trimethyl phosphite to the resultant oil. After heating the mixture for 16 h, phosphonate was then purified *via* distillation under reduced pressure to give phosphonate (**269**) in 75% yield over 2 steps.



Scheme 91. Horner-Wadsworth-Emmons olefination of Iodophenol (**270**)

Upon close inspection of the described Horner-Wadsworth-Emmons olefination procedure towards iodostyrene (**270**) it was of slight surprise to the author that only 2.0 equiv. of NaHMDS was added to the reaction mixture to deprotonate both phenol (**268**; 1.0 equiv.) and phosphonate (**269**; 1.22 equiv.). The author wondered, if a slight excess (2.4 equiv.) of NaHMDS was added to ensure quantitative deprotonation perhaps olefination could be carried out quantitatively (**Scheme 91**). Unfortunately, this only facilitated a marginal increase in yield (86% vs 82%).^q



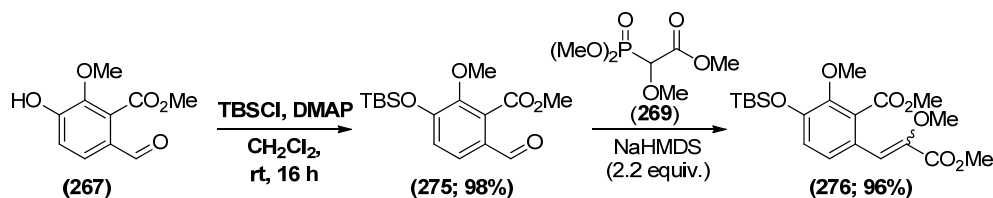
Scheme 92. Proposed chemoselective deprotection of acetal (**266c**)

It was therefore hypothesized that if chemoselective deprotection of the acetal (**Scheme 92**) was carried out prior to olefination, perhaps this transformation could be

^p Due to the extremely exothermic nature of this reaction, this reaction could not safely be carried out on a larger scale.

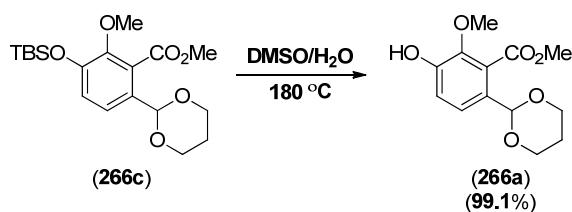
^q When the analogous Wittig olefination was attempted the reaction afforded a complex mixture of products and therefore was discarded as a viable alternative.

achieved quantitatively. To assess this phenol (**267**) was converted to the novel silyl ether (**275**) and subjected to previous olefination conditions (**Scheme 93**).



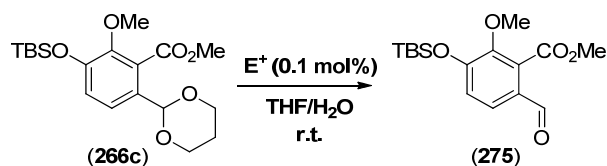
Scheme 93. Horner-Wadsworth-Emmons olefination of (**276**)

The author was pleased to find that olefination could be achieved to furnish the novel olefin (**276**) in 96.2% overall yield upon removal of the acidic phenolic proton from the reaction. The (*E:Z*) ratio was also more favourable (1:5 vs 7:13) than Reißig's protocol for isocoumarin formation. It was therefore deemed worthwhile to investigate a selective acetal deprotection approach. Towards this goal, all relevant cyclic acetal deprotection reactions outlined in "*Protective Groups in Organic Synthesis, Third Edition*"¹⁰⁴ in addition to treatment of (**266c**) with a range of Brønsted-acids on a 25 mg scale, but unfortunately selective protection could not be achieved. Interestingly, during this screening, the author was rather surprised to discover a novel procedure for the chemoselective deprotection of the phenolic silyl ether. This was achieved upon heating a solution of (**266c**) in DMSO/H₂O to reflux to give the novel phenol (**266a**) in 99.1% isolated yield (**Scheme 94**).¹⁰⁵



Scheme 94. Chemoselective phenolic deprotection of silyl ether (**266c**)

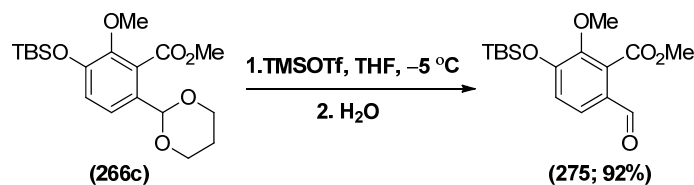
Upon re-examination of the literature it appeared that since the publication of this textbook, there was a report in 2002 by Mohan and co-workers that Bi(OTf)₃·3H₂O can be used as a mild reagent towards the deprotection of acetals in THF/H₂O.¹⁰⁶ A second screening was therefore carried out using all the available metal triflates, present in the laboratory.



Entry	Lewis Acid	Conversion (%)	Yield (%)
1	Y(OTf) ₃	0	0
2	Sc(OTf) ₃	0	0
3	In(OTf) ₃	0	0
4	Zn(OTf) ₂	0	0
5	TMSOTf	85	78
6	Sn(OTf) ₂	74	65

Table 12. Development of a selective deprotection protocol

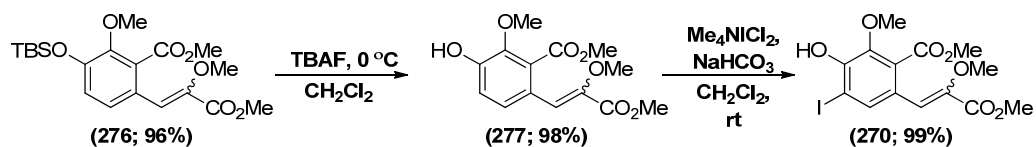
Gratifyingly, both TMSOTf and Sn(OTf)₂ were found to facilitate the desired acetal hydrolysis, while leaving the silyl ether relatively untouched [less than 2-3% hydrolysis in both instances (**entries 5 and 6, Table 12**)].



Scheme 95. Selective deprotection of the acetal

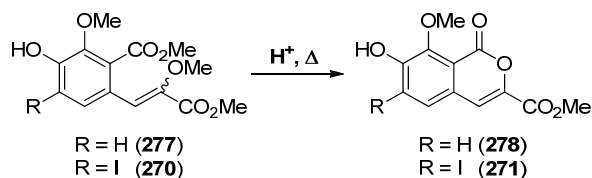
After further optimisation of the reaction conditions it was found that the reaction could essentially be conducted in a manner analogous to a titration (**Scheme 95**). A slight excess of TMSOTf (1.05 equiv.) was added to a solution of the acetal in anhydrous THF at $-5\text{ }^{\circ}\text{C}$, water (10-13 equiv.) was then added dropwise over 90 min until TLC analysis indicates consumption of the starting material. The reaction was robust and reliable enough to be carried out on multi-gram scale in excellent isolated yields (92%)^r and the material isolated was identical to that synthesized *via* TBS protection of (**267**) (**Scheme 93**).

^r Without careful monitoring of the reaction by TLC analysis, yields were reduced due to the formation of (**258**)



Scheme 96 – Deprotection and iodination of of (276)

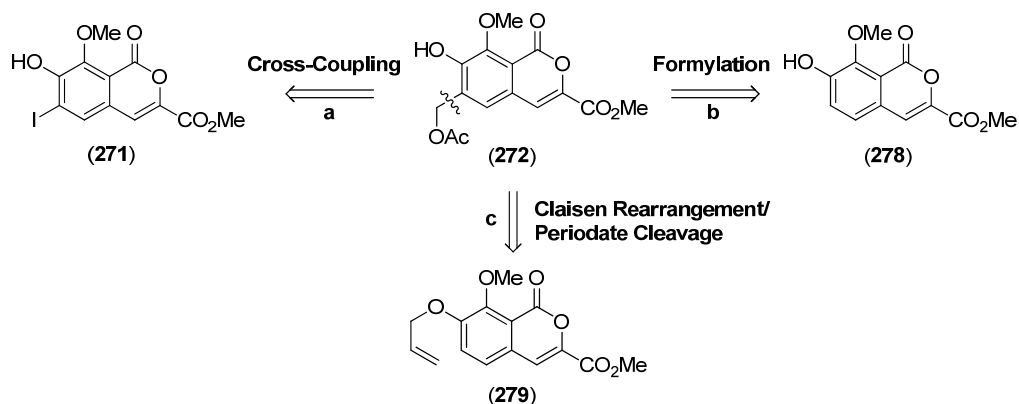
Gratifyingly, removal of the silyl ether and subsequent iodination could be achieved in excellent overall yield (97 % over 2 steps). This procedure was also interesting as it allowed us to explore the synthetic utility of (270) and the novel intermediate (277). Said intermediates were then exposed to Brønsted-acid promoted lactonisation conditions (Table 13) used previously by the groups of Reißig¹⁰³ (entries 1 and 4), Danishefsky^{45,80} (entries 2 and 5) and Kozłowski⁹⁸ (entries 3 and 6) during their total synthesis investigations (Section 3a). In the author's hands, Danishefsky's approach (entry 5, Table 13) was found to be preferential for the synthesis of Reißig's isocoumarin (271) and that Kozłowski's procedure (entry 2, Table 13) appears to to be most favourable for the synthesis of the novel isocoumarin (278).



Entry	R =	Acid	Solvent	Yield (%)
1	H	HBr (47% aq.)	MeOH	64
2	H	H ₂ SO ₄ (3N)	MeOH	85
3	H	PTSA	PhMe	94
4	I	HBr (47% aq.)	MeOH	68
5	I	H ₂ SO ₄ (3N)	MeOH	83
6	I	PTSA	PhMe	75

Table 13. Summary of isocoumarin formation

4.10 Acetate Installation Strategies

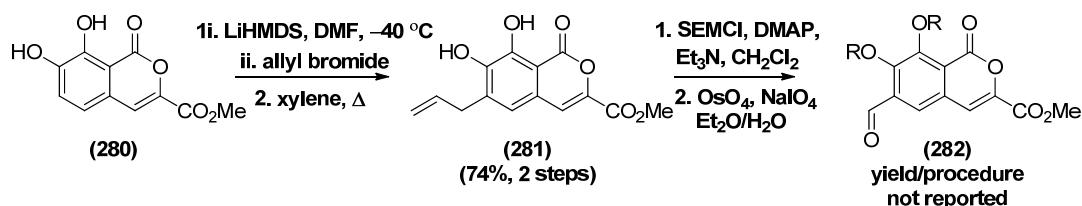


Scheme 97. Overview of acetate installation approaches

With meaningful quantities of various isocoumarins and isocoumarin precursors in hand, the next key step was how to install an acetate functional group *ortho* to the phenol. Due to an entirely different ‘endgame’ to previous strategies a great deal of modification was necessary to install the acetyl leaving group on the methylene carbon *ortho* to the phenol. The three general strategies towards this installation considered were; transition metal catalysed cross-coupling with an acyl-containing organometallic or equivalent synthon (**pathway a, Scheme 91**), direct formylation (**pathway b**), and Claisen rearrangement twinned with periodate cleavage (**pathway c**).^s

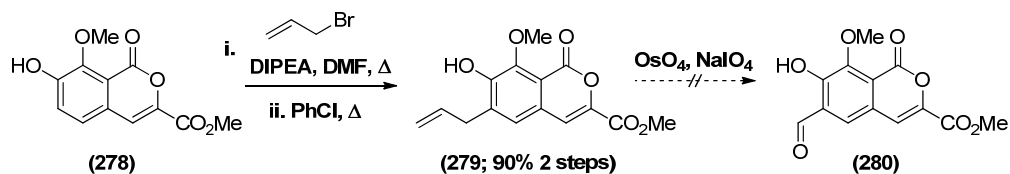
^s In the interest of completeness, lithium-halogen exchange followed by an electrophilic quench with DMF was also attempted, however it was found that methyl ester cleavage ensued even at reaction times of less than 10 seconds at -78°C .

4.11 Claisen Strategy



Scheme 98. Danishefsky's periodate cleavage

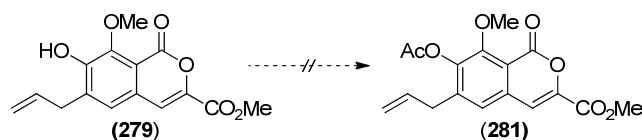
Due to previous observations by Danishefsky and co-workers (Scheme 98), it appears that allylated isocoumarins undergo sequential periodate cleavage to give benzaldehydes and not acetaldehyde products as one might expect. Although there were no reported conditions or yield[†] for this transformation, we anticipated that if successful this would provide a very straightforward route to benzaldehyde (282). It was anticipated that said *ortho*-formylated phenol could subsequently be reduced and acetylated to give the desired *o*-QM precursor (272).



Scheme 99. Attempted Claisen approach to salicaldehyde

Allylation of (271) could be achieved using allyl bromide and Hünigs base in DMF at 80 °C (Scheme 99) and subsequent Claisen rearrangement could be carried out at 210 °C under microwave irradiation in PhCl to give the allyl isocoumarin (279) in 90% overall yield. Unfortunately, the attempted one-pot periodate cleavage of (279) gave an extremely polar ($R_f = 0.0$; 100% EtOAc), clear, colourless oil, which was insoluble in deuterated chloroform, dichloromethane, water, methanol, acetonitrile, toluene and dimethyl sulfoxide, thus making it rather synthetically impractical and thus was not analysed further. It was therefore anticipated that by carrying out acetylation prior to periodate cleavage, the resultant products would be more soluble. Unfortunately after extensive efforts acetylation of (279) could not be achieved (Table 14).

[†] It is therefore not known if the SEM protecting groups survive this procedure.

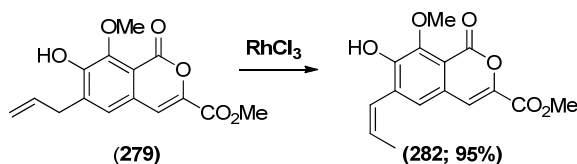


Entry	Base	Electrophile	Solvent	Temp. (°C)	Yield (%)
1	NEt ₃	AcCl ⁱ	CH ₂ Cl ₂	25	0
2	K ₂ CO ₃	AcCl ⁱ	DMF	80	0
3	K ₂ CO ₃	AcCl/NaI ⁱ	DMF	80	0
4	NEt ^t Pr ₂	AcCl	DMF	80	0
5	NEt ^t Pr ₂	AcBr	DMF	150	0
6	NEt ^t Pr ₂	AcBr	DMA	165	0
7	NEt ^t Pr ₂	Ac ₂ O	DMA	165	0
8	NEt ^t Pr ₂	Ac ₂ O	DMA	165	0
9	NEt ^t Pr ₂	Ac ₂ O	Ac ₂ O	25	0
10	NEt ^t Pr ₂	Ac ₂ O	Ac ₂ O	140	0
11	NaHMDS	AcBr	DMF	-40	0
12	NaHMDS	Ac ₂ O	DMF	-40	0
13	-	Ac ₂ O	Ac ₂ O	25-165	0
14	-	Ac ₂ O	AcOH (5% H ₂ SO ₄)	25-165	0

ⁱ DMAP (0.25 equiv.) added

Table 14. Attempted acetylation of (279)

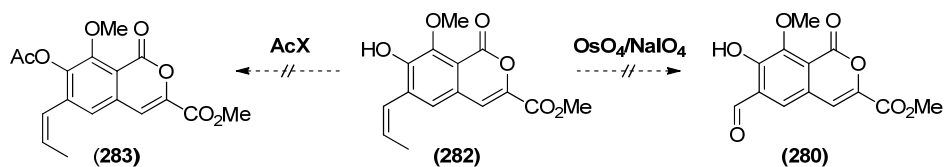
Due to repeated failures to synthesise (281), attempts were then made to try and bring the olefin into conjugation with the aromatic moiety. It was hoped that perhaps this compound may be more soluble and that potential mixtures of compounds recovered from periodate cleavage may be less complicated.



Scheme 100. RhCl₃ conjugation approach to styrene (282)

It was therefore of great satisfaction that alkene (279) could be brought into conjugation upon treatment with catalytic RhCl₃ (Scheme 100), to generate novel styrene in a 19:1

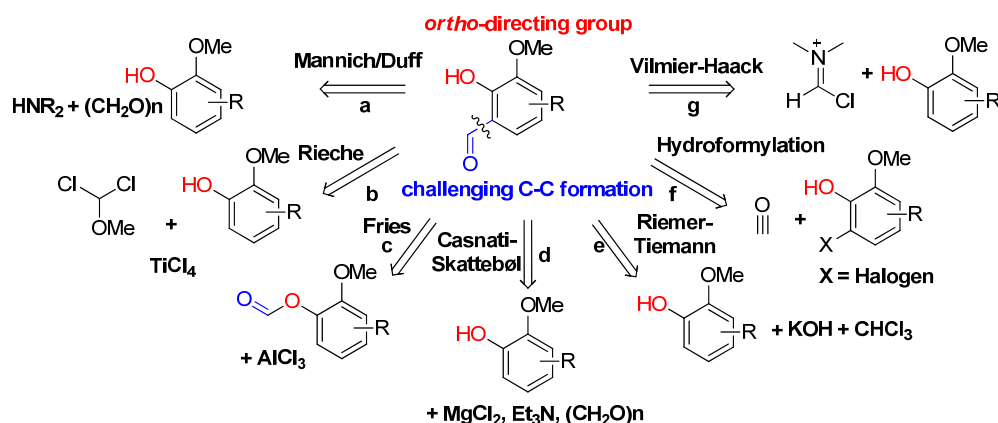
inseparable mixture of (282):(279).¹⁰⁷ It was then hoped that, either acetylation or OsO₄ dihydroxylation of (282) followed by periodate cleavage may be accomplished.



Scheme 101. Attempts to functionalise (282)

Unfortunately subsequent synthetic efforts both *via* stepwise and one-pot dihydroxylation and periodate cleavage also gave a clear colourless oil with the same insoluble properties previously seen (**Scheme 99**) and acetylation could not be achieved after numerous attempts (**Scheme 101**), thus this strategy was abandoned.

4.12 Direct Formylation Strategy



Scheme 102. Direct formylation approaches attempted on (255), (270) and (271) by author

Despite a sizeable amount of literature precedent regarding direct formylation reactions *ortho* to a phenol, finding a suitable reaction to accomplish this initially proved to be extremely fruitless. This difficulty is reflected in the literature, with only a limited number of examples reported with electronically neutral and electronically deficient aromatics.

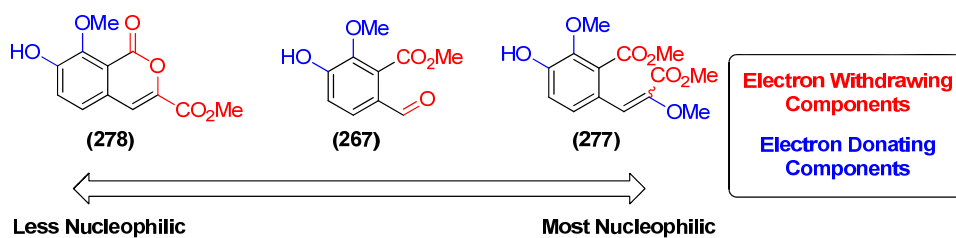
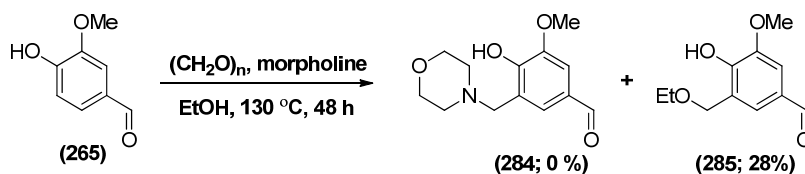


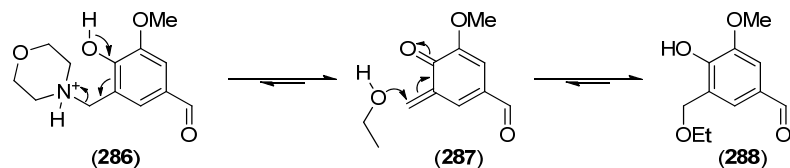
Fig. 19. Electronic characteristics of advanced intermediates

This presented us with an increased level of difficulty due to the ‘electronically schizophrenic’ nature of our functionalised vanillin derivatives (**Fig. 19**). Of all of the reactions attempted (summarised in **Scheme 102**)^{108,109} the only methodology that proved successful in all cases was *via* a simple Mannich reaction with the preformed iminium salt of morpholine and paraformaldehyde in acetic acid (see overleaf).



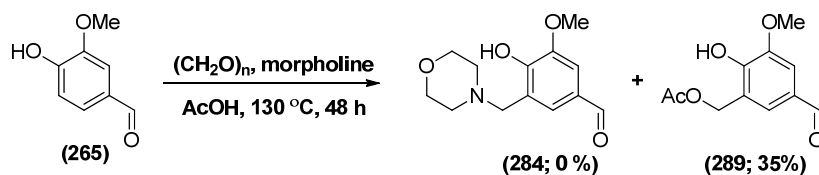
Scheme 103. Model acetylation

When this procedure⁹⁸ was initially tested on vanillin, the author was delighted to discover the major reactio product was *ortho*-benzyl ether (**285**) and not morpholine (**284**) as anticipated (**Scheme 103**).



Scheme 104. Mechanistic proposal for acetate formation

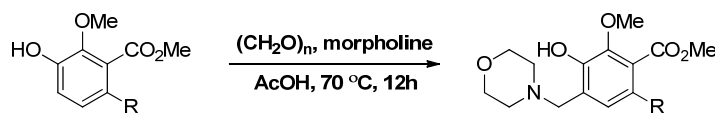
It was proposed that after formation of the Mannich product (**284**), morpholine is then eliminated from the conjugate acid (**286**), generating *o*-QM (**287**) *in situ*, in a similar fashion to that described by Wilson (**Scheme 26**).⁶⁹ The reactive intermediate was then quenched by nucleophilic addition from the solvent to complete this intriguing novel transformation (**Scheme 104**).^u



Scheme 105. Model acetylation

It was therefore proposed that if the reaction was carried out in a solution of acetic acid that perhaps the *ortho*-acetate could be generated *via* the same novel reaction mode (**Scheme 105**). Gratifyingly, this *o*-QM pathway furnished the desired product (**289**) in slightly increased yield (35%), perhaps due to the increased ability of AcOH to protonate the morpholine leaving group.

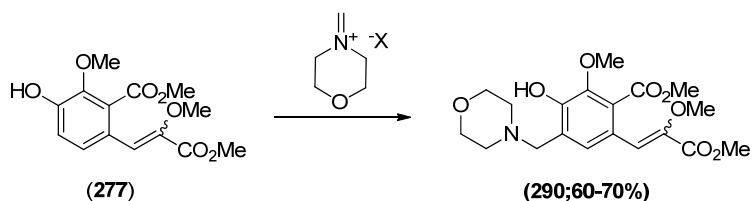
^u Repeating the reaction in the absence of morpholine or paraformaldehyde lead to 0% conversion of (**288**), inferring the initial formation of morpholine (**284**) and morpholinium (**286**).



Entry	Phenol	Yield (%)
1		0
2		60-70
3		0

Table 15. Scope of the Mannich protocol

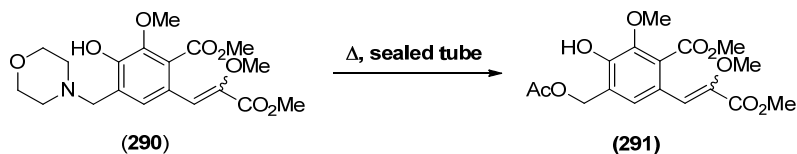
In the author's hands, when either benzaldehyde (**267**) or isocoumarin (**278**) were subjected to the reaction conditions, neither of the corresponding Mannich or benzyl acetate products were observed (**entries 1 and 3, Table 15**). This was believed to be due to reduced nucleophilicity of the π -system, thus demonstrating the high energetic barriers towards electrophilic aromatic substitution. The electron donation contribution of the conjugated methoxy group of styrene (**277**), appears to offer sufficient contribution to subtly overcome this nucleophilicity problem (**entry 2, Table 15**).



Entry	X ⁻	Solvent	Temp. (°C)	Yield (%)
1	AcO ⁻	AcOH	70	60-70
2	AcO ⁻	AcOH	90	84
3	AcO ⁻	AcOH	130	99.9
4	AcO ⁻	AcOH	150	97
5	Cl ⁻	MeCN	90	79
6	Cl ⁻	MeCN	130	90
7	Cl ⁻	MeCN	150	91

Table 16. Optimization of benzylic functionalisation

Gratifyingly, overall yield of **(290)** could be increased to 99.8% upon increasing the temperature to 130 °C, although the author was surprised to see no evidence of *o*-QM formation at 150 °C (**entries 4 and 7, Table 16**). It was therefore our hypothesis that functional group interconversion to the acetate could potentially lower the activation energy of *o*-QM formation, based on comparison of their conjugate acids (pK_a values in H₂O for AcOH = 4.75¹¹⁰ and *N*-methylmorpholine = 7.80).¹¹¹

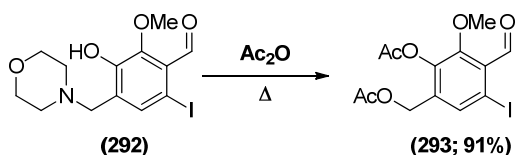


Entry	Nucleophile	Solvent	Temperature (°C)	Yield (%)
1	AcOH	AcOH	150	0
2	NaOAc	AcOH	150	0
3	NaOAc	MeCN	130	0
4	KOAc	MeCN	130	0
5	CsOAc	MeCN	130	0
6	NaOAc	EtOH	110	0
7	KOAc	EtOH	110	0
8	NaOAc	PhMe	160	0
9	KOAc	PhMe	160	0
10	CsOAc	PhMe	160	0

Table 17. Attempted acetate installation^v

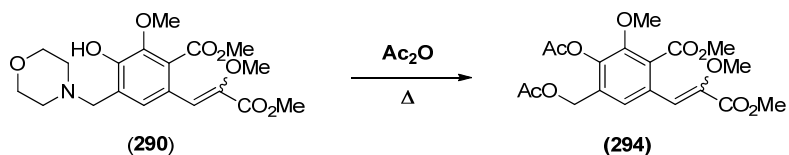
Several attempts were then made to try and perform an isohypsic conversion of the morpholine functionality to an acetate *via* an *o*-QM analogous to (**Scheme 105**). Unfortunately after several attempts a transformation of this nature could not be achieved (**Table 17**).

^v Phenol (**277**) (10 mg, 25.37 μmol, 1.0 equiv.) was dissolved in specified solvent (0.3 mL) at room temperature in a CEM microwave vial under an atmosphere of argon before addition of the specified nucleophile (0.51 mmol, 20.0 equiv.) and the resultant suspension was heated for 16 h. Temperatures reported are that of the external heating block.



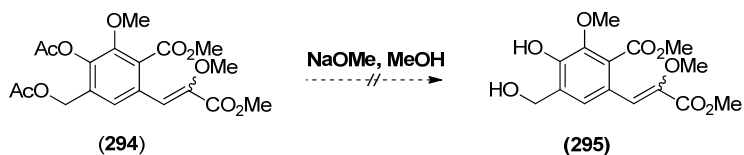
Scheme 106. Kozlowski's acetate installation

Interestingly, upon re-examination of the literature it was discovered that a similar transformation to that attempted in (Table 17) had been achieved by Kozlowski (Scheme 106).⁹⁸ In their report, phenol (292) was dissolved in Ac₂O and heated at 140 °C to promote the isohypsic functional group interconversion of the morpholine to an acetate. The author presumes that this occurs *via* an *o*-QM intermediate, with thermal extrusion of acyl morpholine, before contemporaneous acetylation of the resultant phenol to give diacetate (293).



Scheme 107. Formation of the diacetate

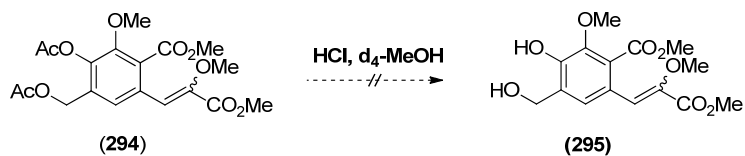
As Kozlowski's procedure appeared to offer an extremely straightforward and high yielding approach for acetate installation the reaction was probed for synthetic utility.⁹⁹ Upon subjection of (290) to the conditions outlined by Kozlowski, the author was delighted to observe formation of the corresponding diacetate (294) in 84% yield. With meaningful quantities of this material in hand, we then attempted to chemoselectively remove either one or both of the acetyl esters.



Scheme 108. Attempted hydrolysis of (294) under basic conditions

Diacetate (294) was then treated with NaOMe (2.0 equiv.), in anhydrous methanol at 0 °C until TLC analysis indicated consumption of the starting material (Scheme 108).¹¹² Unfortunately upon further inspection the reaction appears to afford a mixture of hydrolysis products, although it is difficult to know if this hydrolysis occurs during the reaction or upon addition of a Brønstead acid to neutralise any alkoxides present. No improvement in product recovery was exhibited using a variety of aqueous and anhydrous

acids for this purpose (HCl, NH₄Cl, AcOH, PTSA, citric acid or camphorsulfonic acid), so the approach was abandoned.



Scheme 109. Attempted hydrolysis of (287) under acidic conditions

The analogous reaction was attempted under acidic conditions using anhydrous HCl in MeOH at 0 °C. After 20 minutes TLC analysis indicated complete consumption of the starting material and the reaction mixture was passed through a short plug of alumina and concentrated under reduced pressure. Unfortunately GC/MS and ¹H NMR analysis of the reaction mixture appeared to indicate mixtures of demethylated products. To ascertain the relative rates of hydrolysis, the reaction was carried out in deuterated methanol in a Young's tube at 25 °C (**Figure 20**). Unfortunately from the results of this experiment it appears that the methyl ester hydrolysis occurs at a comparative rate to that of the acetyl group and that this was not a viable approach.^w

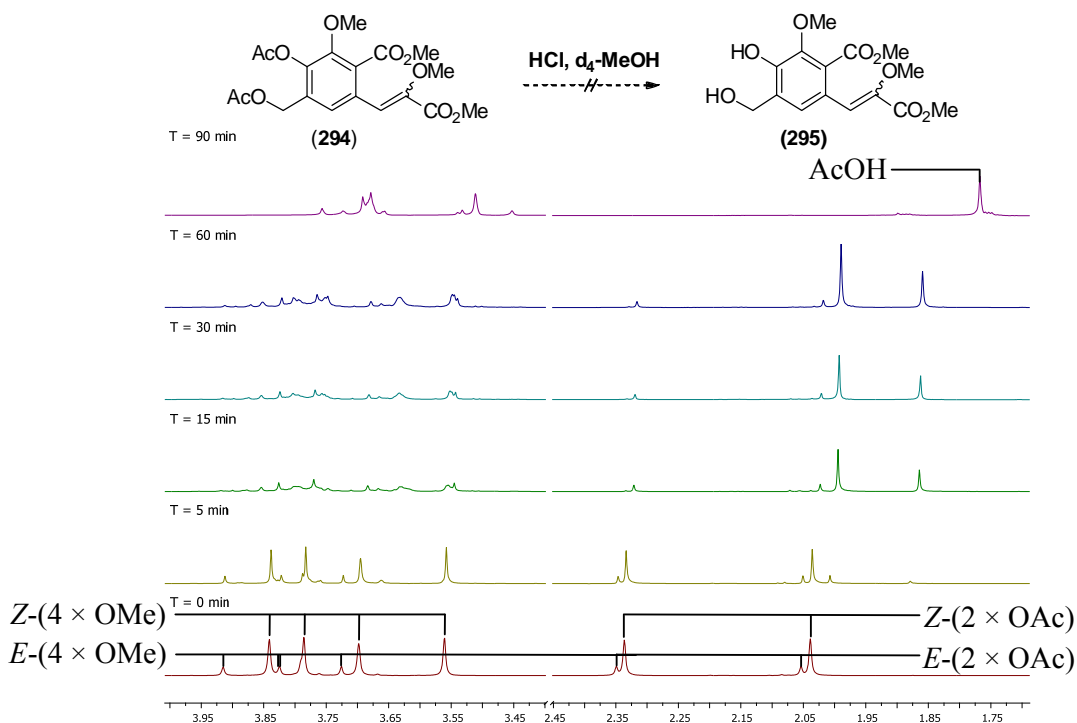
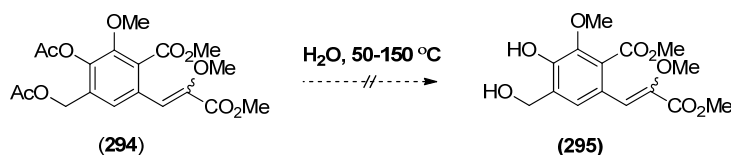


Figure 20. ¹H NMR hydrolysis experiment

^w Product mixtures analysed by ESI and GC/MS appeared to show minimal deuterium incorporation.

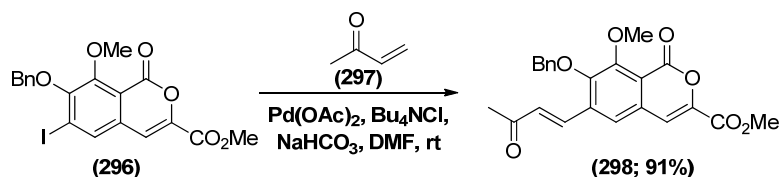


Scheme 110. Attempted hydrolysis of (287) via an *o*-QM

Another *o*-QM approach similar to (Scheme 104) was also considered. In this approach the diacetate was heated in distilled deionised water for 16 hours at a range of temperatures (50-150 °C) (Scheme 110).^x Unfortunately only mixtures of hydrolysis products similar to those isolated previously (Schemes 108 and 109) and hydrolysis approaches were abandoned, in favour of exploring the potential of (290) as an *o*-QM precursor.

Although this was not the desired transformation the author has initially envisaged, it is known from the work of Wilson and co-workers benzylic morpholine substituents can be employed as effective leaving groups to generate an *o*-QM (Scheme 26).⁶⁹

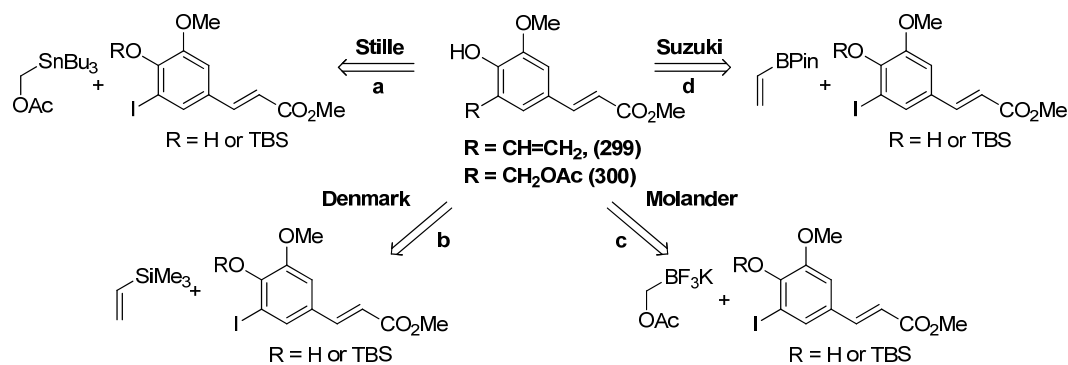
4.13 Cross-Coupling Strategy



Scheme 111. Reißig's isocoumarin cross-coupling reaction

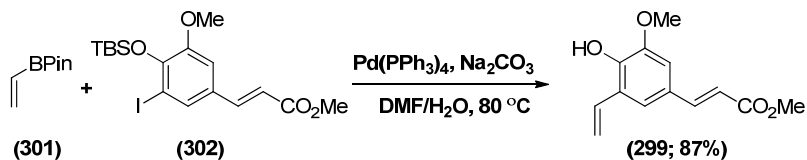
Due to the precedent by Reißig and co-workers that iodide installation *ortho* to the phenol of the desired isocoumarin followed by palladium catalysed cross-coupling is not only possible but also facile and high yielding (Scheme 111), this seemed like an atom efficient method of vinyl installation for an envisaged selective olefin oxidation.

^x Diacetate (294) (10 mg, 24.38 μmol) was dissolved in H₂O (0.2 mL) at room temperature in a CEM microwave vial and heated at the desired temperature for 16 h. Temperatures reported are that of the external heating block.



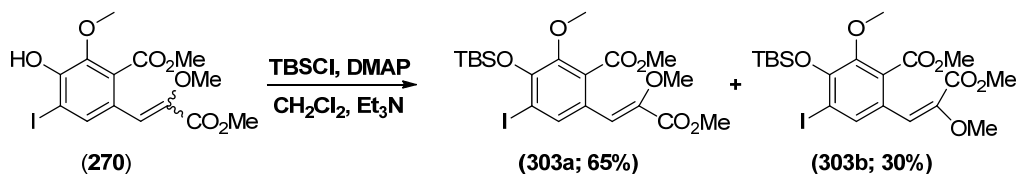
Scheme 112. Overview of initial cross-coupling reactions explored

From a model study (**Scheme 112**)¹¹³ it was found that Suzuki coupling was capable of facilitating this transformation, however this was only possible when the phenol was protected as a silyl ether, which was quantitatively cleaved in the reaction, perhaps in a concerted elimination event inferred from the TLC and GC/MS analysis.



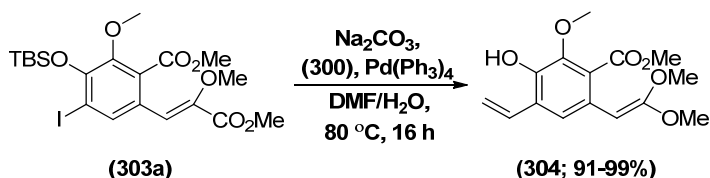
Scheme 113. Model Suzuki conditions

With vinylation conditions from our model system in hand, coupled with the observation that the solubility of advanced intermediates decrease significantly upon annulation to the isocoumarin, iodophenol (**270**) was investigated for synthetic utility. Gratifyingly upon conversion of phenol (**270**) to the requisite novel silyl ether, diastereomers (**303a**) and (**303b**) could be separated *via* silica gel chromatography (**Scheme 114**).^y



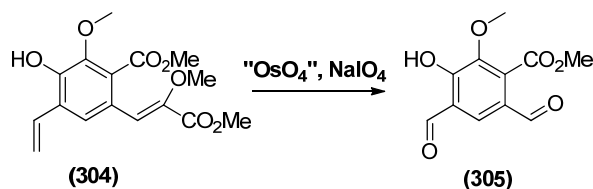
Scheme 114. Silyl ether protection of (**270**)

^y Stereochemical assignment inferred from ¹H NMR spectra was confirmed *via* X-ray crystallography.



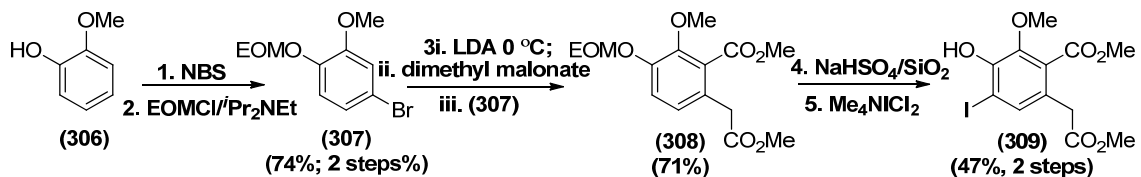
Scheme 115. Vinyl installation

Gratifyingly, upon subjection of **(303a)** to the aforementioned Suzuki reaction conditions (**Scheme 115**), formation of the desired *ortho*-vinylic phenol **(304)** proceeded without incident in excellent yield (91-99%). Unfortunately, using Upjohn¹⁴, Poli¹⁵ and Sharpless asymmetric dihydroxylation¹⁶ conditions, vinyl-selective dihydroxylation could not be achieved (**Scheme 116**), and thus upon *in situ* treatment with sodium periodate resulted in the dialdehyde **(305)**.^z



Scheme 116. Attempted selective olefin oxidation

Having established a cross-coupling route towards benzaldehyde formation *via* the aforementioned route would not tolerate olefin **(304)**, our attention then turned towards Brimble's formal synthesis product (**184**; **Scheme 57**). It was anticipated that removing the olefin and therefore late stage dihydroxylation competition, this would allow for the key acetate product to finally be generated.

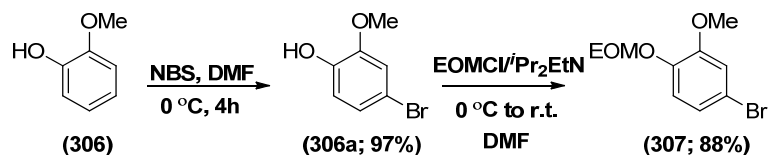


Scheme 117. Brimble's synthesis of iodophenol **(309)**

During the synthesis of advanced intermediate (**190**, **Scheme 56**), Brimble reported that iodophenol **(309)** could be generated in 5 steps from commercially available and

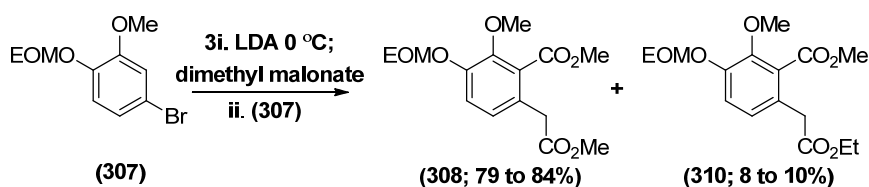
^z Background reaction was ran osmium free with sodium periodate, confirmed no olefinic oxidizing side-reactions were occurring during this step.

inexpensive guaiacol in 25% overall yield. Frustratingly, no supporting information regarding the synthesis or characterisation of intermediates (**307-300**) was reported in Brimble's manuscript and so had to be investigated by the author.



Scheme 118. Synthesis of bromide (**307**)

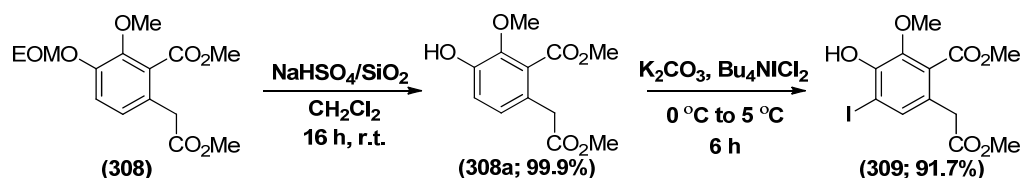
Fortunately in 2012 Kan and co-workers¹¹⁷ published a scalable and high yielding procedure for the synthesis of (**306a**), which could be replicated in the author's hands on 50 g scale. The resultant phenol, could then be protected as the corresponding methyl ethyl ether (**307**) using either Hünigs base (87.7%) or K_2CO_3 (81.2%).^{aa}



Scheme 119. Synthesis of unsaturated diester (**308**)

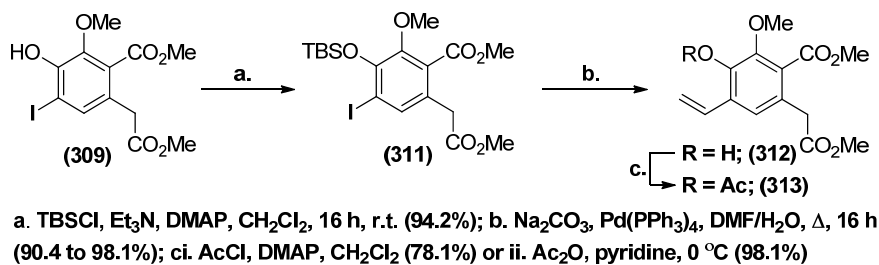
Unfortunately replication of the following step initially proved more challenging as the reaction conditions were simply described as “LDA, THF, 0 °C, 0.5 h, then dimethyl malonate, 0 °C, then [(**307**)], THF, 0 °C”. After a number of attempts the author found that when using freshly distilled solvents and reagents, the reaction could be replicated in a reproducible (79.2 to 81.4%) manner by deprotonation of dimethyl malonate (1.2 equiv.) with LDA (2.4 equiv.) at 0 °C over 30 minutes, before dropwise addition of a solution of (**307**) (1.0 equiv.) in THF over ten minutes (**Scheme 119**). The reaction mixture was then held at 0 °C for a further 30 minutes, before quenching the reaction with MeOH in attempt to limit the formation of the ethyl ester (**310**).

^{aa} Telescoping of this procedure could also be achieved by filtering the reaction mixture after bromination in 71.1% overall yield.



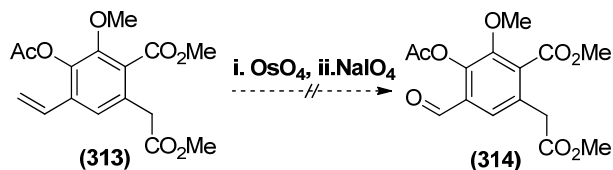
Scheme 120. Deprotection and Iodination

Gratifyingly, deprotection of the phenol (**308**) could be achieved quantitatively and iodination could be achieved in 91.7% yield using K_2CO_3 in place of $NaHCO_3$, and not allowing the reaction temperature to rise above 5 °C, thus avoiding degradation of the starting material.



Scheme 121. TBS protection and vinyl installation

Gratifyingly, after silyl deprotection of (**309**), the resultant iodide (**311**) could be converted to novel styrene (**312**) *via* the previously established Suzuki conditions (**Scheme 121**). It was then found that using Ac_2O in pyridine was the preferred method of acyl protection, to furnish the desired novel styrene (**313**) in up to 86.9% overall yield (three steps).



Scheme 122. Attempted periodate cleavage

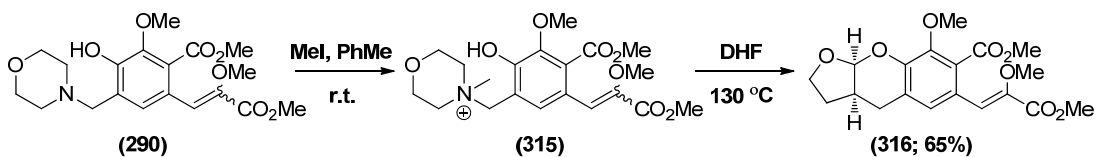
Unfortunately, after several attempts using Upjohn, Poli, and Sharpless asymmetric dihydroxylation conditions, followed by treatment with $NaIO_4$ (1.0 equiv.), compound (**314**) could not be isolated cleanly due to various over oxidation and degradation products. Due to the author's inability to generate the fully elaborated acetate initially envisaged (**272**) in combination with pressure on this projects timeline, attempts were

then focussed upon investigating the employment of morpholine (**290**) in a similar fashion to that described in (**Scheme 26**).

hetero-Diels-Alder

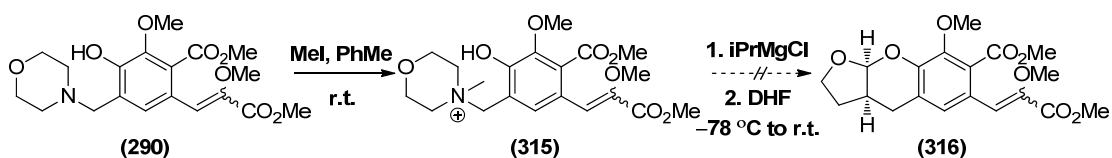
Approaches

4.14 Morpholine *hetero*-Diels-Alder Strategy



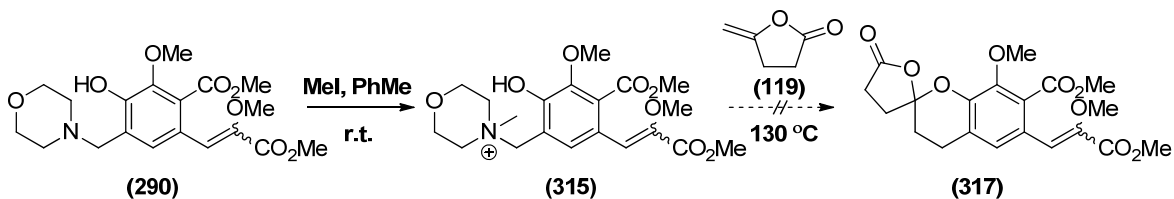
Scheme 123. *h*DA reaction of morpholinium salt

Encouragingly an initial proof of concept reaction using conditions outlined by Wilson (**Scheme 123**) showed that the advanced morpholine intermediate (**290**) can form an *o*-QM, which undergoes [4+2] cycloaddition using DHF as a simple 2π component at 130 °C to give the novel furan (**316**) as the major product in 65% isolated yield. It was therefore anticipated that with further optimisation this reaction could be undertaken using a base mediated approach under kinetic conditions.



Scheme 124. Attempted base initiated *h*DA

Frustratingly no reaction was observed when the morpholinium species was warmed in the presence of DHF and *i*PrMgCl from -78 °C to r.t. and subsequent heating resulted in a complex mixture (**Scheme 124**). Clearly in this case methyl morpholine was not a suitable leaving group for application in a low-temperature initiation approach.



Scheme 125. Attempted spiroketal formation

In an attempt to generate a spiroketal *via* this protocol, the thermal protocol was repeated using γ -methylene- γ -butrolactone¹¹⁸ in a protocol analogous to earlier reports by Bray (**Scheme 34**). Unfortunately attempting the reaction at a range of temperatures (50 to 130 °C) and reaction times (8 to 48 h), just resulted in complex mixtures (**Scheme 125**),

which contained no indicative signs of product formation, so this approach was abandoned. Following on from this, attempts to convert the quaternary ammonium salt (**315**) to an acetate in a similar fashion to previous attempts (**Table 17**), furnished a similar outcome (**Table 18**).

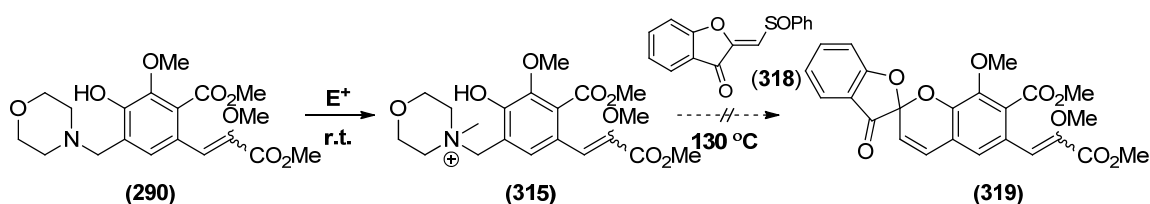
Entry	Electrophile	Nucleophile	Solvent	Temp. (°C)	Yield (%)
1	MeI	NaOAc	PhMe	130	0
2	MeI	KOAc	PhMe	130	0
3	MeI	CsOAc	PhMe	130	0
4	MeI	NaOAc	PhMe	150	0
5	MeI	KOAc	PhMe	150	0
6	MeI	CsOAc	PhMe	150	0
7	(CF ₃ CO) ₂ O	CsOAc	PhMe	150	0
8	Tf ₂ O	CsOAc	PhMe	150	0
9	AcCl	CsOAc	PhMe	150	0
10	BnBr	CsOAc	PhMe	150	0
11	MeI	NaOAc	MeCN	130	0
12	MeI	KOAc	MeCN	130	0
13	MeI	CsOAc	MeCN	130	0

Table 18. Attempted acetate installation^{bb}

As a considerable amount of the starting material had been generated it was envisaged that perhaps the strategy could be adapted towards a thermally stable 2π partner. The most thermodynamically stable benzofuran previously reported to undergo *h*DA reactions with *o*-QMs are those described by Xie and Li (**Scheme 31**). It was therefore hoped that

^{bb} Phenol (**290**) (10 mg, 25.37 μ mol, 1.0 equiv.) was dissolved in specified solvent (0.3 mL) at room temperature in a CEM microwave vial under an atmosphere of argon before addition of an electrophile (25.11 μ mol, 0.99 equiv.) at 0 °C. The reaction mixture was allowed to warm up to r.t. and was stirred for a further 3 h, before addition of the specified nucleophile (0.51 mmol, 20.0 equiv.) and the resultant suspension was heated for 16 h. Temperatures reported are that of the external heating block.

subjection of **(315)** to conditions outlined in Xie and Li's reports would allow for the generation of the unsaturated spiroketal **(319)**.



Scheme 126. Overview of attempts to employ a sulfoxide as an electrophile

Unfortunately initial attempts towards this goal (**entry 1, Table 19**), did not appear to be successful with respect to generation of a spiroketal, with no representative signals present during NMR analysis of the resultant mixture (**Figure 21**).

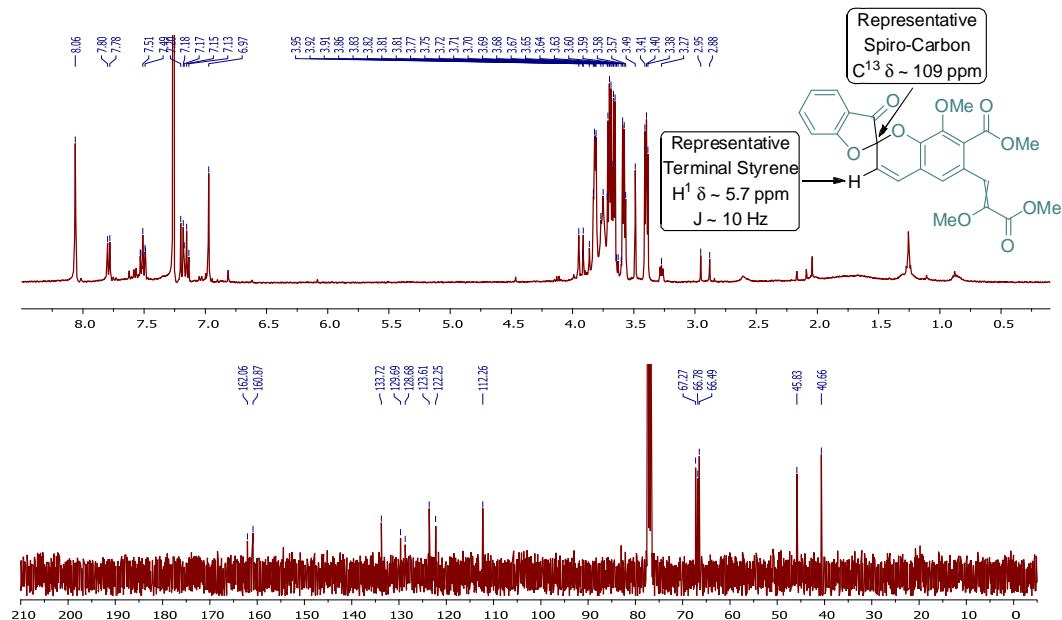
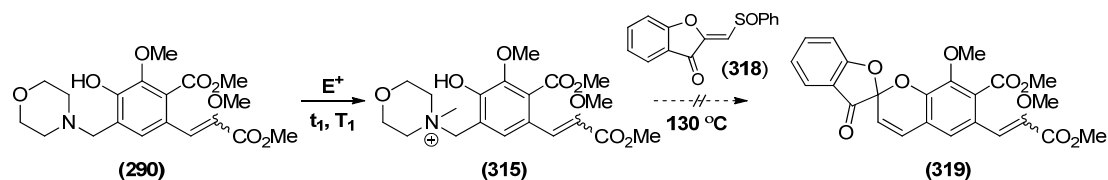


Figure 21. Crude ^1H and ^{13}C NMR analysis from the reaction described in (**Scheme 127**)

Unfortunately, increasing the amount of the sulfoxide **(318)** had no affect of the overall result of this protocol (**entries 2 and 3, Table 19**), even when leaving the reaction for 39 hours. As Li and Xue's procedure was described at 110 °C, it was proposed that above this temperature the sulfoxide may be unstable and therefore degrade before it could react with the *o*-QM. However, when the reaction was repeated at this temperature (**entries 4 and 5**), no product was detected after 16 or 39 hours.



Entry	2 π component		Electrophile		t_1 (h)	T_1 ($^\circ\text{C}$)	t_2 (h)	T_2 ($^\circ\text{C}$)	Conversion (%)
	R =	equiv.	E^+ =	equiv.					
1	SOPh	1.0	MeI	0.99	2.0	0 to rt	16	130	0
2	SOPh	5.0	MeI	0.99	2.0	0 to rt	39	130	0
3	SOPh	10.0	MeI	0.99	2.0	0 to rt	39	130	0
4	SOPh	10.0	MeI	0.99	2.0	0 to rt	16	110	0
5	SOPh	10.0	MeI	0.99	2.0	0 to rt	39	110	0
6	SOPh	10.0	MeI	0.99	2.0	0 to 40	39	110	0
7	SOPh	10.0	MeI	1.05	24.0	0 to rt	39	130	0
8	SOPh	10.0	MeI	1.30	24.0	0 to rt	39	130	0
9	SPh	10.0	MeI	0.99	2.0	0 to rt	39	110	0
10	NMe ₂	10.0	MeI	0.99	2.0	0 to rt	39	110	0
11	SOPh	10.0	(CF ₃ CO) ₂ O	1.05	3.0	0 to rt	39	110	0
12	SOPh	10.0	Tf ₂ O	1.05	3.0	0 to rt	39	110	0
13	SOPh	10.0	AcCl	1.05	5.0	0 to rt	39	110	0
14	SOPh	10.0	BnBr	1.05	4.5	0 to rt	39	110	0
15	SOPh	10.0	<i>p</i> NO ₂ BnCl	1.05	8.5	0 to rt	39	110	0
16	SOPh	10.0	<i>p</i> NO ₂ BnCl+NaI	1.05	6.0	0 to rt	39	110	0

Table 19. Attempted unsaturated spiroketal formation

To try and attenuate the risk that the morpholine wasn't sufficiently alkylated, the temperature of the initial alkylation step was increased to $40\text{ }^\circ\text{C}$ after warming to r.t. but again, this could not promote product formation (**entry 6**). Similar results, were also achieved using an excess of alkylating agent, at r.t. for 24 hours (**entries 7 and 8**).

The reaction was also attempted using the amino and thioether intermediates used to synthesise (318) (**entries 9 and 10**), however this avenue of investigation was equally unsuccessful. It was then proposed that perhaps a more electron withdrawing quaternising agent would lower the activation energy of the *o*-QM initiation and promote

product formation. Unfortunately, our results did not reflect this hypothesis (**entries 11-16**).

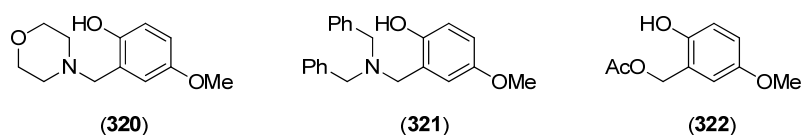


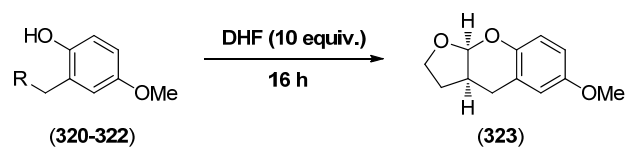
Fig. 21. Model substrates screened

Due to the persistently unsuccessful nature of these protocols, it was hoped that perhaps by comparing the reactivity of some model compounds (**Fig. 21**), a more synthetically useful reaction could be uncovered in order to facilitate the synthesis of γ -rubromycin (**Table 20**). In this study phenols (**320**; R = Morpholine), (**321**; R = NBN₂) and (**322**; R = OAc)^{cc} were compared to establish their relative reactivity rates and to see if the conditions for *o*-QM formation could be carried out in a milder fashion.

Initially, the model phenols were then subjected to the *h*DA conditions (**entries 1-3, Table 20**) previously used to generate benzopyran (**316**; **Scheme 123**). Unfortunately, under these conditions both of the benzylamines (**320**) and (**321**) performed markedly worse than acetate (**322**).

It was again proposed that perhaps a more electron withdrawing quaternising agent would lower the activation energy of the *o*-QM initiation and increase yields but again, our results did not reflect this hypothesis (**entries 4-7**). Having no encouragement for this strategy, our attention was then turned towards concentrating the reaction mixture, in the hope that the 2π component would become more accessible to the reactive intermediate.

^{cc} Compound was synthesised previously by Dr. C.D. Bray as part of a different investigation.



Entry	Electrophile	Phenol	Solvent	Temp. (°C)	Yield (%)
1	MeI	320	PhMe	130	50
2	MeI	321	PhMe	130	51
3	-	322	PhMe	130	67
4	Tf ₂ O	320	PhMe	130	36
5	Tf ₂ O	321	PhMe	130	48
6	(CF ₃ CO) ₂ O	320	PhMe	130	39
7	(CF ₃ CO) ₂ O	321	PhMe	130	45
8	MeI	320	PhMe ^{dd}	130	66
9	MeI	321	PhMe ²³	130	68
10	MeI	320	PhMe ²³	110	48
11	MeI	321	PhMe ²³	110	52
12	-	322	-	110	56
13	MeI	320	PhMe ²³	130 ^{ee}	67
14	MeI	321	PhMe ²³	130 ³⁰	71
15	-	322	-	130 ³⁰	85
16	-	320	-	130 ³⁰	79
17	-	321	-	130 ³⁰	82
18	-	320	-	110 ³⁰	58
19	-	321	-	110 ³⁰	63
20	-	320	-	150 ³⁰	42
21	-	321	-	150 ³⁰	37

Table 20. Optimisation of *h*DA conditions

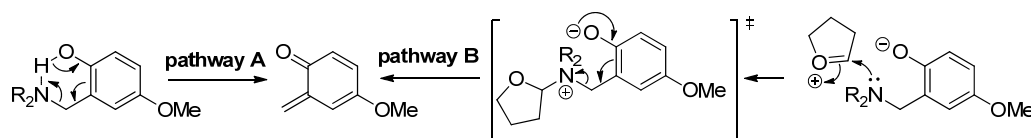
Gratifyingly, upon removal of the toluene after quaternisation, the reaction was found to proceed in comparable yields to that previously observed using the acetate (**entries 3, 8 and 9**). This trend was also observed when the reaction temperature was lowered to 110 °C, however product conversion was markedly reduced (**entries 10-12**).

^{dd} Solvent was removed under reduced pressure at r.t. prior to addition of DHF.

^{ee} Reaction mixture was heated in a microwave.

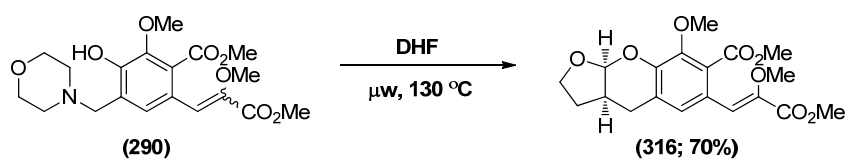
Interestingly, upon repeating the reaction in a microwave reactor at 130 °C yields could be meaningfully increased for the acetate but not for the quaternised benzylamines (**entries 13-15**).

Rather surprisingly, when the reaction was repeated without a quaternising agent, the reaction proceeded in an increased and comparable yield to that acetate (**entries 15-17**). It also appeared that this temperature was reasonably optimised for this transformation, as yields were significantly reduced by decreasing (**entries 18-19**) and increasing (**entries 20-21**) the temperature by 20 °C.



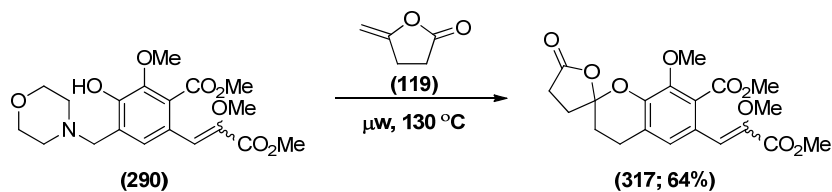
Scheme 127. Potential mechanisms of *o*-QM formation

Although this reaction has not been investigated mechanistically, it is proposed that perhaps the phenolic proton migrates onto the nitrogen atom in a concerted elimination reaction, which is supported by the deshielded nature of the ¹H NMR signals around 10.2 ppm (**pathway A, Scheme 127**). The alternative hypothesis (**pathway B**), may be that DHF is functioning as the quaternising agent, and the reaction proceeds *via* a similar pathway to those seen previously.



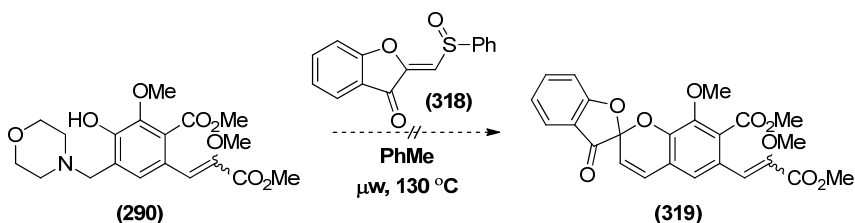
Scheme 128. Microwave assisted *h*DA reaction

Although these reaction conditions (**Table 20, entry 16**) didn't appear to be much milder, repeating the protocol with phenol (**290**), the desired product was furnished in slightly improved overall yield (70%) and perhaps more importantly, purification *via* silica gel chromatography was significantly more facile.



Scheme 129. Microwave assisted spiroketal formation

Upon subjection of phenol **(290)** to the same reaction conditions using γ -methylene- γ -butyrolactone as the solvent, it was with great delight that spiroketal **(317)** was isolated in 64% overall yield. This was a significant step forward in the pursuit of a modular approach to the rubromycins and synthetic analogues *via* a *hetero*-Diels-Alder methodology.

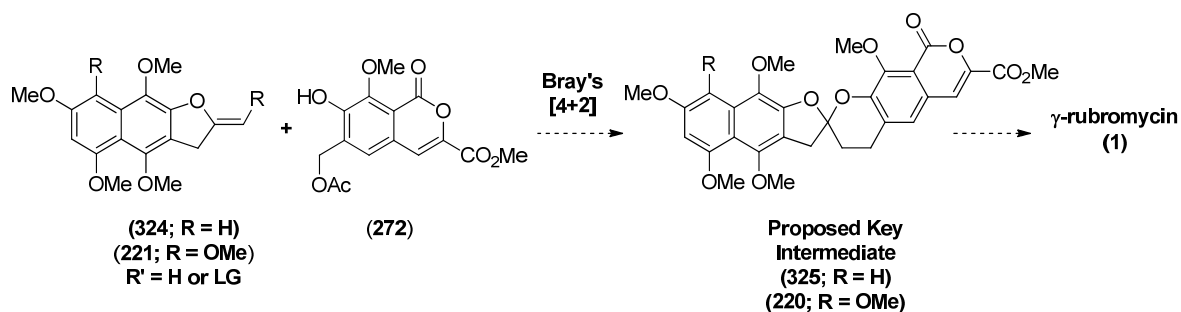


Scheme 130. Attempted microwave assisted *bis*-benzannulated spiroketal formation

Unfortunately, upon resubjection of the sulfoxide **(318)** to the reaction conditions, it was not possible to generate a *bis*-benzannulated [5,6]-spiroketal *via* this approach (**Scheme 130**). For this reaction to prove suitable for the synthesis fully elaborated rubromycins, a great deal of optimisation is still required, to reduce the initiation temperature of *o*-QM formation.

Summary & Conclusions

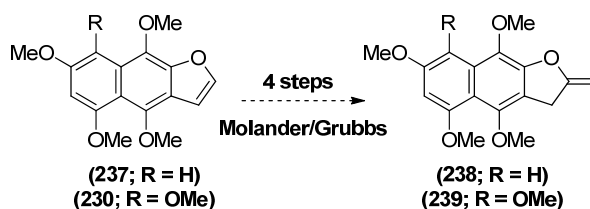
4.15 Summary and Conclusion



Scheme 131. Proposed synthesis of γ -rubromycin

At the outset of this project, our aim was to try and establish a general, robust method of synthesising the rubromycins *via* a [4+2] cycloaddition (**Scheme 131**). Although γ -rubromycin and heliquinomycinone had been synthesised previously by Kita⁴⁵ and Danishefsky¹⁰⁹ respectively, there was still ample scope for development of a definitive, modular approach to these highly intriguing molecular scaffolds.

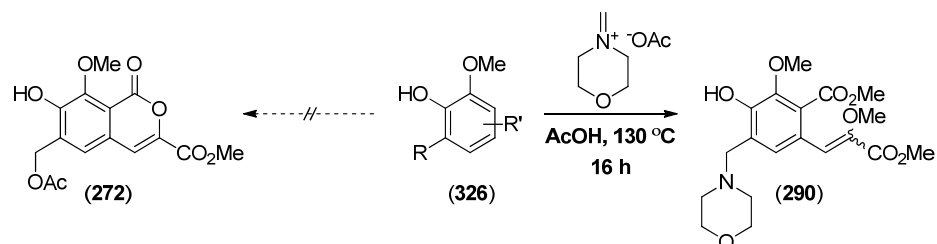
Our motivations to develop this methodology were twofold: firstly to investigate the synthetic utility of Bray's [4+2] cycloaddition chemistry, and secondly to provide a modular approach to unnatural rubromycin analogues to elevate their status as potential medicinal chemistry lead compounds.



Scheme 131. Proposed methylene installation

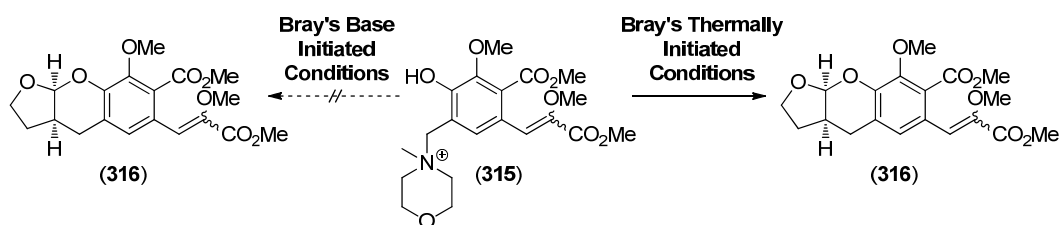
Preliminary investigations allowed us to generate the desired naphthazarin subunits (**Scheme 69 and 73**), and having replicated the literature results of Molander and Grubbs (**Scheme 78**), this appeared to be a promising strategy to synthesise the desired *exo*-enol ethers (**238**) and (**239**) (**Scheme 132**). However, the author believed that it would be prudent not to commit samples of (**230**) or (**237**) to this methylene installation strategy until conditions for generating the key electron deficient *o*-QM (**222**) were established.

This strategy would offer the advantage of allowing us to establish whether or not this reactive 2π species would need to be stabilised in some way (e.g. **221**; $R' = \text{SOPh}$) to tolerate said *o*-QM generation conditions.



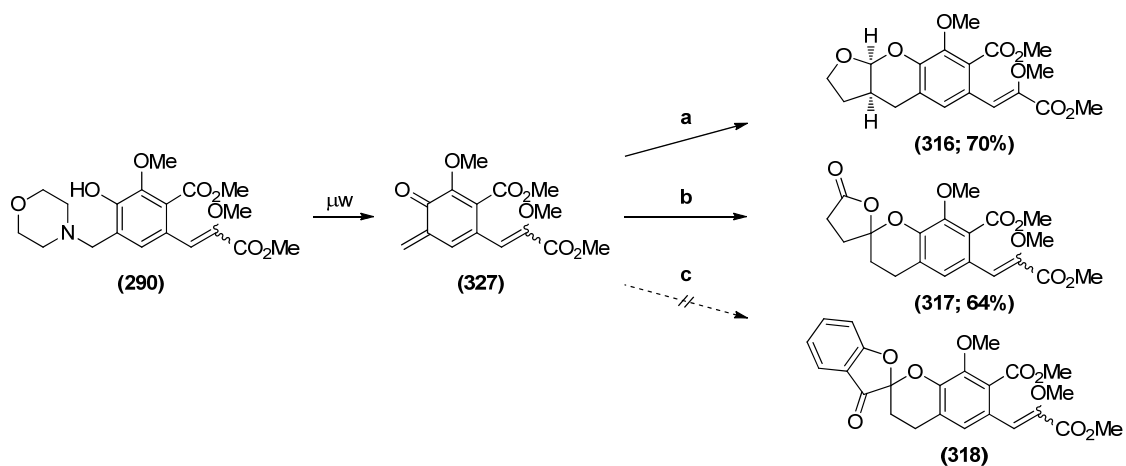
Scheme 132. Adaptation of the strategy towards morpholine leaving groups

In our attempts to achieve this goal, a number of synthetic routes towards the key *o*-QM precursor (**272**) were explored. Although a number of novel isocoumarins, and isocoumarin synthons (**326**) could be generated, unfortunately these could not be converted into (**272**) as anticipated. Fortunately, the author was able to build upon the work of Wilson⁸⁶ and substitute the benzylic acetate leaving group with the more synthetically accessible morpholine (**290**) (**Scheme 132**).



Scheme 133. Synthetic utility of morpholinium (**315**) in Bray's base and thermally initiated methodologies

Although, this compound had no synthetic utility under Bray's base-initiated conditions, gratifyingly under thermal conditions, *o*-QM (**323**) could be generated and trapped reliably by [4+2] cycloaddition with DHF (**Scheme 133**). This was a key achievement for this project as to the author's knowledge, a [4+2] cycloaddition had never been achieved with such an electron-deficient *o*-QM (**Scheme 124**).



a. DHF, 130 °C (μW), 16 h; b. γ -methylene- γ -butyrolactone, 130 °C (μW), 16 h; c. (318, 0.25M in PhMe), 130 °C (μW), 16 h.

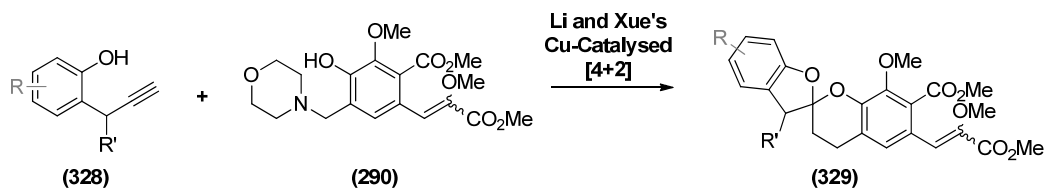
Scheme 134. Scope of the microwave promoted *h*DA reaction

Building on this methodology, the author also discovered that upon irradiation in a microwave reactor, that morpholine (290) could be converted into *o*-QM (327) without the need to alkylate the amine (Scheme 128). This is to the author's knowledge, the first example of such a transformation, however a precise mechanism is currently unknown at this time.

Frustratingly, despite numerous attempts, this protocol could not be adapted towards the synthesis of a [5,6]-*bis*-benzannulated spiroketal during the course of this investigation (Scheme 134). However, after further optimisation of the reaction conditions, [4+2] cycloaddition between *o*-QM (323) and γ -methylene- γ -butyrolactone (119) could be achieved, affording spiroketal (317) (Scheme 130).

Although this reaction could not be achieved at low temperature as originally envisaged, this study does provide a proof of concept that synthetic rubromycin analogues such as (317) can be generated using this novel microwave promoted [4+2] cycloaddition. It is hoped that with further development, this may prove to be a viable strategy for the synthesis of the rubromycins and other synthetic analogues.

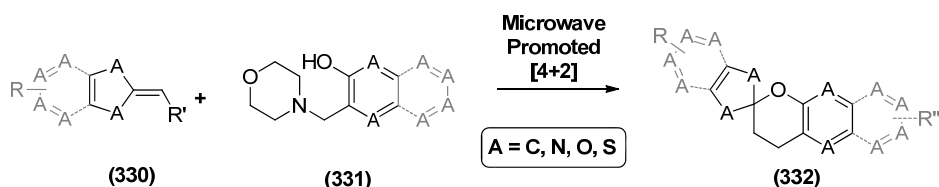
4.16 Future Work



Scheme 135. Adapted [4+2] strategy towards the rubromycins

To adapt this microwave promoted cycloaddition protocol, towards this project's ultimate goal of synthesising members of the rubromycin family, it is proposed that investigation of more thermally stable 2π components may hold the key to achieving this transformation.

One particularly attractive strategy would be to generate both the 2π and 4π components *in situ* by adapting Li and Xue's recently developed copper catalysed [4+2] system (Scheme 44a and 44b) to the author's microwave promoted [4+2] approach (Scheme 135).



Scheme 136. Exploration of microwave promoted [4+2] strategy to generate synthetic rubromycins with improved physicochemical properties

It is also of note that installation and elimination of the benzylic morpholine to generate an *o*-QM requires less synthetic steps compared with all other benzylic leaving group installation/elimination strategies (Scheme 25). As this approach also appears to be more tolerant to electron deficient phenols, this protocol may prove to be a useful general tool for the construction of [5,6]-benzannulated spiroketals in two steps from commercially available phenols and *exo*-enol ethers (Scheme 136).

Chapter 5:
Experimental

5.1 Experimental

I. General Information: Unless otherwise stated, commercially available reagents were used as supplied. All reactions requiring anhydrous conditions were conducted in flame-dried apparatus under an inert atmosphere of nitrogen or argon. Microwave heating was conducted in 10 mL thick walled microwave vials (microwave) fitted with crimp top Teflon seals. Analytical thin-layer chromatography (TLC) was performed on silica gel plates (0.25 mm) precoated with a fluorescent indicator. Standard flash chromatography procedures were performed using Kieselgel 60 (40-63 μm) or with a Varian Superflash automated purification system. Petroleum refers to the fraction boiling between 40-60 $^{\circ}\text{C}$.

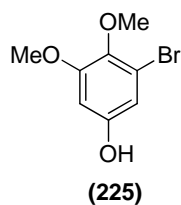
Infrared spectra were recorded in the range 4000-600 cm^{-1} , using a Bruker Tensor 37 FTIR machine equipped with a PIKE MIRacle ATR accessory. IR signals are reported in wavenumbers (cm^{-1}) and signal intensity is subjectively denoted br = broad, brs = broad (strong), brm = broad (medium) s = strong, m = medium and w = weak.

Both ^1H and ^{13}C NMR spectra were recorded using either a Bruker AV400 NMR or AV600 spectrometer. Chemical shifts δ are reported in ppm (relative to δ_{H} CHCl_3 (7.27) and δ_{C} CDCl_3 (77.0) unless otherwise stated) and multiplicity of signals denoted: s = singlet, d = doublet, t = triplet, q = quartet, and m = multiplet respectively with coupling constants (J) reported in hertz (Hz). Structural interpretations and assignments were made based upon COSY, HMQC, HMBC, DEPT 135, DEPT 90 and NOESY experiments and denoted as follows: (^1H NMR) ArCH = aryl proton, Me = CH_3 of a methyl group, MeO = CH_3 of methoxy group, CO_2Me = CH_3 of methylester, CO_2H = H of carboxylic acid, OH = H of alcohol, $\text{CH}_a=\text{CH}_b$ or $\text{CH}=\text{C}_{\text{quat}}$ = single alkenyl proton, CHO = aldehyde proton, SiMe_2^tBu = $2 \times \text{Me}$ groups of TBS, SiMe_2^iBu = ^iBu group of TBS, NCH_2 = methylene protons attached to a nitrogen atom, OCH_2 = methylene protons attached to an oxygen atom; (^{13}C NMR) COMe = C atom bearing a methoxy group, $\text{C}(\text{OMe})_2$ = C atom of methoxy group, COH = C atom bearing an alcohol group, CBr = C atom bearing a bromine atom, $\text{CCN}=\text{C}$ atom bearing a nitrile group, CCN = C atom of

nitrile group, C=O= carbonyl, ArCH = aryl C bearing a hydrogen atom, C_{quat.} = quaternary carbon, ArC_{quat.} = quaternary aromatic carbon, ArCC_{quat.} = quaternary carbon fused to aryl ring, CH₂ = methylene carbon, CH₃ = methyl carbon, CO₂H = C atom of carboxylic acid, CO₂Me = C atom of methyl ester (C=O), CO₂Me = C atom of methyl ester (CH₃), CH_a=CH_b or CH=C_{quat.} = alkenyl carbon.

GC/MS spectra were recorded using an Agilent 6890gc and 5973 msd instrument. High resolution mass spectra (HRMS) were obtained by the EPSRC National Mass Service (Swansea) using a double focussing mass spectrometer (Finnigan MAT 95 XP).

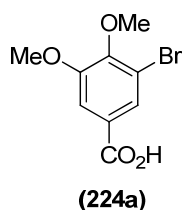
II. Experimental Procedures and Compound Characterisation



5-Bromo-3,4-dimethoxyphenol (225).⁹⁰ *m*-Chloroperbenzoic acid (4.75 g, 27.5 mmol, 1.5 equiv.) was added in one portion to a solution of 5-bromo-3,4-dimethoxybenzaldehyde (**(224)**) (4.50 g, 18.4 mmol, 1.0 equiv.) in CH₂Cl₂/H₂O (68 : 2 mL) before heating to reflux for 16 hours. The reaction mixture was carefully added to vigorously stirred sat. aq. NaHCO₃ solution (30 mL) and stirring was continued for 30 minutes before extracting the aqueous layer with CH₂Cl₂. The combined organic phases were successively washed with sat. aq. NaHCO₃ solution (30 mL), and sat. aq. Na₂S₂O₅ solution (30 mL) (test for peroxides negative) and sat. aq. NaCl solution (30 mL). The organic phase was dried over MgSO₄, before concentrating to a crude tan oily solid under reduced pressure.

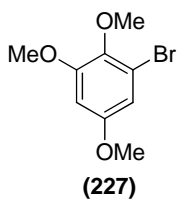
The residue was dissolved in MeOH (10 mL) before addition of 6M HCl (10 mL) and the mixture was stirred at r.t. for 30 minutes. The MeOH was then removed under reduced pressure and the remaining aqueous solution was extracted with Et₂O (3 × 150 mL). The combined organic layers were dried over MgSO₄ before concentrating to an off-white solid under reduced pressure. The title compound was then purified using flash chromatography (EtOAc:Petroleum; 1:4) to afford the title compound (**(225)**) as a white solid (3.75 g, 16.2 mmol, 88%).

mp = 97-98 °C; *R*_f = 0.19 (EtOAc:Petroleum;1:4); *v*_{max} (film)/cm⁻¹ 3286br (OH), 2947w and 2933w (CH), 2836w (CH₃), 1608m and 1578m (C=C); ¹H NMR (400 MHz, d₆-acetone) δ = 8.42 (brs, 1H, OH), 6.59 (d, *J* = 2.7 Hz, 1H, ArCH), 6.50 (d, *J* = 2.7 Hz, 1H, ArCH), 3.80 (s, 3H, OMe), 3.68 (s, 3H, OMe); ¹³C NMR (100.0 MHz, d₆-acetone) δ = 155.2 (COMe), 155.2 (COMe), 140.5 (COH), 117.6 (CBr), 110.9 (ArCH), 101.3 (ArCH), 60.5 (OMe), 56.2 (OMe); HRMS (EI) calcd for [C₈H₈O₃⁷⁹Br]⁻ 230.9662 and [C₈H₈O₃⁸¹Br]⁻ 232.9642; found 230.9664 and 232.9638 [M-H]⁻; spectroscopic data is in agreement with that previously reported.⁹⁰



3-Bromo-4,5-dimethoxybenzoic acid (224a). To a pre-cooled (0 °C, external) solution of 5-bromo-3,4-dimethoxybenzaldehyde (**224**) (980 mg, 4.0 mmol, 1.0 equiv.) in MeOH (25 mL) was slowly added 80% magnesium bis(monoperoxyphthalate) hexahydrate (2.48 g, 4.0 mmol, 1.0 equiv.) at -5 °C. The mixture was allowed to gradually warm to r.t. and stirred for 16 h. The crude mixture was then diluted with Et₂O (200 mL) and washed with H₂O (100 mL). The layers were then separated and the aqueous layer was extracted again further Et₂O (200 mL) and the combined organics were dried over MgSO₄, filtered and concentrated under reduced pressure to afford the *title compound* as a white solid (1.04 g, quant.).

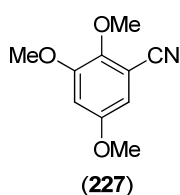
m.p. 176-178 °C; R_f = 0.44 (EtOAc:MeOH; 9:1); ν_{max} (film)/cm⁻¹ 2969br (OH), 2642w, 2605w and 2513w (CH), 1732w (O-CO), 1682s (C=O), 1589m, 1565m and 1490m (C=C); ¹H NMR (400 MHz, d₆-DMSO) δ = 13.19 (brs, 1H, CO₂H), 7.70 (s, 1H, ArCH), 7.59 (s, 1H, ArCH), 3.89 (s, 3H, OMe), 3.82 (s, 3H, OMe); ¹³C NMR (100.0 MHz, d₆-DMSO) δ = 165.6 (CO₂H), 152.1 (COMe), 149.3 (COMe), 127.7 (CCO₂H), 125.3 (ArCH), 116.9 (CBr), 113.0 (ArCH), 60.2 (OMe), 56.1 (OMe); HRMS (EI) calcd for [C₉H₈O₄⁷⁹Br]⁻ 258.9611 and [C₉H₈O₄⁸¹Br]⁻ 260.9592; found 258.9608 and 260.9583 [M-H]⁻.



2,3,5-Trimethoxybromobenzene (226).⁹¹ A solution of 5-bromo-3,4-dimethoxyphenol (**225**) (5.30 g, 22.8 mmol, 1.0 equiv.) in anhydrous acetone (150 mL) was treated with anhydrous K₂CO₃ (6.3 g, 45.5 mmol, 2.00 equiv.) and Me₂SO₄ (6.35 g, 50.4 mmol, 1.1 equiv.) under nitrogen. After 12 h stirring at r.t. under nitrogen, the reaction mixture was diluted with ice-cold distilled water (250 mL), concentrated under reduced pressure to one-third volume and extracted with EtOAc (3 × 50 mL). The organic extracts were washed with water and sat. aq. NaCl solution (30 mL) and dried over MgSO₄ before concentration under reduced pressure to afford a yellow oil that was purified using flash

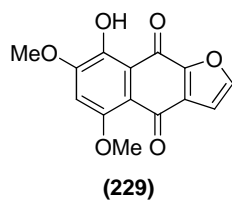
chromatography (EtOAc:Petroleum; 1:4) to afford the title compound as a pale-yellow oil (5.55 g, 22.6 mmol, 99%).

$R_f = 0.28$ (EtOAc:Petroleum,1:4); ν_{\max} (film)/ cm^{-1} 3000w, 2960w and 2937w (CH), 2835w (CH_3), 1599m, 1570m and 1489m (C=C); ^1H NMR (400 MHz, CDCl_3) $\delta = 6.63$ (d, $J = 2.5$ Hz, 1H, ArCH), 6.44 (d, $J = 2.5$ Hz, 1H, ArCH), 3.83 (s, 3H, OMe), 3.80 (s, 3H, OMe), 3.76 (s, 3H, OMe); ^{13}C NMR (100.0 MHz, CDCl_3) $\delta = 156.4$ (COMe), 153.9 (COMe), 140.6 (COMe), 117.3 (CBr), 107.9 (ArCH), 99.9 (ArCH), 60.5 (OMe), 55.6 (OMe), 55.6 (OMe); GCMS (CI) calcd for $[\text{C}_9\text{H}_{12}^{79}\text{BrO}_3]^+$ 247 and $[\text{C}_9\text{H}_{12}^{81}\text{BrO}_3]^+$ 249; found = 247 and 249 $[\text{M}+\text{H}]^+$; spectroscopic data is in agreement with that previously reported.⁹¹



2,3,5-Trimethoxybenzonitrile (227).⁸⁸ To a solution of stirred, 2,3,5-trimethoxybromobenzene (**226**) (9.5 g, 38.5 mmol, 1.0 equiv.) in anhydrous DMF (150 mL) was added copper(I) cyanide (7.2 g, 80.4, 2.1 equiv.) at r t. and the reaction mixture was heated to reflux, under nitrogen with for 16 hours. The solution was allowed to cool to r.t. before being poured into a solution of excess aqueous EDTA and stirred for 2 h. The product was then extracted with ethyl acetate before concentrating under reduced pressure to afford a brown solid. Purification of the crude material was achieved using flash chromatography (EtOAc:Petroleum, 1:4) to give the title compound as an off-white crystalline solid (7.3 g, 37.7 mmol, 98%).

mp 61-63 °C, [lit. 61-62.5 °C]; $R_f = 0.38$ (EtOAc:Petroleum; 1:4); ν_{\max} (film)/ cm^{-1} 3106w, 3006w and 2952w (CH), 2844w (OCH_3), 2233m (CN), 1593m and 1590m (C=C); ^1H NMR (400 MHz, CDCl_3) $\delta = 6.65$ (1H, $J = 2.6$ Hz, ArCH), 6.48 (1H, $J = 2.6$ Hz, ArCH), 3.89 (s, 3H, OMe), 3.81 (s, 3H, OMe), 3.78 (s, 3H, OMe); ^{13}C NMR (100.0 MHz, CDCl_3) $\delta = 156.1$ (COMe), 153.6 (COMe), 146.36 (COMe), 116.3(CCN), 106.8 (CCN), 105.8 (ArCH), 105.7 (ArCH) 61.9 (OMe), 56.0 (OMe), 55.9 (OMe); HRMS (CI) calcd for $[\text{C}_{10}\text{H}_{12}\text{O}_3\text{N}]^+$ 194.0812; found 194.0810 $[\text{M}+\text{H}]^+$; spectroscopic data is in agreement with that previously reported.⁸⁸

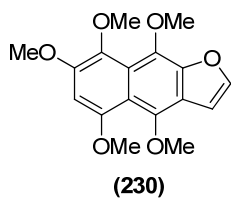


8-Hydroxy-5,7-dimethoxynaphtho[2,3-*b*]furan-4,9-dione (229).^{45,80}

To a stirred solution of 3-furoic acid (260 mg, 2.3 mmol, 1.0 equiv.) in anhydrous THF (15 mL) at $-78\text{ }^{\circ}\text{C}$ was added *t*-butyllithium (3.2 mL, 5.1 mmol, 2.2 equiv., 1.6 M in hexanes) dropwise. The solution was stirred for 2 h at $-78\text{ }^{\circ}\text{C}$, then a solution of nitrile (**227**) (500 mg, 2.6 mmol, 1.1 equiv. in 5 mL THF) was added dropwise. The reaction mixture was allowed to warm slowly from $-78\text{ }^{\circ}\text{C}$ to r.t. over 6 hours and the mixture was then stirred at r.t. for 12 h, before quenching by a slow addition of H_2O (20 mL). The mixture was extracted with Et_2O ($2 \times 30\text{ mL}$) and the dark brown aqueous layer was acidified to pH 1 with 1M HCl, stirred for 2 h, then extracted with EtOAc ($3 \times 30\text{ mL}$). The combined organic layers were dried over MgSO_4 , filtered and concentrated under reduced pressure to afford the furan (**228**) (700 mg, 2.3 mmol, quant.) as a dark brown solid. The compound was carried forward without further purification.

Furan (**228**) was then stirred in 98% sulfuric acid (8 mL) for 3 days at r.t. before carefully pouring the dark red mixture onto ice (50 g). The warmed mixture was extracted with 9:1 $\text{CH}_2\text{Cl}_2/\text{MeOH}$ (200 mL) and the organic layer was separated, dried over MgSO_4 , filtered and concentrated under reduced pressure. The crude compound was purified by flash chromatography (EtOAc:Petroleum; 5:2) to afford the title compound (**229**) as a “haem-red” solid (603 mg, 2.2 mmol, 96% over 2 steps).

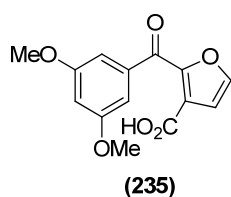
mp = $87\text{--}88\text{ }^{\circ}\text{C}$; R_f = 0.15 (EtOAc:Petroleum; 5:2); ν_{max} (film)/ cm^{-1} 3194w and 2943w (CH), 2361br (OH_{conj}), 1640s (C=O), 1479 (C=C); ^1H NMR (400 MHz, CDCl_3) δ = 13.19 (s, 1H, OH), 7.75 (d, J = 1.8 Hz, 1H, $\text{OCH}_a=\text{CH}_b$), 6.97 (d, J = 1.8 Hz, 1H, $\text{OCH}_a=\text{CH}_b$), 6.74 (s, 1H, ArCH), 4.02 (s, 3H, OMe), 4.01 (s, 3H, OMe); ^{13}C NMR (100.0 MHz, CDCl_3) δ = 178.6 (C=O), 177.7 (C=O), 156.7 (C_{quat}), 155.9 (COMe), 150.2 ($\text{OCH}_a=\text{CH}_b$), 149.9 (COMe), 149.4 (COH), 133.7 (C_{quat}), 114.9 (ArCC $_{\text{quat}}$), 111.4 (ArCC $_{\text{quat}}$), 109.5 ($\text{OCH}_a=\text{CH}_b$), 102.8 (ArCH), 57.0 (OMe), 56.4 (OMe); HRMS (CI) calcd for $[\text{C}_{14}\text{H}_{11}\text{O}_6]^+$ 275.0556; found 275.0547 $[\text{M}+\text{H}]^+$; spectroscopic data is in agreement with that previously reported.^{45,80}



4,5,7,8,9-Pentamethoxynaphtho[2,3-*b*]furan (230).^{45,80} To a solution of quinone (**229**) (97 mg, 0.35 mmol, 1.0 equiv.) in THF (1.8 mL) and H₂O (1.1 mL) were added TBAB (23 mg, 0.07 mmol, 0.2 equiv.) and Na₂S₂O₄ (85% wt., 400 mg, 1.72 mmol, 4.9 equiv.).

The mixture was stirred for 15 min, then KOH (430 mg, 7.7 mmol, 22.0 equiv.) was added to the clear solution and the resultant red/purple solution was stirred for 20 min. Me₂SO₄ (290 μL, 3.15 mmol, 9.0 equiv.) was added and the solution was stirred for a further 2 h before addition of 10% aq. ammonium hydroxide solution (4.0 mL). The orange/yellow solution was stirred for a further 16 h at r.t., diluted with H₂O (20 mL) and extracted with EtOAc (3 × 50 mL). The combined organic layers were collected and dried over MgSO₄ before concentrating under reduced pressure. The crude product was then purified using flash chromatography (EtOAc:Petroleum, 1:2 → 1:1) to provide the title compound as a pale yellow solid (61 mg, 0.19 mmol, 55% yield).

mp = 71-73 °C; *R*_f = 0.30 (EtOAc:Petroleum, 1:1); *v*_{max} (film)/cm⁻¹ 2935w and 2837w (CH), 1487m and 1450m (C=C); ¹H NMR (400 MHz, CDCl₃) δ = 7.59 (d, *J* = 2.4 Hz, 1H, OCH_a=CH_b), 6.94 (d, *J* = 2.4 Hz, 1H, OCH_a=CH_b), 6.66 (s, 1H, ArCH), 4.06 (s, 3H, OMe), 4.02, (s, 3H, OMe), 4.01 (s, 3H, OMe), 3.96 (s, 3H, OMe), 3.89 (s, 3H, OMe); ¹³C NMR (100.0 MHz, CDCl₃) δ = 153.6 (ArC_{quat.}), 148.4 (COMe), 147.2 (COMe), 145.5 (OCH_a=CH_b), 145.3 (COMe), 136.7 (ArC_{quat.}), 134.8 (ArC_{quat.}), 123.5 (COMe), 120.8 (COMe), 114.8 (ArC_{quat.}), 104.4 (OCH_a=CH_b), 95.4 (ArCH), 62.8 (OMe), 62.7 (OMe), 61.9 (OMe), 57.1 (OMe), 56.8 (OMe); HRMS (CI) calcd for [C₁₇H₁₈O₆]⁺ = 318.1103; found 318.1114 [M+H]⁺; spectroscopic data is in agreement with that previously reported.^{45,80}

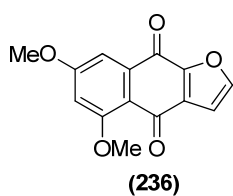


2-(3,5-Dimethoxybenzoyl)furan-3-carboxylic acid (235). To a stirred solution of 3-furoic acid (300 mg, 2.7 mmol, 1.0 equiv.) in anhydrous THF (15 mL) -78 °C was added *t*-butyllithium (1.6 M in hexanes, 3.6 mL, 5.8 mmol, 2.2 equiv.) dropwise. The solution was

stirred for 2 h at -78 °C, then a solution of 3,5-dimethoxybenzotrile (480 mg, 2.94

mmol, 1.1 equiv. in 20 mL THF) was added dropwise. The reaction mixture was allowed to warm from $-78\text{ }^{\circ}\text{C}$ to r.t. over 6 hours and the mixture was stirred for 16 h, before quenching the reaction by slow addition of H_2O (40 mL). The mixture was extracted with Et_2O ($2 \times 60\text{ mL}$) and the dark brown aqueous layer was acidified to pH 1 with 1M HCl, stirred for 2 h, then extracted with EtOAc ($3 \times 50\text{ mL}$). The combined organic layers were dried over MgSO_4 , filtered and concentrated under reduced pressure before purification *via* silica gel chromatography (100% EtOAc) afforded *the title compound* as a yellow solid (670 mg, 2.4 mmol, 90% yield).

mp = $78\text{-}79\text{ }^{\circ}\text{C}$; ν_{max} (film)/ cm^{-1} 2942br (O-H), 1640s (C=O), 1457m and 1483m (C=C); ^1H NMR (400 MHz, CDCl_3) δ = 7.72 (d, J = 1.6 Hz, 1H, OHC=CHR); 7.30-7.28 (m, 3H, $1 \times \text{OCH}_a=\text{CH}_b$, $2 \times \text{ArCH}$), 6.78 (dd, J = 2.2, 1.3 Hz, 1H, ArCH), 3.88 (s, 6H, $2 \times \text{OMe}$); ^{13}C NMR (100.0 MHz, CDCl_3) δ = 185.8 (C=O), 160.8 ($2 \times \text{COMe}$), 160.6 (CO_2H), 149.1 (C_{quat}), 146.4 ($\text{OCH}_a=\text{CH}_b$), 136.3 (ArC_{quat}), 130.6 (C_{quat}), 117.2 ($\text{OCH}_a=\text{CH}_b$), 108.7 ($2 \times \text{ArCH}$), 106.8 (ArCH), 55.8 ($2 \times \text{OMe}$); GCMS (CI) calcd for $[\text{C}_{14}\text{H}_{13}\text{O}_6]^+$ 277; found 277 $[\text{M}+\text{H}]^+$.



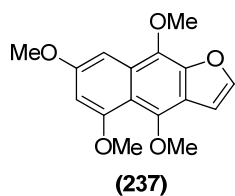
5,7-Dimethoxynaphtho[2,3-*b*]furan-4,9-dione (236). Method A:

Carboxylic acid (**235**) (200 mg, 0.7 mmol, 1.0 equiv.) was dissolved in oxalyl chloride (2.0 mL, 23.6 mmol, 32.8 equiv.) at $-5\text{ }^{\circ}\text{C}$ before addition of DMF (50 μL , 0.65 μmol , 0.1 mol%) liberating fumes of HCl gas. After 2 h the reaction mixture had stopped fuming and was concentrated under reduced pressure, without exposure of the flask to air to give a bright yellow solid, which was subsequently dissolved in CH_2Cl_2 (25 mL). After cooling the reaction mixture to $-5\text{ }^{\circ}\text{C}$, AlCl_3 (140 mg, 1.08 mmol, 1.5 equiv.) was slowly added over 10 minutes and the reaction mixture was warmed slowly to r.t. over 3 h. The reaction mixture was then cooled to $-5\text{ }^{\circ}\text{C}$, before the reaction mixture was carefully quenched by slow addition of ice (15 g) and sat. aq. NH_4Cl solution (10 mL) before extracting with CH_2Cl_2 ($3 \times 40\text{ mL}$). The crude compound was purified by flash chromatography

(EtOAc:Petroleum; 5:2) to afford the *title compound* as an orange solid (163 mg, 0.63 mmol, 88%).

Method B: Furan (**235**) (200 mg, 0.72 mmol) was stirred in 98% sulfuric acid (5 mL) for 3 days at r.t. before carefully being poured onto ice (20 g). The mixture was extracted with 9:1 CH₂Cl₂/MeOH (70 mL) and the organic layer was separated, dried over MgSO₄, filtered and concentrated under reduced pressure. The crude compound was purified by flash chromatography (EtOAc:Petroleum; 5:2) to afford the *title compound* as an orange solid (160 mg, 0.62 mmol, 86%).

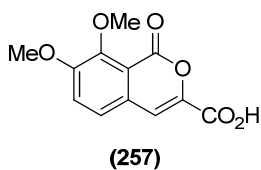
mp = 97-98 °C; R_f = 0.28 (EtOAc:Petroleum; 5:2); ν_{\max} (film)/cm⁻¹ 3193w, 2953w and 2942w (CH), 1640s (C=O), 1454m and 1476m (C=C); ¹H NMR (400 MHz, CDCl₃) δ = 7.65 (d, J = 2.0 Hz, 1H, ArCH), 7.36 (d, J = 2.4 Hz, 1H, OCH_a=CH_b), 6.88 (d, J = 2.0 Hz, 1H, ArCH), 6.68 (d, J = 2.4 Hz, 1H, OCH_a=CH_b), 3.92 (s, 3H, OMe), 3.90 (s, 3H, OMe); ¹³C NMR (100.0 MHz, CDCl₃) δ = 178.3 (C=O), 178.1 (C=O), 155.4 (C_{quat.}), 152.1 (OCH_a=CH_b), 149.6 (COMe), 148.2 (COMe), 131.0 (C_{quat.}), 130.7 (ArC_{quat.}), 110.1 (OCH_a=CH_b), 108.1 (ArCC_{quat.}), 105.8 (ArCH), 103.2 (ArCH), 56.2 (OMe) 55.1; HRMS calcd for [C₁₄H₁₁O₅]⁺ 259.0601; found [M+H]⁺ 259.0605.



4,5,7,9-Tetramethoxynaphtho[2,3-*b*]furan (237**).** To a solution of quinone (**236**) (200 mg, 0.69 mmol, 1.0 equiv.) in THF (3.0 mL) and H₂O (2.0 mL) were added TBAB (44 mg, 0.14 mmol, 0.2 equiv.) and 85% wt. Na₂S₂O₄ (790 mg, 3.40 mmol, 4.9 equiv.). The mixture was stirred for 15 min, before addition of KOH (850 mg, 15.18 mmol, 22.0 equiv.) was added to the clear solution and the resultant red/purple solution was stirred for 20 min before addition of Me₂SO₄ (0.59 mL, 6.21 mmol, 9.0 equiv.). The solution was stirred for a further 2 h before addition of 10% ammonium hydroxide (8.0 mL) and the orange/yellow solution was stirred for a further 16 h at r.t. The mixture was diluted with H₂O (20 mL) and extracted with EtOAc (3 × 75 mL). The combined organic layers were collected and dried over MgSO₄ before concentrating under reduced pressure. The crude

product was then purified using flash chromatography (EtOAc:Petroleum, 1:2 → 1:1) to provide the *title compound* as an orange solid (127 mg, 0.44 mmol, 64% yield).

mp = 86-88 °C; R_f = 0.36 (EtOAc:Petroleum, 1:1); ν_{\max} (film)/cm⁻¹ 2935w, 2867w and 2837w (CH), 1504w, 1486m and 1444m (C=C); ¹H NMR (400 MHz, CDCl₃) δ = 7.56 (d, J = 2.3 Hz, 1H, OCH_a=CH_b), 7.16 (d, J = 2.3 Hz, 1H, ArCH), 6.96 (d, J = 2.3 Hz, 1H, OCH_a=CH_b), 6.48 (d, J = 2.3 Hz, 1H, ArCH), 4.25 (s, 3H, OMe), 4.00, (s, 3H, OMe), 3.95 (s, 6H, 2 × OMe); ¹³C NMR (100.0 MHz, CDCl₃) δ = 157.7 (COMe), 157.2 (COMe), 144.7 (OCH_a=CH_b), 144.5 (COMe), 144.3 (COMe), 134.2 (ArC_{quat.}), 128.2 (ArC_{quat.}), 120.7 (ArC_{quat.}), 113.5 (ArC_{quat.}), 104.5 (OCH_a=CH_b), 97.7 (ArCH), 91.9 (ArCH), 62.9 (OMe), 60.8 (OMe), 56.1 (OMe), 55.3 (OMe); GCMS (CI) = 289 [C₁₆H₁₇O₅]⁺; found 289 [M+H]⁺.



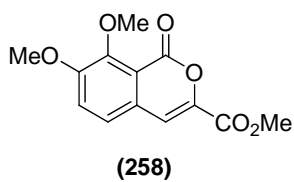
7,8-Dimethoxy-1-oxo-1H-isochromene-3-carboxylic acid

(257)^{99,101} Freshly distilled diethylbromomalonate (0.71 mL, 4.2 mmol, 1.0 equiv.) was added *via* syringe to a suspension of

opianic acid^{ff} (**255**) (0.9 g, 4.3 mmol, 1.0 equiv.) and anhydrous K₂CO₃ (1.5 g, 10.9 mmol, 2.6 equiv.) in freshly distilled but-2-one containing activated 4Å molecular sieves at reflux and heating was continued for a further 3 hours. The solvent was then removed under reduced pressure and the crude oily residue was treated with water (5 mL) and extracted with ether (2 × 10 mL) and the combined organics were concentrated under reduced pressure. The crude residue was subsequently dissolved in a 1:1 mixture of glacial AcOH:23% aq. HCl (10 mL) and refluxed for 1 h. The mixture was allowed to cool to 40 °C and was treated with cold EtOAc (10 mL) causing the title compound to precipitate as a pale green solid. The product was collected by filtration and dried in an oven at 60 °C (0.67 g, 2.7 mmol, 65%).

^{ff} Purification of the commercially available opianic acid was achieved by flash chromatography (EtOAc:Petroleum) before removing the residual solvent *in vacuo*.

mp = 263-264 °C [lit. 261 °C]; ν_{\max} (film)/cm⁻¹ 3100-2600br (OH), 1755s and 1685s (C=O, ester), 1634m (C=C), 1590m (CO-O), 1562m and 1494m (C=C); ¹H NMR (400 MHz, d₆-DMSO) δ = 13.63 (brs, 1H, CO₂H), 7.68 (d, *J* = 8.8 Hz, 1H, ArCH), 7.63 (d, *J* = 8.8 Hz, 1H, ArCH), 7.56 (s, 1H, CH=C_{quat.}), 3.82 (s, 3H, OMe), 3.80 (s, 3H, OMe); ¹³C NMR (100.0 MHz, d₆-DMSO) δ = 161.2 (CO₂H), 157.0 (ArCCO₂), 154.5 (COMe), 149.9 (COMe), 141.2 (CH=C_{quat.}), 128.7 (ArC_{quat.}), 124.6 (ArCH), 120.3 (ArCH), 116.0 (ArC_{quat.}), 112.0 (CH=C_{quat.}), 60.9 (OMe), 56.4 (OMe); HRMS (EI) calcd for [C₁₂H₉O₄]⁻ 249.0405; found 249.0399 [M-H]⁻; spectroscopic data differs to that previously reported as discussed on pages 85-86.^{99,101}



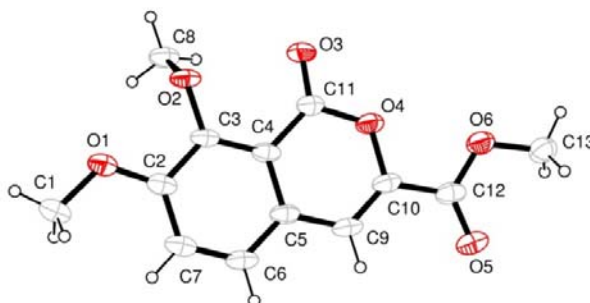
Methyl 7,8-dimethoxy-1-oxo-1H-isochromene-3-carboxylate (258).^{99,101} **Method A:** To a solution of carboxylic acid (**257**)

(100 mg, 0.4 mmol, 1.0 equiv.) in anhydrous CH₂Cl₂ (5 mL) was added a 2M solution of trimethylsilyldiazomethane in Et₂O (0.30 mL, 0.6 mmol, 1.5 equiv.) dropwise at r.t. The brilliant yellow solution was stirred at r.t. for 5 min before it was subsequently treated with dropwise addition of glacial AcOH until returning to a clear solution (ca 0.3 mL). The reaction mixture was then concentrated under reduced pressure to afford the title compound (**250**) as an off-white solid (104 mg, 0.4 mmol, 99%).

Method B: To a solution of carboxylic acid (**257**) (100 mg, 0.40 mmol, 1.0 equiv.) in MeOH (10mL) was added cat. 98% H₂SO₄ (ca. 100 μ l) and the reaction mixture was refluxed for 24 h. The reaction mixture was then concentrated under reduced pressure to afford the title compound (**249**) as a pale yellow solid (102 mg, 0.4 mmol, 97%).

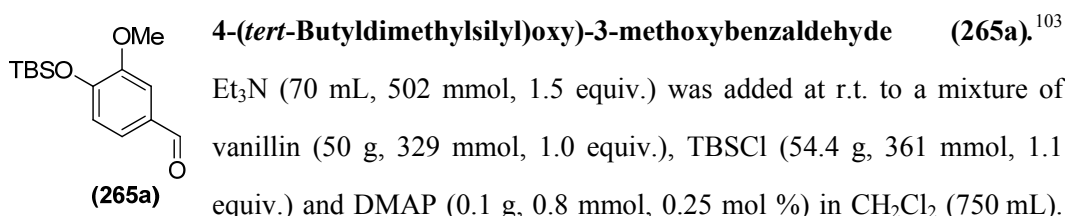
mp 172-173 °C [lit. 174-176 °C]; ν_{\max} (film)/cm⁻¹ 1744m and 1716s (C=O, ester), 1590w (CO-O), 1560w, 1497m and 1438m (C=C); ¹H NMR (600 MHz, CDCl₃) δ = 7.36 (d, *J* = 8.4, 1H, ArCH), 7.35 (s, 1H, CH=C_{quat.}), 7.30 (d, *J* = 8.4 Hz, 1H, ArCH), 3.97 (s, 3H, OMe), 3.96 (s, 3H, OMe), 3.93 (s, 3H, CO₂Me); ¹³C NMR (100.0 MHz, CDCl₃) δ = 161.1 (CO₂Me), 157.3 (ArCCO₂), 155.2 (COMe), 151.6 (COMe), 141.5 (CH=C_{quat.}), 129.1 (ArC_{quat.}), 124.0 (ArCH), 119.5 (ArCH), 117.1 (ArC_{quat.}), 112.5 (CH=C_{quat.}), 61.8

(OMe), 56.7 (OMe), 52.9 (CO₂Me); HRMS (EI) calcd for [C₁₃H₁₂O₆Na]⁺ 287.0532; found 287.0536 [M+H]⁺; spectroscopic data differs to that previously reported as discussed on pages 85-86.^{99,101}



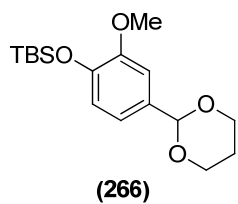
Empirical formula	C ₁₃ H ₁₂ O ₆	
Formula weight	264.23	
Temperature	120 K	
Wavelength	0.71073 Å	
Crystal system	Monoclinic	
Space group	-P 2yn	
Unit cell dimensions	a = 3.8703(2)Å	a = 90°
	b = 19.8892(14)Å	b = 96.022(4)°
	c = 15.1977(9)	g = 90°
Volume	1163.42(12)Å ³	
Z	4	
Density	1.509 Mg/m ³	
Absorption coefficient	0.121 mm ⁻¹	
F(000)	552	
Crystal size	0.18 × 0.07 × 0.06 mm ³	
Theta range for data collection	0.979 to 0.993°	
Index ranges	4 ≤ h ≤ 5, -25 ≤ k ≤ 25, -18 ≤ l ≤ 19	
Reflections collected	20129	
Independent reflections	2631 [R(int) = 0.0986]	

Completeness to theta = 25.00°	98.2%
Absorption correction	Multiscan
Refinement method	Full-matrix least-squares on F ²
Data/restraints/parameters	2631/ 0/175
Goodness-of-fit F ²	1.026
Final R indices [I.2sigma(I)]	R1 = 0.0647, wR2 = 0.1214
R indices (all data)	R1 = 0.1193, wR2 = 0.1411
Largest diff. peak and hole	0.187 and -0.273 e.Å ⁻³



Et₃N (70 mL, 502 mmol, 1.5 equiv.) was added at r.t. to a mixture of vanillin (50 g, 329 mmol, 1.0 equiv.), TBSCl (54.4 g, 361 mmol, 1.1 equiv.) and DMAP (0.1 g, 0.8 mmol, 0.25 mol %) in CH₂Cl₂ (750 mL). After stirring at r.t. for 24 h, the organic layers were washed with sat. aq. NH₄Cl solution (2 × 500 mL). The separated organic layers were dried over MgSO₄, filtered and concentrated under reduced pressure to a brown oil. Flash chromatography (EtOAc:Petroleum, 1:3) afforded the title compound (**265a**) as a yellow oil (84.3 g, 317 mmol, 96%).

R_f = 0.65 (EtOAc:Petroleum, 1:3); ν_{\max} (film)/cm⁻¹ 2958w and 2930w (C-H), 2857w (OCH₃), 1696s (C=O, aldehyde), 1593m (C=C), 1284m (SiMe₂), 1033m (Si-O), and 838m (SiMe₂); ¹H NMR (400 MHz, CDCl₃) δ = 9.85 (s, 1H, CHO), 7.40 (d, J = 1.8 Hz, 1H, ArCH), 7.36 (dd, J = 8.0 Hz, 1.8 Hz, 1H, ArCH), 6.96 (d, J = 8.0 Hz, 1H, ArCH), 3.87 (s, 3H, OMe), 1.00 (s, 9H, SiMe₂^{*t*}Bu), 0.19 (s, 6H, SiMe₂^{*t*}Bu); ¹³C NMR (100.0 MHz) δ = 191.1 (CHO), 151.8 (COMe), 151.5 (COTBS), 131.1 (CCHO), 126.3 (ArCH), 120.9 (ArCH), 110.3 (ArCH), 55.6 (OMe), 25.7 (SiC(CH₃)₃), 18.7 (SiC(CH₃)₃), -4.4 (SiMe₂); HRMS (CI) calc for [C₁₄H₂₃O₃Si]⁺ 267.1412; found 267.1411 [M+H]⁺; spectroscopic data is in agreement with that previously reported.¹⁰³



(4-(1,3-Dioxan-2-yl)-2-methoxyphenoxy)(tert-butyl)dimethylsilane

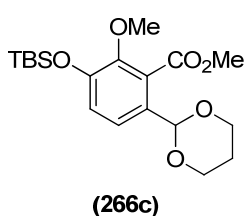
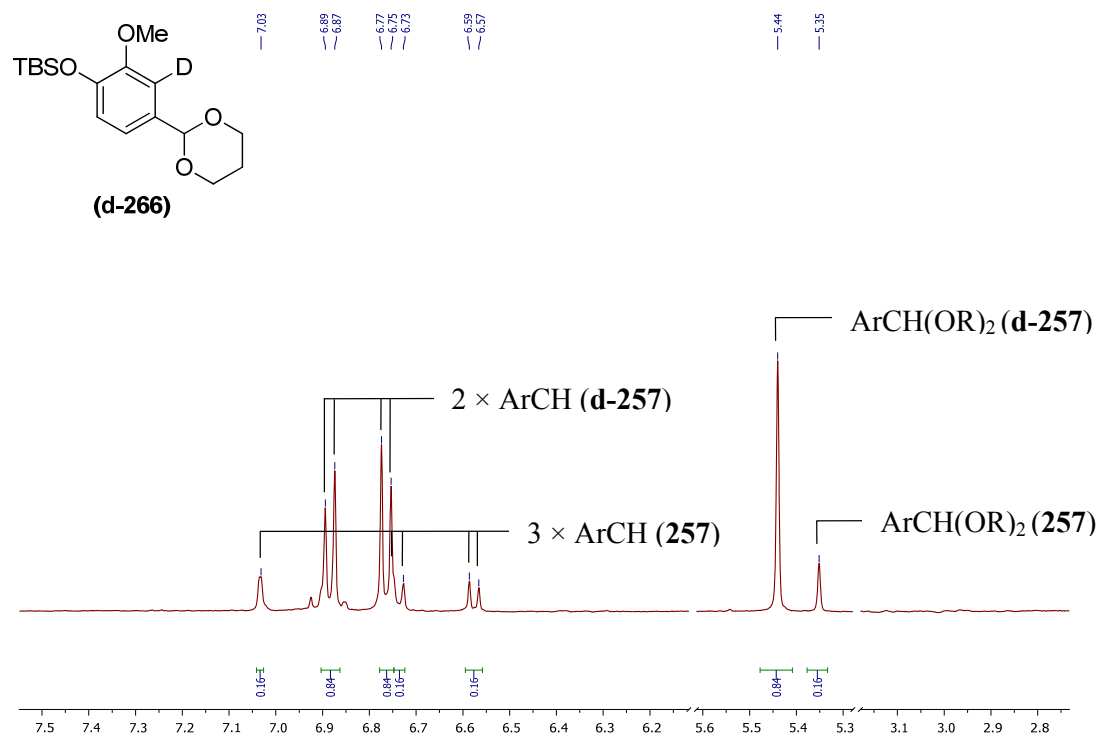
(266).¹⁰³ 4-(tert-Butyldimethylsilyloxy)3-methoxybenzaldehyde

(265a) (80 g, 246 mmol, 1.0 equiv.) was dissolved in CH₂Cl₂ (210 mL), before addition of 1,3-propanediol (82 mL, 1.14 mol, 4.6 equiv.), trimethyl orthoformate (49 mL, 477 mmol, 1.9 equiv.) and *n*-Bu₄NBr₃ (7.6 g, 24.2 mmol, 0.01 equiv.) were added and the resultant mixture was stirred at r.t. for 2.5 days. Sat. aq. Na₂CO₃ solution (250 mL) and H₂O (250 mL) were added and the layers were separated. The aqueous layer was then extracted with CH₂Cl₂ (200 mL) and the combined organic were dried over MgSO₄ and filtered before concentrating under reduced pressure. The crude oil was then purified by flash chromatography (EtOAc:*n*-hexane, 1:19) furnishing the title compound **(266)** as colourless oil (71.7 g, 22.1 mmol, 90%).

$R_f = 0.64$ (EtOAc:Petroleum, 1:19); ν_{\max} (film)/cm⁻¹ 2955w and 2929w (CH), 2855w (OCH₃), 1282m (SiMe₂), 1123m (SiO) and 838m (SiMe₂); ¹H NMR (400 MHz, CDCl₃) $\delta = 7.03$ (d, $J = 1.7$ Hz, 1H, ArCH), 6.93 (dd, $J = 8.2, 1.7$ Hz, 1H, ArCH), 6.83 (d, $J = 8.1$ Hz, 1H, ArCH), 5.44 (s, 1H, HCO₂), 4.23 (dd, $J = 11.2, 5.0$ Hz, 2H, 2 × OCH_aH_b), 3.96-3.86 (m, 2H, 2 × OCH_aH_b), 3.82 (s, 3H, ArOMe), 2.08-2.22 (m, 1H, OCH₂CH_aH_b), 1.39 (m, 1H, OCH₂CH_aH_b), 0.99 (s, 9H, SiMe₂*t*-Bu), 0.16 (s, 6H, SiMe₂*t*-Bu); ¹³C NMR (100.0 MHz) $\delta = 151.1$ (COMe), 145.6 (COTBS), 132.6 (CCHO₂), 120.8 (ArCH), 118.8 (ArCH), 109.8 (ArCH), 101.9 (CCHO₂), 67.6 (2 × OCH₂CH₂), 55.6 (OMe), 25.9 (SiC(CH₃)₃), 25.9 (2 × OCH₂CH₂), 18.6 (SiC(CH₃)₃), -4.5 (SiMe₂); HRMS (CI) calcd for [C₁₇H₂₉O₄Si]⁺ 325.1826; found 325.1830 [M+H]⁺; spectroscopic data is in agreement with that previously reported.¹⁰³

Representative procedure for deuteration of (266).

n-Butyllithium (0.25 mL, 0.6 mmol, 2.0 equiv., 2.5 M in hexanes) was added to anhydrous cyclohexane (5.0 mL) at 2 °C and the resultant mixture was further cooled to -1 °C (external). Acetal (266) (100 mg, 0.3 mmol, 1.0 equiv.) was added and the reaction was further cooled to -6 °C and allowed to stir at that temperature for 20 h, at which point 0.2 mL of the reaction mixture was removed *via* syringe and added to a 5 mL round bottom flask containing CD₃OD (3 mL) under an atmosphere of argon at room temperature. After 30 minutes a ¹H NMR was recorded to determine conversion of starting material upon integration of the signals highlighted overleaf (84%).

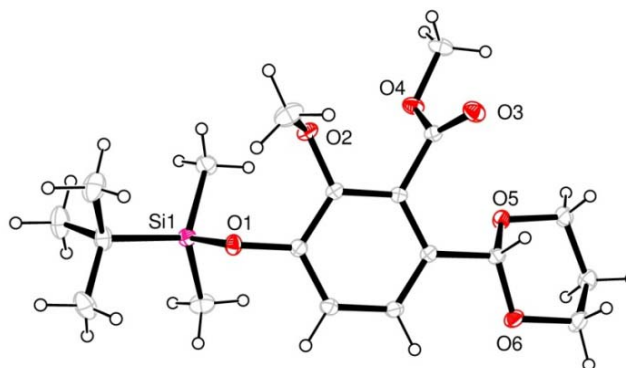


Methyl 3-((*tert*-butyldimethylsilyloxy)-6-(1,3-dioxan-2-yl)-2-methoxybenzoate (266c).¹⁰³ *n*-Butyllithium (59 mL, 146 mmol, 2.5 M in hexanes, 1.2 equiv.) was added to a solution of acetal

(266) (39 g, 120 mmol, 1.0 equiv.) in anhydrous cyclohexane (750 mL) at 0 °C. The mixture was allowed to warm to r.t. and stirred for 4.5 h before

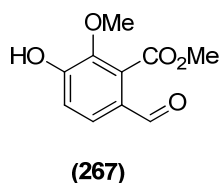
recoiling the solution to 0 °C. The reactive mixture was quenched by addition of methyl chloroformate (31 mL, 401 mmol, 3.3 equiv.) dropwise. The reaction was allowed to warm slowly to r.t. and stirring was continued for a further 16 h. The reaction mixture was quenched with sat. aq. Na₂CO₃ solution (200 mL), the layers were separated and the aqueous layer was extracted with Et₂O (3 × 400 mL) and the combined organics were dried over MgSO₄ and concentrated under reduced pressure before purifying the crude product by column chromatography (EtOAc:*n*-Hexane, 1:5). The title compound was furnished as clear colourless solid (33.1 g, 86.6 mmol, 72%).

mp. 74-76 °C; [lit. 76-78 °C]; $R_f = 0.51$ (EtOAc:*n*-Hexane 1:5); ν_{\max} (film)/cm⁻¹ 2951w and 2930w (CH), 2857w (OCH₃), 1724s (C=O, ester), 1599w (CO-O), 1492w, 1453w and 1437w (C=C), 1271s (SiMe₂), 1143m (SiO) and 838s (SiMe₂); ¹H NMR (400 MHz, CDCl₃) $\delta = 7.23$ (d, 1H, $J = 8.6$ Hz, ArCH), 6.87 (d, 1H, $J = 8.6$ Hz, ArCH), 5.55 (s, 1H, CHO₂), 4.21 (dd, $J = 11.3, 1.2$, 2H, 2 × OCH_aH_b), 3.95-3.86 (m, 2H, 2 × ROCH_aH_b), 3.89 (s, 3H, OMe), 3.81 (s, 3H, CO₂Me), 2.21-2.08 (m, 1H, OCH₂CH_aH_b) 1.43-1.35 (m, 1H, OCH₂CH_aH_b), 0.99 (s, 9H, SiMe₂*t*-Bu), 0.16 (s, 6H, SiMe₂*t*-Bu); ¹³C NMR (100.0 MHz) $\delta = 167.9$ (CO₂Me), 149.3 (COMe), 148.3 (COTBS), 129.6 (CCHO₂), 127.9 (CCO₂Me), 122.2 (ArCH), 122.0 (ArCH), 99.2 (CCHO₂), 67.4 (2 × OCH₂CH₂), 61.4 (OMe), 52.2 (CO₂Me), 25.8 (SiC(CH₃)₃), 25.7 (OCH₂CH₂), 18.5 (SiC(CH₃)₃), -4.7 (SiMe₂); HRMS (CI) calcd for [C₁₉H₃₁O₆Si]⁺ 383.1885; found 383.1884 [M+H]⁺; spectroscopic data is in agreement with that previously reported.¹⁰³



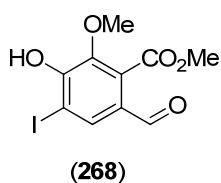
Empirical formula	C ₁₉ H ₃₀ O ₆ Si
Formula weight	382.52
Temperature	100(2) K
Wavelength	0.71073 Å
Crystal system	Monoclinic
Space group	-P 2 ₁ /c
Unit cell dimensions	a = 14.6051(10)Å a = 90° b = 15.8731(11)Å b = 97.9860(10)° c = 8.9463(6)Å g = 90°
Volume	2053.9(2) Å ³
Z	4
Density	1.237 Mg/m ³
Absorption coefficient	0.145 mm ⁻¹
F(000)	824
Crystal size	0.40 × 0.10 × 0.10 mm ³
Theta range for data collection	2.57 to 34.99°
Index ranges	-23 ≤ h ≤ 23, 25 - ≤ k ≤ 24, -14 ≤ l ≤ 7
Reflections collected	8987
Independent reflections	43509 [R(int) = 0.0304]
Completeness to theta = 25.00°	99.3%
Absorption correction	Multiscan

Refinement method	Full-matrix least-squares on F ²
Data/restraints/parameters	8987/0/242
Goodness-of-fit F ²	1.025
Final R indices [I.2sigma(I)]	R1 = 0.0421, wR2 = 0.1192
R indices (all data)	R1 = 0.0590, wR2 = 0.1329
Largest diff. peak and hole	1.474 and -0.383e.Å ⁻³



Methyl 6-formyl-3-hydroxy-2-methoxybenzoate (267).¹⁰³ Acetal **(266c)** (5.0 g, 13.1 mmol, 1.0 equiv.) was dissolved in THF (100 mL) in a PTFE bottle before addition of conc. aq.HCl (37%, 16 mL), KF (2.8 g, 48.4 mmol, 3.7 equiv.) and H₂O (20 mL) and the mixture was stirred at r.t. for 9 h. The layers were then separated and the aqueous layer was extracted with CH₂Cl₂ (3 × 80 mL). The combined organics were dried over MgSO₄ and concentrated under reduced pressure. Silica gel chromatography (EtOAc:Petroleum; 2:3) afforded the title compound as a light pink solid (1.92 g, 9.1 mmol, 70%).

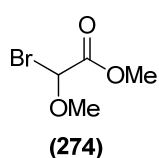
mp = 101-103 °C; [lit. 106 °C]; *R*_f = 0.42 (EtOAc:Petroleum 2:3); *v*_{max} (film)/cm⁻¹ 3147br (OH), 3010w, 2975w, 2847w (C-H), 1742m (C=O, ester) 1661s (C=O, aldehyde), 1597m, 1560m, 1505m (C=C); ¹H NMR (400 MHz, CDCl₃) δ = 9.81 (s, 1H, CHO), 7.57 (d, *J* = 7.9 Hz, 1H, ArCH), 7.13 (d, *J* = 7.9 Hz, 1H, ArCH), 6.42 (s, 1H, OH), 4.00 (s, 3H, OMe), 3.92 (s, 3H, CO₂Me); ¹³C NMR (100.0 MHz) δ = 189.2 (CHO), 167.1 (CO₂Me), 154.5 (ArCOH), 144.5 (COMe), 130.1 (CCHO), 127.6 (ArCH), 127.2 (ArCH), 116.7 (CCO₂Me), 62.7 (OMe), 53.2 (CO₂Me); GCMS (CI) calcd for [C₁₀H₉O₅]⁻ 209; found 209 [M-H]⁻; spectroscopic data is in agreement with that previously reported.¹⁰³



Methyl 6-formyl-3-hydroxy-4-iodo-2-methoxybenzoate (268).¹⁰³ To a solution of phenol **(267)** (1.2 g, 5.7 mmol, 1.0 equiv.) in CH₂Cl₂ (25 mL) was added tetramethylammonium dichloroiodate¹¹⁹ (1.86 g, 6.9 mmol, 1.2 equiv.) and NaHCO₃ (1.1 g, 12.6 mmol, 2.2 equiv.) at 0 °C and the reaction was allowed to stir at r.t. for 4 h. The reaction mixture was then re-cooled to 0 °C before addition of aq. HCl solution (1M, 20 mL) and CH₂Cl₂

(25 mL) and the organics were then washed with sat. aq. Na₂S₂O₃ solution (30 mL). The organics were dried over MgSO₄ and concentrated under reduced pressure before silica gel chromatography (EtOAc:Petroleum; 3:1) afforded the title compound as a yellow oil, which solidified to give a faintly yellow solid upon storage (1.90 g, 5.7 mmol, 99%) at 3 °C for 30 min.

mp = 37-39 °C; *R*_f = 0.81(EtOAc:Petroleum 3:1); *v*_{max} (film)/cm⁻¹ 3315br (OH), 3017w, 2978w and 2846w (CH), 1739m (C=O, ester), 1678s (C=O, carbonyl), 1570m, 1491m and 1471m (C=C); ¹H NMR (400 MHz, CDCl₃) δ = 9.76 (s, 1H, CHO), 7.98 (s, 1H, ArCH), 3.99 (s, 3H, OMe), 3.93 (s, 3H, CO₂Me); ¹³C NMR (100.0 MHz) δ = 187.8 (CHO), 166.3 (CO₂Me), 154.5 (COH), 143.8 (COMe), 138.3 (ArCH), 128.2 (CCHO), 128.0 (CCO₂Me), 84.0 (CI), 62.7 (OMe), 53.3 (CO₂Me); GCMS (CI) calcd for [C₁₀H₈IO₅]⁻ 335, found 335 [M-H]⁻; spectroscopic data is in agreement with that previously reported.¹⁰³

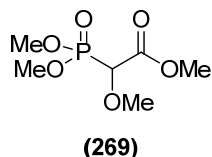


Methyl bromomethoxyacetate (274).¹²⁰ ****Caution, this reaction is**

extremely exothermic, take care to heat the reaction gently, in a vessel no smaller than 2 litres with extremely efficient vapour cooling.** Methyl methoxyacetate (20.0 g, 192 mmol, 1.0 equiv.) was dissolved in CCl₄ (250 mL), before addition of NBS (34.2 g, 192 mmol, 1.0 equiv) and benzoyl peroxide (75% in H₂O) (400 mg, 1.2 mmol, 0.6 mol. %) and the mixture was gently heated to 77 °C over 6 hours so as to control the potentially explosive reaction. The reaction was stirred at 77 °C for a further 16 hours and the mixture was then filtered and concentrated under reduced pressure to afford the title compound (**274**) as a brown oil (26.3 g, 144 mmol, 75%). A sample of the resultant residue was then distilled under reduced pressure (43-45 °C/0.1 mbar) to afford the title compound as clear, pale yellow oil and the remainder was carried forward without further purification.

*v*_{max} (film)/cm⁻¹ 2957w (CH₃), 2843w (CH₃), 1747s (C=O), 1378m (CO₂C-H₃); ¹H NMR (400 MHz, CDCl₃) δ = 6.01 (s, 1H, CH), 3.85 (s, 3H, OMe) 3.58 (s, 3H, CO₂Me); ¹³C NMR (100.0 MHz) δ = 166.0 (CO₂Me), 83.2 (CBr), 58.9 (OMe),

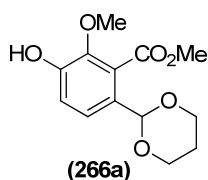
53.4 (CO₂Me); GCMS (CI) = 182 [C₄H₇⁷⁹BrO₃]⁺ and 184 [C₄H₇⁸¹BrO₃]⁺; found 182 and 184; spectroscopic data is in agreement with that previously reported.¹²¹



Methyl (Dimethylphosphono)methoxyacetate (269).¹²¹ ****Caution, this reaction is extremely exothermic, take care to add the trimethyl phosphite dropwise at r.t.**** To a 100 ml round bottomed

flask fitted with an air condenser was added crude methyl bromomethoxyacetate (26.3 g, 144 mmol, 1.0 equiv.) was carefully added trimethyl phosphite (18 mL, 153 mmol, 1.1 equiv.) dropwise at r.t. and the resultant, gently bubbling mixture was stirred at r.t for 20 min before heating to 185 °C for 5 hours. The cooled reaction mixture was then distilled under reduced pressure (111-112 °C/0.1 mbar) to afford the title compound **(269)** as a clear, colourless oil (30.5 g, 144 mmol, 99%).

ν_{\max} (film)/cm⁻¹ 2900w (CO₂C-H₃), 2853w and 2849w (OCH₃), 1750s (C=O), 1262s (P=O); ¹H NMR (400 MHz, CDCl₃) δ = 4.25 (d, J = 19.5 Hz, 1H, PCH), 3.86 (d, J = 5.2 Hz, 3H, POMe), 3.84 (s, 3H, OMe), 3.83 (d, J = 5.2 Hz, 3H, POMe), 3.52 (d, J = 0.5 Hz, 3H, CO₂Me); ¹³C NMR (100.0 MHz, CDCl₃) δ = 167.3 (CO₂Me), 78.8 (d, J = 158.3 Hz, (PCH), 60.3(d, J = 12.9 Hz, COMe), 54.2 (d, J = 8.0 Hz, POMe), 54.1 (d, J = 8.0 Hz, POMe), 52.8 (CO₂Me); ³¹P (161.9, MHz, CDCl₃) δ = 16.3 (P=O); HRMS (CI) calcd for [C₆H₁₄O₆P]⁺ 213.0528; found 213.0519 [M+H]⁺; spectroscopic data is in agreement with that previously reported.¹²²

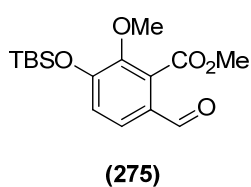


Methyl 6-(1,3-dioxan-2-yl)-3-hydroxy-2-methoxybenzoate (266a).

Method A: To a solution of silyl ether **(266c)** (70 mg, 0.22 mmol, 1.0 equiv.) in DMSO (1.4 mL, 19.7 mmol, 90 equiv.) and H₂O (79 μ L, 4.4 mmol, 20 equiv.) was heated at 170 °C for 2 h. The reaction mixture was cooled to r.t. diluted with Et₂O (10 mL) and washed with sat. aq. NaCl solution (5 \times 6 mL), dried over MgSO₄, and concentrated under reduced pressure. Purification of the crude reaction mixture by silica gel chromatography (EtOAc:Petroleum; 1:3) afford the *title compound* as a white solid (58 mg, 0.22 mmol, 99%).

Method B: To a solution of silyl ether (**266c**) (500 mg, 1.3 mmol, 1.0 equiv.) in THF (10 mL) was added 1M TBAF in THF (1.4 mL, 1.4 mmol 1.1 equiv.) and stirred at r.t. for 60 min before addition of saturated aq. NH₄Cl (10 mL). The mixture was extracted with Et₂O (3 × 35 mL), dried over MgSO₄ before concentrating under reduced pressure before silica gel chromatography (EtOAc:Petroleum; 1:3) afforded the *title compound* as a white solid (344 mg, 1.3 mmol., 98%).

mp = 174-176 °C; *R*_f = 0.21 (EtOAc:Petroleum;1:3); *v*_{max} (film)/cm⁻¹ 3214br (-OH), 3006w, 2987w and 2924w (CH), 2857w (OCH₃), 1699s (C=O), 1587m (C=C); ¹H NMR (400 MHz, CDCl₃) δ = 7.31 (dd, 1H, *J* = 8.5, 0.5 Hz, ArCH), 7.00 (d, 1H, *J* = 8.5 Hz, ArCH), 5.70 (brs, 1H, OH), 5.58 (s, 1H, CHO₂), 4.22 (ddd, *J* = 11.9, 5.0, 1.3 Hz, 2H, 2 × OCH_aH_bCH₂), 3.92 (s, 3H, OMe), 3.91 (ddd, *J* = 12.3, 2.5, 1.3 Hz, 2H, 2 × ROCH_aH_bCH₂), 3.85 (s, 3H, CO₂Me), 2.16 (dddd, *J* = 17.4, 13.2, 12.3, 5.0Hz, 1H, OCH₂CH_aH_b), 1.41 (dddd, *J* = 13.5, 4.0, 2.5 Hz, 1.3 Hz, 1H, OCH₂CH_aH_b); ¹³C NMR (100.0 MHz) δ = 167.5 (CO₂Me), 149.2 (COH), 144.3 (COMe), 129.0 (CCHO₂), 126.0 (CCO₂Me), 122.9 (ArCH), 116.9 (ArCH), 99.1 (CCHO₂), 67.5 (2 × OCH₂CH₂), 62.6 (OMe), 52.5 (CO₂Me), 25.7 (OCH₂CH₂); HRMS (CI) calcd for [C₁₃H₁₇O₆]⁺ 269.1020; found 269.1023 [M+H]⁺.

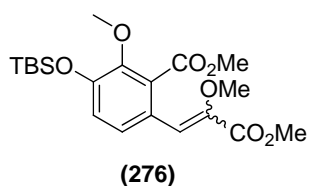


Methyl 3-((tert-butyldimethylsilyloxy)-6-formyl-2-methoxybenzoate (275). **Method A:** Et₃N (0.07 mL, 0.50 mmol, 1.5 equiv.) was added at r.t. to a mixture of phenol (**267**) (69 mg, 0.33 mmol, 1.0 equiv.), TBSCl (54.3 mg, 0.36 mmol, 1.1 equiv.)

and DMAP (2 mg, 0.01 mmol, 5 mol %) in CH₂Cl₂ (1.0 mL). After stirring at r.t. for 24 h, the reaction was diluted with CH₂Cl₂ (10 mL) and washed with sat. aq. NH₄Cl solution (2 × 5 mL). The organic layer was separated, dried over MgSO₄, filtered and concentrated under reduced pressure to a pale yellow/brown oil. Flash chromatography (EtOAc:Petroleum, 1:3) afforded the *title compound* (**268**) as a pale yellow oil (102 mg, 0.31 mmol, 95%).

Method B: To a solution of acetal (**266c**) (16.9 g, 44.2 mmol, 1.0 equiv.) in reagent grade THF (1.5 L) at $-5\text{ }^{\circ}\text{C}$ was added TMSOTf (8.4 mL, 46.4 mmol, 1.05 equiv.) dropwise and left to stir at that temperature for 15 minutes. H_2O (8.8 mL, 488.9 mmol, 11.1 equiv.) was then added dropwise to the reaction over 180 min (at which time TLC analysis indicated complete consumption of the starting material) before diluting the reaction mixture with EtOAc (1.5 L). Saturated aq. Na_2CO_3 solution (1.5 L) was then added to the solution. The organics were then separated before further extraction of the aqueous layer with EtOAc (1.5 L) and the combined organic layers were dried over MgSO_4 and concentrated under reduced pressure at $30\text{ }^{\circ}\text{C}$. The resultant brown oil was then purified by flash chromatography on silica gel (EtOAc:Petroleum, 1:5) to afford the *title compound* as a pale yellow oil (13.2 g, 92%).

$R_f = 0.41$ (EtOAc:Petroleum, 1:5); ν_{max} (film)/ cm^{-1} 2952w and 2933w (CH), 2859w (OCH_3), 1737s (C=O, ester), 1695s (C=O, aldehyde), 1584m (CO-O), 1264s and 834s (SiMe_2) and 1138m (SiO); $^1\text{H NMR}$ (400 MHz, CDCl_3) $\delta = 9.82$ (s, 1H, CHO), 7.52 (d, 1H, $J = 8.5$, ArCH), 7.00 (d, 1H, $J = 8.5$, ArCH), 3.97 (s, 3H, OMe), 3.85 (s, 3H, CO_2Me), 1.02 (s, 9H, $\text{SiMe}_2t\text{-Bu}$), 0.25 (s, 6H, $\text{SiMe}_2t\text{-Bu}$); $^{13}\text{C NMR}$ (100.0 MHz) $\delta = 189.0$ (CHO), 167.1 (CO_2Me), 154.8 (COMe), 148.9 (COTBS), 130.3 (CCHO), 128.9 (ArCH), 127.7 (CCO_2Me), 121.9 (ArCH), 61.8 (OMe), 52.9 (CO_2Me), 25.7 ($\text{SiC}(\text{CH}_3)_3$), 18.4 ($\text{SiC}(\text{CH}_3)_3$), -4.3 (SiMe_2); HRMS (CI) calcd for $[\text{C}_{16}\text{H}_{25}\text{O}_5\text{Si}]^+$ 324.1466; found 325.1467 $[\text{M}+\text{H}]^+$.

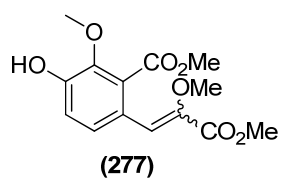


(E/Z)-Methyl-3-((tert-butyldimethylsilyloxy)-6-(2,3-dimethoxy-3-oxoprop-1-en-1-yl)-2-methoxybenzoate (276).

To a solution of phosphonate (**269**) (3.5 g, 16.5 mmol, 1.3 equiv.) in THF (40 mL) was added NaHMDS (2 M in THF, 8.6 mL, 17.1 mmol, 1.35 equiv.) dropwise at $-78\text{ }^{\circ}\text{C}$ over 10 minutes before stirring at this temperature for 20 minutes. A solution of aldehyde (**275**) (4.1g, 12.7 mmol, 1.0 equiv.) in THF (20 mL) was added dropwise and the reaction mixture was allowed to

warm slowly warm to r.t. and stirred for 16 h. A saturated solution of aq. NH_4Cl (45 mL) was introduced and the crude mixture was extracted with Et_2O (3×50 mL). The combined organics were dried over MgSO_4 and concentrated under reduced pressure to afford the *title compound* (5.0 g, 12.2 mmol, 96%) of as an inseparable mixture of (*E*:*Z*: 1:5) isomers respectively as a pale yellow oil. Stereochemical assignments were made on the basis of NOESY experiments and correlation of chemical shifts of closely related literature compounds.¹⁰³

$R_f = 0.28$ (EtOAc;Petroleum 1:19); ν_{max} (film)/ cm^{-1} 2953w and 2931w (CH), 2858w (OCH_3), 1722s (C=O, ester), 1636w (C=C, conj), 1590m (CO-O), 1484m (C=C), 1236s and 836s (SiMe_2) and 1138m (SiO); HRMS (CI) calcd for $[\text{C}_{19}\text{H}_{28}\text{O}_7\text{N}_1\text{Si}_1]^+$ 428.2099; found $[\text{M}+\text{NH}_4]^+$ 428.099; (**Z**)-isomer: ^1H NMR (400 MHz, CDCl_3) δ 7.80 (d, 1H, $J = 8.63$, ArCH), 6.91 (d, 1H, $J = 8.63$, ArCH), 6.83 (s, 1H, $\text{HC}=\text{C}_{\text{quat}}$), 3.95 (s, 3H, OMe), 3.83 (s, 3H, OMe), 3.82 (s, 3H, CO_2Me), 3.73 (s, 3H, CO_2Me), 1.02 (s, 9H, $\text{SiMe}_2\text{-Bu}$), 0.22 (s, 6H, $\text{SiMe}_2\text{-Bu}$); ^{13}C NMR (100.0 MHz, CDCl_3) δ 167.7 (CO_2Me), 164.6 (CO_2Me), 149.3 (COMe), 148.1 (ArC_{quat}), 145.6 (COTBS), 130.6 (ArC_{quat}), 126.3 (ArCH), 124.3 ($\text{HC}=\text{C}_{\text{quat}}$), 122.3 (ArCH), 119.4 ($\text{HC}=\text{C}_{\text{quat}}$), 61.3 (OMe), 59.3 (OMe), 52.4 (CO_2Me), 52.2 (CO_2Me), 29.5 ($\text{SiC}(\text{CH}_3)_3$), 18.2 ($\text{SiC}(\text{CH}_3)_3$), -4.49 (SiMe_2); (**E**)-isomer: ^1H NMR (400 MHz, CDCl_3) $\delta = 6.84\text{-}6.79$ (m, 2H, $2 \times$ ArCH), 6.11 (s, 1H, $\text{HC}=\text{C}_{\text{quat}}$), 3.85 (s, 3H, OMe), 3.82 (s, 3H, OMe), 3.69 (s, 3H, CO_2Me), 3.60 (s, 3H, CO_2Me), 1.00 (s, 9H, $\text{SiMe}_2\text{-Bu}$), 0.19 (s, 6H, $\text{SiMe}_2\text{-Bu}$); ^{13}C NMR (100.0 MHz, CDCl_3) δ 167.8 (CO_2Me), 163.9 (CO_2Me), 148.3 (COMe), 147.9 (ArC_{quat}), 147.9 (COTBS), 128.9 (ArC_{quat}), 126.5 ($\text{HC}=\text{C}_{\text{quat}}$), 125.2 (ArCH), 122.1 (ArCH), 107.0 ($\text{HC}=\text{C}_{\text{quat}}$), 61.3 (OMe), 56.0 (OMe), 52.1 (CO_2Me), 52.0 (CO_2Me), 25.7 ($\text{SiC}(\text{CH}_3)_3$), 18.2 ($\text{SiC}(\text{CH}_3)_3$), -4.6 (SiMe_2).

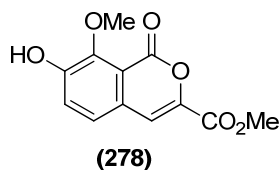


Methyl 6-(2,3-dimethoxy-3-oxoprop-1-en-1-yl)-3-hydroxy-2-methoxybenzoate (277). To a solution of (**276**) (340 mg, 0.82 mmol, 1.0 equiv.) in THF (3.5 mL) was added 1M TBAF in THF (1.05 mL, 1.05 mmol 1.28 equiv.) and stirred at r.t. for 30

min before addition of sat. aq. NH_4Cl solution (5 mL). The mixture was extracted with

Et₂O (3 × 20 mL), dried over MgSO₄ before concentrating under reduced pressure to afford the *title compound* (*E:Z*; 1:5) as a yellow oil that could be further purified using column chromatography (EtOAc:Petroleum, 1:3) to give a pale yellow oil (238 mg, 97%). Stereochemical assignments were made on the basis of NOESY experiments and correlation of chemical shifts of closely related literature compounds.¹⁰³

$R_f = 0.23$ (EtOAc:Petroleum 1:8); ν_{\max} (film)/cm⁻¹ 3283br (OH), 2998w and 2939w (CH), 2834w (OCH₃), 1730s and 1701s (C=O, ester), 1629 (C=C, conj.) 1573m (C=C), 1275s and 1063 (C-O-CH₃); HRMS (CI) calcd for [C₁₄H₁₇O₇]⁺ 297.0972; found 297.0696 [M+H]⁺; **(Z)-isomer**: ¹H NMR (400 MHz, CDCl₃) δ 7.81 (d, 1H, $J = 7.50$, ArCH), 7.03 (d, 1H, $J = 7.5$, ArCH), 6.88 (s, 1H, HC=C_{quat.}) 5.89 (brs, 1H, OH), 3.97 (s, 3H, OMe), 3.86 (s, 3H, OMe), 3.83 (s, 3H, CO₂Me), 3.71 (s, 3H, CO₂Me); ¹³C NMR (100.0 MHz, CDCl₃) δ 167.8 (CO₂Me), 165.2 (CO₂Me), 149.7 (COH), 146.0 (COMe), 127.6 (ArCH), 124.2 (HC=C_{quat.}), 120.0 (ArCH), 117.8 (HC=C_{quat.}), 62.9 (OMe), 59.9 (OMe), 53.2 (CO₂Me), 52.7 (CO₂Me); **(E)-isomer**: ¹H NMR (400 MHz, CDCl₃) δ 6.85-6.78 (m, 2H, ArCH), 6.12 (s, 1H, HC=C_{quat.}), 5.85 (brs, 1H, OH), 3.87 (s, 3H, OMe), 3.84 (s, 3H, OMe), 3.70 (s, 3H, CO₂Me), 3.61 (s, 3H, CO₂Me); ¹³C NMR (100.0 MHz, CDCl₃) δ 167.8 (CO₂Me), 164.1 (CO₂Me), 148.2 (COH), 147.0 (COMe), 128.76 (ArC_{quat.}), 128.2 (CH=C_{quat.}), 125.7 (ArCH), 122.7 (ArCH), 107.1 (HC=C_{quat.}), 63.0 (OMe), 56.3 (OMe), 52.4 (CO₂Me), 52.0 (CO₂Me).



Methyl 7-hydroxy-8-methoxy-1-oxo-1H-isochromene-3-carboxylate (278). **Method A:** A solution of (277) (100 mg, 0.34 mmol) dissolved in a 1:1 mixture of MeOH:HBr (37%) was

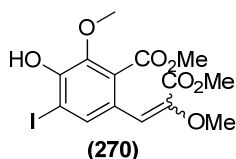
heated to 95 °C in a sealed microwave vial for 12 h before slowly cooling to -25 °C. The resultant creamy precipitate was filtered and washed with cold Et₂O (15 mL). The mother liquors were then diluted with H₂O (10 mL) before further extraction with EtOAc (3 × 15 mL), the organics were then concentrated under reduced pressure to give a mixture of white solid in a pale yellow oil. The subsequent oil/solid mixture was washed with cold Et₂O (15 mL) and the combined solids were further purified *via* column chromatography

(EtOAc: Petroleum 4:1) to afford the *title compound* as a pale white solid (55 mg, 0.22 mmol, 64%).

Method B: A solution of (**277**) (100 mg, 0.34 mmol) dissolved in a 2:1 mixture of MeOH:3N H₂SO₄ (2 mL) was heated to 95 °C in a sealed microwave vial for 4 h before slowly cooling to -25 °C. The resultant creamy precipitate was filtered and washed with cold Et₂O (15 mL). The mother liquors were then diluted with H₂O (10 mL) before further extraction with EtOAc (3 × 15 mL), the organics were then concentrated under reduced pressure to give a mixture of white solid in a pale yellow oil. The subsequent oil/solid mixture was washed with cold Et₂O (15 mL) and the combined solids were further purified *via* column chromatography (EtOAc: Petroleum 4:1) to afford the *title compound* as a pale white solid (72 mg, 0.29 mmol, 85%).

Method C: Methyl ester (**277**) (100 mg, 0.34 mmol, 1.00 equiv.) and PTSA monohydrate (66 mg, 0.35 mmol, 1.02 equiv.) were added PhMe (2 ml) under stirring in a microwave vial, the reaction vessel was then sealed and heated to 135 °C (external) for 21 h. The reaction mixture was then slowly cooled to -25 °C and the resultant creamy precipitate was filtered and washed with cold Et₂O (15 mL). The resultant white solid was further purified *via* column chromatography (EtOAc: Petroleum 4:1) to afford the *title compound* as a pale white solid (80 mg, 0.32 mmol, 94%).

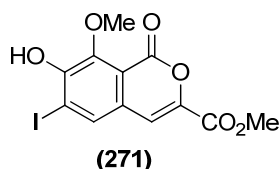
mp = 136-138 °C; R_f = 0.21 (EtOAc:Petroleum 4:1); ν_{\max} (film)/cm⁻¹ 3241br (-OH), 3083w (CH), 2944w (OCH), 1695 (C=O ester), 1592m, 15992m, 1509m, 1494m (C=C), 1306s (-O-H) 1237s and 1071s (C-O-CH₃); ¹H NMR (400 MHz, d₆-DMSO) δ 10.36 (brs, 1H, COH), 7.58 (s, 1H, CH=C_{quat.}), 7.51 (d, 1H, J = 8.49, ArCH), 7.42 (d, 1H, J = 8.49, ArCH), 3.85 (s, 3H, OMe), 3.80 (s, 3H, CO₂Me); ¹³C NMR (100.0 MHz, d₆-DMSO) δ = 160.3 (CO₂Me), 156.8 (ArCCO₂), 153.2 (COH), 148.3 (COMe), 139.7 (CH=C_{quat.}), 127.7 (ArC_{quat.}), 124.9 (ArCH), 124.4 (ArCH), 116.3 (ArC_{quat.}), 112.9 (CH=C_{quat.}), 60.9 (OMe), 52.50 (CO₂Me); HRMS (EI) calcd for [C₁₂H₁₁O₆]⁺251.0550; found [M+H]⁺ 251.0552.



Methyl 6-(2,3-dimethoxy-3-oxoprop-1-en-1-yl)-3-hydroxy-4-iodo-2-methoxybenzoate (270).¹⁰³

To a solution of phenol (277) (1.69 g, 5.7 mmol, 1.0 equiv.) in CH₂Cl₂ (25 mL) was added tetramethylammonium dichloroiodate¹²² (1.86 g, 6.9 mmol, 1.2 equiv.) and NaHCO₃ (1.1 g, 12.6 mmol, 2.2 equiv.) at 0 °C and the reaction was allowed to stir at r.t. for 8 h. The reaction mixture was then re-cooled to 0 °C before addition of a solution of aq. HCl (1M, 20 mL) and CH₂Cl₂ (25 mL) and the organics were then washed with Na₂S₂O₃ (30 mL). The organics were dried over MgSO₄ and concentrated under reduced pressure before silica gel chromatography (EtOAc:Petroleum; 3:1) afforded the title compound (*E:Z*; 1:5) as a yellow oil, which solidified to give a faintly yellow solid (2.01 g, 86%) upon storage at 3 °C for 60 min.

mp = 103-105 °C [lit. 109 °C (7:13)]; *R*_f = 0.23 (EtOAc:Petroleum 3:1); *v*_{max} (film)/cm⁻¹ 3380br (OH), 2950w (CH), 2849w (OCH₃), 1717s (C=O, ester), 1633m (C=C, conj.), 1561m (C=C), 1434m (C-H), 1407m (C-H), 1235s, 1199s, 1133s, 1106s (C-O-CH₃); GCMS (CI) calc for [C₁₄H₁₆IO₇]⁺ 423; found 423 [M+H]⁺; (**Z**)-**isomer**: ¹H NMR (400 MHz, CDCl₃) δ = ¹H NMR (400 MHz, CDCl₃) δ = 8.24 (s, 1H, ArCH), 6.76 (s, 1H, CH=C_{quat.}), 3.94 (s, 3H, OMe), 3.85 (s, 3H, OMe), 3.81 (s, 3H, CO₂Me), 3.72 (s, 3H, CO₂Me); ¹³C NMR (100.0 MHz, CDCl₃) δ = 166.6 (CO₂Me), 164.3 (CO₂Me), 149.2 (COH), 146.2 (COMe), 143.5 (CH=C_{quat.}), 135.6 (ArCH) 128.6 (ArC_{quat.}), 125.2 (ArC_{quat.}), 117.8 (CH=C_{quat.}) 85.5 (CI), 62.2 (OMe), 59.4 (OMe), 52.6 (CO₂Me), 52.2 (CO₂Me); (**E**)-**isomer**: ¹H NMR (400 MHz, CDCl₃) δ = ¹H NMR (400 MHz, CDCl₃) δ = 7.33 (s, 1H, ArCH), 6.06 (s, 1H, CH=C_{quat.}), 3.88 (s, 6H, 2 × OMe), 3.71 (s, 3H, CO₂Me), 3.66 (s, 3H, CO₂Me); ¹³C NMR (100.0 MHz, CDCl₃) δ = 166.7 (CO₂Me), 163.4 (CO₂Me), 148.2 (COH), 148.1 (COMe), 143.3 (CH=C_{quat.}), 134.6 (ArCH) 127.4 (ArC_{quat.}), 126.9 (ArC_{quat.}), 105.8 (CH=C_{quat.}) 84.6 (CI), 62.2 (OMe), 56.0 (OMe), 52.4 (CO₂Me), 52.3 (CO₂Me); spectroscopic data is in agreement with that previously reported.¹⁰³



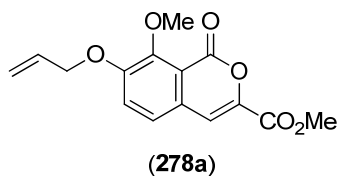
Methyl 7-hydroxy-8-methoxy-1-oxo-1H-isochromene-3-carboxylate (271).¹⁰³

Method A: A solution of (270) (128 mg, 0.34 mmol) dissolved in a 1:1 mixture of MeOH:HBr_(aq) (37%) was heated to 95 °C in a sealed microwave vial for 12 h before slowly cooling to -25 °C. The resultant creamy precipitate was filtered and washed with cold Et₂O (15 mL). The mother liquors were then diluted with H₂O (10 mL) before further extraction with EtOAc (3 × 15 mL), the organics were then concentrated under reduced pressure to give a mixture of white solid in a pale yellow oil. The subsequent oil/solid mixture was washed with cold Et₂O (15 mL) and the combined solids were further purified *via* column chromatography (EtOAc: Petroleum 4:1) to afford the title compound as a pale pink solid (87 mg, 0.23 mmol, 68%).

Method B: A solution of (270) (128 mg, 0.34 mmol) dissolved in a 2:1 mixture of MeOH:3N H₂SO₄ (2 mL) was heated to 95 °C in a sealed microwave vial for 4 h before slowly cooling to -25 °C. The resultant creamy precipitate was filtered and washed with cold Et₂O (15 mL). The mother liquors were then diluted with H₂O (10 mL) before further extraction with EtOAc (3 × 15 mL), the organic layers were then concentrated under reduced pressure to give a mixture of white solid in a pale yellow oil. The subsequent oil/solid mixture was washed with cold Et₂O (15 mL) and the combined solids were further purified *via* column chromatography (EtOAc: Petroleum 4:1) to afford the title compound as a pale pink solid (107 mg, 0.28 mmol, 83%).

Method C: Methyl ester (270) (128 mg, 0.34 mmol, 1.00 equiv.) and PTSA monohydrate (66 mg, 0.35 mmol, 1.02 equiv.) were added to PhMe (2 ml) under stirring in a microwave vial, the reaction vessel was then sealed and heated to 135 °C (external) for 21 h. The reaction mixture was then slowly cooled to -25 °C and the resultant creamy precipitate was filtered and washed with cold Et₂O (15 mL). The resultant white solid was further purified *via* column chromatography (EtOAc: Petroleum 4:1) to afford the title compound as a pale pink solid (71 mg, 0.26 mmol, 75%)

mp = >200 °C; [lit. 249 °C, dec.]; R_f = 0.12 (EtOAc:Petroleum 3:1); ν_{\max} (film)/ cm^{-1} 3450br (OH), 3091w and 2984w (CH), 2940 (OCH₃), 1741s and 1715m (C=O, ester), 1572m, 1553m and 1497m (C=C); ¹H NMR (400 MHz, d₆-DMSO) δ = 10.80 (brs, 1H, OH), 8.14 (s, 1H, ArCH), 7.57 (s, 1H, ArCH=CR₂), 3.84 (s, 3H, OMe), 3.79 (s, 3H, CO₂Me); ¹³C NMR (100.0 MHz, d₆-DMSO) δ = 160.3 (CO₂Me), 156.9 (CO₂R), 153.0 (ArOH); 147.0 (ArOMe); 140.6 (ArCH=CHR), 134.0 (ACrH), 129.0 (ArCH=CHR), 116.0 (ArCO₂Me), 111.9 (ArCH=CHR), 96.6 (ArI); 62.1 (OMe), 52.8 (CO₂Me); GCMS (CI) calcd [C₁₂H₁₀IO₆]⁺ 377; found 377 [M+H]⁺; spectroscopic data is in agreement with that previously reported.¹⁰³

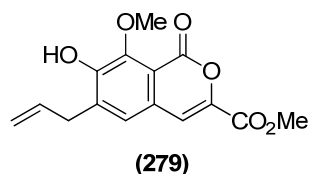


Methyl 7-(allyloxy)-8-methoxy-1-oxo-1H-isochromene-3-carboxylate (278a).⁹⁸

To a solution of (278) (250 mg, 1.0 mmol 1.0 equiv) in DMF (8 mL) in a microwave microwave vial fitted with a rubber septum was added Hünig's base (0.35 mL, 2.0 mmol, 2.0 equiv.) and ally bromide (175 μ L, 2.0 mmol, 2.0 equiv.). The reaction vessel was then fitted with a "crimp cap" and heated at 80 °C for 24 h. After cooling the reaction mixture to r.t. the reaction mixture was filtered through a short plug of silica (1 cm w \times 1 cm h), washing through with EtOAc (50 mL) and MeCN (20 mL). The combined organics were then washed with sat. aq. NaCl solution (10 \times 15 mL), dried over MgSO₄ and concentrated under reduced pressure before silica gel chromatography (EtOAc:Petroleum; 4:5) afforded the title compound as a pale yellow/green solid (272 mg, 0.94 mmol, 90%).

mp = 120-121 °C [lit. 120-122 °C]; R_f = 0.14 (EtOAc:Petroleum 1:2); ν_{\max} (film)/ cm^{-1} 3090w, 2999w, 2941w and 2845w (CH), 1723s (2 \times C=O, ester), 1634m (CO-O), 1594m, 1490m and 1478m (C=C); ¹H NMR (400 MHz, CDCl₃) δ = 6.85 (d, 1H, J = 8.3 Hz, ArCH), 6.83 (s, 1H, HC=C_{quat.}), 6.76 (d, 1H, J = 8.3 Hz, ArCH), 5.63-5.48 (m, 1H, OCH₂CH=CH₂), 4.93 (d, 1H, J = 17.4 Hz, OCH₂CH=CH_aH_b), 4.81 (d, 1H, J = 10.0 Hz, OCH₂CH=CH_aH_b), 4.17 (d, 2H, J = 4.4 Hz, OCH₂CH=CH₂) 3.46 (s, 3H, OMe), 3.40 (s, 3H, CO₂Me); ¹³C NMR (100.0 MHz, CDCl₃) δ = 161.0 (CO₂Me), 157.6 (CCO₂), 149.8

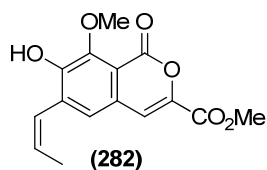
(COMe), 147.3 (COAllyl), 141.5 (CH=C_{quat.}), 136.2 (OCH₂CH=CH₂), 134.4 (ArCH), 128.8 (ArC_{quat.}), 124.7 (ArCH), 117.8 (OCH₂CH=CH₂), 113.9 (ArC_{quat.}), 113.0 (CH=C_{quat.}), 63.1 (OMe), 53.0 (CO₂Me), 34.5 (OCH₂); GCMS (CI) calcd for [C₁₅H₁₅O₆]⁺ 291; found 291 [M+H]⁺; spectroscopic data is in agreement with that previously reported.⁹⁸



Methyl 6-allyl-7-hydroxy-8-methoxy-1-oxo-1H-isochromene-3-carboxylate (279).⁹⁸ To a microwave microwave vial fitted with a septum was added isocoumarin (**278a**) (265 mg, 0.92 mmol, 1.0 equiv.) and chlorobenzene (3

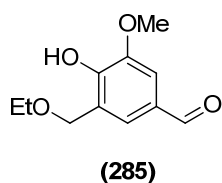
mL). The reaction vessel was fitted with a “crimp-cap” and heated in a microwave reactor at 150 °C (0-300 W, variable power) for 6 h. After the reaction vessel was cooled to r.t., the reaction mixture was diluted with EtOAc (30 mL) and washed with sat. aq. NH₄Cl solution (3 × 20 mL). The organics were dried over MgSO₄ and concentrated under reduced pressure before silica gel chromatography (EtOAc) afforded the title compound as an off-white solid.

mp 188-189 °C [lit. 188-190.5 °C]; *R*_f = 0.65 (EtOAc); *v*_{max} (film)/cm⁻¹ 3400br (OH), 3080w, 2999w and 2964w (CH), 2853w (OCH₃), 1724s (C=O, ester), 1649m (C=O, ester), 1600m, 1490m and 1465 cm (C=C); ¹H NMR (400 MHz, CDCl₃) δ 7.37 (s, 1H, ArCH), 7.16 (s, 1H, CH=C_{quat.}), 6.59 (brs, 1H, OH), 6.04-5.94 (m, 1H, CH₂CH=CH₂), 5.19-5.12 (m, 2H, CH₂CH=CH₂), 4.02 (s, 3H, OMe), 3.93 (s, 3H, OMe), 3.52 (d, 2H, *J* = 5.3 Hz, CH₂CH=CH₂); ¹³C NMR (100.0 MHz, CDCl₃) δ = 160.9 (CO₂Me), 157.4 (CCO₂), 149.7 (COH), 147.2 (COMe), 141.3 (CH=C_{quat.}), 136.1 (ArC_{quat.}), 134.3 (ArCH), 128.6 (ArC_{quat.}), 124.6 (ArC_{quat.}), 117.6 (CH₂CH=CH₂), 113.8 (CH=C_{quat.}), 112.9 (CH₂CH=CH₂), 62.9 (OMe), 52.8 (CO₂Me), 34.3 (CH₂CH=CH₂); GCMS (CI) calcd for [C₁₅H₁₅O₆]⁺ 291; found 291 [M+H]⁺; spectroscopic data is in agreement with that previously reported.⁹⁸



(Z)-Methyl 7-hydroxy-8-methoxy-1-oxo-6-(prop-1-en-1-yl)-1H-isochromene-3-carboxylate (282). To a suspension of phenol (**279**) (30 mg, 0.10 mmol, 1.0 equiv.) in EtOH (2 mL) was added $\text{RhCl}_3 \cdot x\text{H}_2\text{O}$ (38-40% Rh, 10 mg, ~0.03 mmol, 0.32 equiv.) and the reaction mixture was stirred at r.t. for 16 h. The reaction mixture was then diluted with EtOAc (50 mL) and MeOH (5 mL) and the filtered through a silica plug (0.5 cm w \times 0.3 cm h) and the filtrate was concentrated under reduced pressure at r.t. to provide the *title compound* as light brown solid (28 mg, 0.09 mmol, 95%).

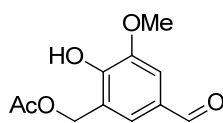
mp = > 200°C; R_f = 0.42 (EtOAc); ν_{max} (film)/ cm^{-1} 3430br (OH), 3075w, 2990w and 2972w (CH), 2848w (OCH₃), 1719s (C=O, ester), 1630m (C=O, ester), 1610m, 1490m and 1465 cm (C=C); ¹H NMR (400 MHz, CDCl₃) δ = 7.37 (d, J = 1.8 Hz, 1H, ArCH), 7.34 (d, J = 1.8 Hz, CH=C_{quat.}), 6.75-6.68 (m, 1H, CH=CHCH₃), 6.65 (brs, 1H, OH), 6.62-6.58 (dq, J = 6.5, 1.9 Hz, 1H, CH=CHCH₃), 4.03 (s, 3H, OMe), 3.94 (s, 3H, CO₂Me), 2.05-1.96 (m, 3H, ArCH=CHCH₃); ¹³C NMR (100.0 MHz) δ = 160.7 (CO₂Me), 156.0 (CCO₂), 148.4 (COH), 147.7 (COMe), 141.4 (CH=C_{quat.}), 132.9 (ArC_{quat.}), 128.5 (ArC_{quat.}), 124.2 (ArCH=C_{quat.}), 121.0 (ArCH=CHCH₃), 116.0 (ArCO₂R), 112.9 (ArCH), 111.9 (CH=C_{quat.}), 62.9 (OMe), 52.8 (CO₂Me), 19.2 (CH₃); GCMS (CI) calcd for [C₁₅H₁₅O₆]⁺ 291, found 291 [M+H]⁺.



3-(Ethoxymethyl)-4-hydroxy-5-methoxybenzaldehyde (285). To a solution of morpholine (0.86 g, 9.9 mmol, 1.5 equiv.) in EtOH (3 mL) over 3Å molecular sieves was added paraformaldehyde (1.0 g, 9.9 mmol, 1.5 equiv.) at r.t. and the suspension was stirred for 24 h before a solution of vanillin (1.0 g, 6.6 mmol, 1.0 equiv.) in EtOH (4 mL) was added *via* cannula and the reaction mixture was stirred at 120 °C for 48 h. The reaction mixture was cooled to r.t. and the crude mixture was concentrated under reduced pressure to give a grey sticky residue, which was partly dissolved in EtOAc (100 mL) and then eluted through a short silica plug (1 cm \times 1 cm). The filtrate was dried over MgSO₄ and

concentrated under reduced pressure and the resultant pale yellow oil was purified by silica gel chromatography (EtOAc) to give the *title compound* as an off-white solid (0.58 g, 2.8 mmol, 28%).

mp = 64-66 °C; R_f = 0.87 (EtOAc); ν_{\max} (film)/ cm^{-1} 3163br (OH), 2971w and 2958w (CH), 2866w and 2852w (OCH_3), 1666s (C=O, aldehyde), 1592m, 1465m and 1434m (C=C); $^1\text{H NMR}$ (400 MHz, CDCl_3) δ = 9.55 (s, 1H, CHO), 7.21 (dd, J = 1.7, 1.6 Hz, 1H, ArCH), 7.09 (d, 1H, J = 1.6 Hz, ArCH), 4.40 (s, 2H, CH_2OEt), 3.65 (s, 3H, OMe), 3.37 (dq, J = 6.9, 1.7 Hz, 2H, OCH_2CH_3), 1.02 (dt J = 6.9, 1.7, 3H, CH_2CH_3); $^{13}\text{C NMR}$ (100.0 MHz) δ = 191.3 (CHO), 150.2 (COH), 147.8 (COMe), 129.5 (ArC_{quat.}), 126.7 (ArCH), 124.3 (CCHO), 108.6 (ArCH), 68.3 (CH_2OEt), 66.8 (OCH_2CH_3), 56.8(OMe), 15.5 (OCH_2CH_3); GCMS (CI) calcd for $[\text{C}_{11}\text{H}_{15}\text{O}_4]^+$ 211; found 211 $[\text{M}+\text{H}]^+$.



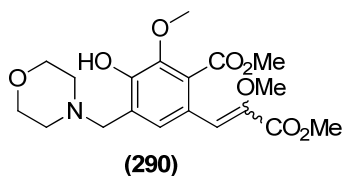
(289)

5-Formyl-2-hydroxy-3-methoxybenzyl acetate (289). To a solution of morpholine (0.86 g, 9.9 mmol, 1.5 equiv.) in AcOH (3 mL) over 3Å molecular sieves was added paraformaldehyde (1.0 g, 9.9 mmol, 1.5 equiv.) at r.t. and the suspension was stirred for

24 h before a solution of vanillin (1.0 g, 6.6 mmol, 1.0 equiv.) in AcOH (4 mL) was added *via* cannula and the reaction mixture was stirred at 120 °C for 48 h. The reaction mixture was cooled to r.t. and the crude mixture was concentrated under reduced pressure to give a grey sticky residue, which was partly dissolved in EtOAc (100 mL) and then eluted through a short silica plug (1 cm × 1 cm). The filtrate was dried over MgSO_4 and concentrated under reduced pressure and the resultant pale yellow oil was purified by silica gel chromatography (EtOAc:Petroleum; 1:1) to give the *title compound* as an off-white solid (0.77 g, 3.5 mmol, 35%).

mp = 90-92 °C; R_f = 0.77 (EtOAc:Petroleum; 1:1); ν_{\max} (film)/ cm^{-1} 3133br (OH), 2974w (CH), 2855w (OCH_3), 1729s (C=O, ester), 1664s (C=O, aldehyde), 1592m, 1501m and 1470m (C=C); $^1\text{H NMR}$ (400 MHz, CDCl_3) δ = 9.84 (s, 1H, CHO), 7.49 (s, 1H, ArCH), 7.41 (s, 1H, ArCH), 6.62 (s, 1H, OH), 5.23 (s, 2H, CH_2OAc), 3.98 (s, 3H, OMe), 2.14 (s, 3H, CH_3CO); $^{13}\text{C NMR}$ (100.0 MHz) δ = 190.9 (CHO), 171.3 (CH_3CO), 150.0

(COH), 147.4 (COMe), 129.4 (ArC_{quat}), 127.9 (ArCH), 122.1 (CCHO), 108.8 (ArCH), 60.9 (OMe), 56.5 (CH₂OAc), 21.1 (MeCO); GCMS (CI) calcd for [C₁₁H₁₃O₅]⁺ 225; found 225 [M+H]⁺.



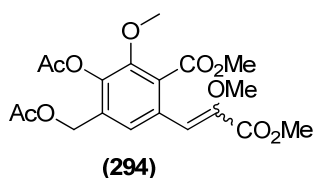
Methyl 6-(2,3-dimethoxy-3-oxoprop-1-en-1-yl)-3-hydroxy-2-methoxy-4-(morpholinomethyl)benzoate (290).

Method A: To a solution of phenol (**277**; *E:Z*; 1:5) (50 mg, 0.17 mmol, 1.0 equiv.) in MeCN (1 mL) in a microwave vial fitted with a septa, was added 4-methylenemorpholin-4-ium chloride¹²³ (46 mg, 0.34 mmol, 2.0 equiv.), the vial was then sealed with a “crimp cap” and then headed at 150 °C for 16 h. The clear yellow solution was allowed to cool to r.t. and then diluted with EtOAc (10 mL) and filtered before concentration under reduced pressure afforded a pale yellow oil. Purification *via* column chromatography (EtOAc: Petroleum 1:2) afforded a isomeric mixture (*E:Z*; 16:84) of the *title compound* (**290**) as a clear colourless oil which solidified upon storage at -5 °C (61 mg, 0.15 mmol, 91%). Stereochemical assignments were made on the basis of NOESY experiments.

Method B: To a microwave vial fitted with a septa, was added paraformaldehyde (101 mg, 3.9 mmol, 2.0 equiv.), acetic acid (6 mL) and then morpholine (0.3 mL, 3.9 mmol, 2.0 equiv.). The resultant slurry was left to stir at r.t. for 24 h before addition of (**277**) (574 mg, 1.9 mmol, 1.0 equiv.). The vial was then sealed and then headed at 130 °C for 16 h. The clear yellow solution was allowed to cool to r.t. and then diluted with EtOAc (30 mL) and filtered before concentration under reduced pressure afforded a pale yellow oil. Purification *via* column chromatography (EtOAc: Petroleum 1:2) afforded a isomeric mixture (*E:Z*; 13:87) of the *title compound* (**290**) as a clear colourless oil which solidified upon storage at -5 °C (76.5 mg, 1.94 mmol, quant.). Stereochemical assignments were made on the basis of NOESY experiments.

mp = 22-23 °C; *R*_f = 0.23 (CH₂Cl₂:MeCN; 9:1); *v*_{max} (film)/cm⁻¹ 2948w (CH), 2841w (OCH₃), 1726s (C=O, ester), 1636m (C=C, conj.), 1450m (C-H), 1274s and 1057s (C-O-

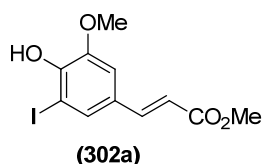
CH₃); HRMS (CI) calcd for [C₁₉H₂₆O₈N₁]⁺ 396.1653; found 396.1653 [M+H]⁺; **(Z)-isomer:** ¹H NMR (400 MHz, CDCl₃) δ = 9.77 (s, 1H, OH), 6.62 (s, 1H, ArCH), 6.09 (s, 1H, HC=C_{quant.}), 3.92 (s, 3H, OMe), 3.86 (s, 3H, OMe), 3.78-3.75 (m, 4H, 2 × NCH₂CH₂O), 3.71-3.68 (brs, 5H, 1 × CO₂Me and CCH₂), 3.63 (s, 3H, CO₂Me), 2.57 (brs, 4H, 2 × OCH₂CH₂N); ¹³C NMR (100.0 MHz) δ = 167.8 (CO₂Me), 163.9 (CO₂Me), 149.7 (ArOH), 147.8 (ArOMe), 144.9 (CH=C_{quat.}), 124.7 (ArCH), 124.5 (ArC_{quat.}), 123.6 (ArC_{quat.}), 122.9 (ArC_{quat.}), 107.1 (CH=C_{quat.}), 66.7 (2 × RNCH₂CH₂O), 61.60 (CH₂N), 61.20 (OMe), 55.98 (OMe), 52.86 (2 × OCH₂CH₂N), 52.11 (CO₂Me), 51.96 (CO₂Me); **(E)-isomer:** δ = ¹H NMR (400 MHz, CDCl₃) δ = 9.87 (s, 1H, OH), 7.62 (s, 1H, ArCH), 6.81 (s, 1H, ArHC=CR₂), 3.95 (s, 3H, OMe), 3.94 (s, 2H, ArCH₂), 3.91 (s, 3H, OMe), 3.81 (s, 3H, OMe), 3.76-3.73 (m, 4H, 2 × NCH₂CH₂O), 3.72 (s, 3H, OMe), 2.57 (brs, 4H, 2 × OCH₂CH₂N); The ¹³C NMR spectrum could not be clearly distinguished from the major (Z)-isomer.



Methyl 3-acetoxy-4-(acetoxymethyl)-6-(2,3-dimethoxy-3-oxoprop-1-en-1-yl)-2-methoxybenzoate (294). To a microwave vial fitted with a septa, was added a solution of **(290)** (100 mg, 0.25 mmol, 1.0 equiv.) in Ac₂O (2 mL, 21.2 mmol, 84.6 equiv), the vial was then sealed and then headed at 155 °C for 24 h. Once cooled the solution was washed into a round-bottomed flask with MeOH (10 mL) and concentrated under reduced pressure to give a clear pale brown oil. Purification *via* column chromatography (CH₂Cl₂:MeCN; 19:1) afforded a isomeric mixture (*E:Z*; 1:4) of the *title compound* as a clear, pale yellow oil (89 mg, 0.20 mmol, 84%). Stereochemical assignments were made on the basis of NOESY experiments.

$R_f = 0.26$ (CH₂Cl₂:MeCN; 19:1); ν_{\max} (film)/cm⁻¹ 2953w (CH), a 2851w (OCH₃), 1770m (C=O, ester), 1727s (C=O, ester), 1635m (C=C, conj.), 1454m (C-H), 1221s, 1183s and 1154s (C-O-CH₃); HRMS (CI) calcd for [C₁₉H₂₆O₁₀N₁]⁺ 428.1551; found 428.1551 [M+NH₄]⁺; **(Z)-isomer:** ¹H NMR (400 MHz, CDCl₃) δ = ¹H NMR (400 MHz, CDCl₃) δ =

7.01 (s, 1H, ArCH), 6.13 (s, H, CH=C_{quat.}), 5.02 (s, 2H, CH₂OAc), 3.85 (s, 3H, OMe), 3.81 (s, 3H, OMe), 3.72 (s, 3H, CO₂Me), 3.61 (s, 3H, CO₂Me), 2.33 (s, 3H, OAc), 2.06 (s, 3H, OAc); ¹³C NMR (100.0 MHz) δ = 171.1 (OCOMe), 168.8 (OCOMe), 167.3 (CO₂Me), 164.8 (CO₂Me), 150.2 (COMe), 147.8 (CH=C_{quat.}), 142.9 (COAc), 132.3 (ArCH), 131.9 (Ar_{quat.}), 130.4 (Ar_{quat.}), 127.1 (Ar_{quat.}), 118.8 (CH=C_{quat.}), 62.9 (OMe), 61.6 (CH₂OAc), 60.3 (OMe), 53.3 (CO₂Me), 53.0 (CO₂Me), 21.4 (OCOMe), 21.1 (OCOMe); **(E)-isomer:** ¹H NMR (400 MHz, CDCl₃) δ = ¹H NMR (400 MHz, CDCl₃) δ = 7.91 (s, 1H, ArCH), 6.86 (s, H, CH=C_{quat.}), 5.05 (s, 2H, CH₂OAc), 3.93 (s, 3H, OMe), 3.83 (s, 6H, 1 × OMe, 1 × CO₂Me), 3.74 (s, 3H, CO₂Me), 2.35 (s, 3H, OAc), 2.09 (s, 3H, OAc); ¹³C NMR (100.0 MHz) δ = 171.1 (OCOMe), 168.9 (OCOMe), 167.4 (CO₂Me), 164.1 (CO₂Me), 150.3 (COMe), 149.2 (CH=C_{quat.}), 141.9 (COAc), 133.0 (ArCH), 130.2 (CH₂), 128.8 (ArC_{quat.}), 127.1 (ArC_{quat.}), 118.8 (CH=C_{quat.}), 62.8 (OMe), 61.4 (ArCH₂), 56.7 (OMe), 53.0 (CO₂Me), 52.8 (CO₂Me), 21.4 (COMe), 21.1 (COMe).



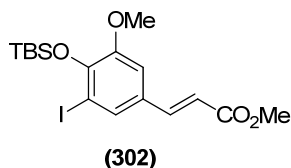
(E)-Methyl 3-(4-hydroxy-3-iodo-5-methoxyphenyl)acrylate

(302a).¹²⁴ To a solution of iodovanillin (1.12 g, 4.0 mmol, 1.0 equiv.) in THF (50 mL) was added methyl

(triphenylphosphoranylidene)acetate (3.8 g, 11.3 mmol, 2.8 equiv.) and the resultant suspension was heated to reflux for 12 h. The reaction mixture was then cooled to r.t. before the filtered reaction mixture was dried over MgSO₄ and concentrated under reduced pressure to give a pale yellow solid, which was purified *via* silica gel chromatography (EtOAc:Petroleum; 1:4) to afford the title compound as an off-white solid (1.31 g, 3.9 mmol, 98%).

mp 138-139 °C [lit. 140-143°C]; *R*_f = 0.25 (EtOAc:Petroleum; 1:4); *v*_{max} (film)/cm⁻¹ 3232br (OH), 2971w and 2940w (CH), 2854w (OCH₃), 1667s (C=O, ester), 1590s, 994m and 914m (RH=CH₂); ¹H NMR (400 MHz, CDCl₃) δ = 7.51 (d, *J* = 16.3 Hz, 1H, CH=CHCO₂Me), 7.49 (s, 1H, ArCH), 6.95 (s, 1H, ArCH), 6.51 (brs, 1H, COH), 6.27 (d, *J* = 16.3 Hz, 1H, CH=CHCO₂Me), 3.90 (s, 3H, OMe), 3.78 (s, 3H, CO₂Me); ¹³C NMR (100.0 MHz, CDCl₃) δ = 167.4 (CO₂Me), 147.8 (COH), 146.2 (COMe),

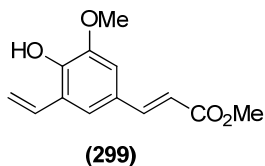
143.4 (CH=CHCO₂Me), 132.1 (ArC_{quat.}), 128.5 (ArCH), 116.4 (CH=CHCO₂Me), 109.4 (ArCH), 81.3 (CI), 56.0 (OMe), 51.7 (CO₂Me); GCMS (CI) calc [C₁₁H₁₀IO₄]⁺ 335; found 335 [M+H]⁺; spectroscopic data is in agreement with that previously reported.¹²⁵



(E)-Methyl 3-(4-((*tert*-butyldimethylsilyloxy)-3-iodo-5-methoxyphenyl)acrylate (302).¹²⁵ Et₃N (0.8 mL, 5.8 mmol, 1.5 equiv.) was added at r.t. to a mixture of phenol (**302a**) (1.3 g, 3.9

mmol, 1.0 equiv.), TBSCl (650 mg, 4.3 mmol, 1.1 equiv.) and DMAP (24 mg, 0.2 mmol, 5 mol %) in CH₂Cl₂ (1.0 mL). After stirring at r.t. for 24 h, the organics were diluted with CH₂Cl₂ (10 mL) and washed with sat. aq. NH₄Cl solution (2 × 10 mL). The organic layer was then separated and dried over MgSO₄, filtered and concentrated under reduced pressure to a pale yellow/brown oil. Flash chromatography (EtOAc:Petroleum, 1:5) afforded the *title compound* as a pale yellow solid (1.69 g, 3.8 mmol, 97%).

mp = 105-107 °C; *R*_f = 0.23 (EtOAc:Petroleum; 1:6); *v*_{max} (film)/cm⁻¹ 2952w and 2928w (C-H), 2854w (OCH₃), 1730m (C=O, ester), 1698s (C=O, aldehyde), 1550w, 1479m and 1460m (C=C); ¹H NMR (400 MHz, CDCl₃) δ = 7.53 (d, *J* = 1.7 Hz, 1H, ArCH), 7.52 (dd, *J* = 16.4 Hz, 2.0 Hz, 1H, CH=CHCO₂Me), 6.95 (d, *J* = 1.7 Hz, 1H, ArCH), 6.28 (dd, *J* = 16.4 Hz, 2.0 Hz, 1H, CH=CHCO₂Me), 3.81 (s, 3H, OMe), 3.79 (s, 3H, CO₂Me), 1.04 (s, 9H, SiMe₂^{*t*}Bu), 0.25 (s, 6H, SiMe₂^{*t*}Bu); ¹³C NMR (100.0 MHz, CDCl₃) δ = 167.6 (CO₂Me), 149.6 (COMe), 147.7 (COTBS), 143.5 (CH=CHCO₂Me), 131.9 (ArC_{quat.}), 129.2 (ArCH), 116.7 (CH=CHCO₂Me), 110.5 (ArCH), 90.7 (CI), 55.1 (OMe), 55.9 (CO₂Me), 26.2 (SiC(CH₃)₃), 19.2(SiC(CH₃)₃), -3.2 (SiMe₂); GCMS (CI) calc [C₁₇H₂₆IO₄Si]⁺ 449; found 449 [M+H]⁺; spectroscopic data is in agreement with that previously reported.¹²⁵

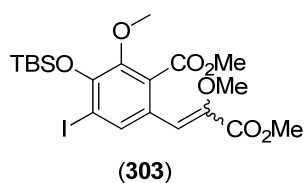


(E)-methyl 3-(4-hydroxy-3-methoxy-5-vinylphenyl)acrylate (302). To a microwave vial fitted with a septa, was added (**301**) (100 mg, 0.2 mmol, 1.0 equiv.), Na₂CO₃ (140 mg, 1.3 mmol,

6.0 equiv.), DMF (4 mL), H₂O (0.4 mL) and vinylboronicacid pinacol ester (120 μl,

0.7 mmol, 3.5 equiv.) and the solution was thoroughly deoxygenated with argon before addition of Pd(PPh₃)₄ (25 mg, 0.02 mmol., 10 mol %). The vial was then fitted with a ‘crimp-cap’ and then heated to 80 °C for 5 h. The reaction mixture was then diluted with Et₂O (50 mL) and filtered through a small plug of silica under suction filtration to remove any inorganic impurities before concentration of the organics under reduced pressure. The crude residue was then dissolved in H₂O (10 mL) and extracted with Et₂O (2 × 15mL) before further washing of the organic layer with sat. aq. NaCl solution (5 × 10 mL) to remove any remaining DMF. The organics were dried over MgSO₄, filtered and concentrated under reduced pressure before purification by silica gel chromatography (Petroleum:Et₂O; 1:1) furnished the *title compound* as a clear colourless oil (27 mg, 0.12 mmol 53%).

mp 138-139 °C; *R*_f = 0.25 (EtOAc:Petroleum; 1:4); *v*_{max} (film)/cm⁻¹ 3232br (OH), 2971w and 2940w (CH), 2854w (OCH₃), 1667s (C=O, ester), 1590s, 994m and 914m (RH=CH₂); ¹H NMR (400 MHz, CDCl₃) δ = 7.64 (d, *J* = 16.2 Hz, 1H, CH=CHCO₂Me), 7.27-7.22 (m, 1H, ArH), 7.02-6.93 (m, 2H, 1 x ArH, 1 x CH=CH₂), 6.31 (d, *J* = 16.2 Hz, 1H, CH=CHCO₂Me), 5.84 (d, *J* = 16.9 Hz, 1H, CH=CH_aH_b), 5.36 (d, *J* = 10.3 Hz, 1H, CH=CH_aH_b), 3.94 (s, 3H, OMe), 3.80 (s, 3H, CO₂Me); ¹³C NMR (100.0 MHz, CDCl₃) δ = 167.4 (CO₂Me), 147.8 (COH), 146.2 (COMe), 143.4 (CH=CHCO₂Me), 132.1 (ArC_{quat.}), 128.5 (ArCH), 116.4 (CH=CHCO₂Me), 109.4 (ArCH), 81.3 (CI), 56.0 (OMe), 51.7 (CO₂Me); GCMS (CI) calc [C₁₃H₁₅O₄]⁺ 335; found 335 [M+H]⁺.



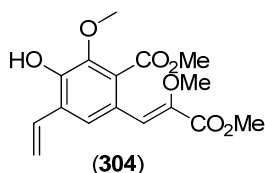
Methyl 3-((tert-butyldimethylsilyloxy)-6-(2,3-dimethoxy-3-oxoprop-1-en-1-yl)-4-iodo-2-methoxybenzoate (303). To a solution of (270) (280 mg, 0.66 mmol, 1.0 equiv.) in CH₂Cl₂ (7 mL) was added Et₃N (0.13 mL, 0.90 mmol, 1.35 equiv.),

4-(dimethylaminopyridine (12.5 mg, 0.10 mmol, 0.15 equiv.) and *tert*-butyldimethylsilyl chloride (125 mg, 0.83 mmol, 1.25 equiv.). The solution was stirred at rt for 16 h before addition of sat. aq. Na₂CO₃ solution (15 mL), the layers were then separated and the aqueous layer was then extracted further with CH₂Cl₂ (3 × 30 mL). The combined

organics were dried over MgSO₄ and concentrated under reduced pressure, before purification of the crude residue by silica gel chromatography (Et₂O:Petroleum; 1:4) afforded (**Z-303**) as an off white solid (230 mg, 0.43 mmol, 65%) and (**E-303**) as a pale yellow oil (106 mg, 0.20 mmol, 30%). Stereochemical assignments were made on the basis of NOESY experiments and correlation of chemical shifts of closely related literature compounds.¹⁰³

(Z)-isomer: mp = 38-39 °C, R_f = 0.23 (Et₂O:Petroleum; 1:4); ν_{max} (film)/cm⁻¹ 2943w, 2926w and 2895w (CH), 2855 (O-C-H₃), 1722s (2 × C=O, ester), 1633w (O-CO), 1570w, 1536w and 1446m (C=C); ¹H NMR (400 MHz, CDCl₃) δ = 8.34 (s, 1H, ArCH), 6.72 (s, 1H, CH=C_{quat.}), 3.94 (s, 3H, OMe), 3.83 (s, 3H, OMe), 3.76 (s, 3H, CO₂Me), 3.73 (s, 3H, CO₂Me), 1.07 (s, 9H, SiMe₂^tBu), 0.29 (s, 6H, SiMe₂^tBu); ¹³C NMR (100.0 MHz, CDCl₃) δ = 167.0 (CO₂Me), 164.1 (CO₂Me), 149.1 (CH=C_{quat.}), 147.4 (COMe), 146.1 (COTBS), 136.3 (ArCH), 130.3 (ArC_{quat.}), 125.8 (ArC_{quat.}), 117.4 (CH=C_{quat.}), 93.5 (CI), 61.5 (OMe), 59.3 (OMe), 52.4 (CO₂Me), 52.1 (CO₂Me), 26.1 (SiC(CH₃)₃), 18.6 (SiC(CH₃)₃), -3.4 (SiMe₂); HRMS (EI) calcd for [C₂₀H₃₀I₁O₇Si]⁺ 537.0800; found [M+H]⁺ 537.0794.

(E)-isomer: R_f = 0.25 (Et₂O:Petroleum; 1:4); ν_{max} (film)/cm⁻¹ 2933w and 2927w (CH), 2850 (O-C-H₃), 1734s (2 × C=O, ester), 1612w (O-CO), 1510m, and 1454m (C=C); ¹H NMR (400 MHz, CDCl₃) δ = 7.39 (s, 1H, ArCH), 6.02 (s, 1H, CH=C_{quat.}), 3.85 (s, 3H, OMe), 3.74 (s, 3H, OMe), 3.70 (s, 3H, CO₂Me), 3.64 (s, 3H, CO₂Me), 1.07 (s, 9H, SiMe₂^tBu), 0.28 (s, 6H, SiMe₂^tBu); ¹³C NMR (100.0 MHz, CDCl₃) δ = 167.0 (CO₂Me), 164.1 (CO₂Me), 149.1 (CH=C_{quat.}), 147.4 (COMe), 146.1 (COTBS), 136.8 (ArCH), 130.4 (ArC_{quat.}), 125.7 (ArC_{quat.}), 107.8 (CH=C_{quat.}), 93.5 (CI), 61.4 (OMe), 59.3 (OMe), 52.4 (CO₂Me), 52.1 (CO₂Me), 26.1 (SiC(CH₃)₃), 18.6 (SiC(CH₃)₃), -3.4 (SiMe₂); HRMS (EI) calcd for [C₂₀H₃₀IO₇Si]⁺ 537.0800; found 537.0795 [M+H]⁺.

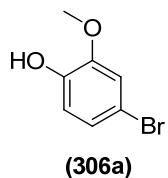


(Z)-Methyl 6-(2,3-dimethoxy-3-oxoprop-1-en-1-yl)-3-hydroxy-2-methoxy-4-vinylbenzoate (304). To a microwave vial fitted

with a septa, was added **(303a)** (144 mg, 0.27 mmol, 1.0 equiv.), Na₂CO₃ (170 mg, 1.6 mmol, 6.0 equiv.), DMF (5 mL), H₂O

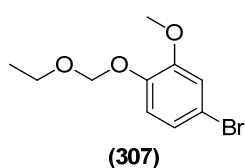
(0.5 mL) and vinylboronic acid pinacol ester (158 μl, 0.94 mmol, 3.5 equiv.) and the solution was thoroughly deoxygenated with argon before addition of Pd(PPh₃)₄ (31 mg, 10 mol %). The vial was then fitted with a ‘crimp-cap’ and then heated to 80 °C for 5 h. The reaction mixture was then diluted with Et₂O (50 mL) and filtered through a small plug of silica under suction filtration to remove any inorganic impurities before concentration of the organics under reduced pressure. The crude residue was then dissolved in H₂O (75 mL) and extracted with Et₂O (15 mL) before further washing of the organic layer (5 × 75 mL) to remove any remaining DMF. The organic layers were dried over MgSO₄, filtered and concentrated under reduced pressure before purification by silica gel chromatography (Petroleum:Et₂O; 1:2) afforded the *title compound* as a pale orange oil (86 mg, 0.27 mmol, quant.).

$R_f = 0.36$ (Petroleum:Et₂O; 1:2); ν_{\max} (film)/cm⁻¹ 3406br (OH), 2952w (CH), 2582w (OCH₃), 1720s (C=O, ester), 1634w (C=C, conj.), 1596w (C=C), 1454m and 1435m (C-H), 1286s, 1242s, 1198m and 1168m C-O-CH₃); ¹H NMR (400 MHz, CDCl₃) $\delta = 7.97$ (s, 1H, ArCH), 6.91 – 6.99 (m, 1H, CH=CH₂), 6.92 (s, 1H, CH=C_{quat.}), 6.08 (s, 1H, OH), 5.89 (dd, 1H, $J = 17.7$ Hz, $J = 1.3$ Hz, CH=CH_aH_b) 5.41 (dd, 1H, $J = 11.2$ Hz, $J = 1.3$ Hz, CH=CH_aH_b), 3.96 (s, 3H, OMe), 3.87 (s, 3H, OMe), 3.84 (s, 3H, CO₂Me), 3.72 (s, 3H, CO₂Me); ¹³C NMR (100.0 MHz) $\delta = 167.3$ (CO₂Me), 164.9 (CO₂Me), 146.9 (COH), 145.9 (COMe), 144.9 (CH=C_{quat.}), 130.7 (CH=CH₂), 126.8 (ArC_{quat.}), 126.4 (ArC_{quat.}), 124.7 (ArCH), 123.5 (ArC_{quat.}), 120.1 (CH=CH₂), 117.3 (CH=C_{quat.}), 62.8 (OMe), 59.7 (OMe), 52.9 (CO₂Me), 52.5 (CO₂Me); HRMS (CI) calcd for [C₁₆H₁₉O₇]⁺ 323.1131; found 323.1130 [M+H]⁺.



4-Bromo-2-methoxyphenol (306a).¹²⁵ To a solution of guaiacol (**306**) (22.2 mL, 201 mmol, 1.0 equiv) in DMF (175 mL) at 0 °C was added a solution of N-bromosuccinamide (35.6 g, 200 mmol, 1.0 equiv.) in DMF (175 mL) dropwise *via* a pressure equalised dropping funnel. After stirring at this temperature for 1 h, the reaction mixture was diluted with Et₂O (300 mL), filtered and then washed thoroughly with sat. aq. Na₂S₂O₃ solution (700 mL), sat. aq. NaCl solution (700 mL) and H₂O (700 mL). The combined aqueous extracts were then extracted with Et₂O (2 × 250 mL) and the combined organics were dried over MgSO₄. After filtration and concentration under reduced pressure the crude residue was purified by short silica gel chromatography (dimensions; 10 cm d × 20 cm h; Petroleum:Et₂O; 4:1) to afford the title compound (**306a**) as a pale yellow oil (39.8 g, 196 mmol, 97%). spectroscopic data is in agreement with that previously reported.¹²⁶

$R_f = 0.21$ (Petroleum:Et₂O; 4:1); ν_{\max} (film)/cm⁻¹ 3511br (O-H), 3011w, 2969w, 2940w (CH), 2844w (OCH₃), 1496s (C=C), 1443s (C=C)s, 1255s (O-H), 873s (C-Br). ¹H NMR (400 MHz, CDCl₃) $\delta = 6.99$ (dd, $J = 8.3, 2.3$ Hz, 1H, ArCH), 6.97 (d, $J = 2.3$ Hz, 1H, ArCH), 6.80 (d, $J = 8.3$ Hz, 1H, ArCH), 5.53 (s, 1H, OH), 3.32 (s, 3H, OMe). ¹³C NMR (100.0 MHz) $\delta = 147.3$ (COH), 145.0 (COMe), 124.3 (ArCH), 115.9 (ArCH), 114.3 (ArCH), 111.7 (CBr), 56.3 (OMe); HRMS (EI) calcd for [C₇H₈O₂⁷⁹Br]⁺ 202.9702 and [C₇H₈O₂⁸¹Br]⁺ 204.9682; found 202.9704 and 204.9681 [M+H]⁺.



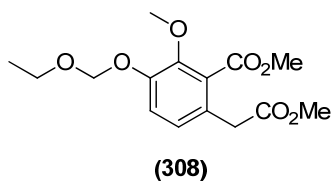
4-Bromo-1-(ethoxymethoxy)-2-methoxybenzene (307).⁸⁶

Method A: To a mixture of phenol (**306a**) (19.33 g, 95.2 mmol, 1.0 equiv.) and K₂CO₃ (15.6 g, 112.9 mmol, 1.19 equiv.) in DMF (50 mL) was slowly added chloromethyl ethyl ether (10 mL, 107.8 mmol, 1.13 equiv.) at 0 °C. After 10 minutes at that temperature the external cooling bath was removed and the reaction vessel was stirred at ambient temperature for 16 h. The mixture was then diluted with Et₂O (100 mL), filtered and then the filtrate solution was washed with water (300 mL). The organic layer was separated, and the aqueous layer was extracted with Et₂O (2 × 100 mL). The combined organic layers were washed with brine (200 mL), and dried over

MgSO₄. After filtration and concentration under reduced pressure, the crude residue was purified by silica gel column chromatography (Petroleum:CH₂Cl₂; 3:2) to the title compound (**307**) (20.2 g, 77.3 mmol, 81%) as a yellow oil.

Method B: To a mixture of phenol (**306a**) (30.2 g, 148.8 mmol, 1.0 equiv.) and Hünig's base (31.1 mL, 178.5 mmol, 1.20 equiv.) in DMF (200 mL) was slowly added chloromethyl ethyl ether (15.6 mL, 168.1 mmol, 1.13 equiv.) at 0 °C. After 10 minutes at that temperature the external cooling bath was removed and the reaction vessel was stirred at ambient temperature for 16 h. The mixture was then diluted with Et₂O (400 mL), filtered and then the filtrate solution was washed with water (600 mL). The organic layer was separated, and the aqueous layer was extracted with Et₂O (2 × 400 mL). The combined organic layers were washed with brine (400 mL), and dried over MgSO₄. After filtration and concentration under reduced pressure, the crude residue was purified by silica gel column chromatography (Petroleum:CH₂Cl₂; 3:2) to the title compound (**307**) (34.1 g, 130.5 mmol, 88%) as a yellow oil.

$R_f = 0.21$ (Petroleum:CH₂Cl₂; 3:2); ν_{\max} (film)/cm⁻¹ 2974w and 2532w (CH), 2948w (OCH₃), 1589m, 1496s, 1463m, 1444m (C=C), 898s (C-Br); ¹H NMR (400 MHz, CDCl₃) $\delta = 6.99$ -7.07 (m, 3H, 3 × ArCH), 5.24 (s, 2H, OCH₂O), 3.86 (s, 3H, OMe), 3.76 (q, 2H, $J = 7.0$ Hz, OCH₂CH₃), 1.22 (t, 3H, $J = 7.0$ Hz, OCH₂CH₃); ¹³C NMR (100.0 MHz) $\delta = 150.4$ (COMe), 145.9 (COEOM), 123.5 (ArCH), 117.6 (ArCH), 114.3 (ArCH), 94.2 (OCH₂O), 64.4 (OCH₂CH₃), 56.0 (OMe), 15.0 (OCH₂CH₃); HRMS (EI) calcd for [C₁₀H₁₄⁷⁹Br₁O₃]⁺ 261.0121 and [C₁₀H₁₄⁸¹Br₁O₃]⁺ 263.0100; found 261.0124 and 263.0103 [M+H]⁺; spectroscopic data was not previously reported.⁸⁶

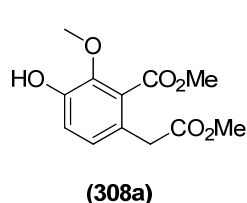


Methyl 3-(ethoxymethoxy)-2-methoxy-6-(2-methoxy-2-oxoethyl)benzoate (308).⁸⁶ To a solution of HNⁱPr₂ (11.2 mL, 80 mmol, 2.45 equiv.), in THF (300 mL) was added *n*-BuLi (2.5 M in hexanes, 31.2 mL, 78 mmol,

2.4 equiv.) dropwise at -78 °C. After the addition, the external cooling bath temperature

was increased to 0 °C and the solution was stirred at this temperature for 30 minutes. Freshly distilled diethyl malonate (4.5 mL, 39 mmol, 1.2 equiv.) was added dropwise and left to stir at that temperature for a further 30 min. This was followed by dropwise addition (over 10 minutes) of bromide (**307**) (8.50 g, 32.6 mmol, 1.0 equiv) in THF (30 mL) and the solution was left to stir at 0 °C for a further 30 min, at which point TLC analysis (3:1; Petroleum:Et₂O) indicated complete consumption of the starting material. The reaction mixture was then quenched at 0 °C by addition of MeOH (50 mL) and the mixture was allowed to warm to r.t. before concentration under reduced pressure. The crude residue was then dissolved in EtOAc (300 mL) and filtered through a short silica gel plug (10 cm w × 3 cm h) and the filtrate was dried over MgSO₄, filtered and concentrated under reduced pressure before silica gel chromatography (1% THF in CH₂Cl₂) afforded the title compound as a pale yellow oil (8.55g, 27.4 mmol, 84%).

$R_f = 0.23$ (3:1; Petroleum:Et₂O); ¹H NMR (400 MHz, CDCl₃) $\delta = 7.19$ (d, $J = 8.6$ Hz, 1H, ArCH), 9.69 (d, $J = 8.6$ Hz, 1H, ArCH), 5.26 (s, 2H, OCH₂O), 3.90 (s, 3H, OMe), 3.89 (s, 3H, CO₂Me), 3.77-3.73 (m, 2H, CH₂CH₃), 3.68 (s, 3H, CO₂Me), 3.67 (s, 2H, CH₂CO₂Me), 1.23 (t, 3H, $J = 7.1$ Hz, OCH₂CH₃); ¹³C NMR (100.0 MHz) $\delta = 171.7$ (CO₂Me), 167.7 (CO₂Me), 149.9 (COMe), 147.8 (COEOM), 129.2 (ArC_{quat.}), 126.6 (ArCH), 125.8 (ArC_{quat.}), 118.2 (ArCH), 93.9 (OCH₂O), 64.7 (OCH₂CH₃), 61.8 (OMe), 56.0 (CO₂Me), 52.2 (CO₂Me), 38.5 (CH₂CO₂Me), 15.2 (OCH₂CH₃); GCMS (CI) calc [C₁₅H₂₁O₇]⁺ 313; found 313 [M+H]⁺; spectroscopic data was not previously reported.⁸⁶

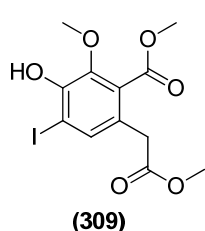


Methyl 3-hydroxy-2-methoxy-6-(2-methoxy-2-oxoethyl)benzoate (308a).⁸⁶ To a solution of (**308**, 8.6g, 27.4 mmol, 1.0 equiv.) in CH₂Cl₂ (200 mL) was added NaHSO₄-SiO₂⁸⁸

⁸⁸ To a solution of 18.0 g (150.0 mmol) of NaHSO₄ in 100 mL of H₂O was added 50.0 g of SiO₂ and the mixture was stirred for 30 min at r.t. The mixture was then

at rt and the resultant suspension was stirred for a further 16 h. The reaction mixture was then filtered through a short silica plug (w = 10 cm × h = 5 cm) under gravity, washing with EtOAc (300 mL) and the combined organic layers were concentrated under reduced pressure. The resultant oil was then triturated with a mixture of 1% THF in cyclohexane (2 × 75 mL) and the the resultant clear colourless oil was dried under vacuum, before addition of a mixture of 5% CH₂Cl₂ in cyclohexane (150 mL). The mixture was left in an ultrasonic bath for 60 minutes, heated to gentle boiling before allowing to cool gradually to r.t. before being cooled to 3 °C for 48 h, at which time, needle like crytals had formed. The needles were collected *via* filtration and dried in a vacuum desiccator over silica gel to provide the title compound as colourless crystals (7.0 g, 27.4 mmol, quant.).

mp = 52-53 °C; $\nu_{\max}/\text{cm}^{-1}$ 3415br (O-H), 3001w (CH), 2957w and 2853w (OCH₃), 1728s (C=O, ester), 1601w and 1586w (CO-O), 1501m and 1436m (C=C); ¹H NMR (400 MHz, CDCl₃) δ = 7.00 (d, 1H, *J* = 8.3 Hz, ArCH), 6.93 (1H, d, *J* = 8.3 Hz, ArCH), 4.75 (brs, 1H, OH), 3.92 (s, 3H, CO₂Me), 3.85 (s, 3H, OMe), 3.68 (s, 3H, CO₂Me), 3.65 (s, 3H, OMe); ¹³C NMR (100.0 MHz) δ = 172.0 (CO₂Me), 167.6 (CO₂Me), 148.6 (ArOH), 145.6 (*Ar*OMe), 127.7 (ArCH), 127.1 (*Ar*CH₂), 125.2 (*Ar*CO₂Me), 117.8 (ArCH), 62.7 (OMe), 52.7 (CO₂Me), 52.4 (CO₂Me), 39.0 (CH₂); HRMS (CI) calcd for [C₁₂H₁₅O₆]⁺ 255.0863; found 255.0865 [M+H]⁺; spectroscopic data was not previously reported.⁸⁶

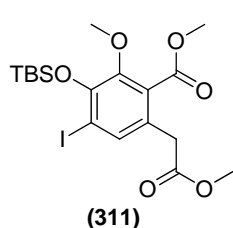


Methyl 3-hydroxy-4-iodo-2-methoxy-6-(2-methoxy-2-oxoethyl)benzoate (309).⁸⁶ To a mixture of (308a) (840 mg, 3.3 mmol, 1.01 equiv.) and K₂CO₃ (680 mg, 4.9 mmol, 1.50 equiv.) in CH₂Cl₂ (25 mL) was added Me₄NiCl₂ (890 mg, 3.3 mmol, 1.00 equiv.) in five approximately equal portions over 2 hours at 0 °C and

the reaction mixture was allowed to warm to 5 °C over 6 h. The reaction mixture was concentrated under reduced pressure to give a fine white powder, which was further dried at 120 °C under reduced pressure for 16 h prior to use.

then quenched with sat. aq. NH_4Cl solution (40 mL), the aqueous layer was extracted with CH_2Cl_2 (2×20 mL) and the combined organics were combined, dried over MgSO_4 and concentrated under reduced pressure. The crude residue was then purified by silica gel chromatography (Petroleum:EtOAc; 2:1) to afford the title compound as a pale yellow oil (1.15 g, 3.04 mmol, 92%).

$R_f = 0.85$ (Petroleum:EtOAc; 2:1); ν_{max} (film)/ cm^{-1} 3399 br (OH), 2947w, (OCH₃), 1727 brs ($2 \times \text{C}=\text{O}$, ester), 1563w (CO-O), 1452w, 1443m and 1408m (C=C); ^1H NMR (400 MHz, CDCl_3) $\delta = 7.39$ (s, 1H, ArCH), 6.01 (brs, OH), 3.91 (s, 3H, OMe), 3.88 (s, 3H, CO_2Me), 3.68 (s, 3H, CO_2Me), 3.62 (s, 2H, $\text{CH}_2\text{CO}_2\text{Me}$); ^{13}C NMR (100 MHz, CDCl_3) $\delta = 171.5$ (CO_2Me), 167.0 (CO_2Me), 149.0 (COH), 144.8 (COMe), 136.3 (ArCH), 127.5 (ArC_{quat}), 126.6 (ArC_{quat}), 85.7 (CI), 62.7 (OMe), 52.8 (CO_2Me), 52.5 (CO_2Me), 38.5 ($\text{CH}_2\text{CO}_2\text{Me}$); HRMS (NSI) calcd for $[\text{C}_{12}\text{H}_{12}\text{I}_1\text{O}_6]^-$ 378.9684; found 378.9677 $[\text{M}-\text{H}]^-$; spectroscopic data was not previously reported.⁸⁶

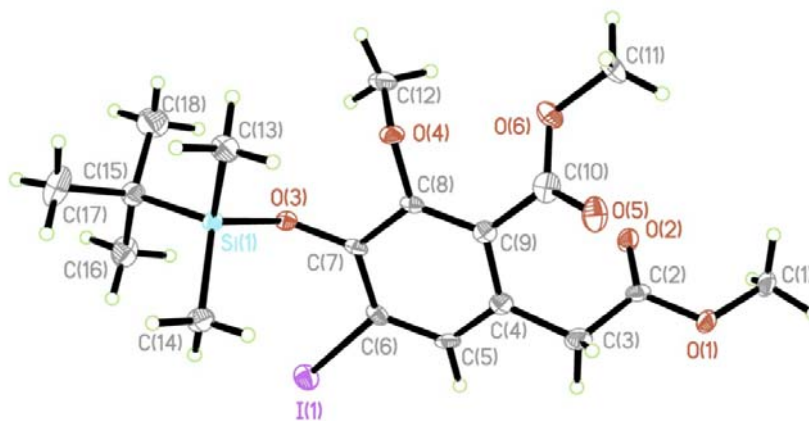


Methyl 3-((*tert*-butyldimethylsilyloxy)-4-iodo-2-methoxy-6-(2-methoxy-2-oxoethyl)benzoate (311). To a solution of (309)

(400 mg, 1.05 mmol, 1.0 equiv.) in CH_2Cl_2 (4.0 mL) at 0°C was added NEt_3 (0.25 mL, 1.78 mmol, 1.7 equiv.), then TBSCl (240 mg, 1.6 mmol, 1.5 equiv.) followed by DMAP (32 mg, 0.26 mmol, 0.25 equiv.). The external cooling bath was then removed and the reaction mixture was allowed to stir at r.t. for 16 h. The reaction mixture was then quenched with sat. aq. Na_2CO_3 solution (40 mL), the aqueous layer was extracted with CH_2Cl_2 (2×20 mL) and the combined organics were combined, dried over MgSO_4 and concentrated under reduced pressure. The crude residue was then purified by silica gel chromatography (Petroleum:EtOAc; 8:1) to afford the *title compound* as a pale yellow crystalline solid (489 mg, 0.99 mmol, 94%).

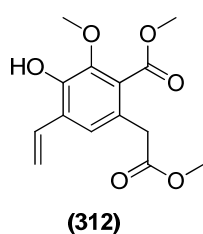
$\text{Mp} = 36^\circ\text{C}$, $R_f = 0.31$ (Petroleum:EtOAc; 8:1); ν_{max} (film)/ cm^{-1} 3003w (CH), 2958w, 2928w, 2852w (OCH₃), 1734s, 1709s (C=O, ester), 1579w and 1548w (CO-O), 1463m, 1443s and 1430m (C=C); ^1H NMR (400 MHz, CDCl_3) $\delta = 7.46$ (s, 1H, ArCH), 3.88 (s,

3H, CO₂Me), 3.74 (s, 3H, OMe), 3.68 (s, 3H, CO₂Me), 3.57 (s, 2H, CH₂CO₂Me), 1.06 (s, 9H, SiMe₂^tBu), 0.26 (s, 6H, SiMe₂^tBuSi); ¹³C NMR (100.0 MHz) δ = 171.2 (CO₂Me), 167.3 (CO₂Me), 149.2 (COTBS), 149.2 (COMe), 136.8 (ArCH), 129.5 (ArC_{quat.}), 127.1 (ArC_{quat.}), 93.9 (CI), 61.6 (OMe), 52.4 (CO₂Me), 52.3 (CO₂Me), 38.0 (CH₂CO₂Me), 26.4 (SiC(CH₃)₃), 18.8 (SiC(CH₃)₃), 3.1 (SiMe₂); HRMS (CI) calcd for [C₁₈H₂₈IO₆Si₁]⁺ 495.0694; found 495.0690 [M+H]⁺.



Empirical formula	C ₁₈ H ₂₇ O ₆ Si I	
Formula weight	494.39	
Temperature	100.(2)	
Wavelength	1.54178 Å	
Crystal system	Orthorhombic	
Space group	-P 2ac 2ab	
Unit cell dimensions	a = 7.5894(3) Å	a = 90
	b = 22.4932(10) Å	b = 90
	c = 25.2819(10)	g = 90
Volume	4315.9(3)	
Z	8	
Density	1.522 Mg/m ³	
Absorption coefficient	12.443 mm ⁻¹	
F(100)	2000	

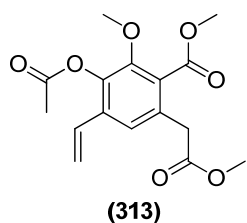
Crystal size	0.300 × 0.040 × 0.040 mm ³
Theta range for data collection	3.4964 to 64.9843°
Index ranges	-6 ≤ h ≤ 8, -26 ≤ k ≤ 26, -29 ≤ l ≤ 29
Reflections collected	9980
Independent reflections	3640 [R(int) = 0.0556]
Completeness to theta = 25.00°	98.9%
Absorption correction	Multi-scan
Refinement method	Full-matrix least-squares on F ²
Data/restraints/parameters	3640/0 /243
Goodness-of-fit F ²	1.233
Final R indices [I.2sigma(I)]	R1 = 0.0540, wR2 = 0.1357
R indices (all data)	R1 = 0.0556, wR2 = 0.1351
Largest diff. peak and hole	1.035 and -1.870 eÅ ⁻³



Methyl 3-hydroxy-2-methoxy-6-(2-methoxy-2-oxoethyl)-4-vinylbenzoate (312). In a microwave vial fitted with a septa was added **(311)** (100 mg, 0.20 mmol, 1.0 equiv.), DMF (4 mL), H₂O (0.4 mL), vinylboronic acid pinacol ester (120 μl 0.71 mmol, 3.5 equiv.), Na₂CO₃ (130 mg, 1.2 mmol, 6.1 equiv.) and Pd(PPh₃)₄

(23 mg, 0.02 mmol, 0.1 equiv.). The solution was degassed with Ar for 30 minutes before the reaction vessel was sealed with a 'crimp-cap' before heating to 80 °C for 16 h. The reaction mixture was then cooled to rt, diluted with Et₂O (10 mL) and washed with H₂O (2 × 25 mL). The combined aqueous layers were then further extracted with Et₂O (2 × 20 mL) and the combined organics were dried over MgSO₄, filtered and concentrated under reduced pressure. The crude extract was then purified by silica gel chromatography (4:1 to 0:1; Petroleum:EtOAc) to give the *title compound* as a pale brown oil (55 mg, 0.20 mmol, 98%).

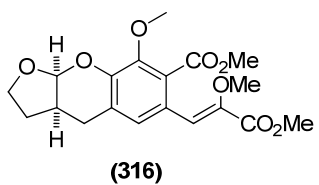
$R_f = 0.20$ (100% EtOAc); ν_{\max} (film)/ cm^{-1} 3342br (OH), 2958w and 2955w, (OCH₃), 1718brs, (2 × C=O, ester), 1630m (C=C, conj.), 1530w (CO-O), 1481m, 1454s and 1423m (C=C); ¹H NMR (400 MHz, CDCl₃) $\delta = 7.08$ (s, 1H, ArCH), 6.92 (dd, $J = 17.6$, 11.5 Hz, 1H, CH=CH₂), 6.02 (s, 1H, OH), 5.86 (d, $J = 17.6$ Hz, 1H, CH=CH_aH_b), 5.39 (d, $J = 11.5$ Hz, 1H, CH=CH_aH_b), 3.91 (s, 3H, OMe), 3.85 (s, 3H, CO₂Me), 3.68 (s, 3H, CO₂Me); ¹³C NMR (100.0 MHz) $\delta = 171.9$ (CO₂Me), 167.3 (CO₂Me), 146.0 (COH), 146.0 (COMe), 130.6, (CH=CH₂), 127.0 (ArC_{quat.}), 125.0 (ArC_{quat.}), 124.9 (ArCH), 124.6 (ArC_{quat.}), 117.2 (CH=CH₂), 62.65 (OMe), 52.55 (CO₂Me), 52.25 (CO₂Me), 39.21 (CH₂CO₂Me); HRMS (CI) calcd for [C₁₄H₁₇O₆]⁺ 281.1020; found 281.1022 [M+H]⁺.



Methyl 3-acetoxy-2-methoxy-6-(2-methoxy-2-oxoethyl)-4-vinylbenzoate (313). To a solution of **(312)** (50 mg, 0.18 mmol, 1.0 equiv.) in pyridine (1.0 mL) at 0 °C was slowly added Ac₂O (0.15 mL, 1.0 mmol, 8.3 equiv.), dropwise. The reaction mixture

was allowed to warm to r.t. over 16 h, before being concentrated under reduced pressure in an ice bath. The resultant oil was diluted with MeOH (10 mL), and concentrated under reduced pressure in an ice bath again, before purification of the resultant oil *via* silica gel chromatography (Petroleum:Et₂O; 4:1) afforded the *title compound* as a pale orange oil (56.4 mg, 0.17 mmol, 98%)

$R_f = 0.24$ (Petroleum:Et₂O; 4:1); ν_{\max} (film)/ cm^{-1} 2952w and 2947w (OCH₃), 1768m and 1734s, (C=O, ester), 1606w (C=C, conj.), 1562w (CO-O), 1455m, 1434m and 1413m (C=C); ¹H NMR (400 MHz, CDCl₃) $\delta = 7.23$ (s, 1H, ArCH), 6.67 (dd, $J = 17.6$, 11.1 Hz, 1H, CH=CH₂), 5.80 (dd, 17.6, 0.8 Hz, CH=CH_aH_b), 5.41 (d, $J = 11.5$ Hz, CH=CH_aH_b), 3.89 (s, 3H, OMe), 3.81 (CO₂Me), 3.73 (s, 2H, CH₂CO₂Me), 3.69 (s, 3H, OMe), 2.35 (s, 3H, OAc); ¹³C NMR (100.0 MHz) $\delta = 171.2$ (OCOMe), 168.4 (CO₂Me), 167.0 (CO₂Me), 150.9 (COMe), 145.2 (COAc), 141.1 (CH=CH₂), 133.8 (ArC_{quat.}), 131.1 (ArC_{quat.}), 129.6 (ArC_{quat.}), 127.7 (CH=CH₂), 124.0 (ArCH), 118.7 (CH=CH₂), 62.3 (OMe), 52.5 (CO₂Me), 52.3 (CO₂Me), 39.2 (CH₂CO₂Me), 20.6 (OAc); HRMS (EI) calcd for [C₁₆H₁₉O₇]⁺ 323.1125; found 323.1122 [M+H]⁺.



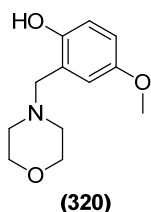
(3a±,9a±)-methyl 6-((Z)-2,3-dimethoxy-3-oxoprop-1-en-1-yl)-8-methoxy-3,3a,4,9a-tetrahydro-2H-furo[2,3-b]chromene-7-carboxylate (316). **Method A:** To a solution of phenol (**290**)

(20 mg, 51 μmol , 1.0 equiv.) dissolved in PhMe (0.2 mL) was added a 0.1 M solution of MeI in PhMe (0.5 mL, 50 μmol , 0.99 equiv.) in a microwave tube at 0 $^{\circ}\text{C}$. The reaction was warmed to r.t. and stirred for a further 2 h, at which time TLC analysis indicated complete consumption of the starting material. 2,3-Dihydrofuran (0.38 μl , 500 μmol , 10.0 equiv.) was then added to the reaction mixture and the reaction vessel was then fitted with a “crimp-cap” and heated at 130 $^{\circ}\text{C}$ for 16 h. The reaction mixture was cooled to r.t., diluted with EtOAc and filtered through a short pad of silica ($w = 1 \text{ cm} \times h = 0.5 \text{ cm}$). The filtrate was then concentrated under reduced pressure and purified *via* silica gel chromatography (Petroleum:EtOAc; 3:1) to give the *title compound* isolated as clear colourless oil (12.4 mg, 33 μmol , 65%). Stereochemical assignments were made on the basis of NOESY experiments.

Method B: Morpholine (**290**) (20 mg, 51 μmol , 1.0 equiv.) was dissolved in 2,3-dihydrofuran (0.10 mL, 6.81 mmol) in a microwave vial, fitted with a “crimp cap” and heated at 130 $^{\circ}\text{C}$ for 16 h in a microwave reactor. The reaction mixture was then cooled to r.t., concentrated under reduced pressure and purified by silica gel chromatography (Petroleum:EtOAc; 1 to 10% Et₂O) to furnish the title compound as a clear colourless oil (14.0 mg, 35 μmol , 70%).

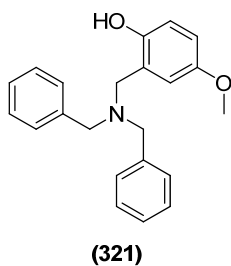
$R_f = 0.19$ (Petroleum:EtOAc; 3:1); ν_{max} (film)/ cm^{-1} 2938w and 2924w (CH), 2854 (O-C-H₃), 1724s ($2 \times \text{C}=\text{O}$, ester), 1645w (O-CO), 1452m, and 1438m (C=C); ^1H NMR (400 MHz, CDCl_3) $\delta = 7.58$ (s, 1H, ArCH), 6.78 (s, 1H, CH=C_{quat.}), 5.71 (d, $J = 5.3$ Hz, 1H, O₂CH), 3.98-3.88 (m, 2H, OCH₂), 3.87 (s, 3H, OMe), 3.84 (s, 3H, OMe), 3.75 (s, 3H, CO₂Me), 3.66 (s, 3H, CO₂Me), 3.01 (dd, $J = 15.9, 5.3$ Hz, 1H, O₂CHCH), 2.78-2.72 (m, 1H, ArH_aH_b), 2.68 (dd, $J = 15.9, 2.6$ Hz, 1H, ArH_aH_b), 2.03-1.96 (m, 1H, OCH₂CH_aH_b), 1.62-1.57 (m, 1H, OCH₂CH_aH_b); ^{13}C NMR (100.0 MHz) $\delta = 164.5$ (CO₂Me), 163.5 (CO₂Me), 153.1 (COMe), 148.3 (CH=C_{quat.}), 142.0 (ArC_{quat.}), 129.8 (ArC_{quat.}), 127.2

(ArC_{quat.}), 119.0 (ArC_{quat.}), 103.6 (CH=C_{quat.}), 103.2 (O₂CH), 74.5 (OCH₂), 67.0 (OMe), 66.1 (OMe), 61.9 (CO₂Me), 59.6 (CO₂Me), 52.8 (O₂CHCH), 30.7 (OCH₂CH₂), 29.8 (CH₂); HRMS (EI) calcd for [C₁₉H₂₆O₈N]⁺ 396.1653; found 396.1654 [M+NH₄]⁺.



4-Methoxy-2-(morpholinomethyl)phenol (320). To a solution of morpholine (0.7 mL, 8.3 mmol, 0.9 equiv.) in acetonitrile (5 mL) in a microwave microwave vial fitted with a septum was added paraformaldehyde (0.25 g, 8.3 mmol, 0.9 equiv.) and the reaction mixture was stirred at r.t. for 4 h, at which time the reaction mixture had become a clear solution. Paramethoxyphenol (1.15 g, 9.3 mmol, 1.0 equiv.) was added and the reaction vessel was fitted with a “crimp cap” and the resultant solution was heated to 100 °C for 10 h. The reaction mixture was then cooled to r.t., diluted with EtOAc (30 mL) and washed with sat. aq. NH₄Cl solution (2 × 20 mL). The organics were dried over MgSO₄, concentrated under reduced pressure and purified by silica gel chromatography (Petroleum:Et₂O; 3:1) afforded the *title compound* as an orange/brown oil (1.62 g, 7.24 mmol, 87%).

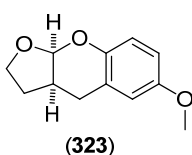
ν_{\max} (film)/cm⁻¹ 3490br (OH), 2952w, 2900w (CH), 2872w (OCH₃), 1497m and 1448w (C=C), 1208m (CN); ¹H NMR (400 MHz, CDCl₃) δ = 10.17 (br, 1H, OH), 6.78-6.72 (m, 2H, ArCH), 6.57 (d, *J* = 2.2 Hz, ArCH), 3.74 (s, 7H, OMe, 2 × OCH₂), 3.67 (s, 2H, ArCH₂), 2.56 (br, 4H, 2 × NCH₂); ¹³C NMR (100.0 MHz) δ = 152.4 (ArOH) 151.1 (ArOMe), 121.2 (ArCH₂), 116.3 (ArCH), 114.5 (ArCH), 113.6 (ArCH), 66.6 (2 × OCH₂), 63.8 (ArCH₂), 55.6 (OMe), 52.8 (2 × NCH₂); HRMS (EI) calcd for [C₁₂H₁₈N₁O₃]⁺ 224.1281; found 224.1282 [M+H]⁺.



2-((Dibenzylamino)methyl)-4-methoxyphenol (321). To a solution of dibenzylamine (1.6 mL, 8.3 mmol, 0.9 equiv.) in acetonitrile (5 mL) in a microwave microwave vial fitted with a septum was added paraformaldehyde (0.25 g, 8.3 mmol, 0.9 equiv.) and the reaction mixture was stirred at r.t. for 16 h, at which time the reaction mixture had become a clear solution. Paramethoxyphenol (1.15 g, 9.3 mmol, 1.0 equiv.) was added and the reaction vessel was fitted with a “crimp cap” and the resultant

solution was heated to 100 °C for 5 h. The reaction mixture was then cooled to r.t., diluted with EtOAc (30 mL) and washed with sat. aq. NH₄Cl solution (2 × 20 mL). The organics were dried over MgSO₄, concentrated under reduced pressure and purified by silica gel chromatography (Petroleum:Et₂O; 3:1) afforded the *title compound* as a pale orange solid (2.35 g, 7.0 mmol, 85%).

ν_{\max} (film)/cm⁻¹ 3025w and 2921w (CH), 2836w (OCH₃), 1598w, 1490s and 1469m (C=C), 1206m (CN); ¹H NMR (400 MHz, CDCl₃) δ = 10.25 (br, 1H, OH), 7.38-7.27 (m, 10H, 10 × ArCH), 6.77 (d, J = 8.8, 1H, ArCH), 6.72 (dd, J = 8.8, 2.5 Hz, 1H, ArCH), 6.59 (d, J = 2.5 Hz, 1H, ArCH), 3.74 (s, 3H, OMe), 3.69 (s, 2H, NCH₂), 3.61 (s, 4H, 2 × PhCH₂); ¹³C NMR (100.0 MHz) δ = 152.2 (COH), 150.8 (COMe), 136.4 (2 × PhCH₂), 129.1 (4 × PhH), 128.2 (4 × PhH), 127.2 (2 × PhH), 122.2 (ArC_{quat.}), 116.0 (ArCH), 114.5 (ArCH), 113.1 (ArCH), 57.4 (2 × PhCH₂), 56.5 (ArCH₂), 55.3 (OMe); HRMS (EI) calcd for [C₂₂H₂₄N₁O₂]⁺ 334.1802; found 334.1805 [M+H]⁺.

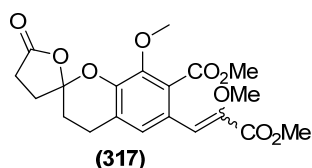


(3a±,9a±)-6-Methoxy-3,3a,4,9a-tetrahydro-2H-furo[2,3-b]chromene.

Morpholine (**320**) (50 mg, 0.22 mmol, 1.0 equiv.) was dissolved in 2,3-dihydrofuran (0.16 mL, 2.20 mmol, 10. Equiv.) in microwave tube, fitted with a “crimp cap” and heated at 130 °C for 16 h in a microwave reactor. The reaction mixture was then cooled to r.t., concentrated under reduced pressure and purified by silica gel chromatography (Petroleum:Et₂O; 1 to 10% Et₂O) to furnish the title compound as a clear colourless oil (35.9 mg, 0.17 mmol, 79%).

R_f = 0.18 (Petroleum:Et₂O; 9:1); ν_{\max} (film)/cm⁻¹ 2932br (multiple CH), 1496s 1463w and 1437w (C=C); ¹H NMR (400 MHz, CDCl₃) δ = 6.82 (d, J = 8.7 Hz, 1H, ArCH), 6.69 (dd, J = 8.7, 2.9 Hz, 1H, ArCH), 6.63 (d, J = 2.9 Hz, 1H, ArCH), 5.64 (d, J = 5.5 Hz, O₂CH), 3.97 (dt, J = 8.5, 4.5 Hz, 1H, OCH_aH_b), 3.88 (d, J = 7.9 Hz, 1H, OCH_aH_b), 3.03 (dd, J = 15.4, 5.7 Hz, 1H, ArCH_aH_b), 2.78-2.70 (m, 1H, ArCH₂CHR₂), 2.66 (dd, J = 15.8, 2.6 Hz, 1H, ArCH_aH_b), 2.08-1.99 (m, 1H, OCH₂CH_aH_b), 1.69-1.63 (m, 1H, OCH₂CH_aH_b); ¹³C NMR (100.0 MHz) δ = 154.2 (COMe), 147.3 (ArC_{quat.}), 123.4 (ArC_{quat.}), 117.8 (ArCH), 114.2 (ArCH), 112.99 (ArCH), 102.1 (O₂CR), 68.1 (OCH₂), 55.7 (OMe), 38.1

(O₂CHCH), 28.73 (OCH₂CH₂), 27.08 (ArCH₂); HRMS (EI) calcd for [C₁₂H₁₅O₃]⁺ 207.1016; found 207.1016 [M+H]⁺.



Methyl 6-(2,3-dimethoxy-3-oxoprop-1-en-1-yl)-8-methoxy-5'-oxo-4',5'-dihydro-3'H-spiro[chroman-2,2'-furan]-7-carboxylate (317). Morpholine (**290**) (20 mg, 51 μmol, 1.0 equiv.) was dissolved in γ-methylene-γ-

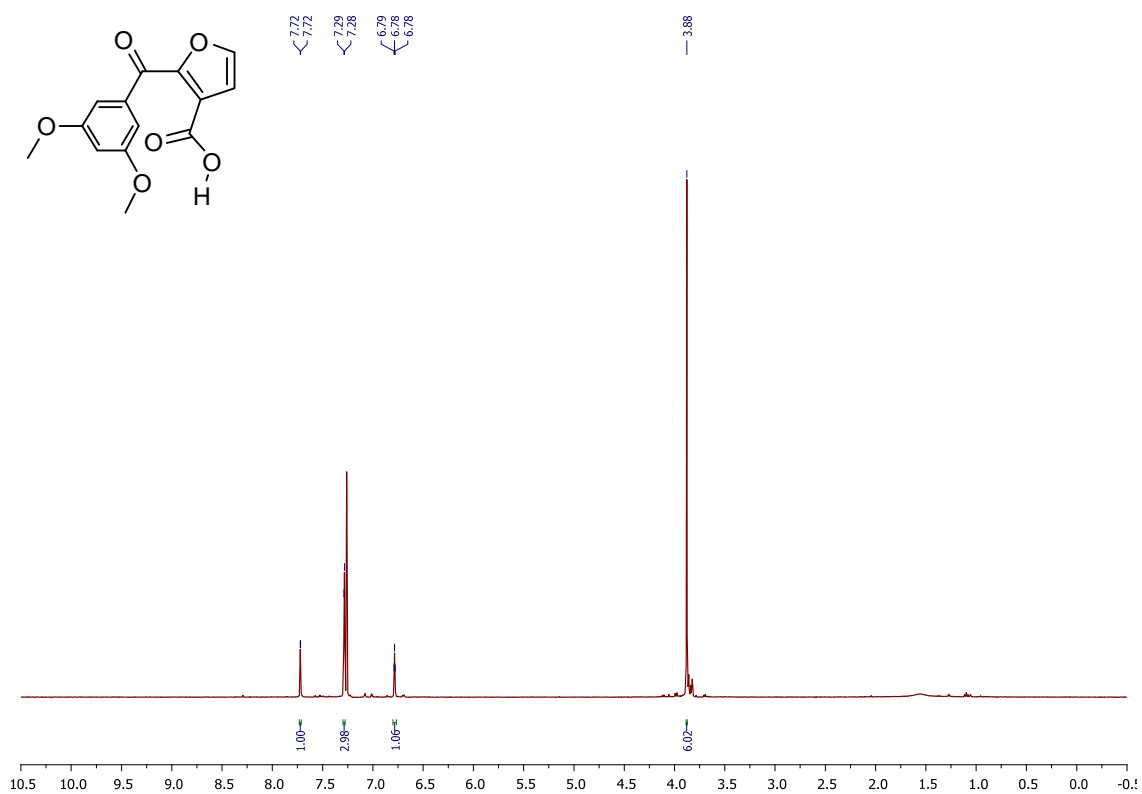
butyrolactone (0.10 mL, 1.12 mmol) in microwave tube, fitted with a “crimp cap” and heated at 130 °C for 16 h in a microwave reactor. The reaction mixture was then cooled to r.t., concentrated under reduced pressure and purified by silica gel chromatography (Petroleum:EtOAc; 1 to 10% EtOAc) to furnish the *title compound* as a clear colourless oil (14.2 mg, 35 μmol, 64.1%) in 1:3 ratio of *E:Z* isomers.

R_f = 0.15 (Petroleum:Et₂O); ν_{max} (film)/cm⁻¹ 2939w and 2930w (CH), 2854 (O-C-H₃), 1792s and 1725s (C=O, ester), 1645w (O-CO), 1567m, 1475m, 1440m, 1436m (C=C); HRMS (EI) calcd for [C₂₀H₂₃O₉]⁺407.1337; found 407.1339 [M+H]⁺.

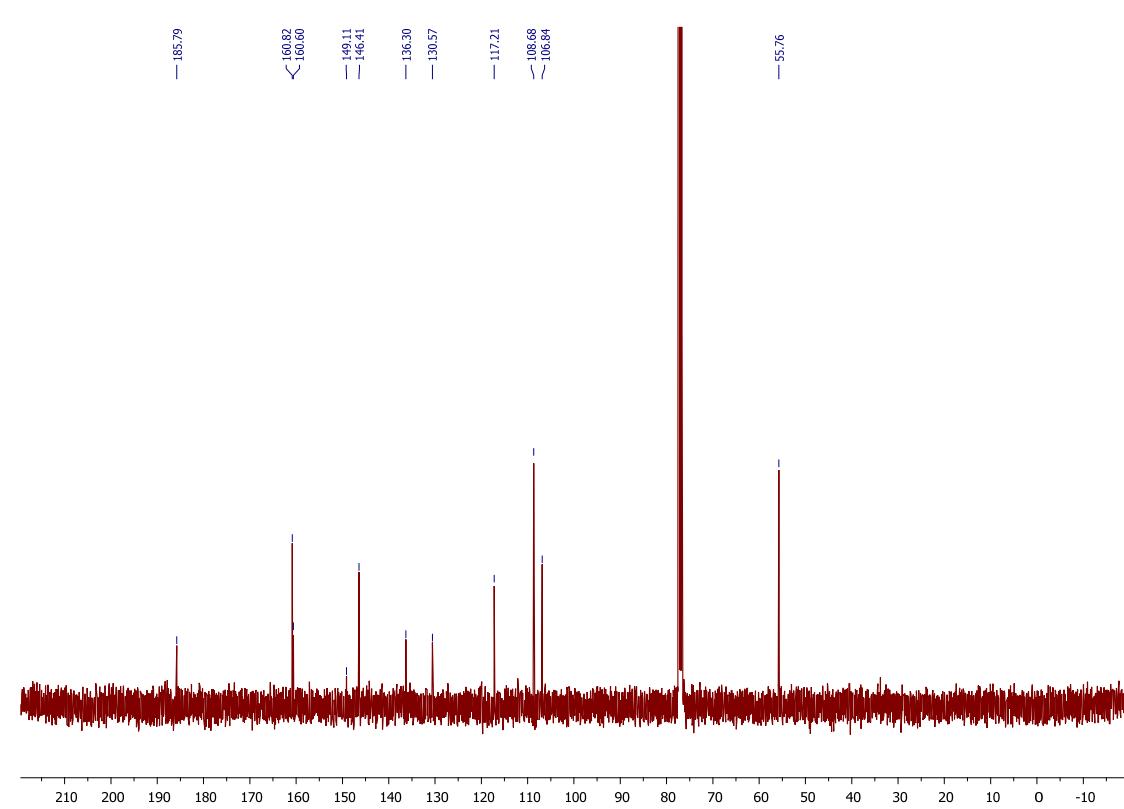
(Z)-isomer; ¹H NMR (400 MHz, CDCl₃) δ = 7.67 (s, 1H, ArCH), 6.81 (s, 1H, CH=C_{quat.}), 3.96 (s, 3H, OMe), 3.91 (s, 3H, OMe), 3.82 (s, 3H, CO₂Me), 3.74 (s, 3H, CO₂Me), 3.09-2.94 (m, 2H, CH₂), 2.72-2.52 (m, 2H, CH₂), 2.41-2.23 (m, 2H, CH₂), 2.19-2.08 (m, 1H, CH_aH_b), 2.04 (m, 1H, CH_aH_b); ¹³C NMR (100.0 MHz) δ = 173.5 (CO₂), 167.2 (CO₂Me), 164.3 (CO₂Me), 147.3 (RH=C_{quat.}), 146.2 (COMe), 142.2 (ArC_{quat.}), 125.5 (ArC_{quat.}), 125.4 (ArC_{quat.}), 124.9 (ArCH), 118.6 (CH=C_{quat.}), 109.0 (spiro-C), 61.9 (OMe), 59.4 (OMe), 52.6 (CO₂Me), 52.3 (CO₂Me), 38.8 (CH₂), 32.9 (CH₂), 26.9 (CH₂), 25.7 (CH₂); **(E)-isomer;** ¹H NMR (400 MHz, CDCl₃) δ = 7.65 (s, 1H, ArCH), 6.84 (s, 1H, CH=C_{quat.}), 3.93 (s, 3H, OMe), 3.82 (s, 3H, OMe), 3.81 (s, 3H, CO₂Me), 3.72 (s, 3H, CO₂Me), 3.09-2.94 (m, 2H, CH₂), 2.72-2.52 (m, 2H, CH₂), 2.41-2.23 (m, 2H, CH₂), 2.19-2.08 (m, 1H, CH_aH_b), 2.04 (m, 1H, CH_aH_b); The ¹³C NMR spectrum could not be clearly distinguished from the major (*Z*)-isomer.

Chapter 6:
Selected Spectra

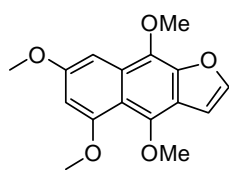
¹H NMR Spectrum (Compound 235)



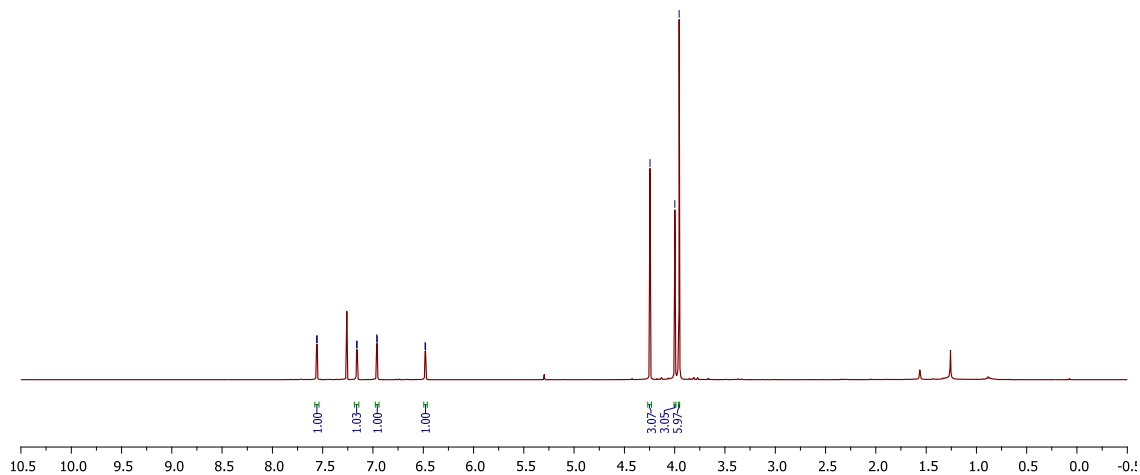
¹³C NMR Spectrum (Compound 235)



¹H NMR Spectrum (Compound 236)

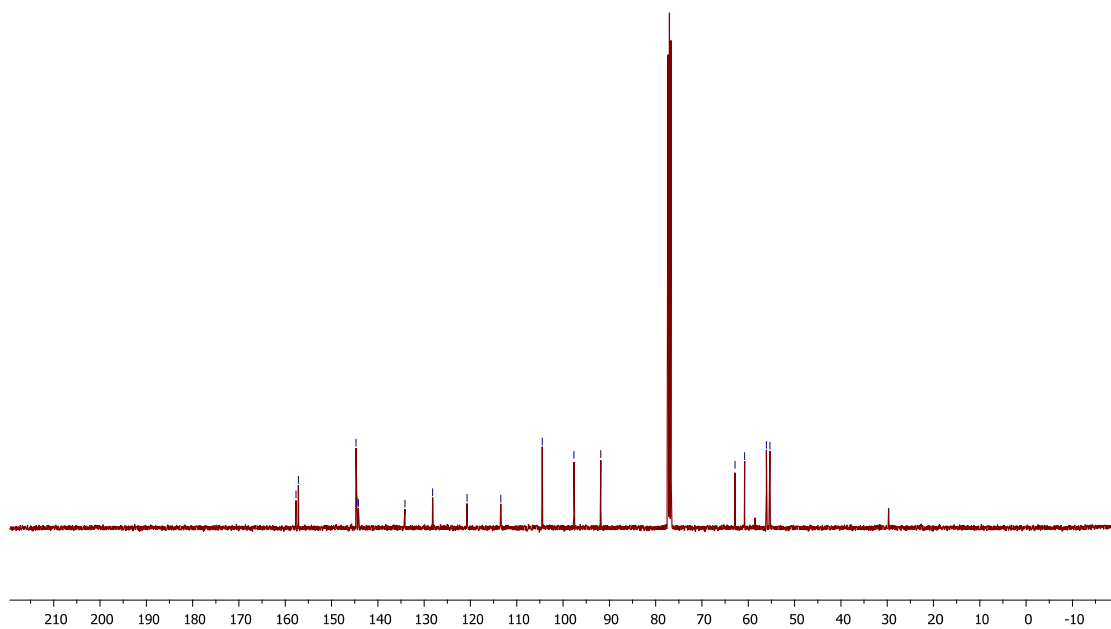


7.56
7.55
7.16
6.96
6.96
6.48
6.48
4.25
4.00
3.95

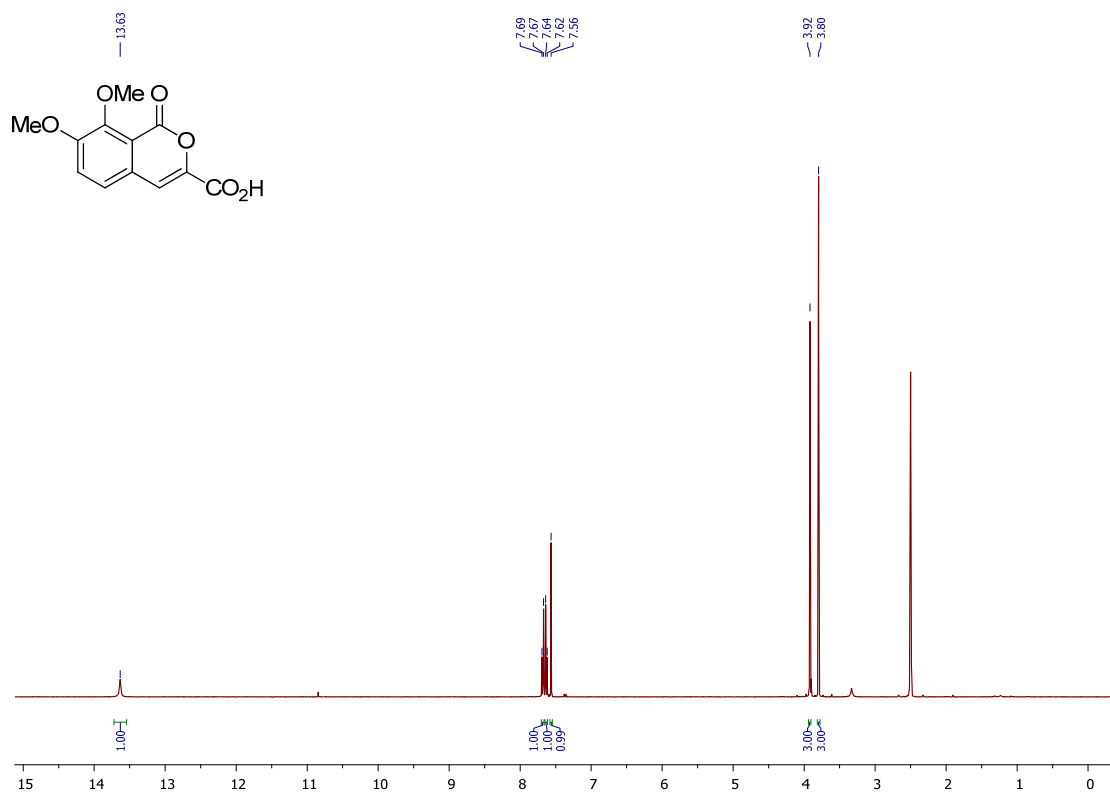


¹³C NMR Spectrum (Compound 236)

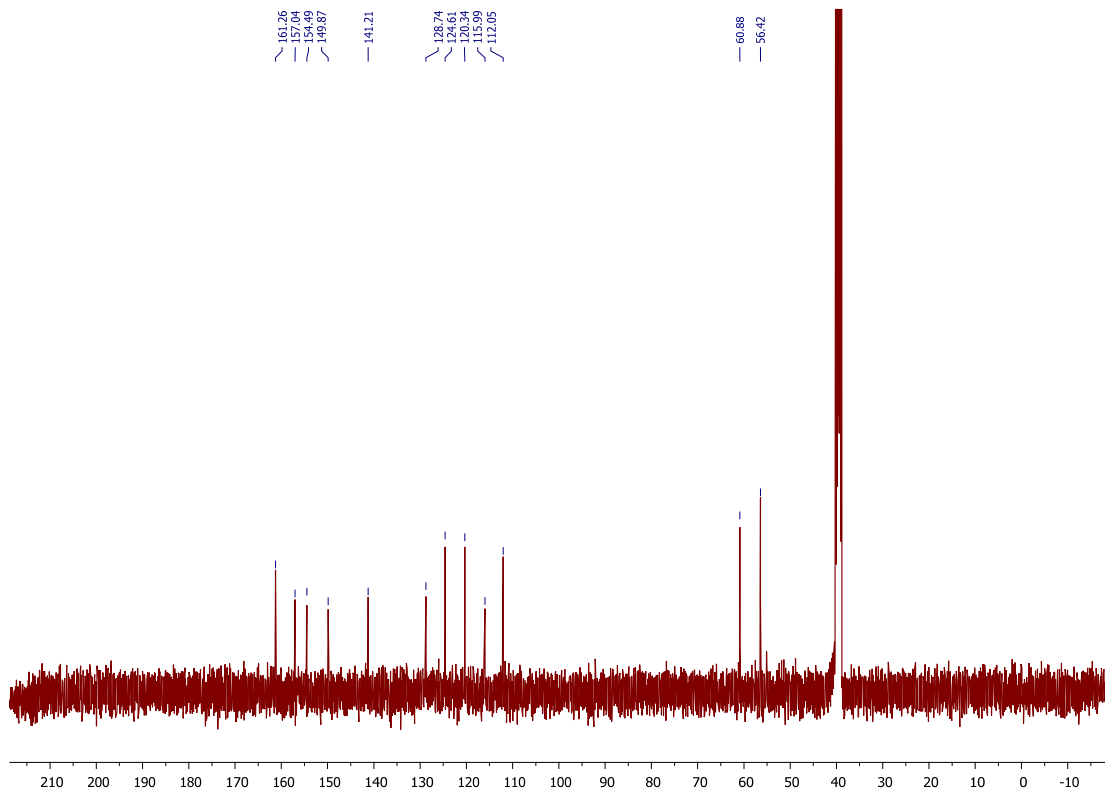
157.69
157.17
144.71
144.51
144.19
134.16
128.15
120.74
113.46
104.50
97.65
91.86
63.86
60.86
56.09
55.33



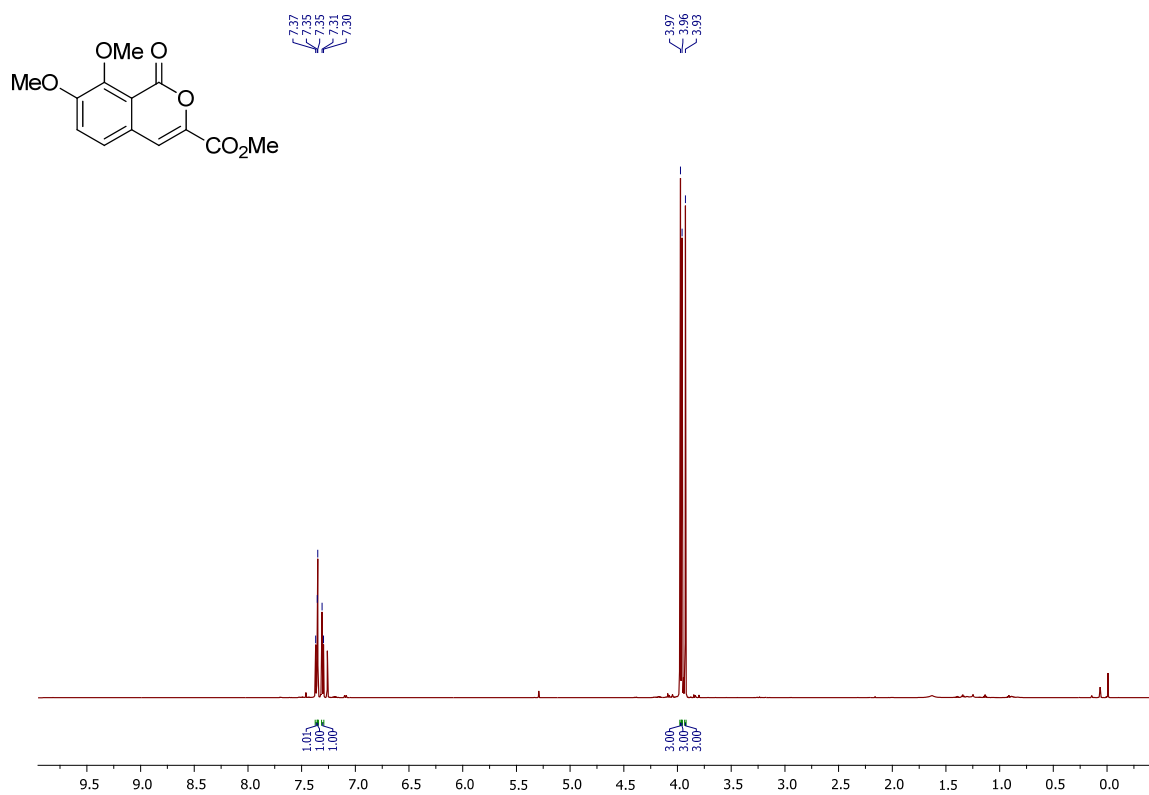
¹H NMR Spectrum (Compound 257)



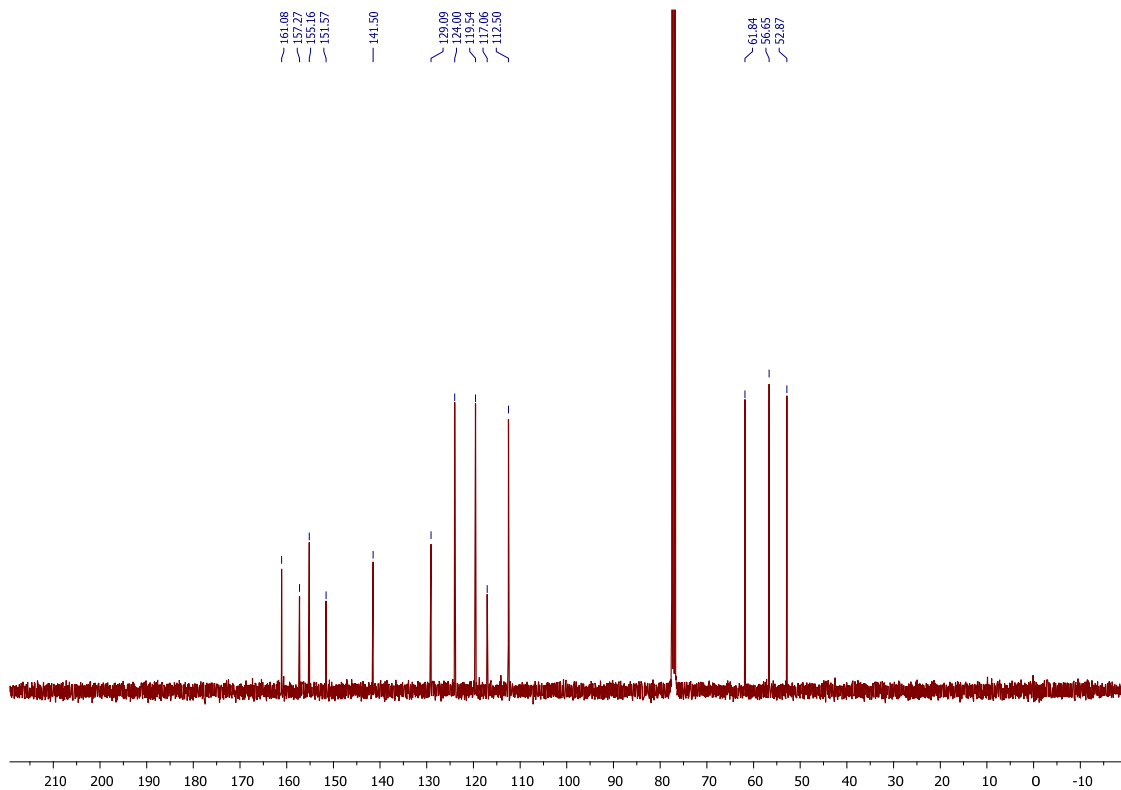
¹³C NMR Spectrum (Compound 257)



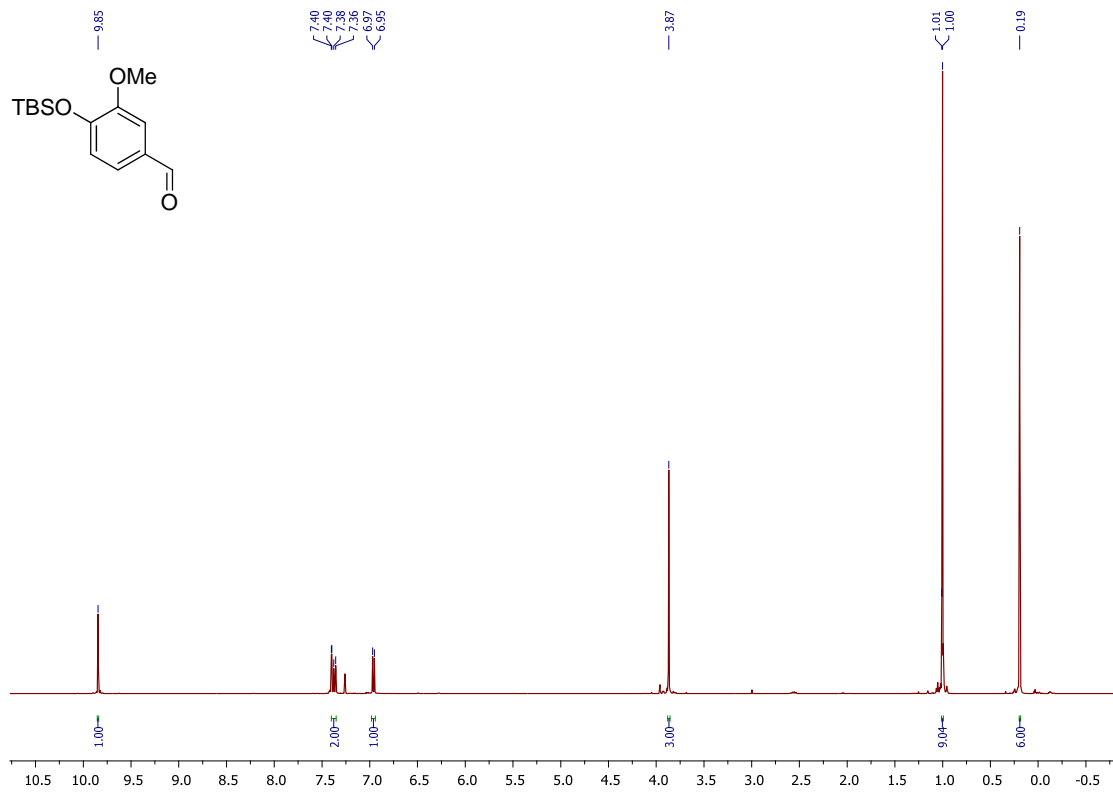
¹H NMR Spectrum (Compound 258)



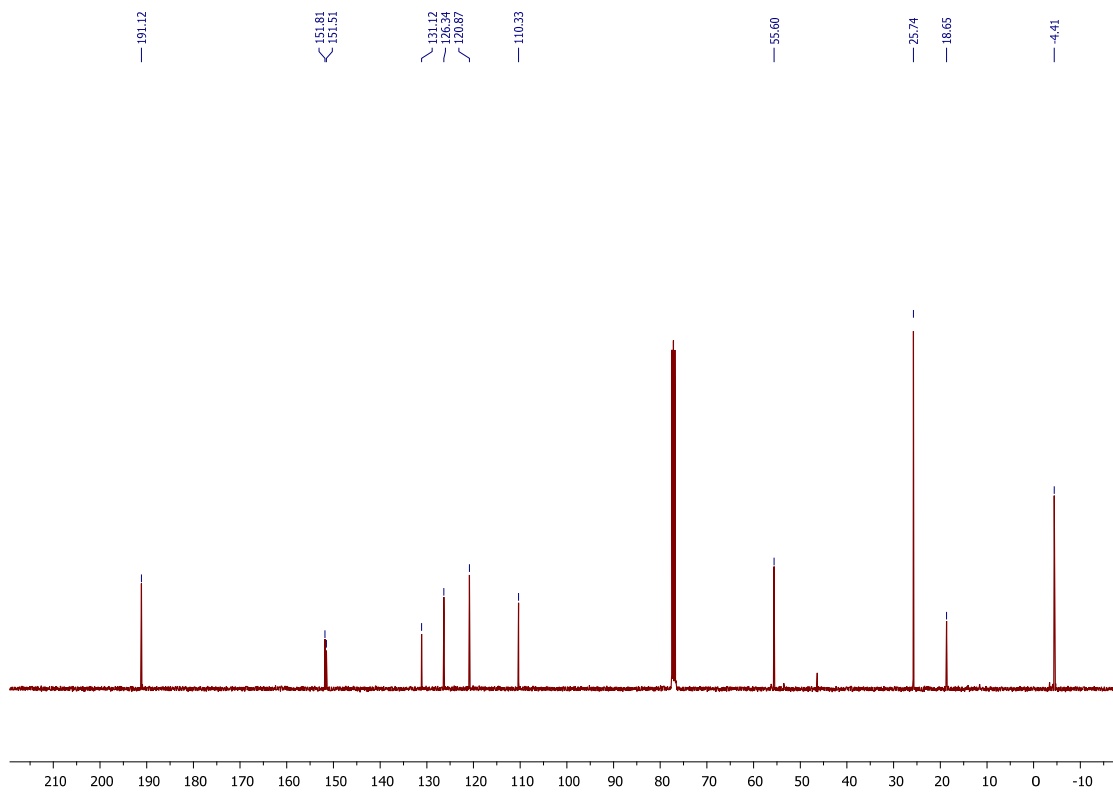
¹³C NMR Spectrum (Compound 258)



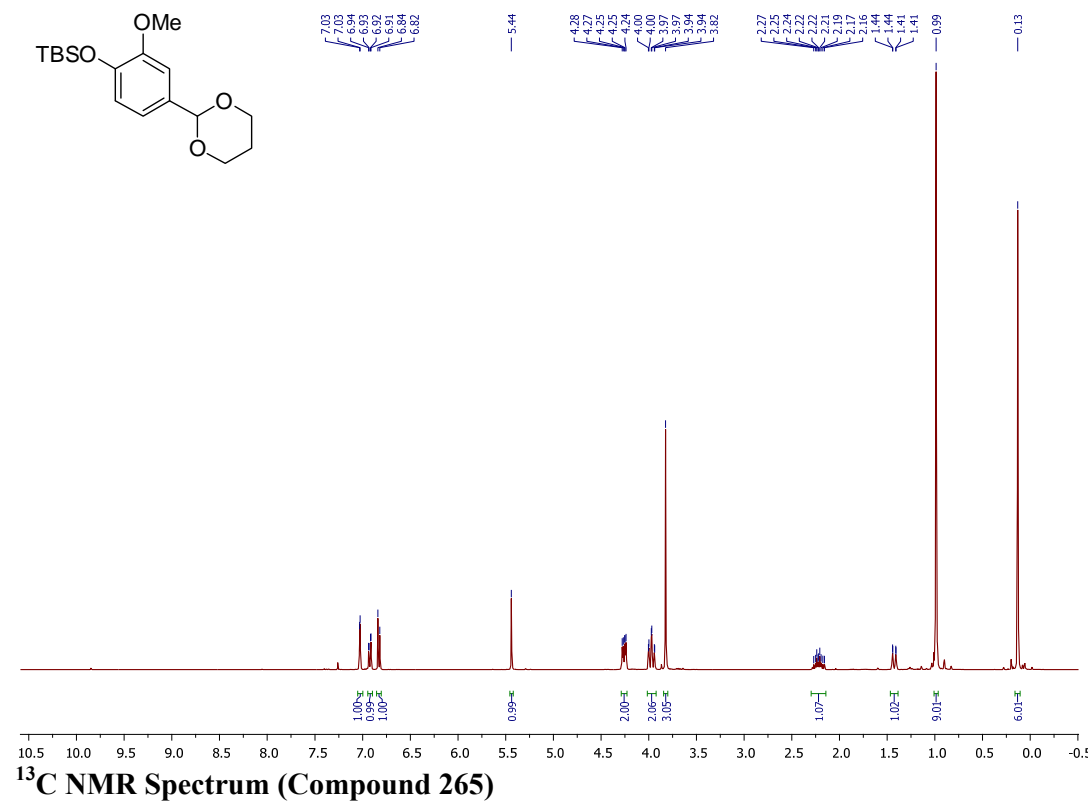
¹H NMR Spectrum (Compound 265a)



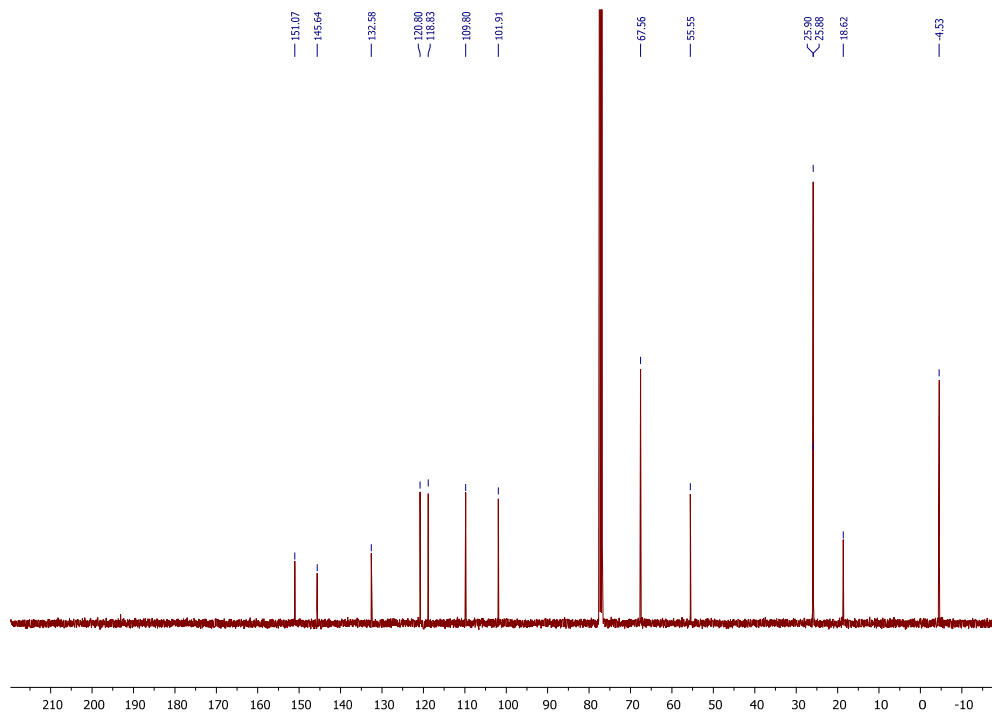
¹³C NMR Spectrum (Compound 265a)



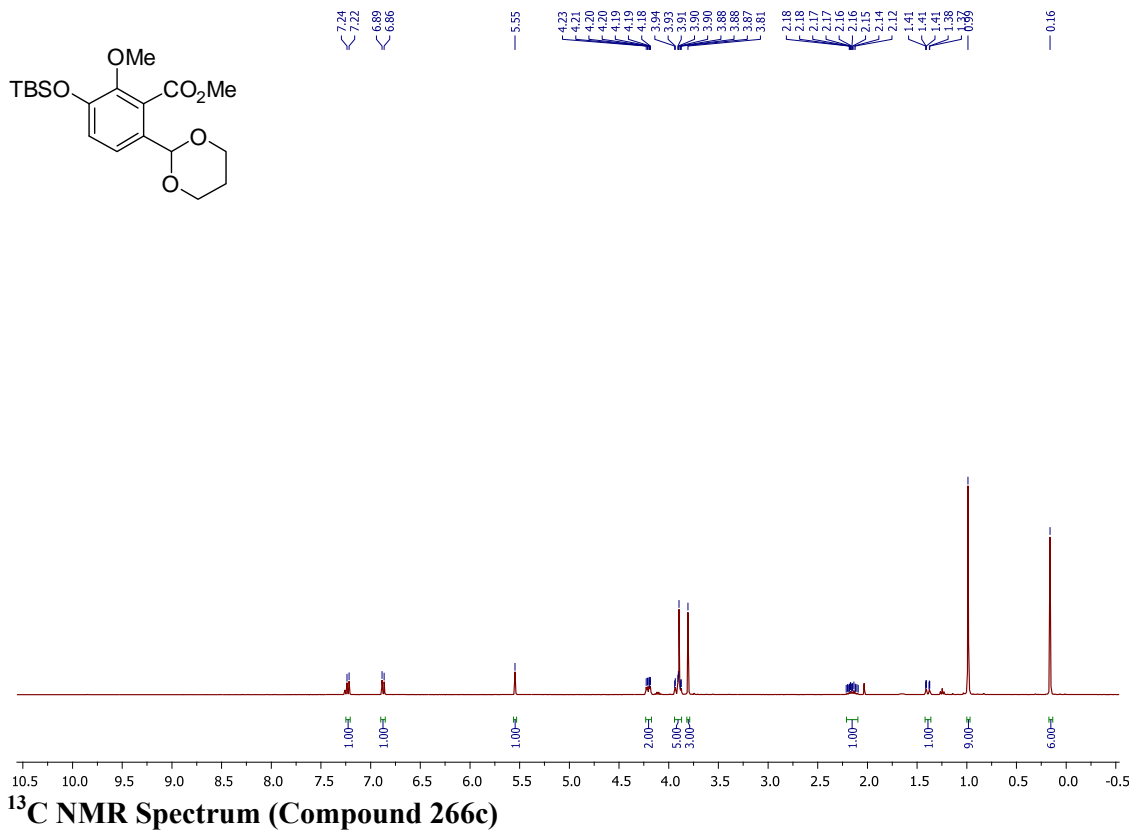
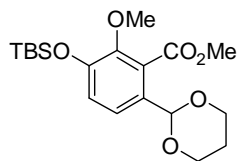
¹H NMR Spectrum (Compound 265)



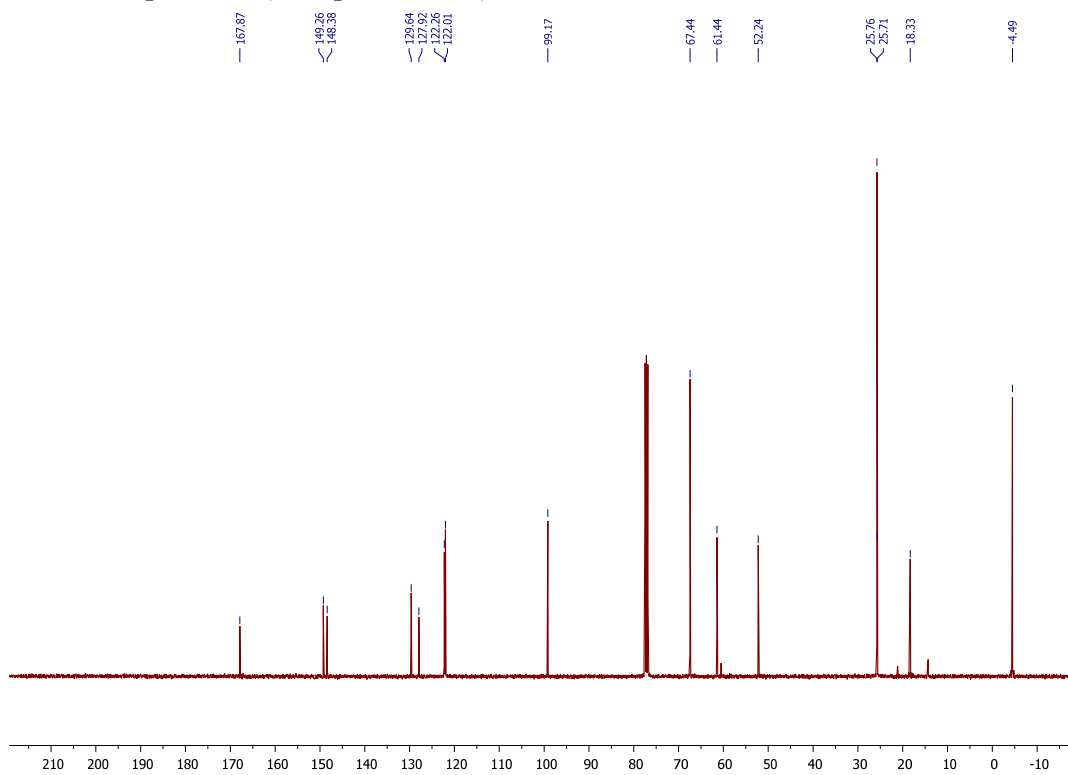
¹³C NMR Spectrum (Compound 265)



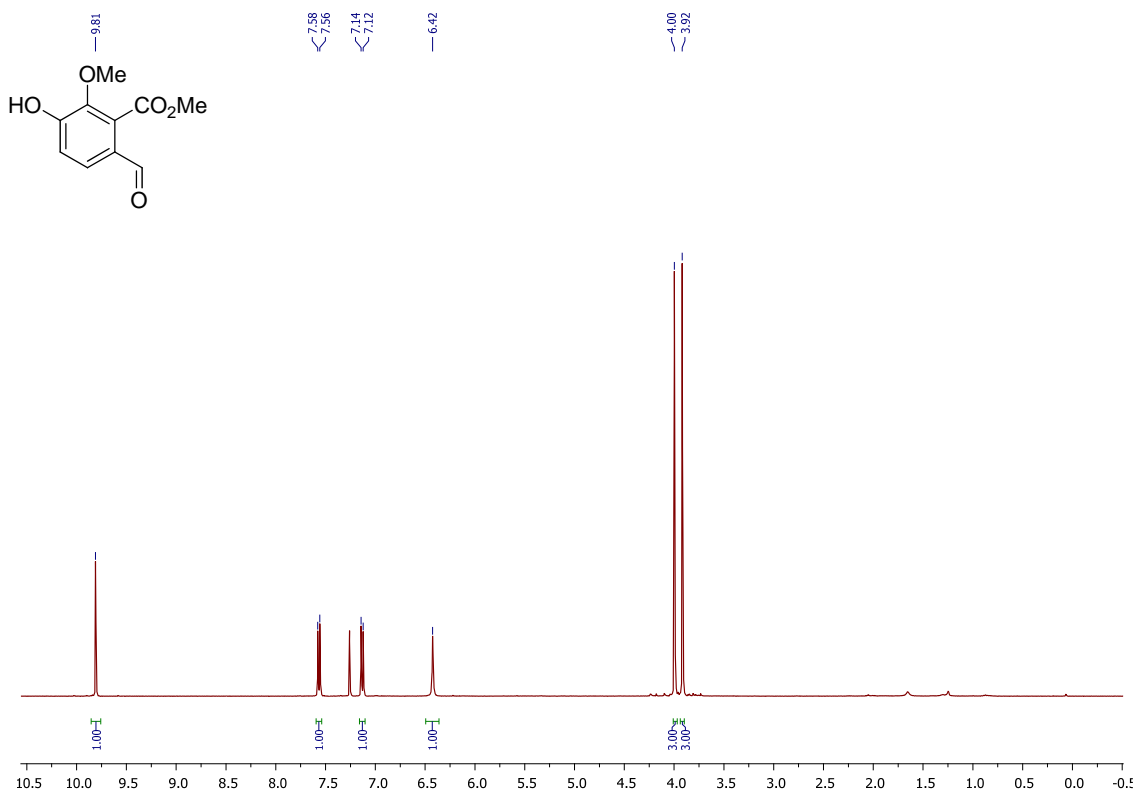
¹H NMR Spectrum (Compound 266c)



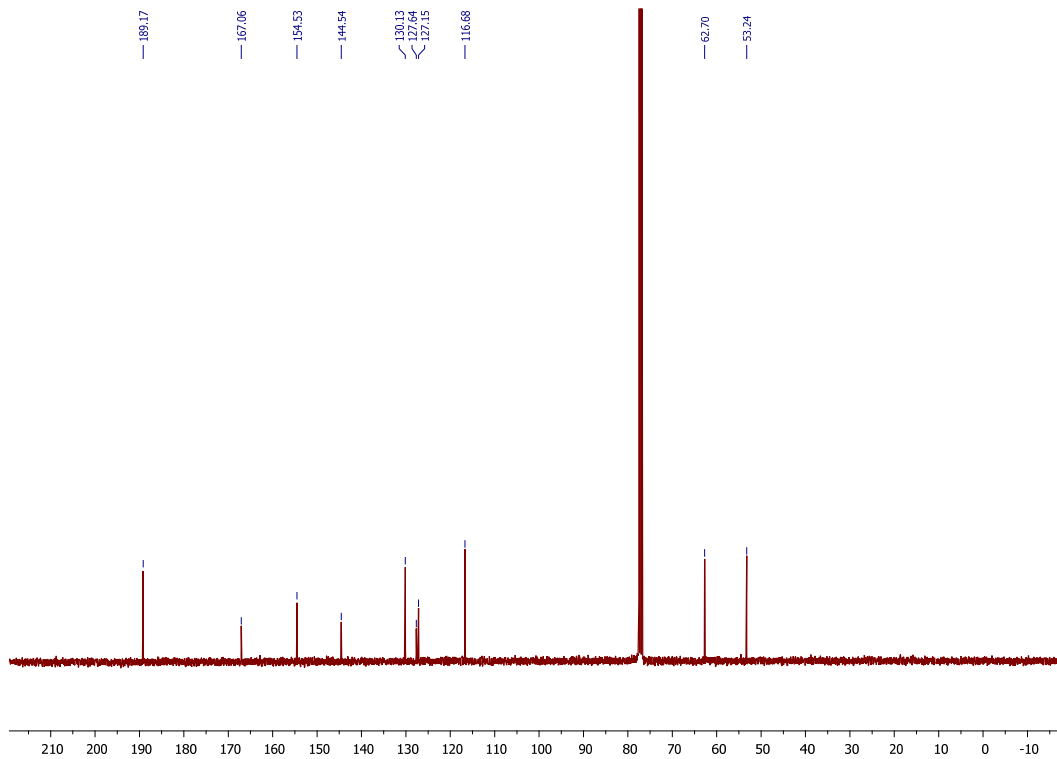
¹³C NMR Spectrum (Compound 266c)



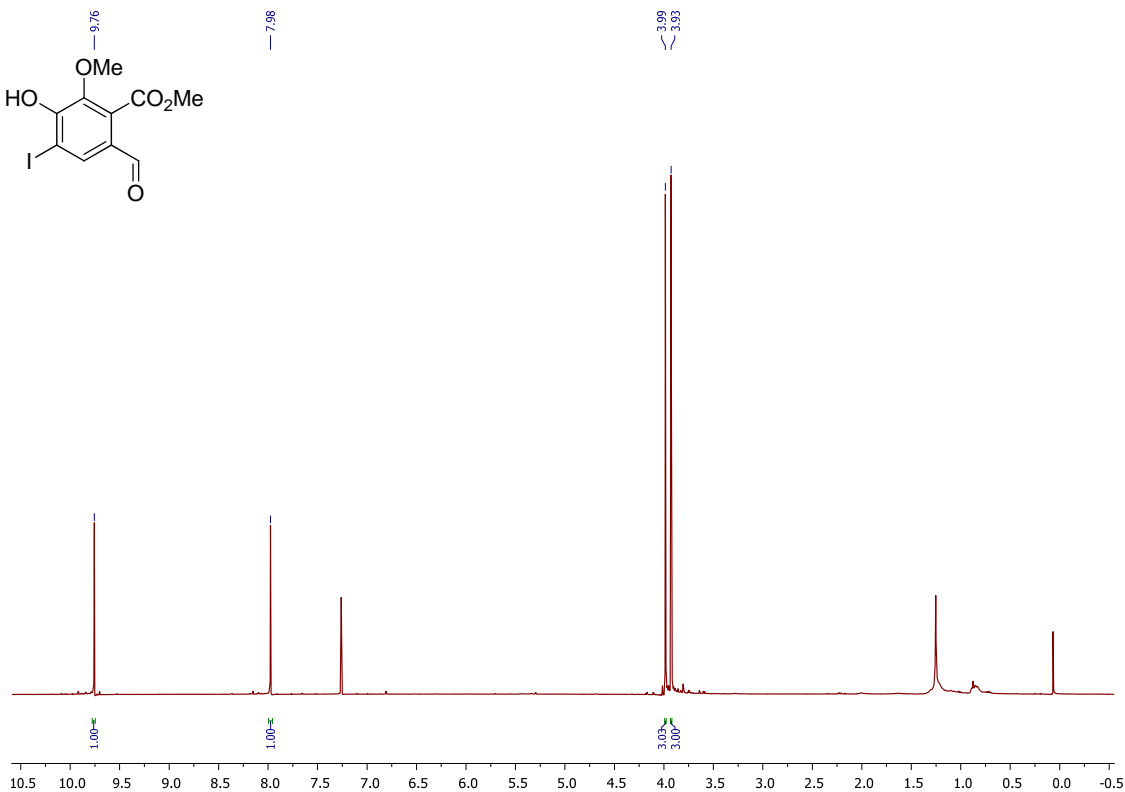
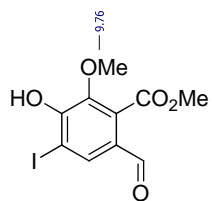
¹H NMR Spectrum (Compound 267)



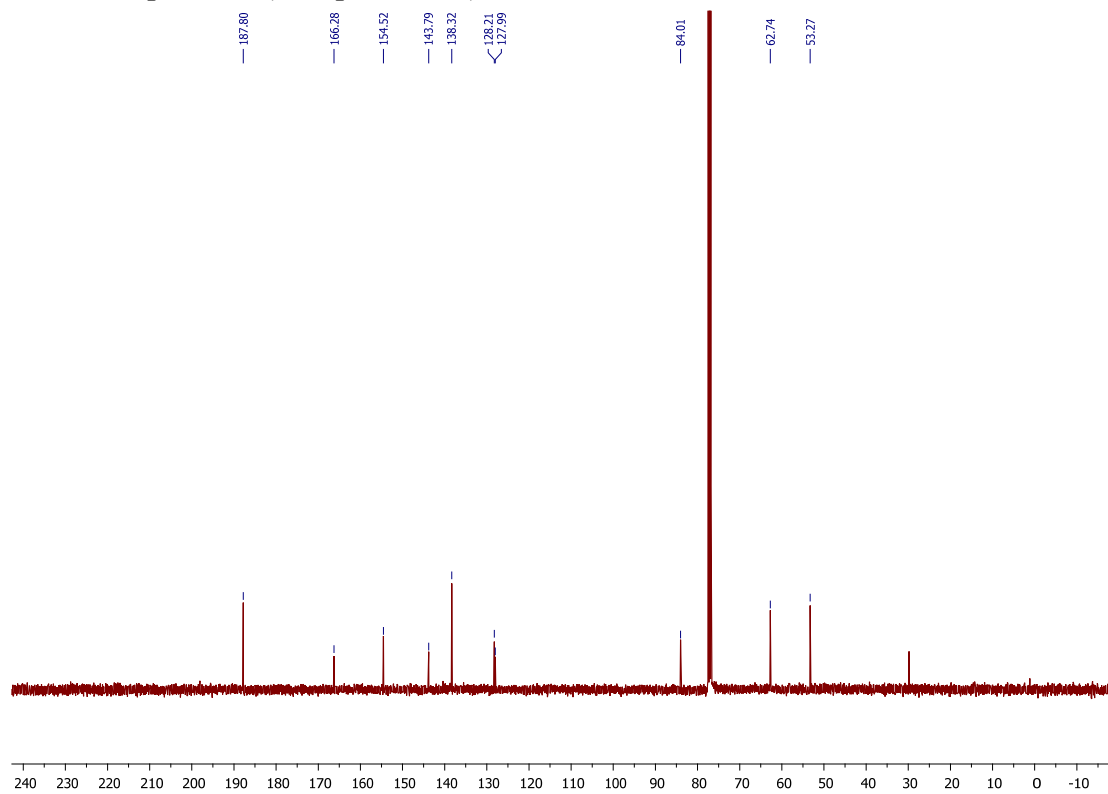
¹³C NMR Spectrum (Compound 267)



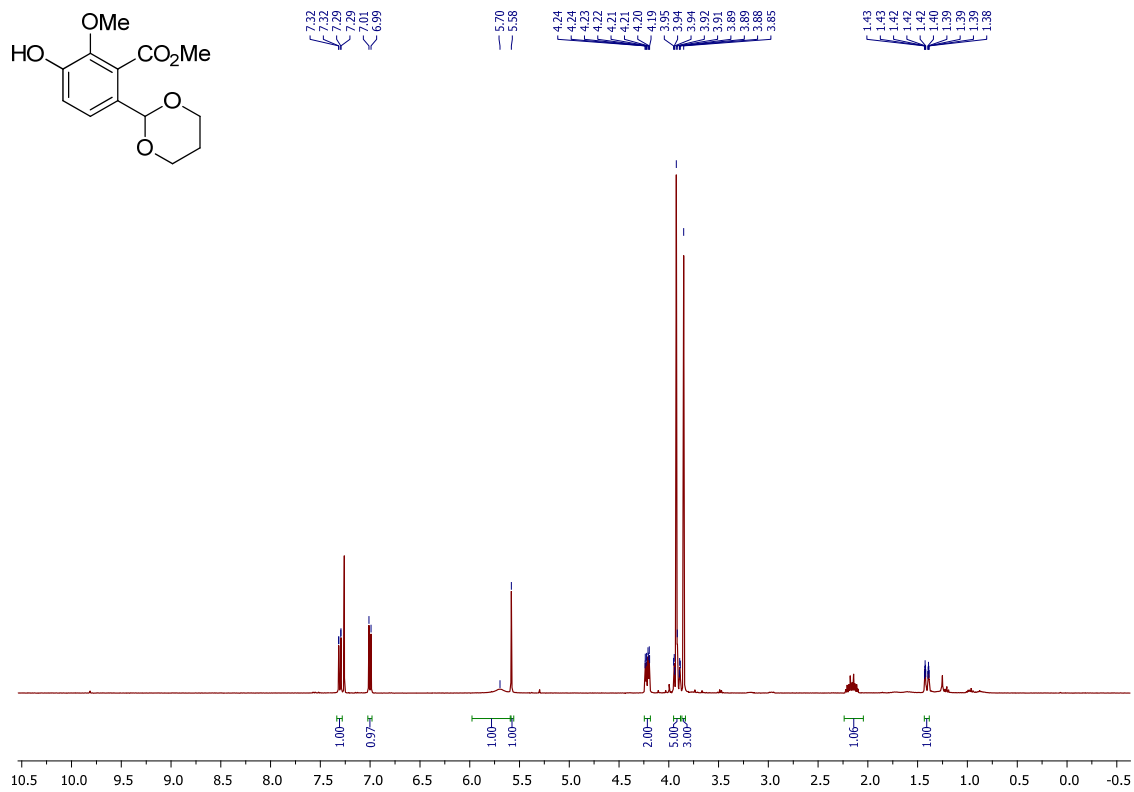
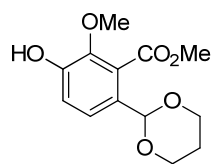
¹H NMR Spectrum (Compound 268)



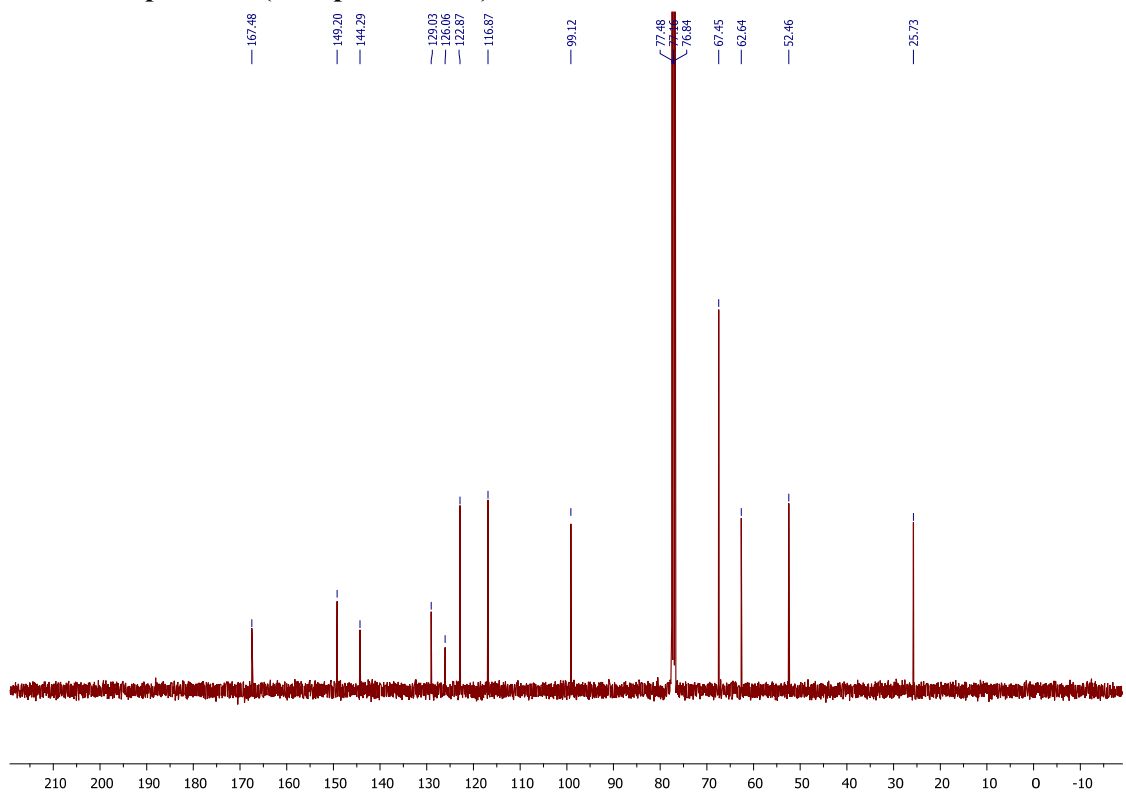
¹³C NMR Spectrum (Compound 268)



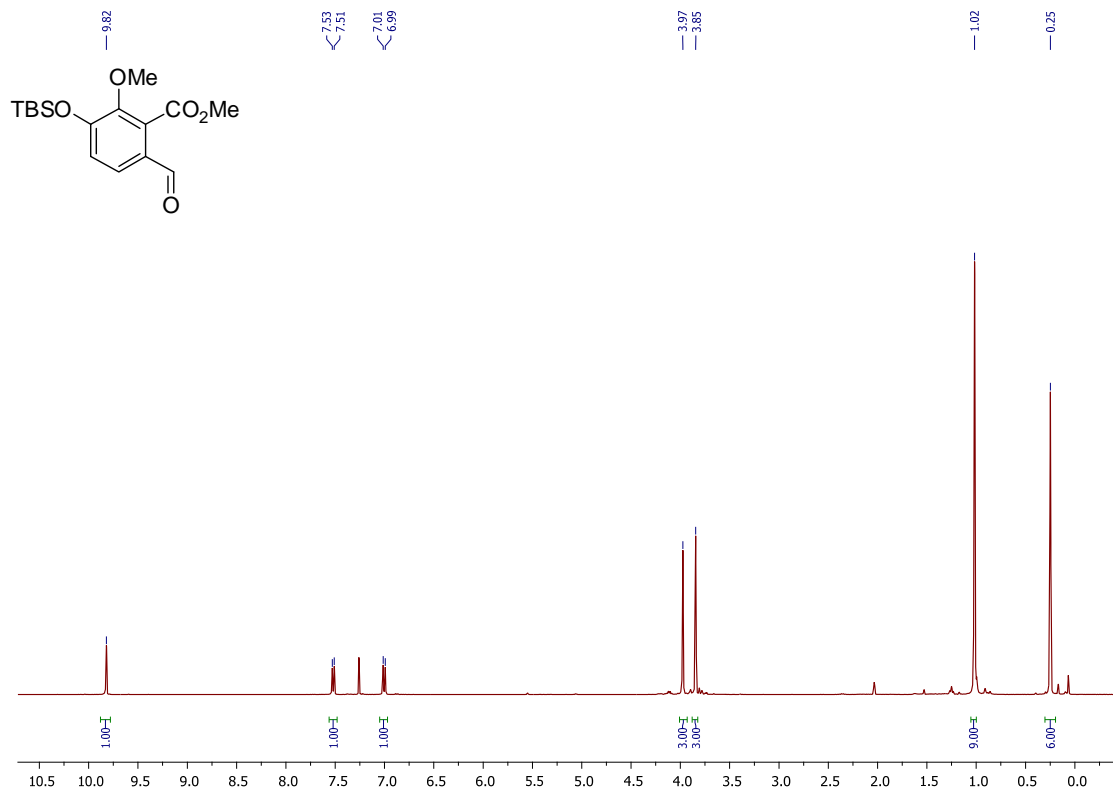
¹H NMR Spectrum (Compound 266c)



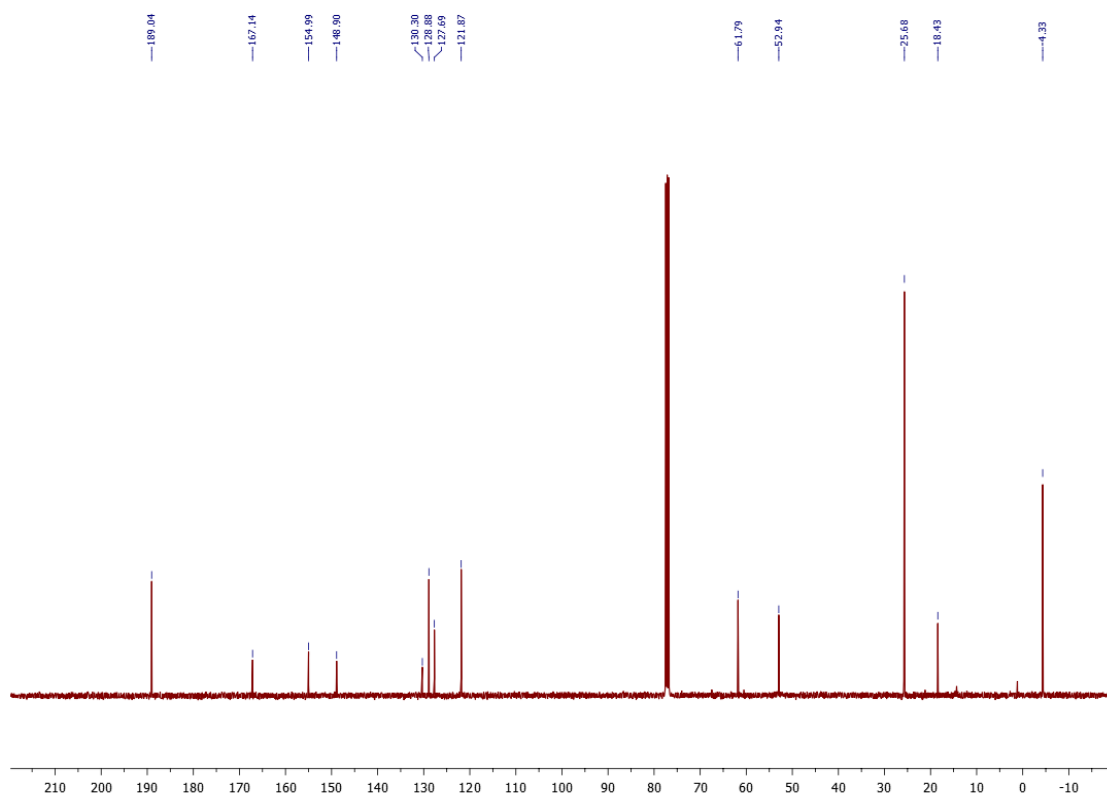
¹³C NMR Spectrum (Compound 266c)



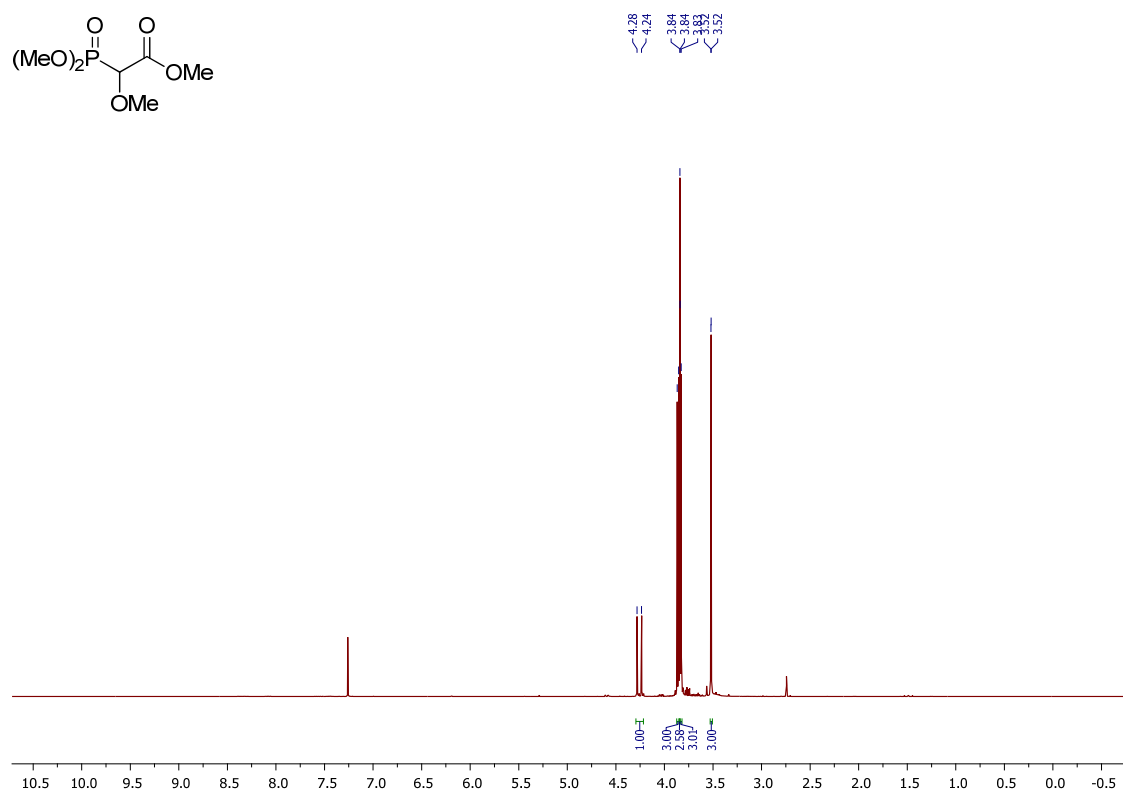
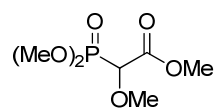
¹H NMR Spectrum (Compound 275)



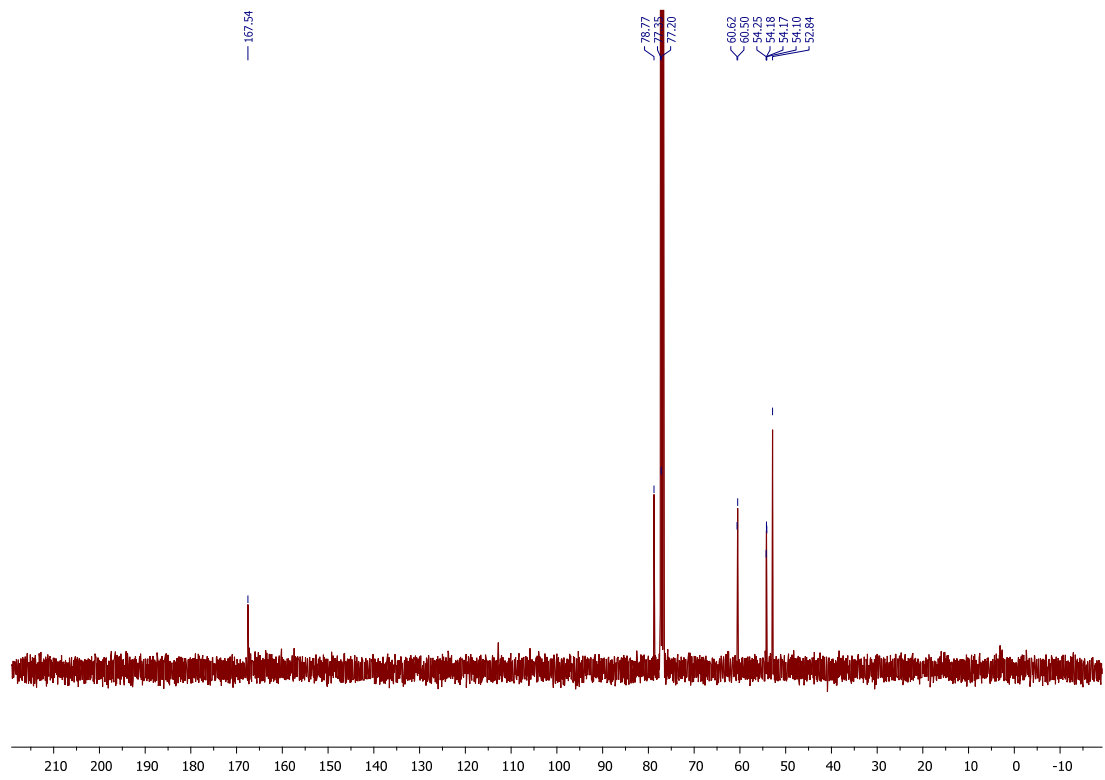
¹³C NMR Spectrum (Compound 275)



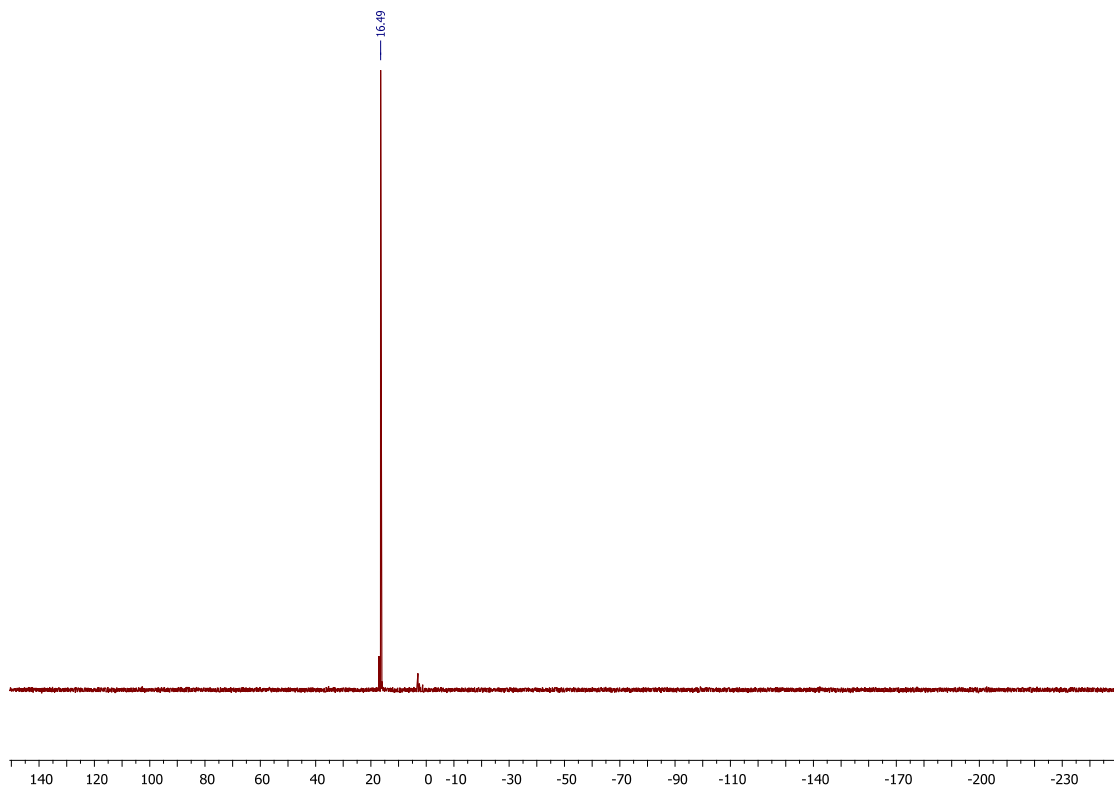
¹H NMR Spectrum (Compound 269)



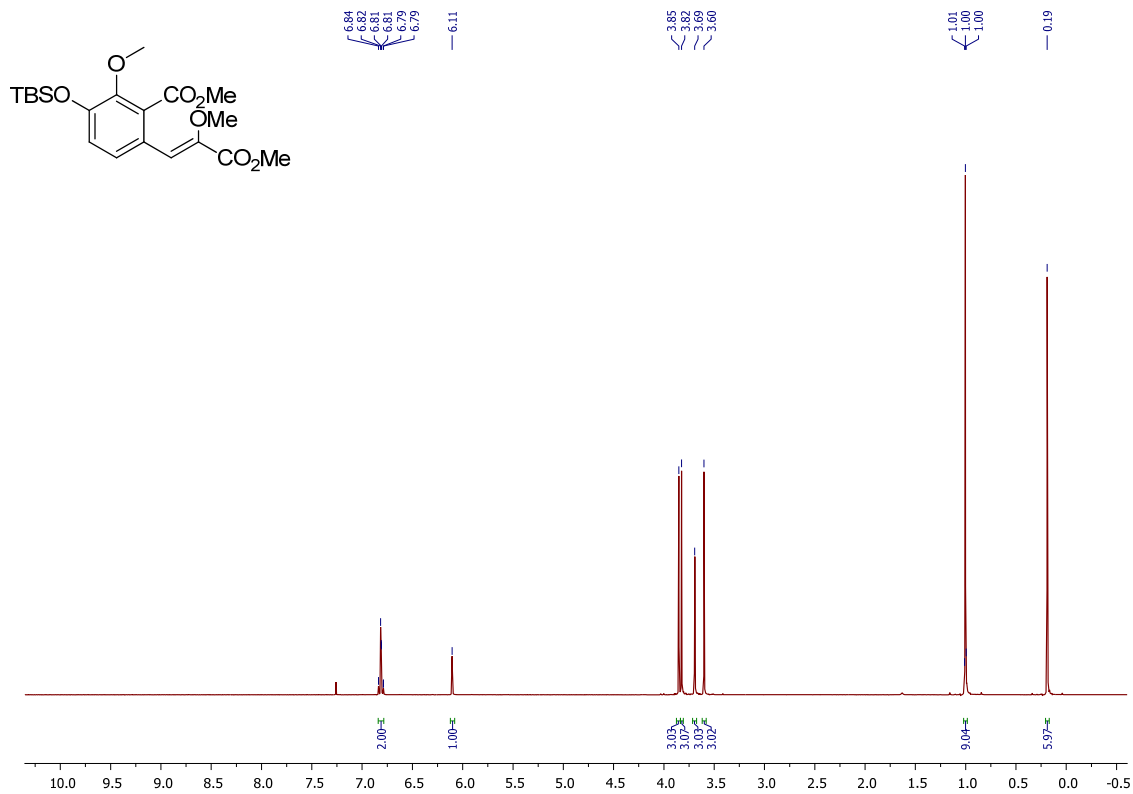
¹³C NMR Spectrum (Compound 269)



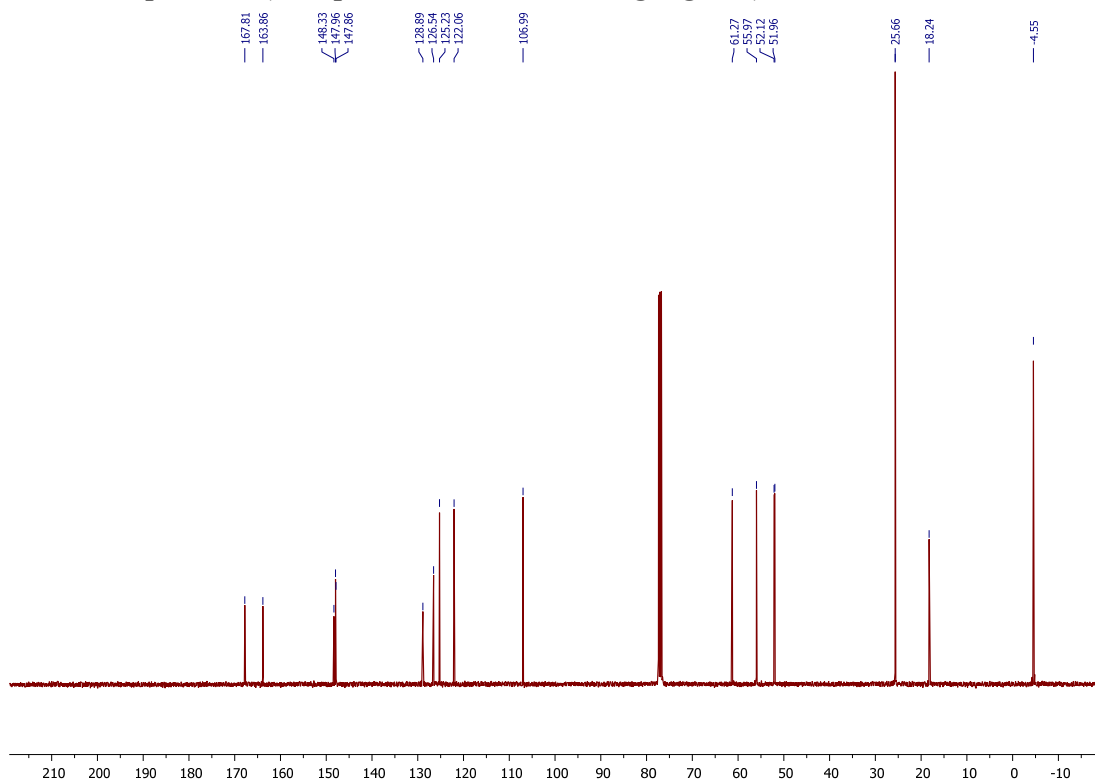
^{31}P NMR Spectrum (Compound 269)



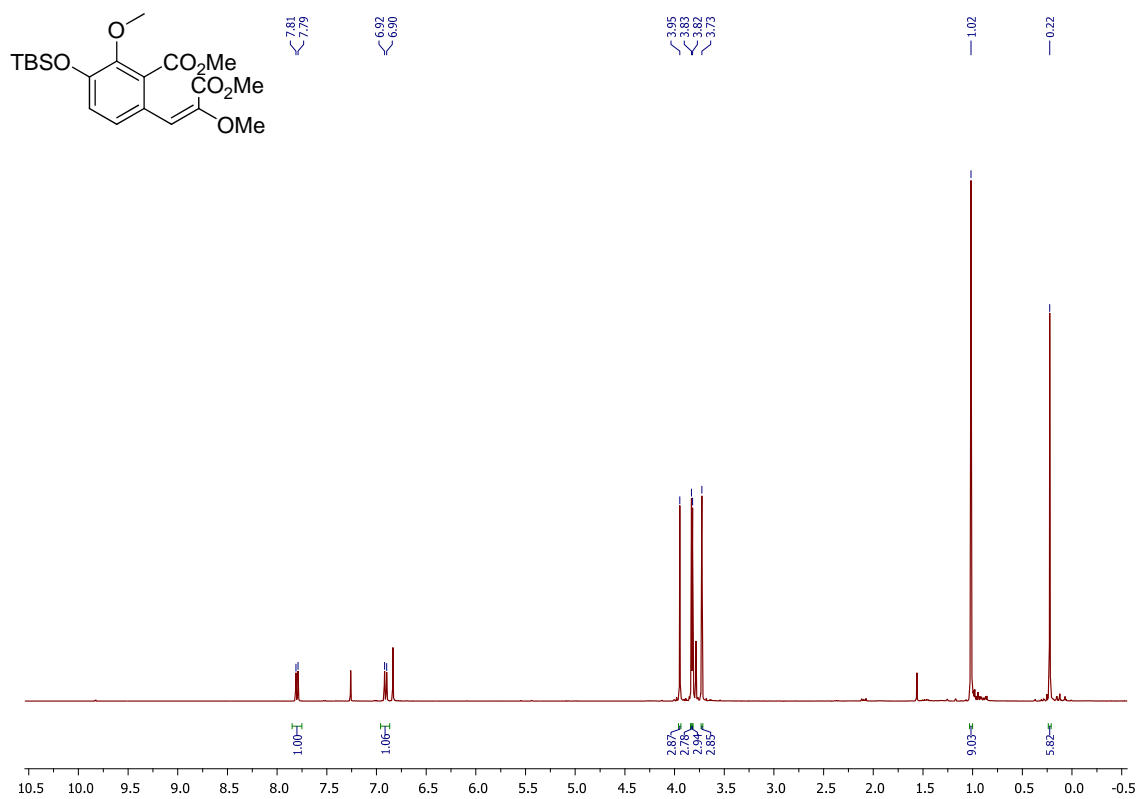
¹H NMR Spectrum (Compound 276; Z-isomer highlighted)



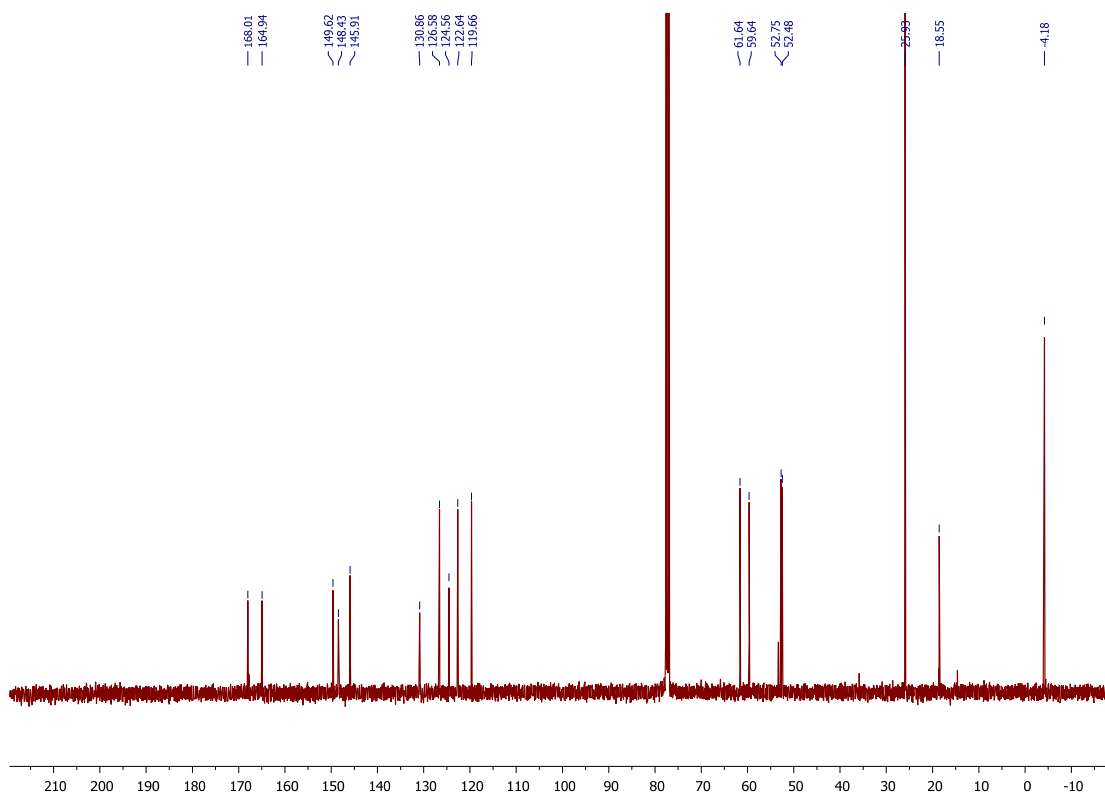
¹³C NMR Spectrum (Compound 276; Z-isomer highlighted)



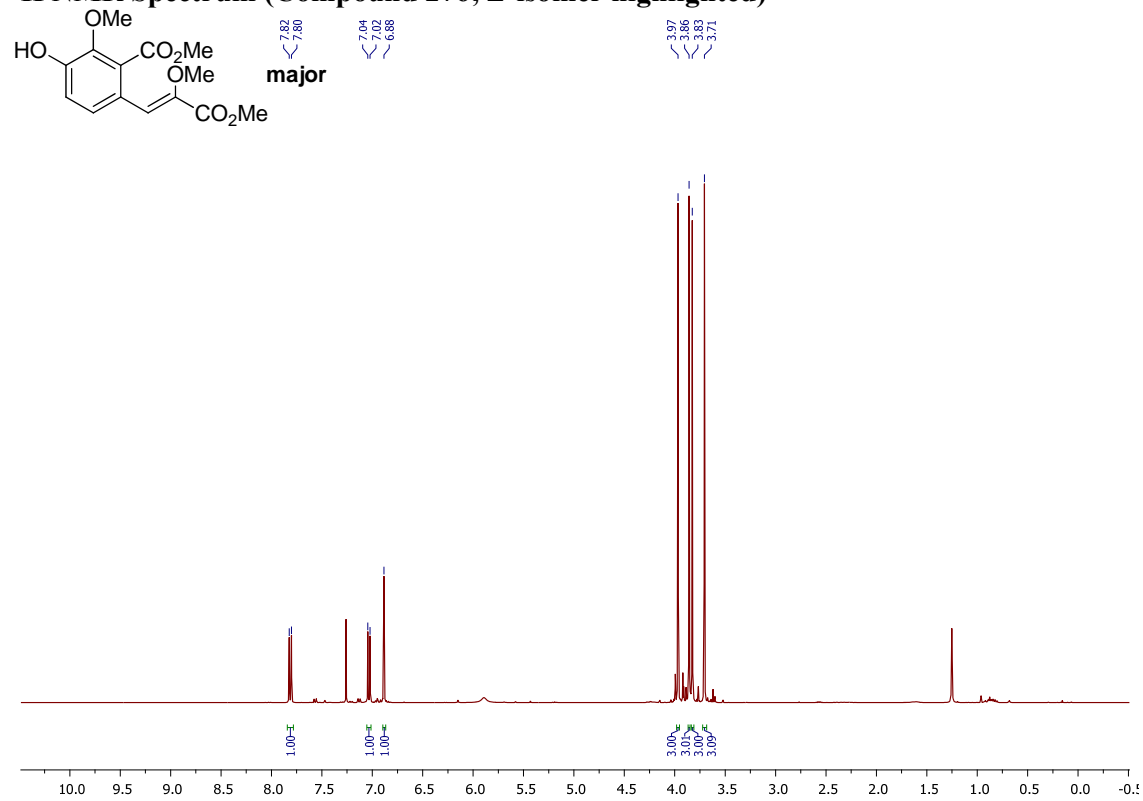
¹H NMR Spectrum (Compound 276; *E*-isomer highlighted)



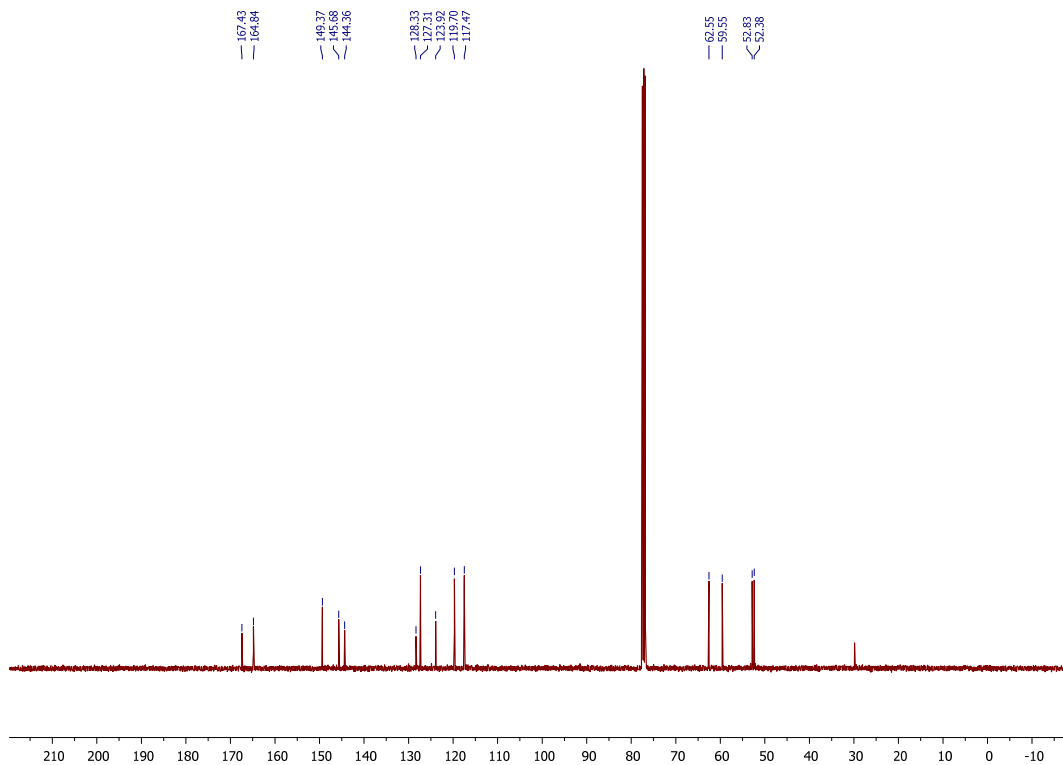
¹³C NMR Spectrum (Compound 276; *E*-isomer highlighted)



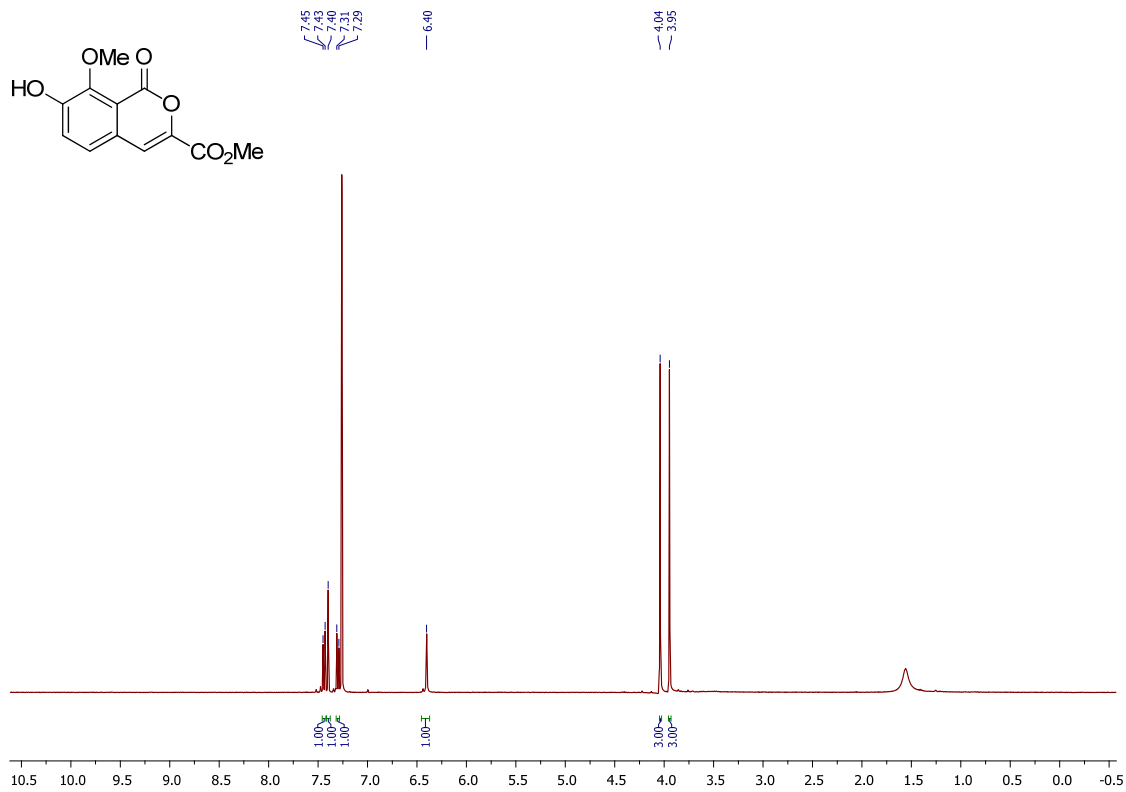
¹H NMR Spectrum (Compound 276; Z-isomer highlighted)



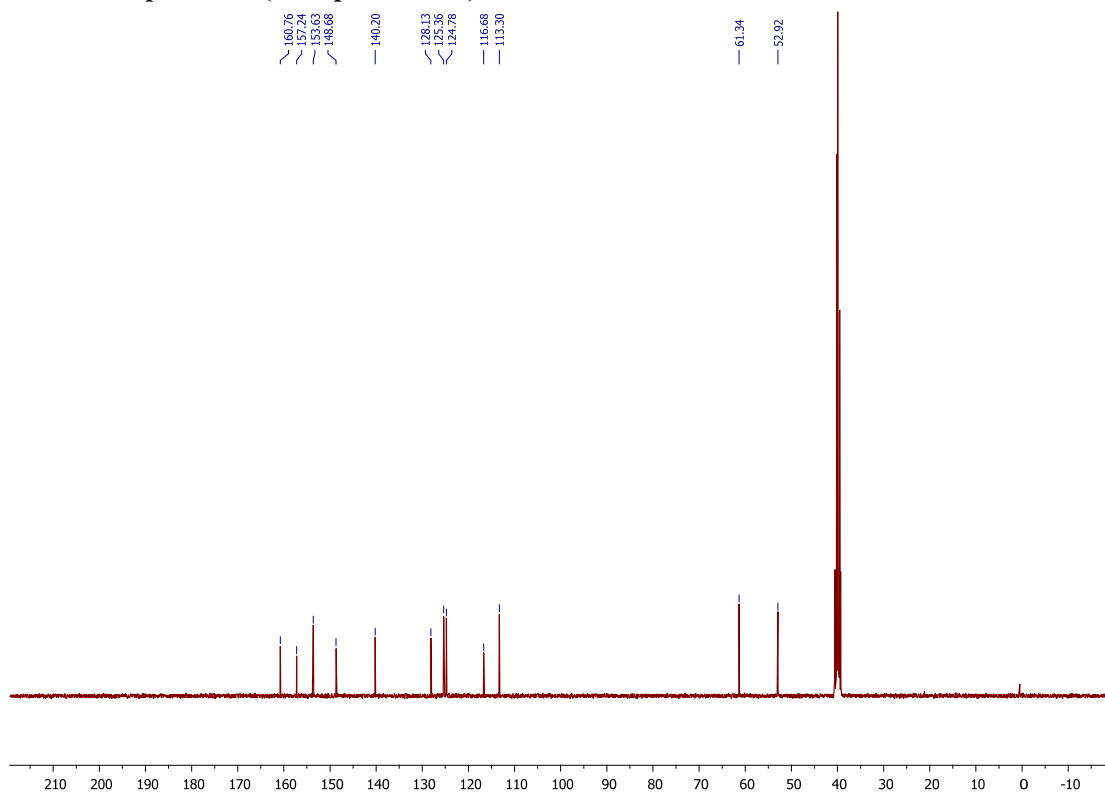
¹³C NMR Spectrum (Compound 276; Z-isomer highlighted)



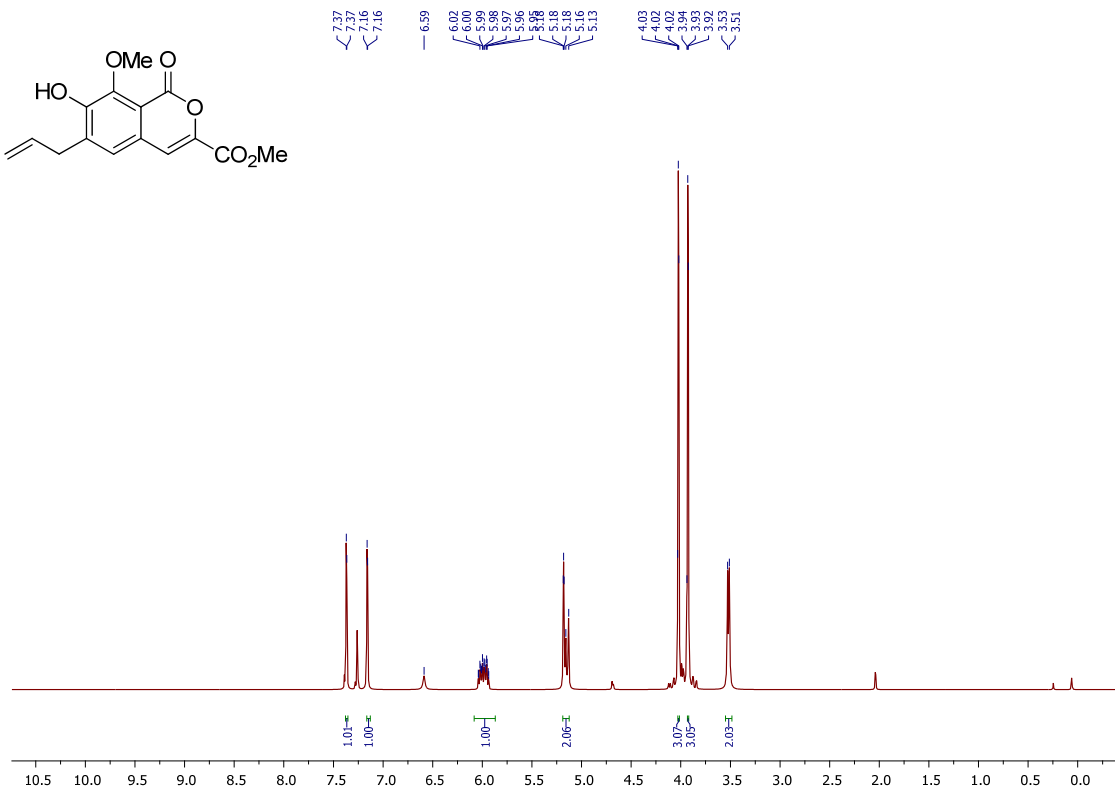
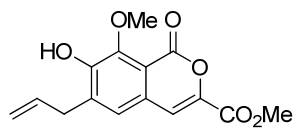
¹H NMR Spectrum (Compound 278)



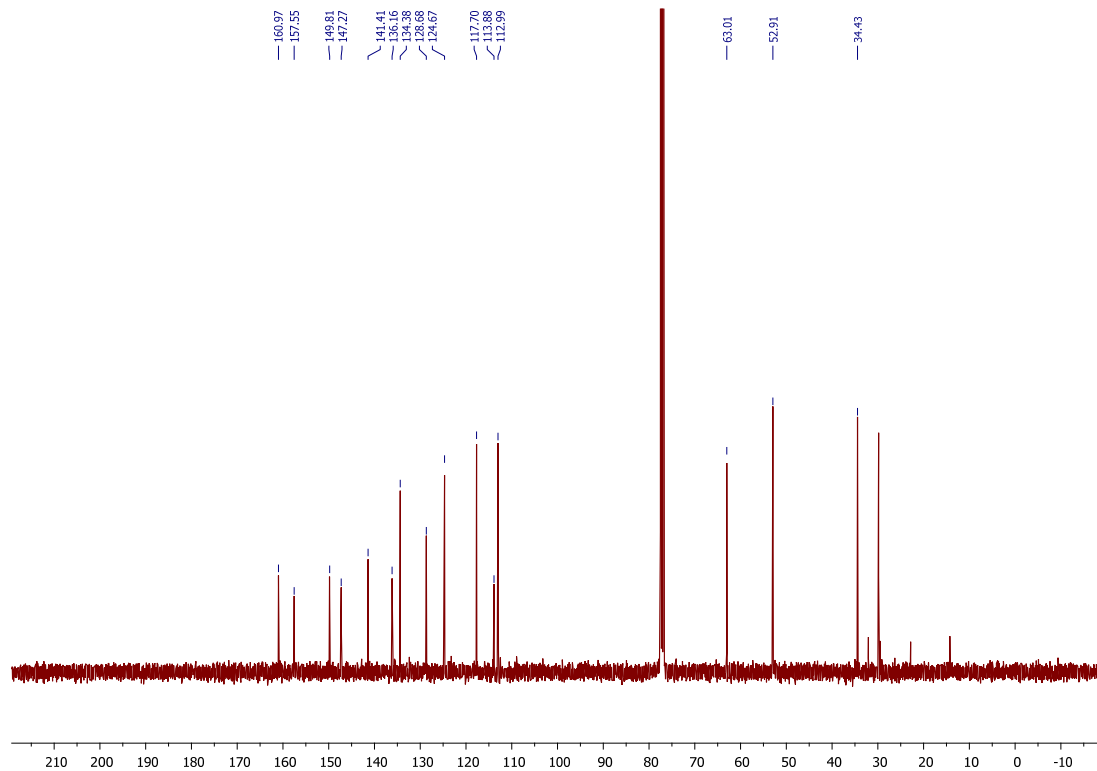
¹³C NMR Spectrum (Compound 278)



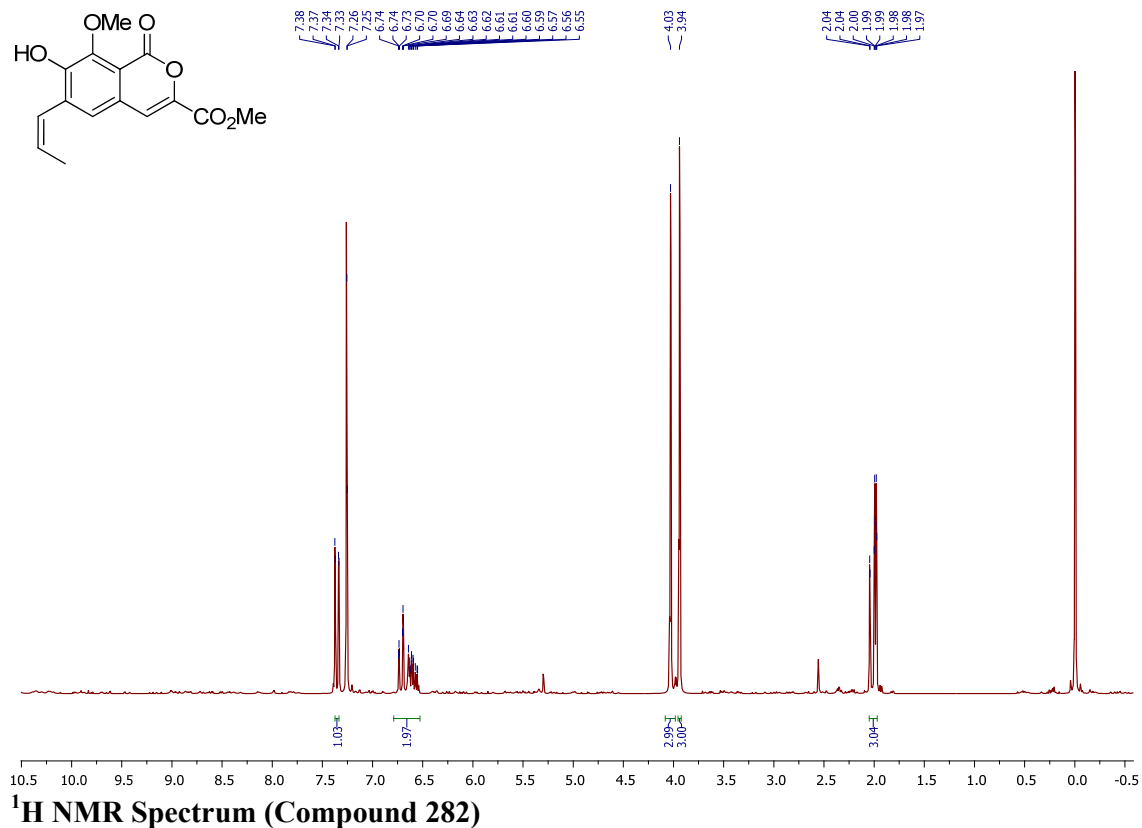
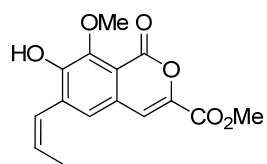
¹H NMR Spectrum (Compound 279)



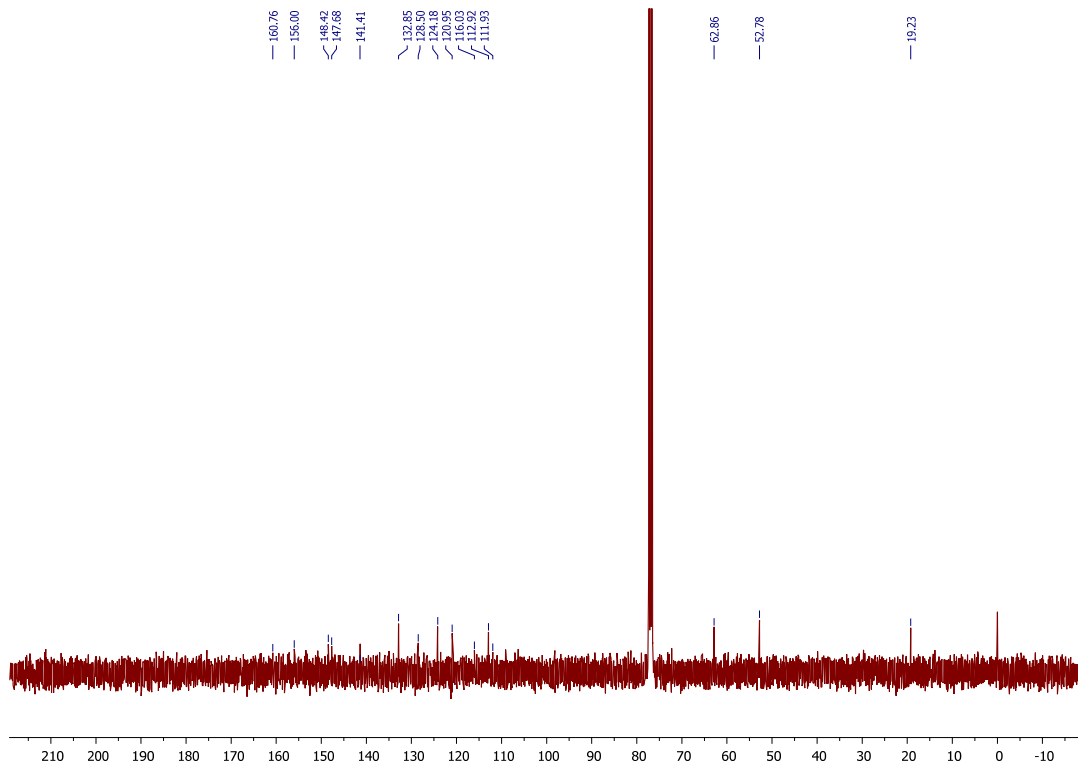
¹³C NMR Spectrum (Compound 279)



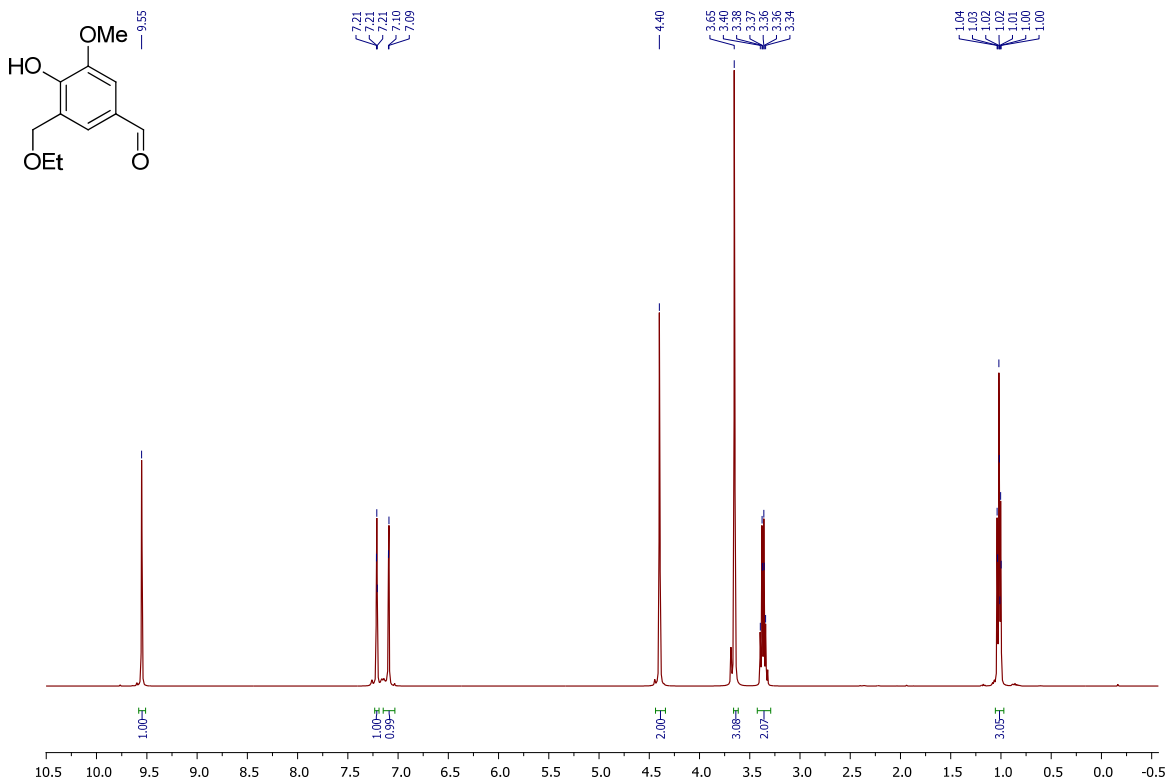
¹H NMR Spectrum (Compound 282)



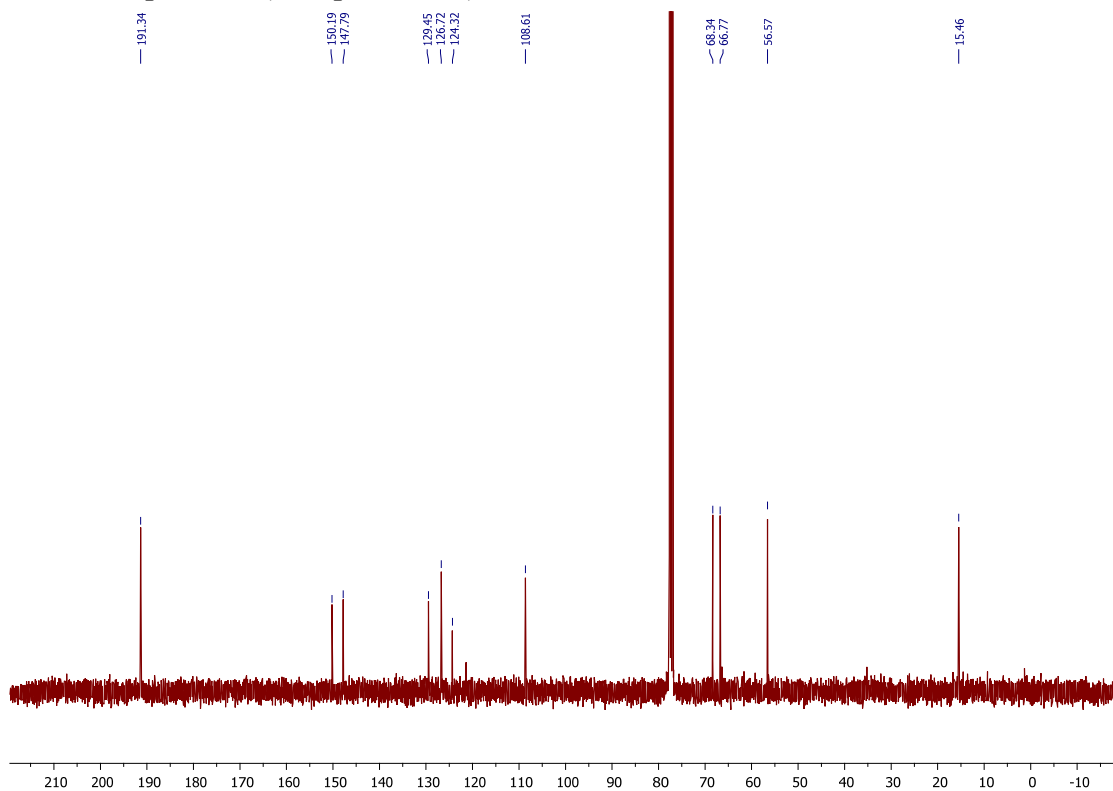
¹³C NMR Spectrum (Compound 282)



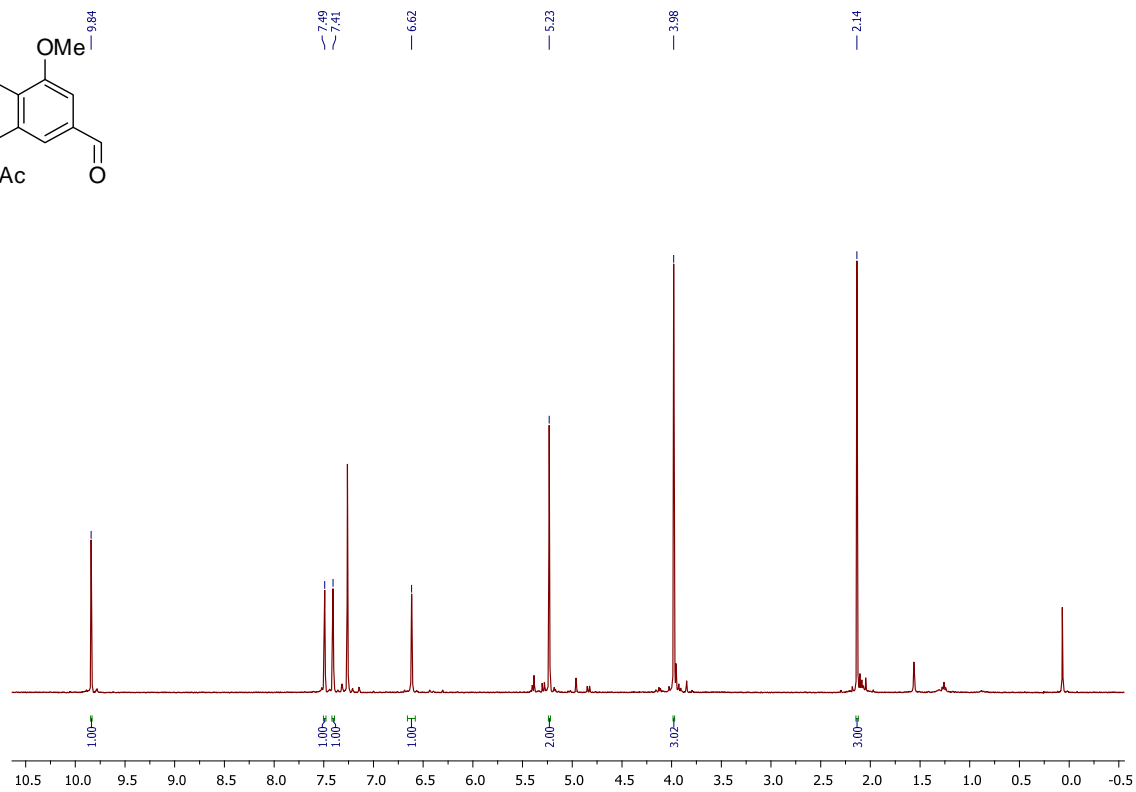
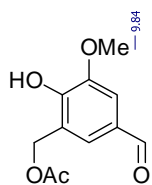
¹H NMR Spectrum (Compound 285)



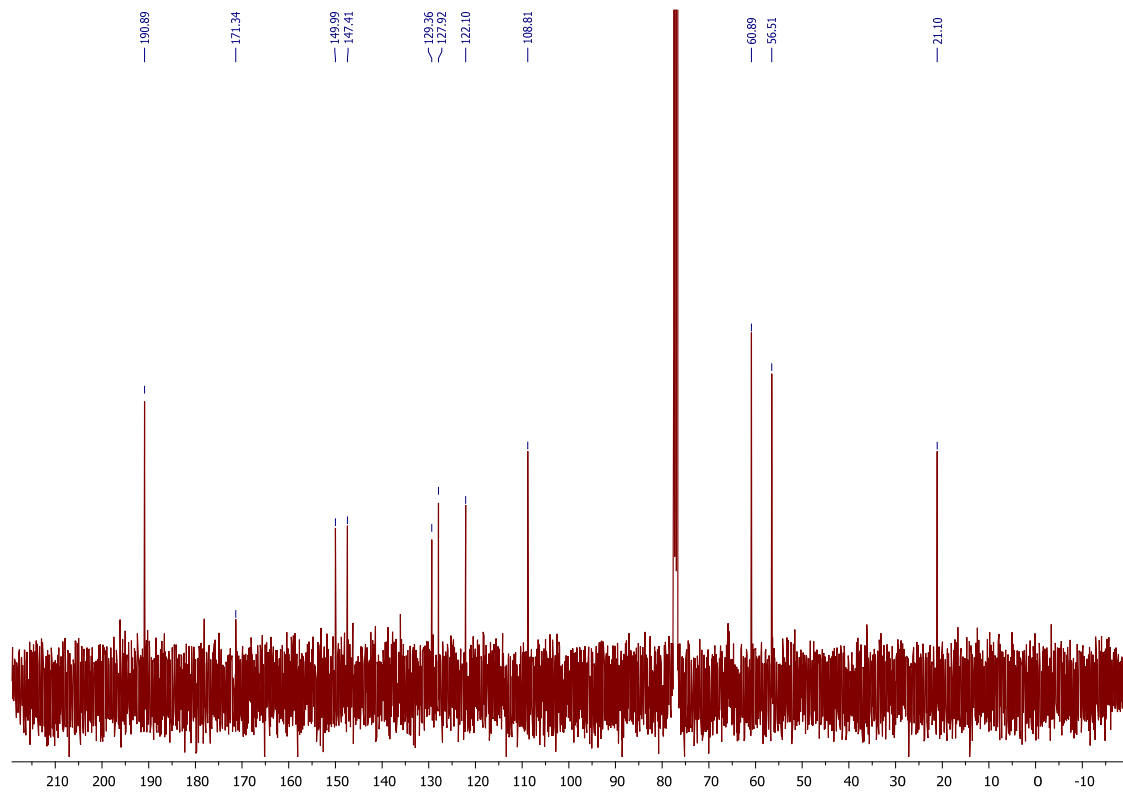
¹³C NMR Spectrum (Compound 285)



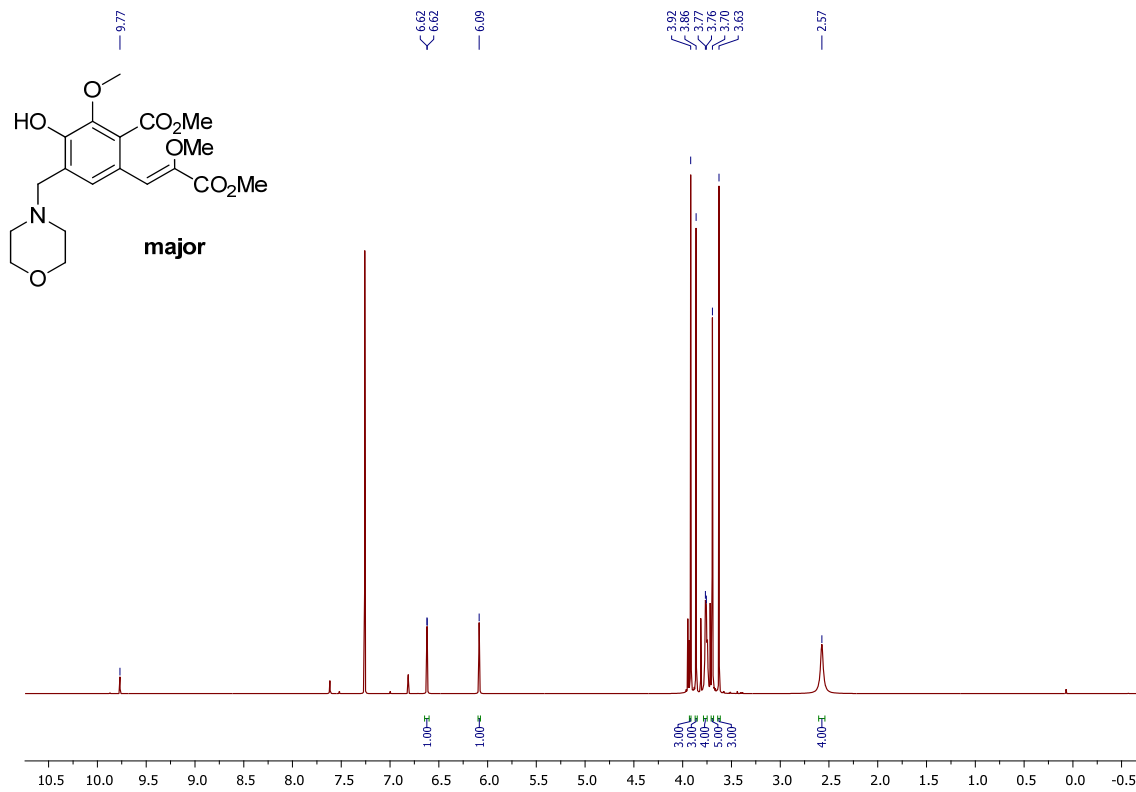
¹H NMR Spectrum (Compound 289)



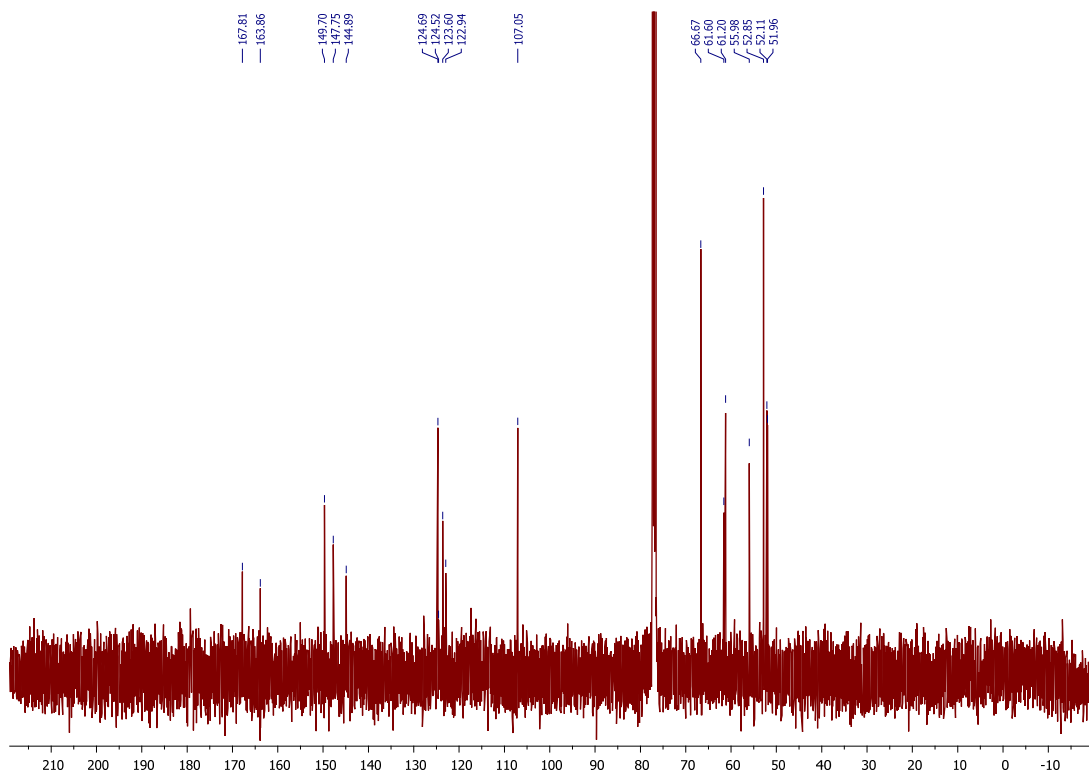
¹³C NMR Spectrum (Compound 289)



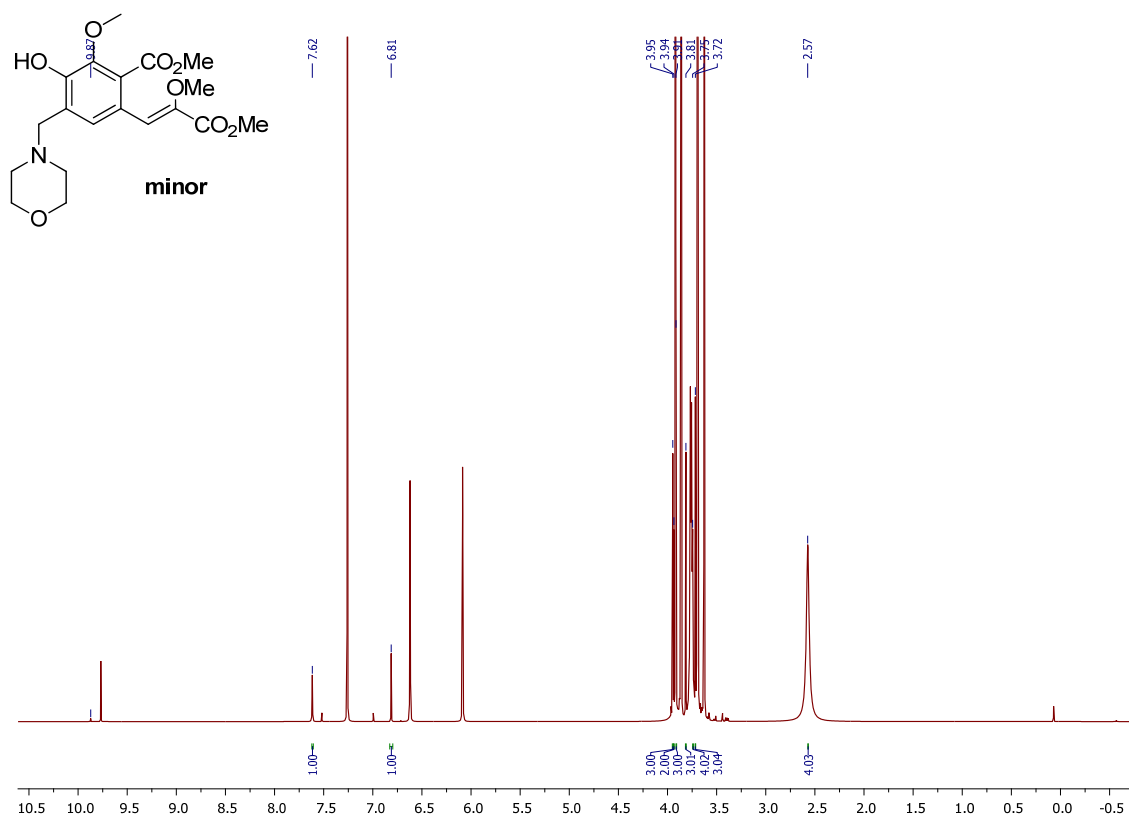
¹H NMR Spectrum (Compound 290; Z-isomer highlighted)



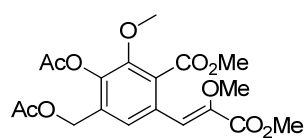
¹³C NMR Spectrum (Compound 290)



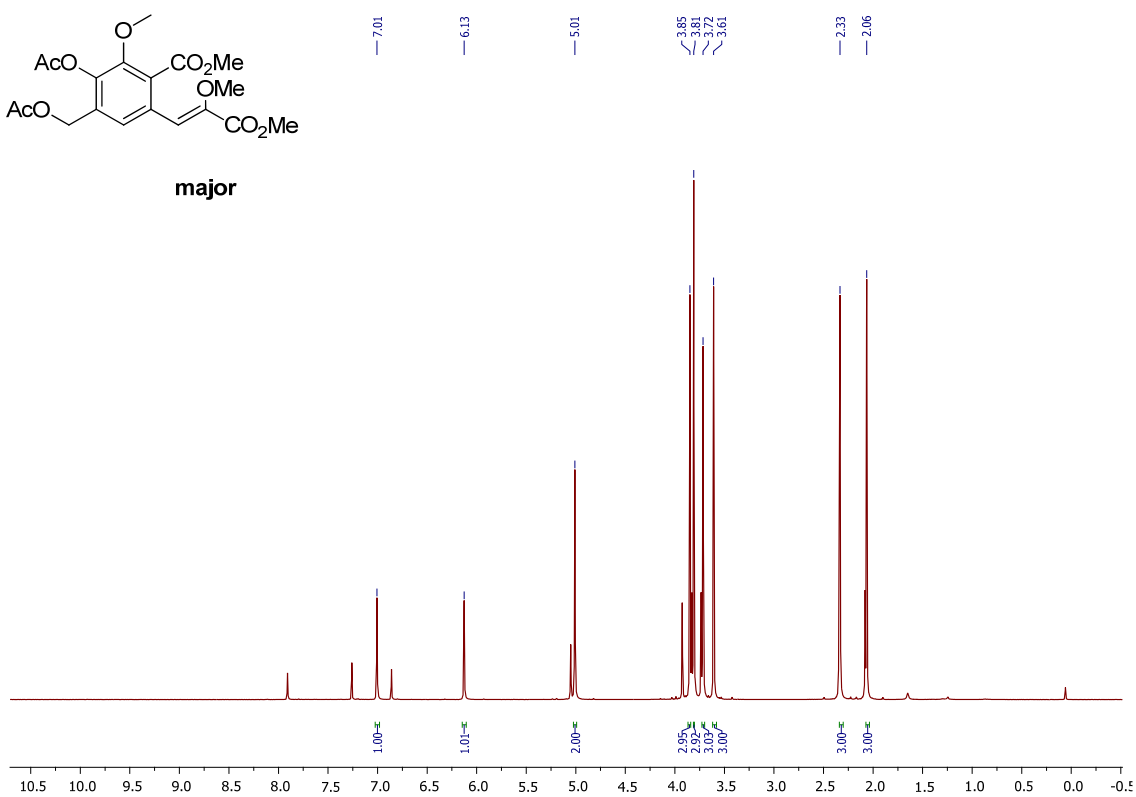
¹H NMR Spectrum (Compound 290; *E*-isomer highlighted)



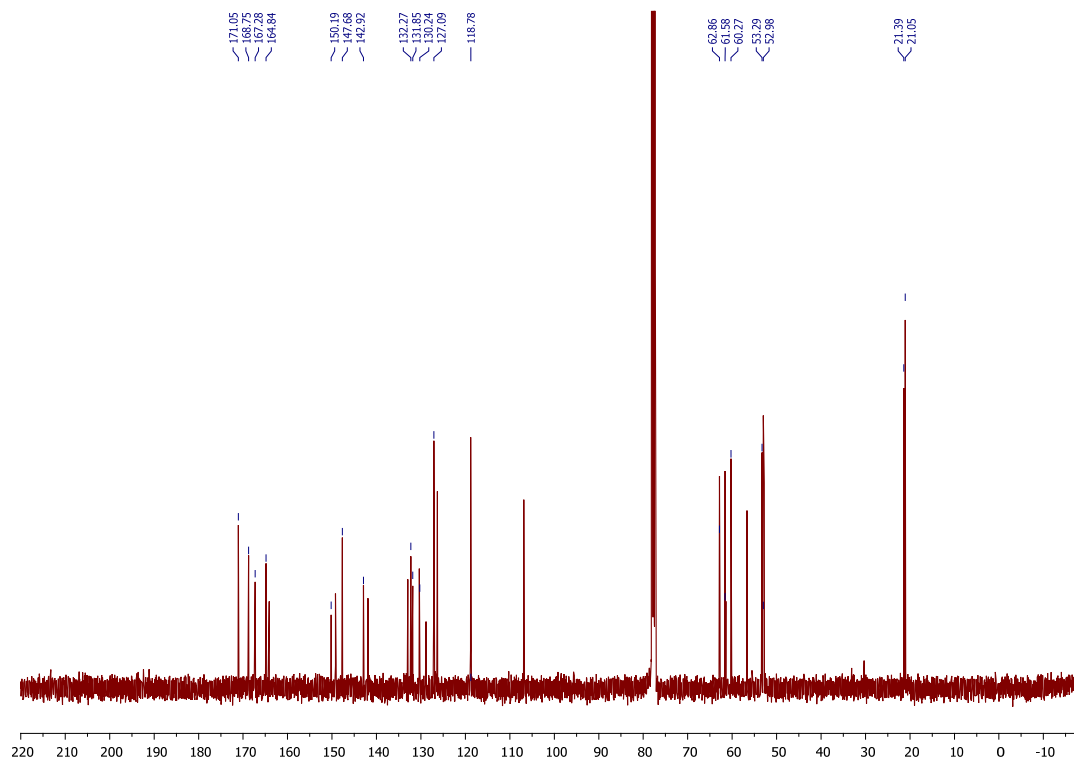
¹H NMR Spectrum (Compound 294; Z-isomer highlighted)



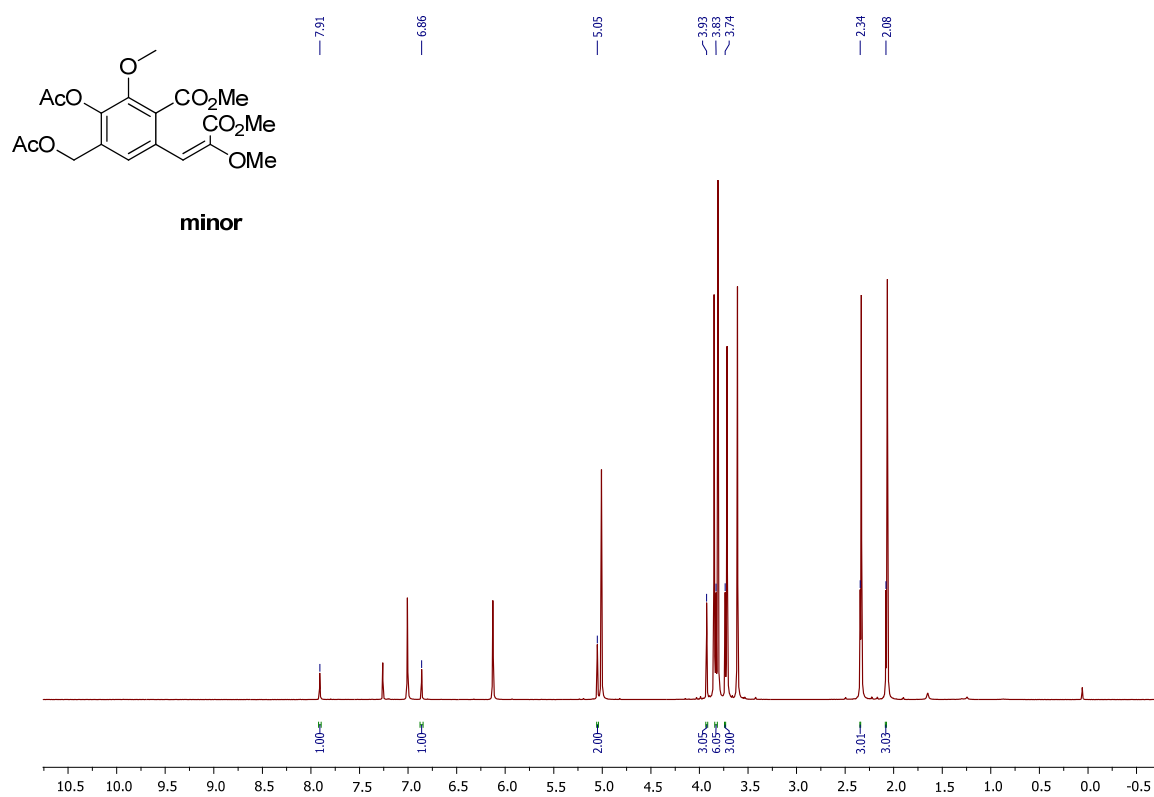
major



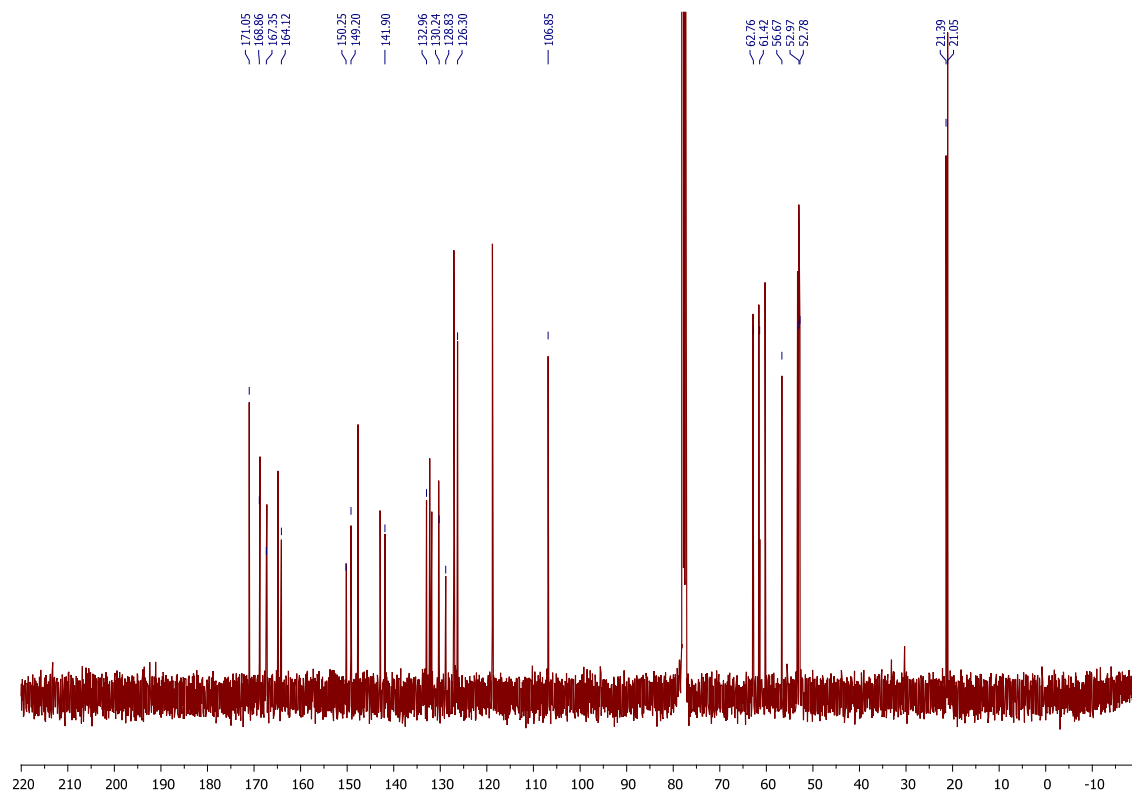
¹³C NMR Spectrum (Compound 294; Z-isomer highlighted)



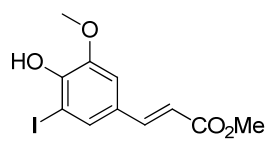
¹H NMR Spectrum (Compound 294; E-isomer highlighted)



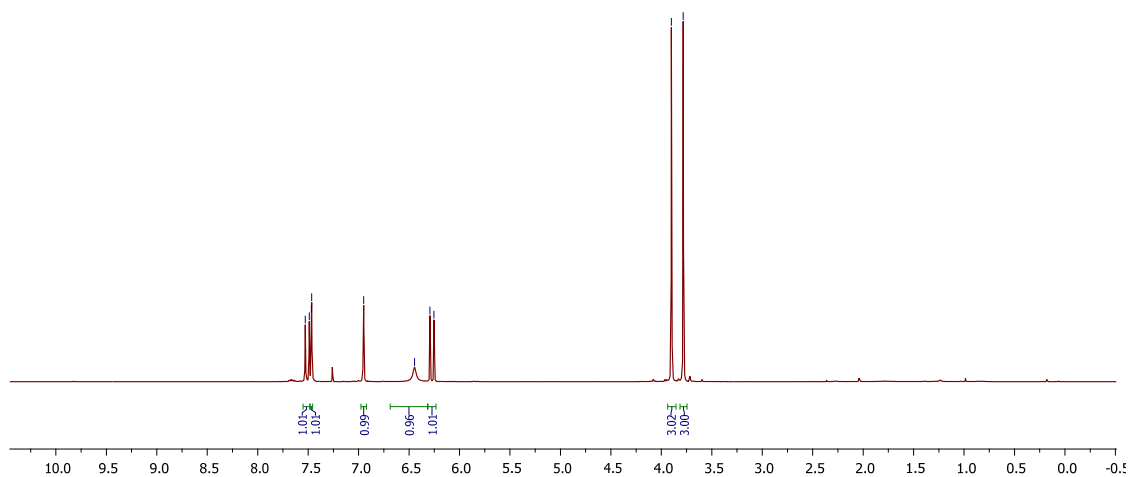
¹³C NMR Spectrum (Compound 294; E-isomer highlighted)



¹H NMR Spectrum (Compound 301a)

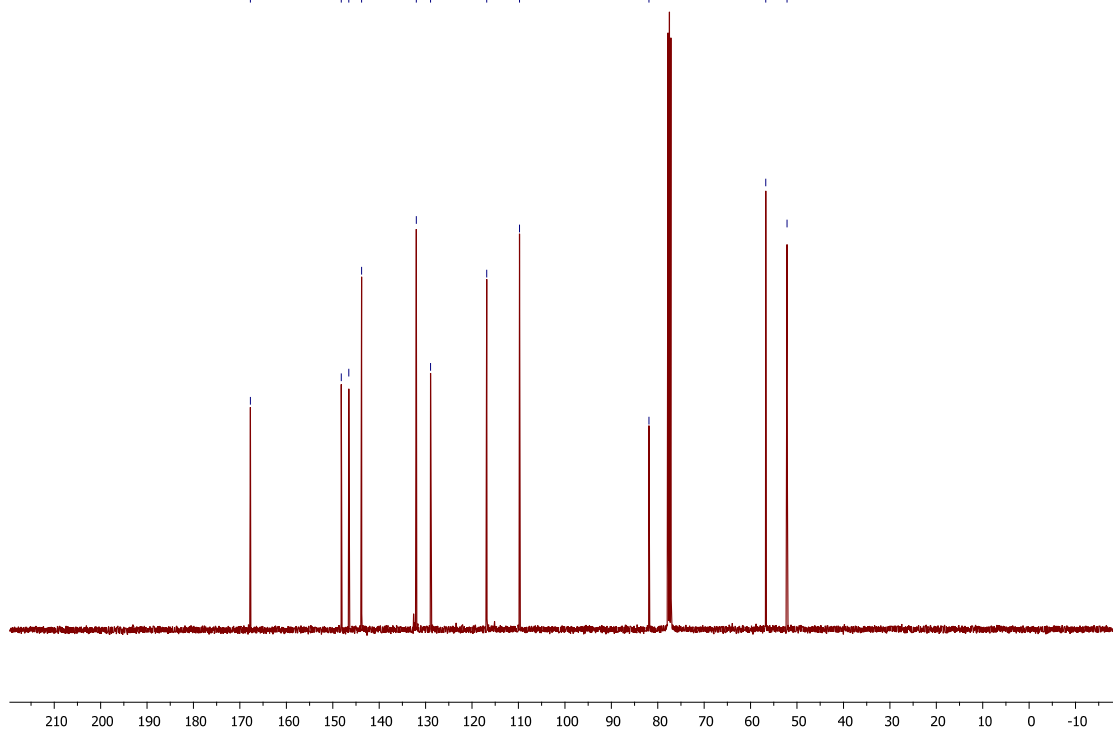


7.53
7.49
7.47
6.95
6.45
6.29
6.25
3.90
3.78

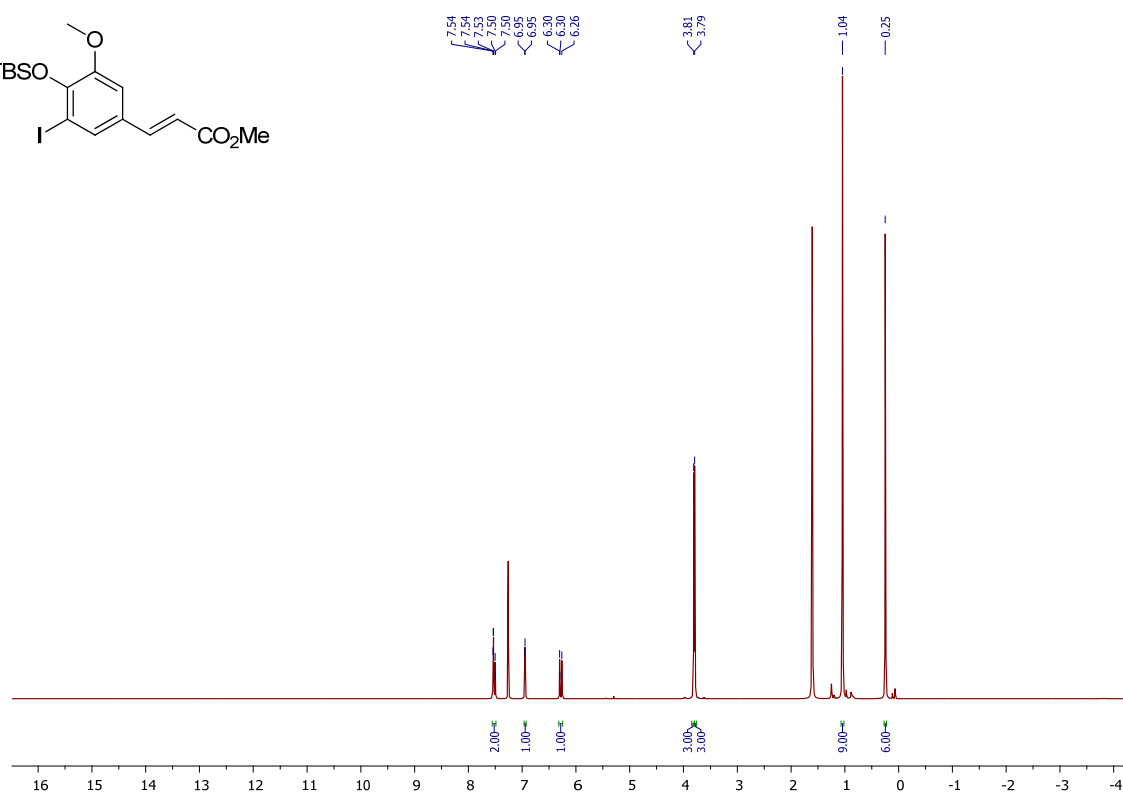
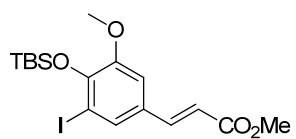


¹³C NMR Spectrum (Compound 301a)

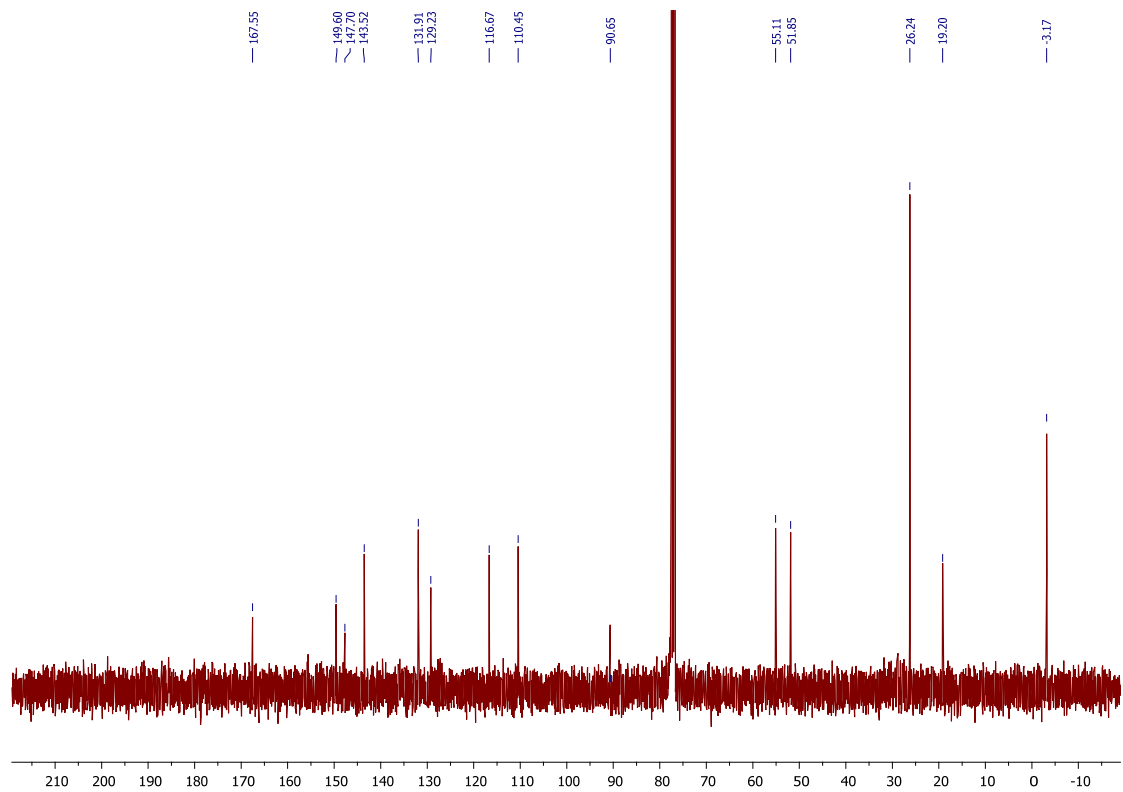
167.75
148.17
146.53
143.79
132.00
128.92
116.83
109.76
81.88
56.72
52.15



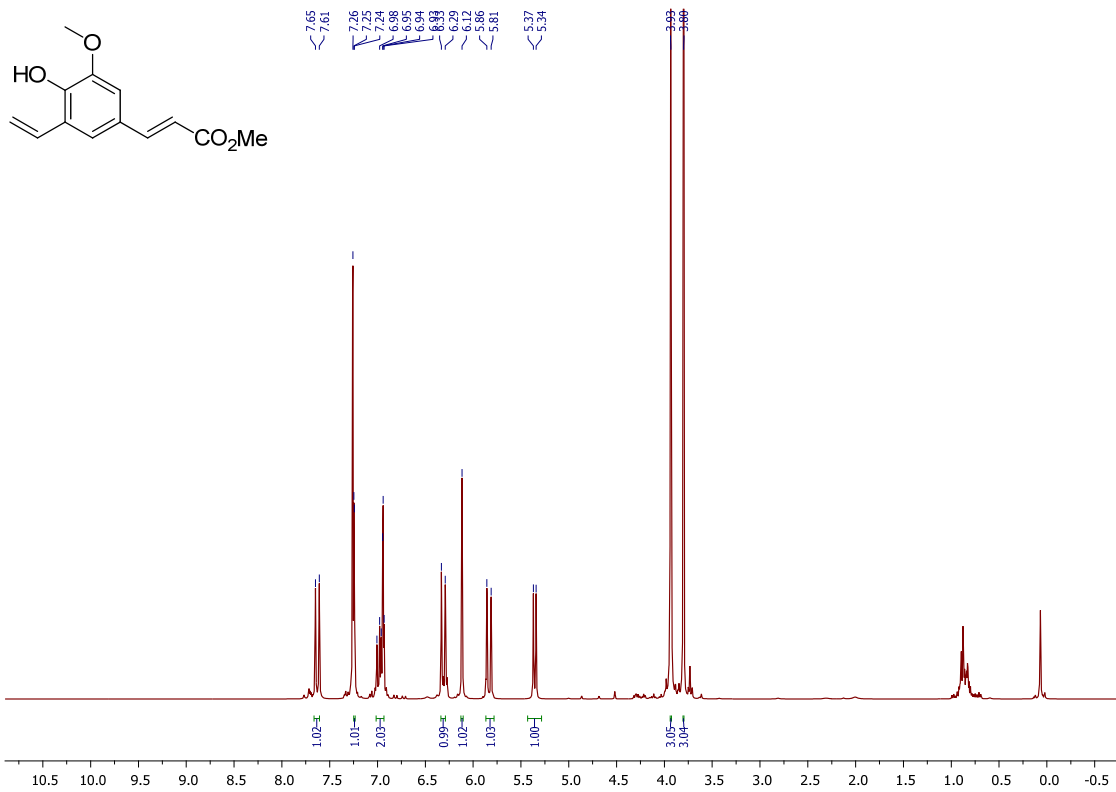
¹H NMR Spectrum (Compound 301)



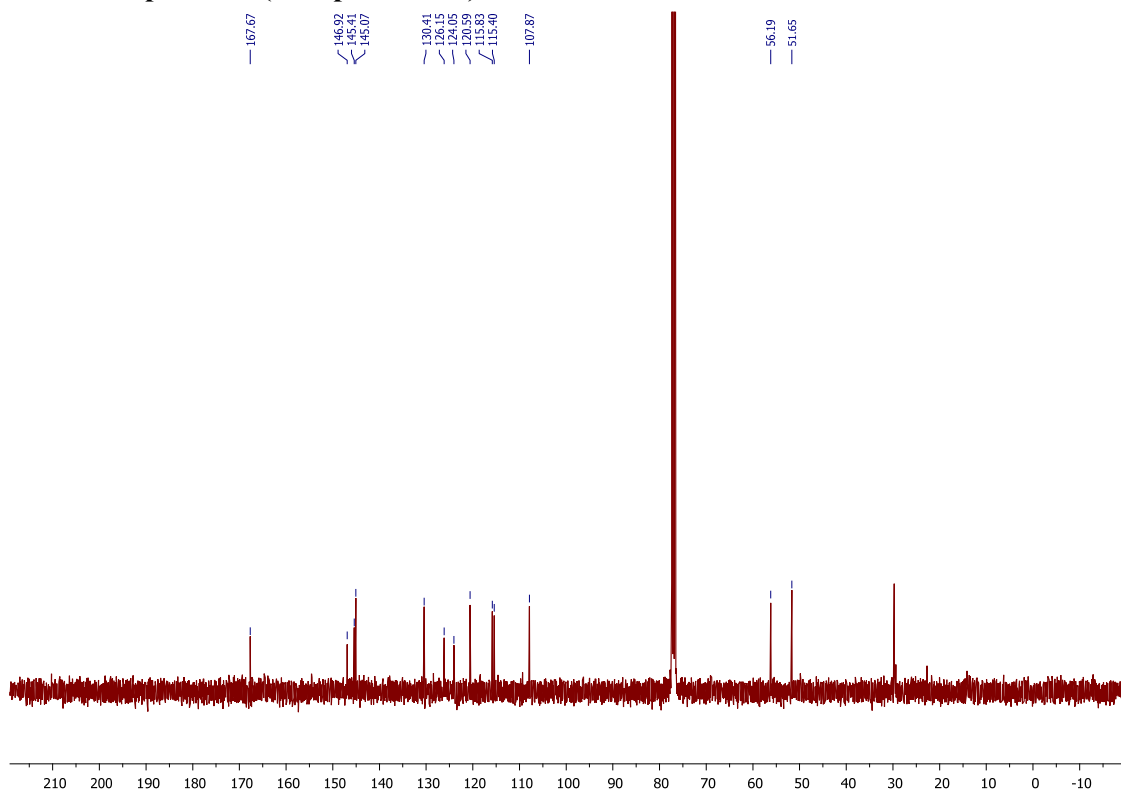
¹³C NMR Spectrum (Compound 301)



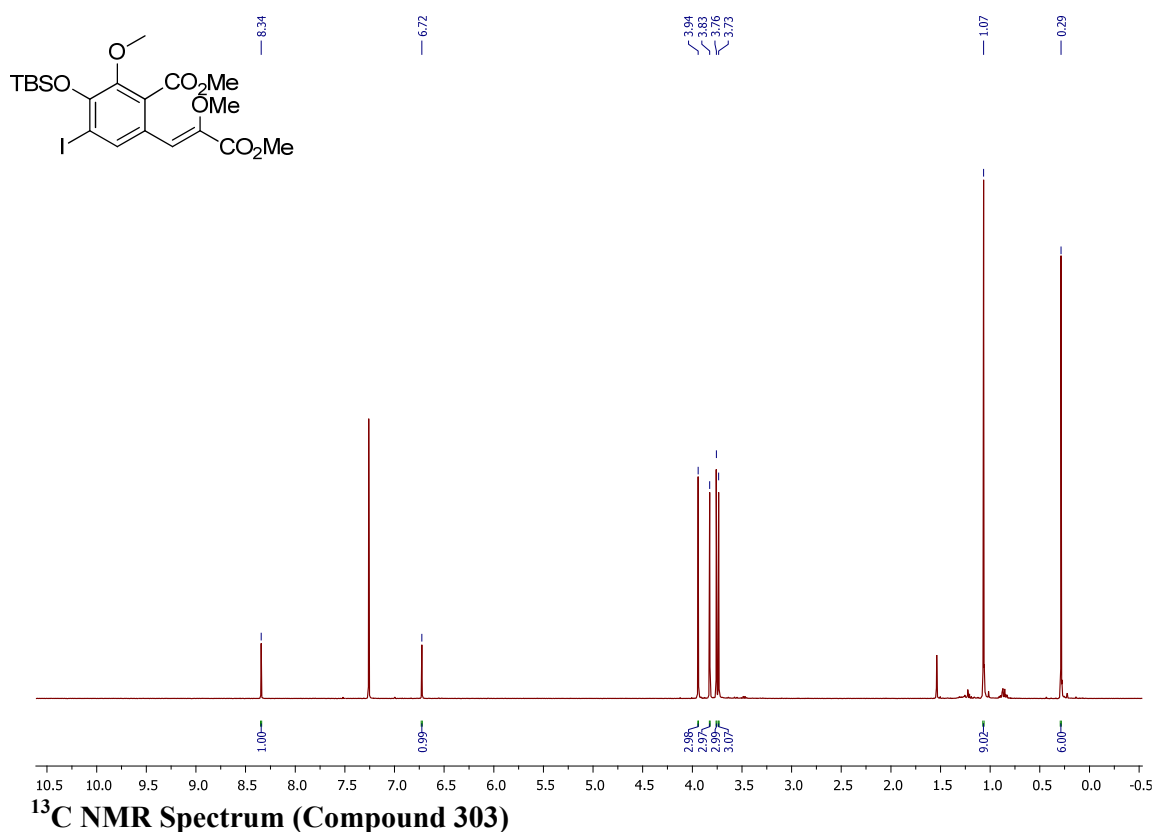
¹H NMR Spectrum (Compound 302)



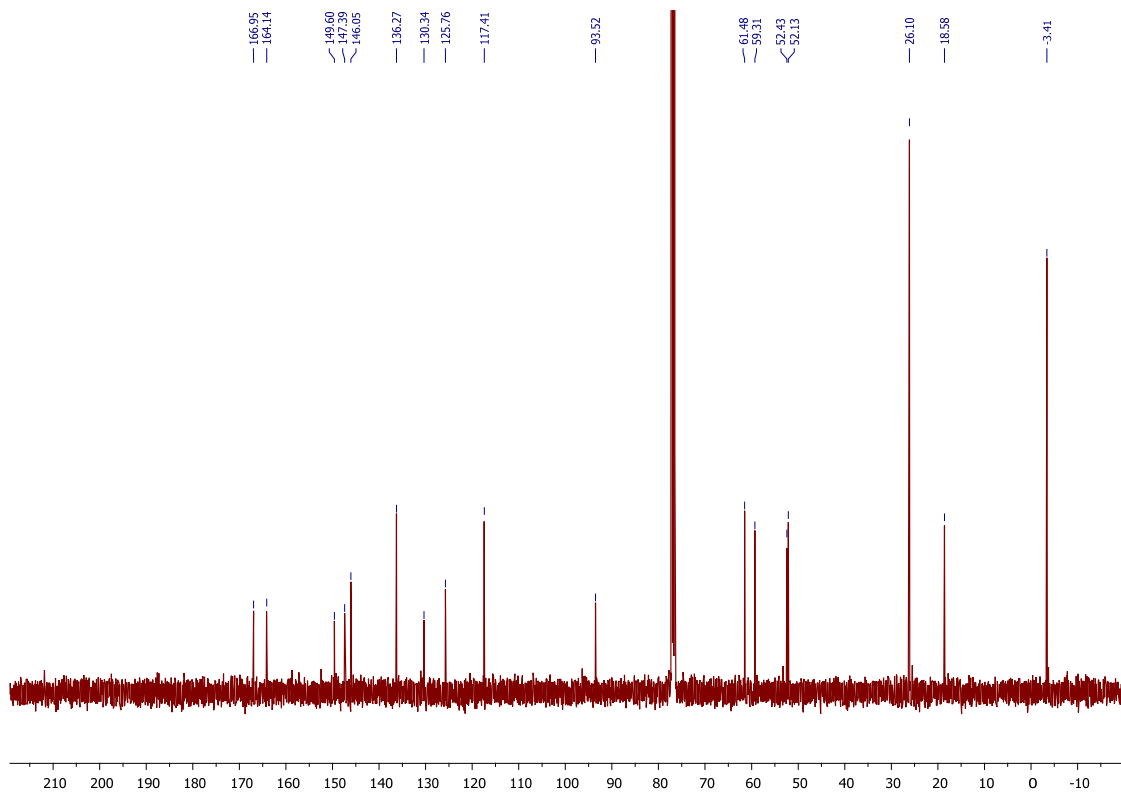
¹³C NMR Spectrum (Compound 302)



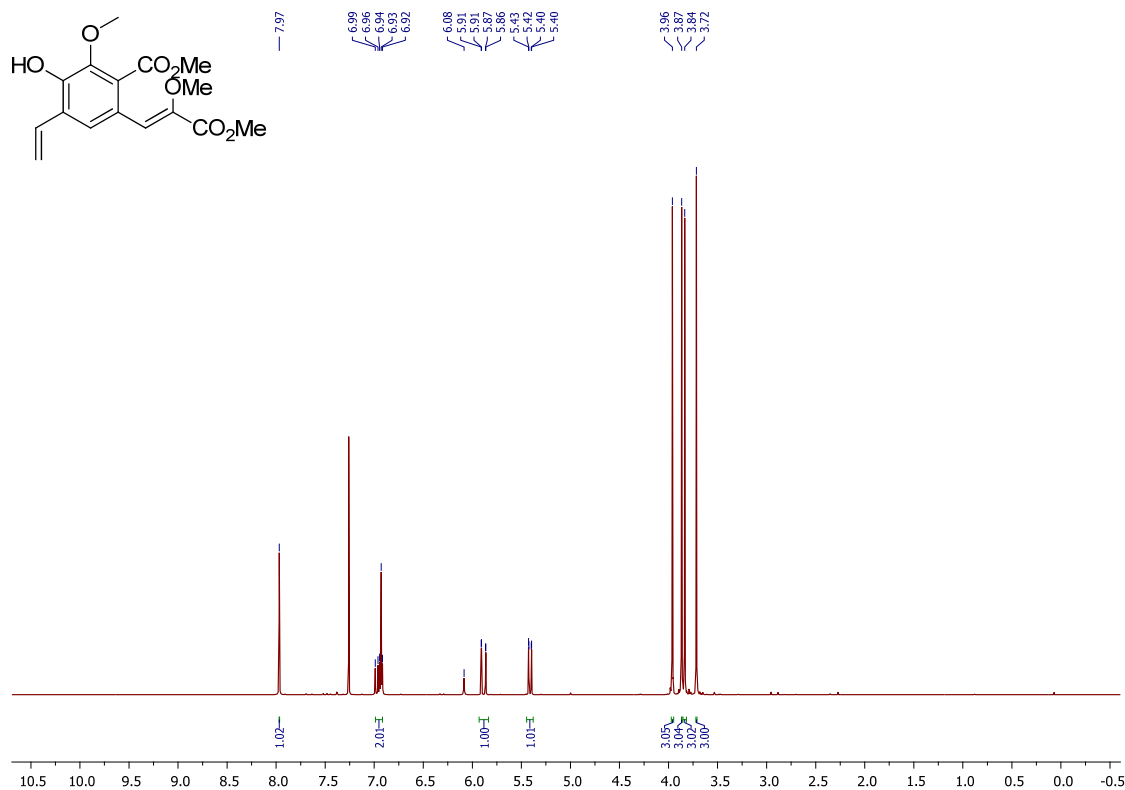
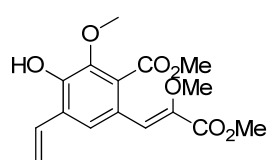
¹H NMR Spectrum (Compound 303)



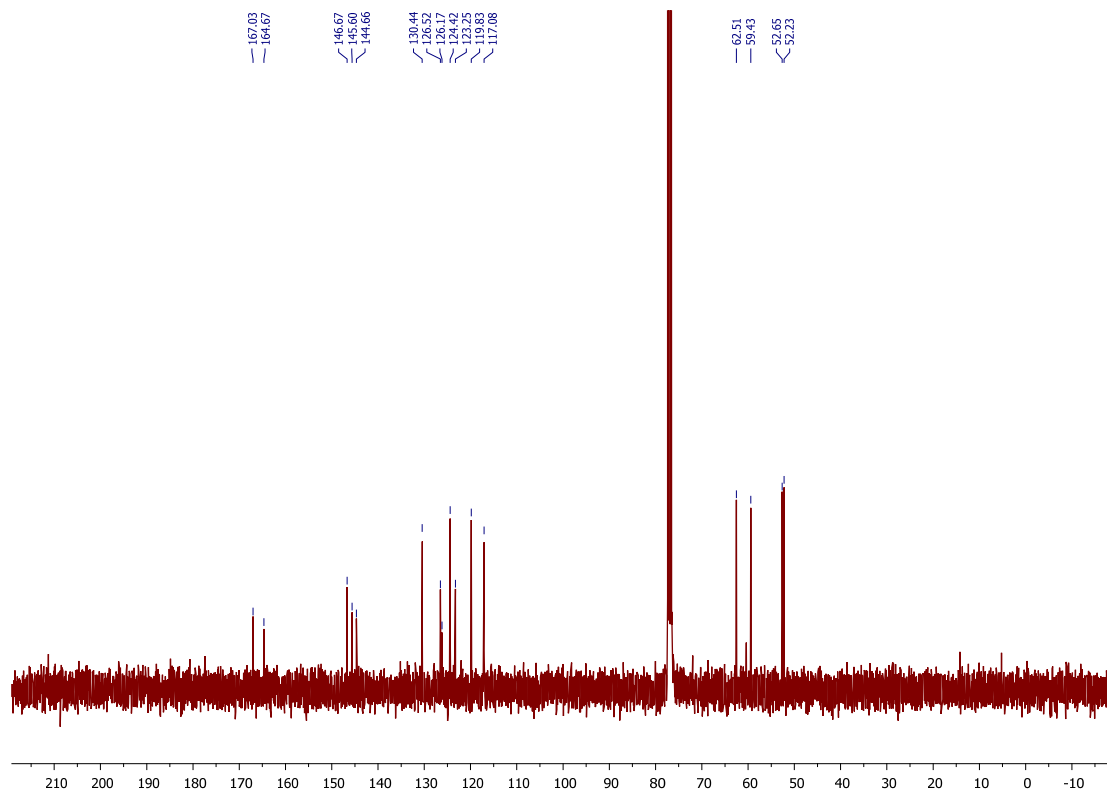
¹³C NMR Spectrum (Compound 303)



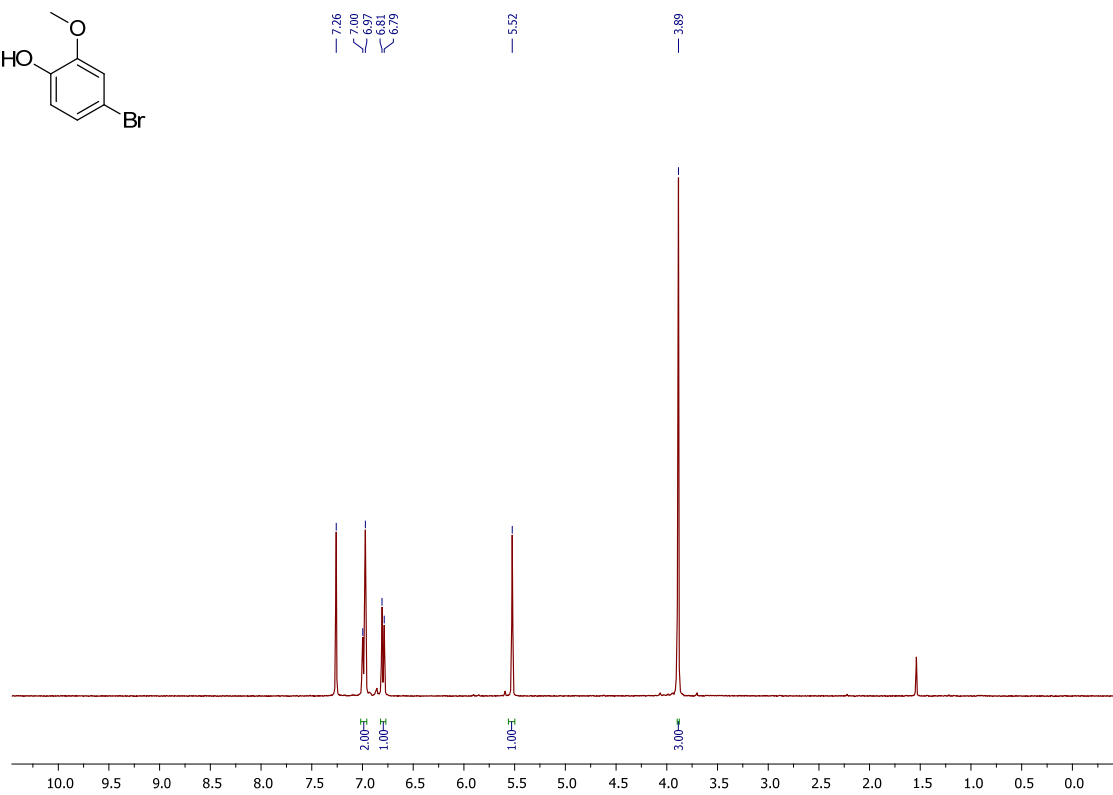
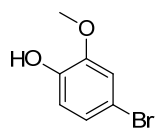
¹H NMR Spectrum (Compound 304)



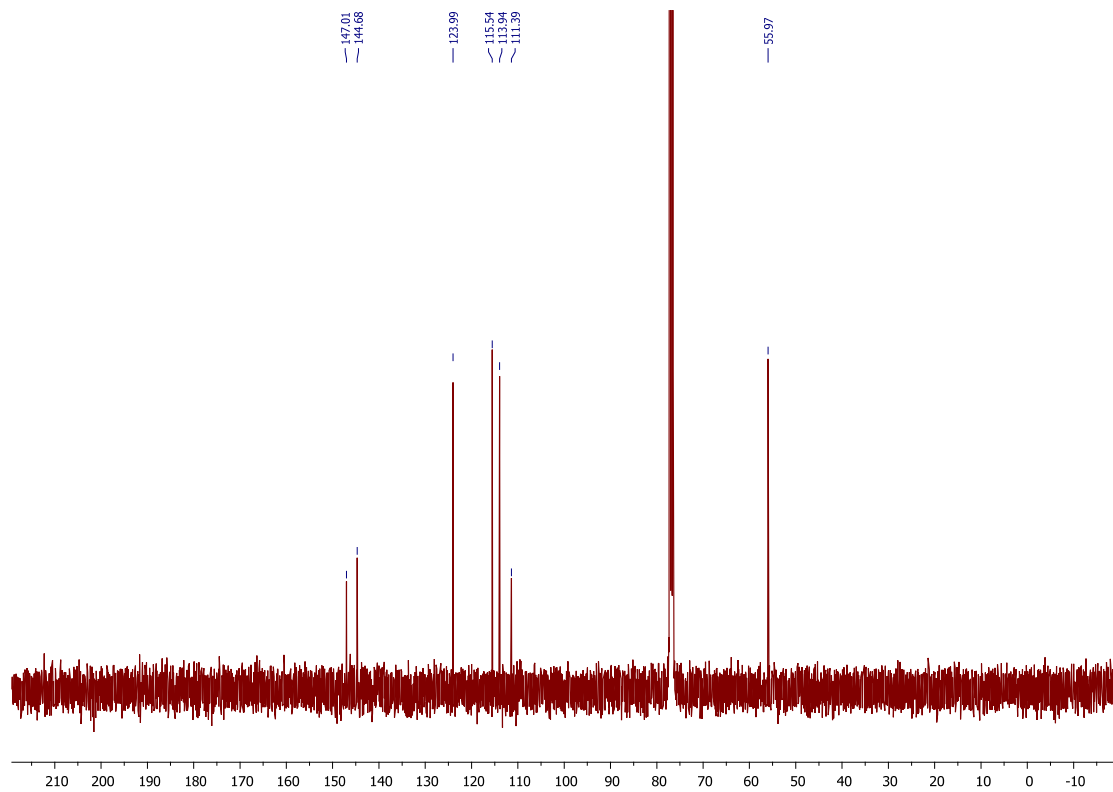
¹³C NMR Spectrum (Compound 304)



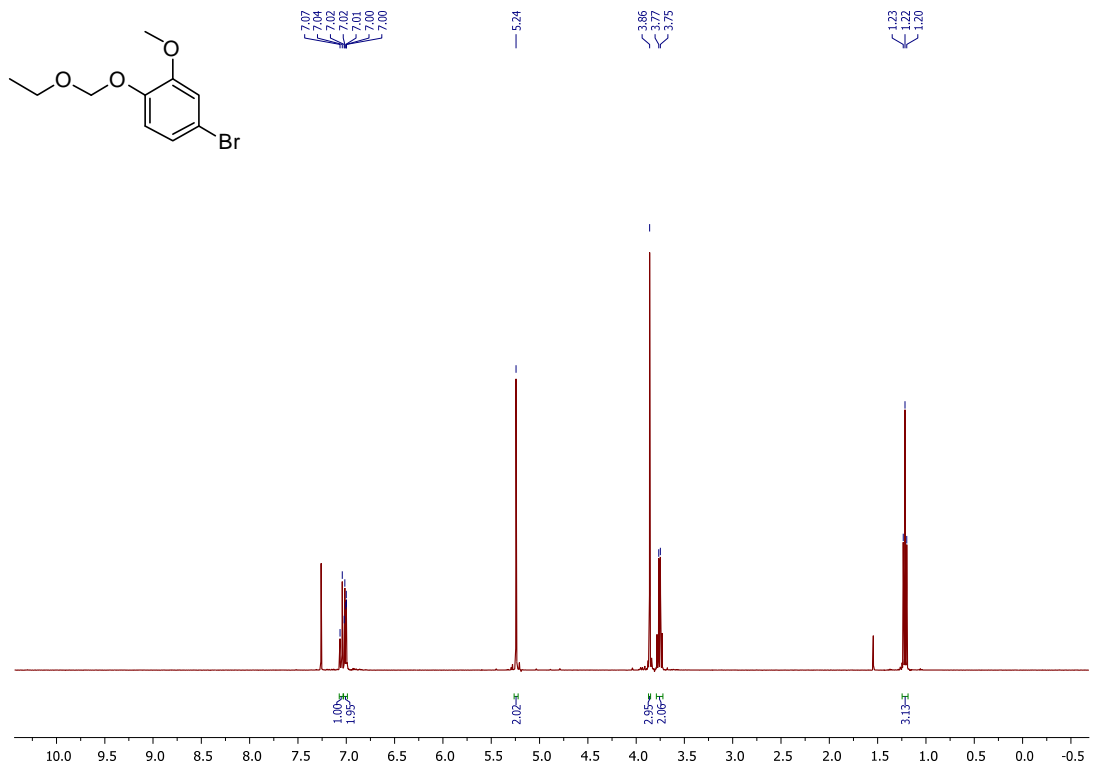
¹H NMR Spectrum (Compound 306a)



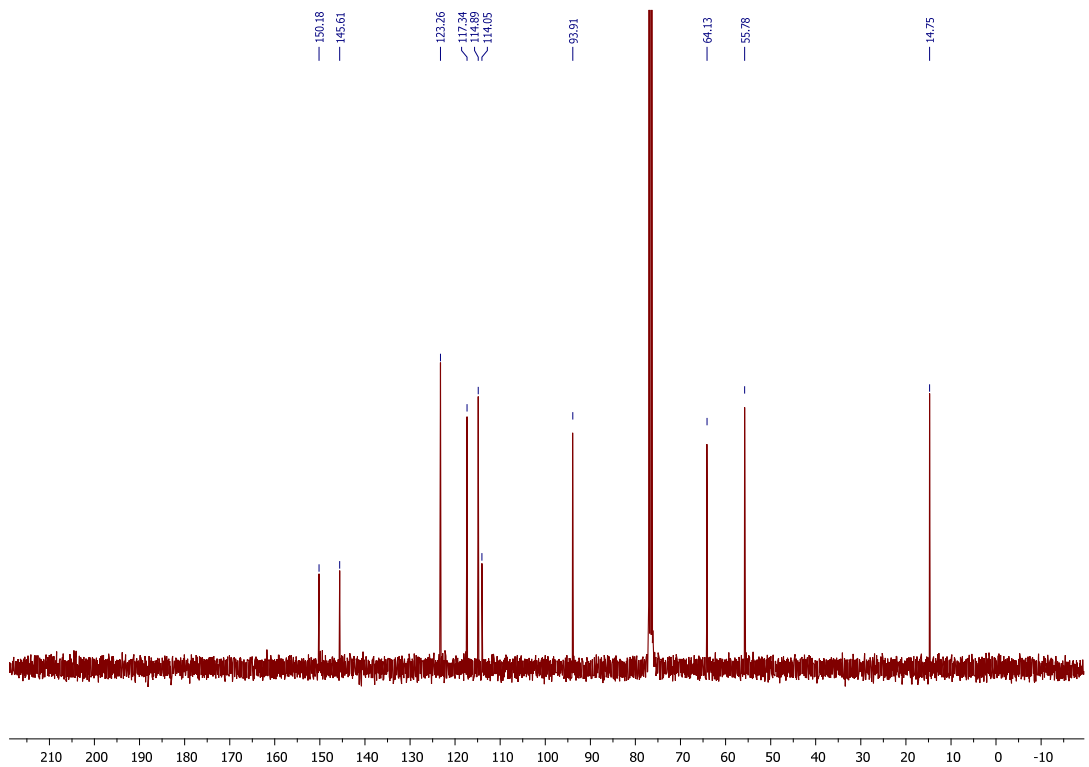
¹³C NMR Spectrum (Compound 306a)



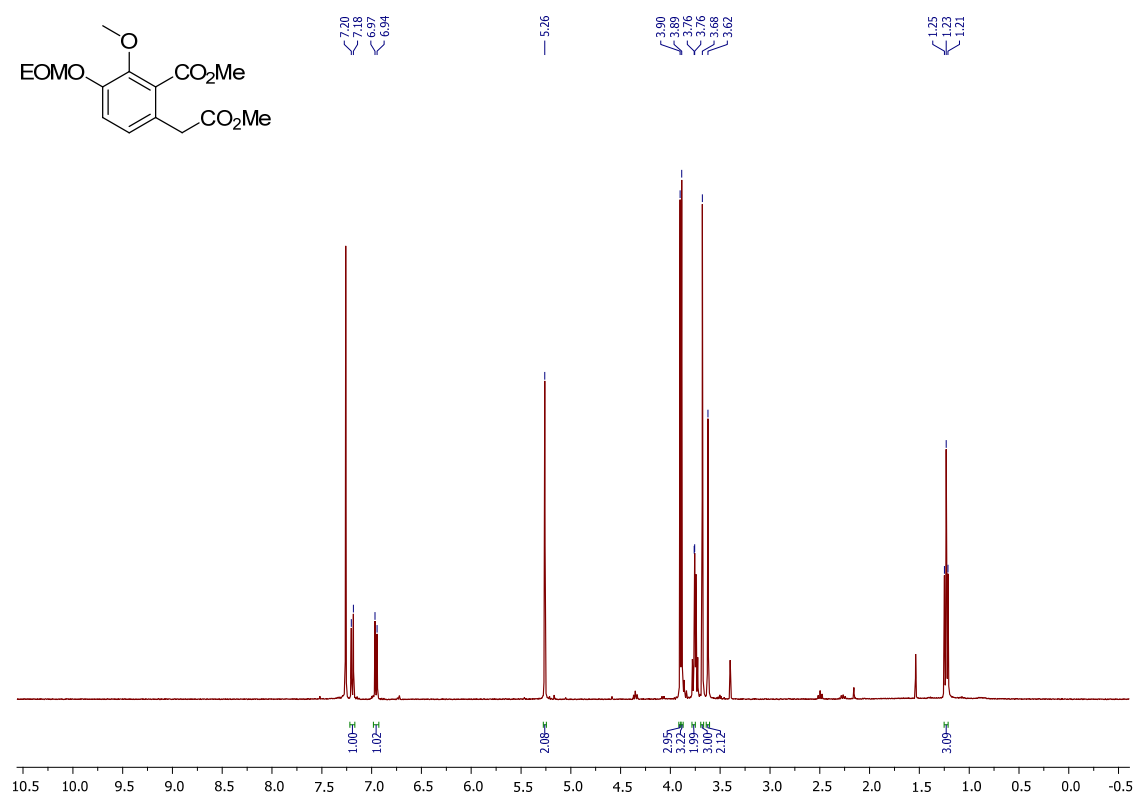
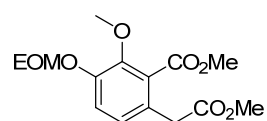
¹H NMR Spectrum (Compound 307)



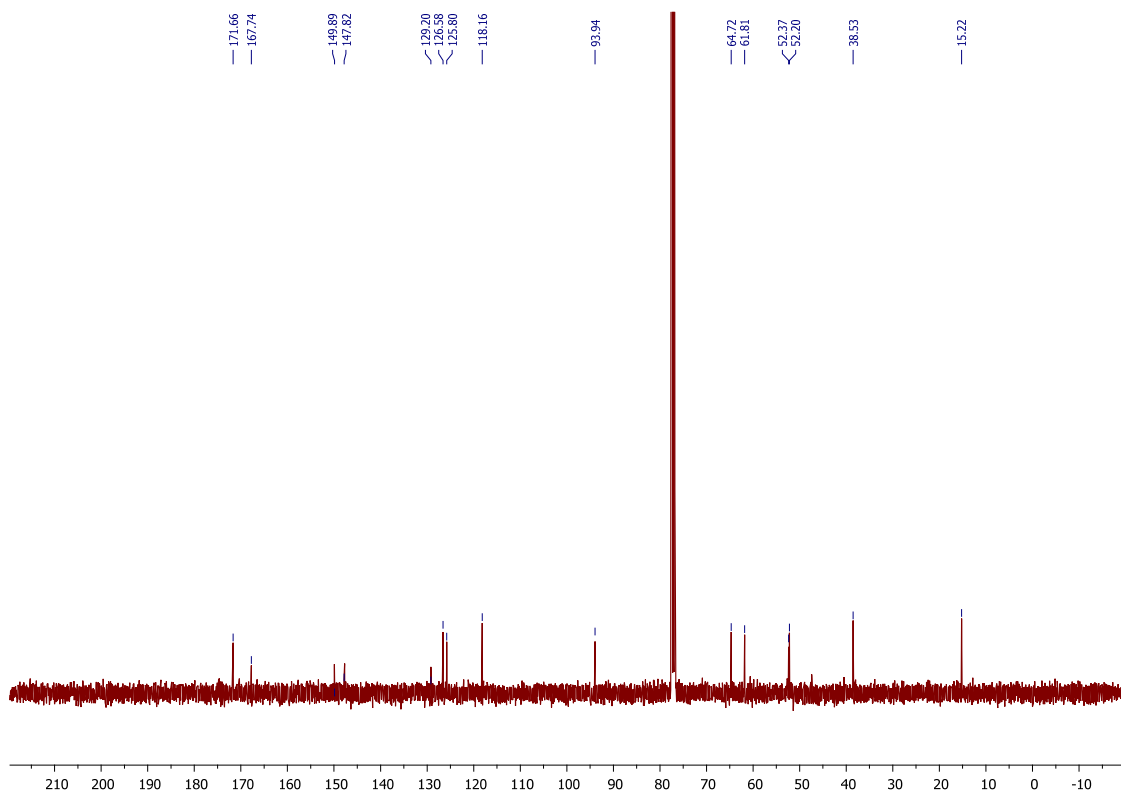
¹³C NMR Spectrum (Compound 307)



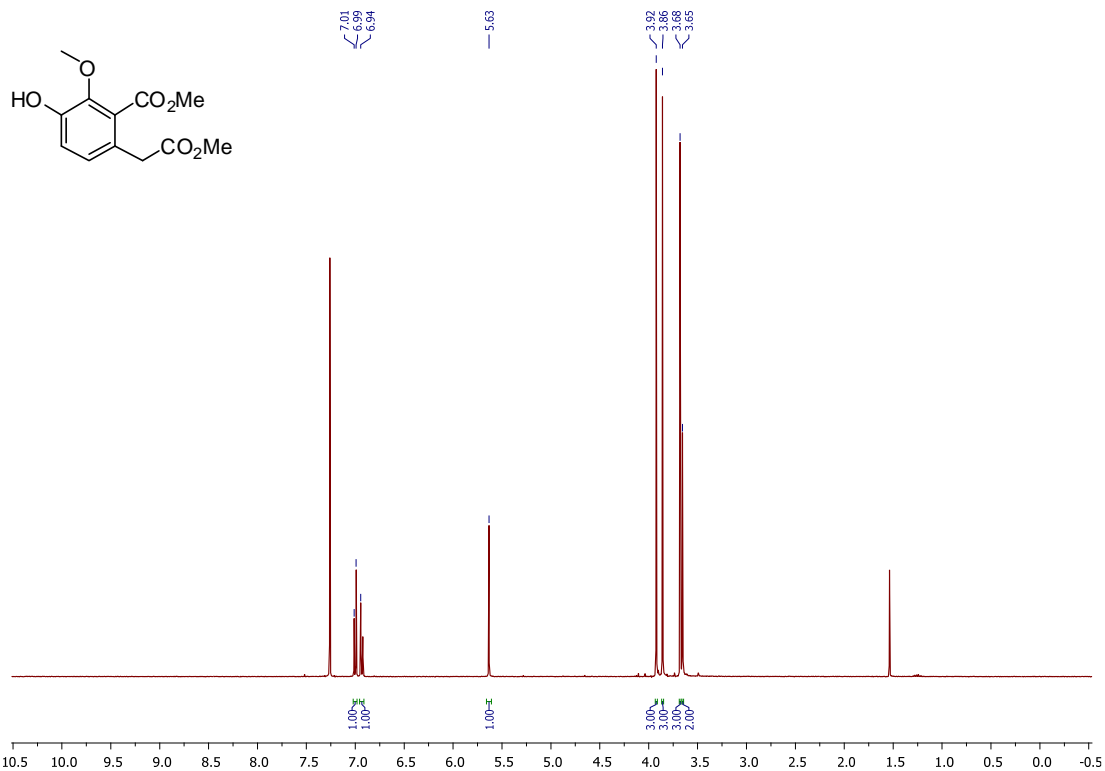
¹H NMR Spectrum (Compound 308)



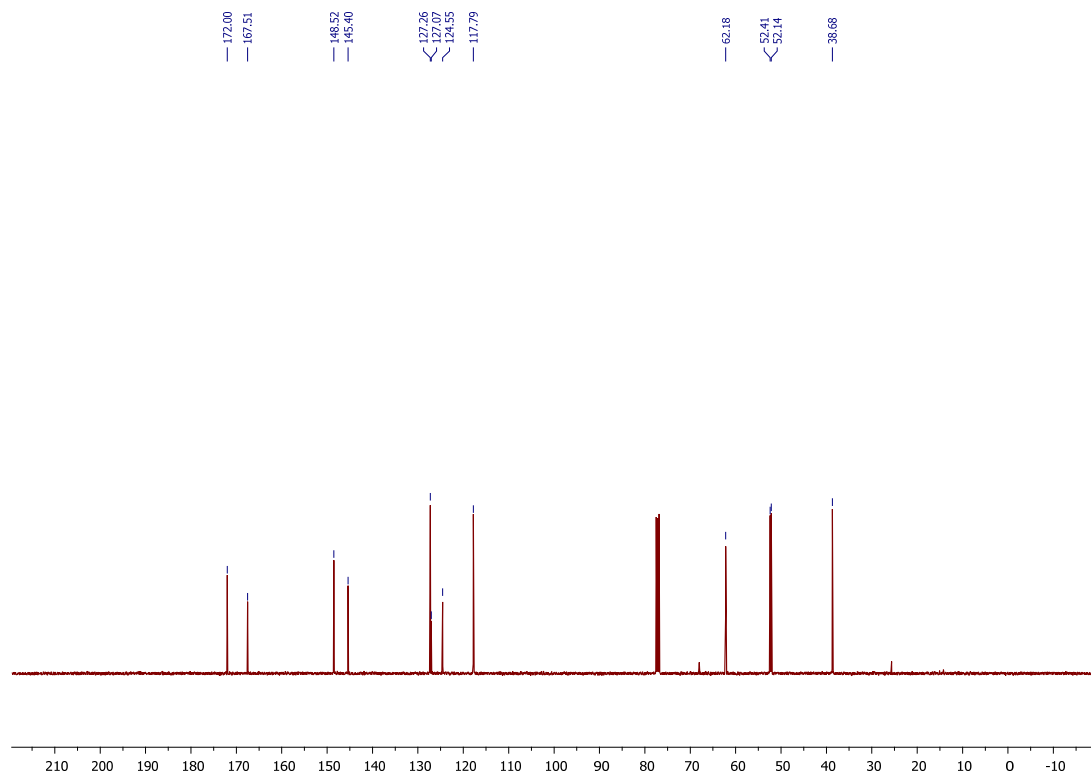
¹³C NMR Spectrum (Compound 308)



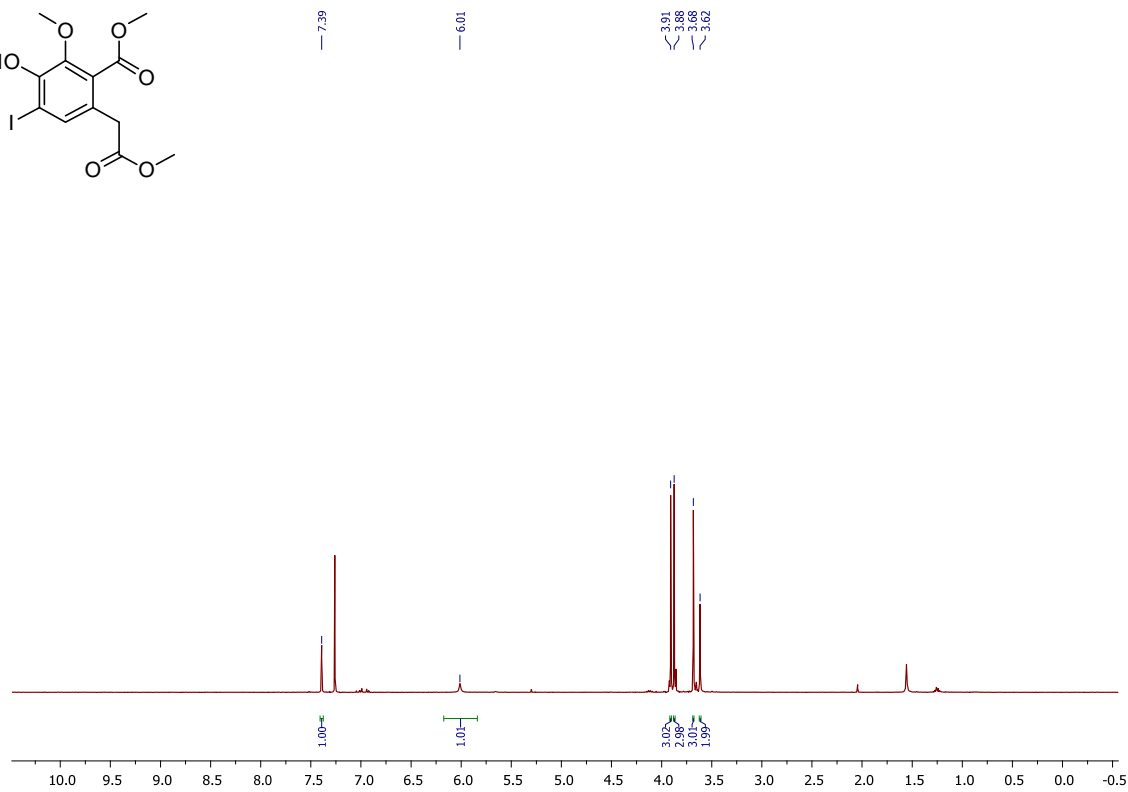
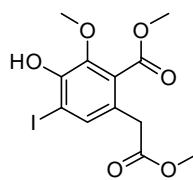
¹H NMR Spectrum (Compound 308a)



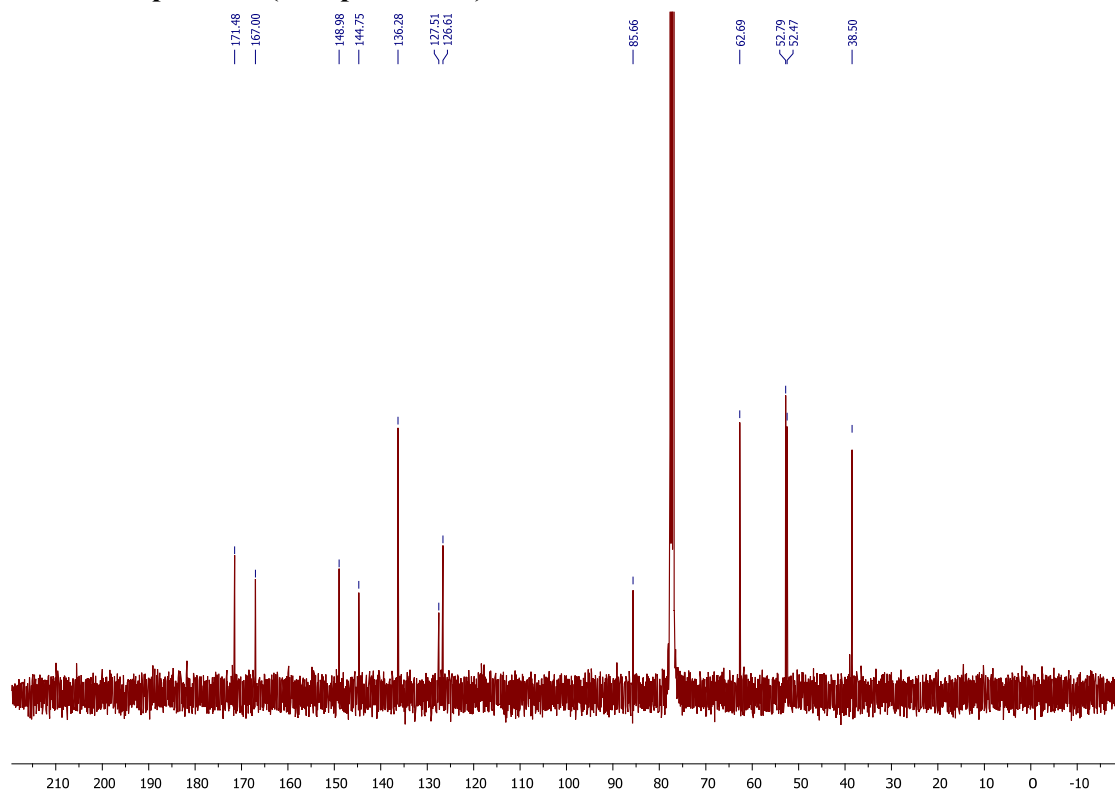
¹³C NMR Spectrum (Compound 308a)



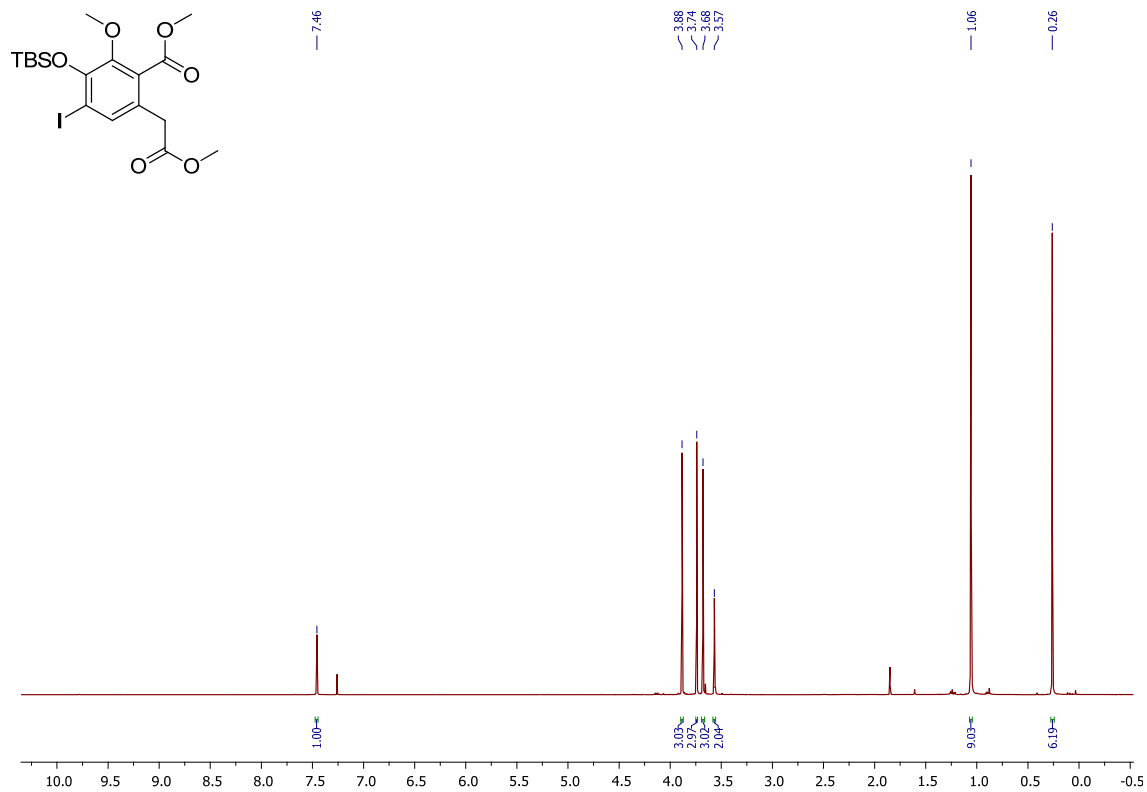
¹H NMR Spectrum (Compound 309)



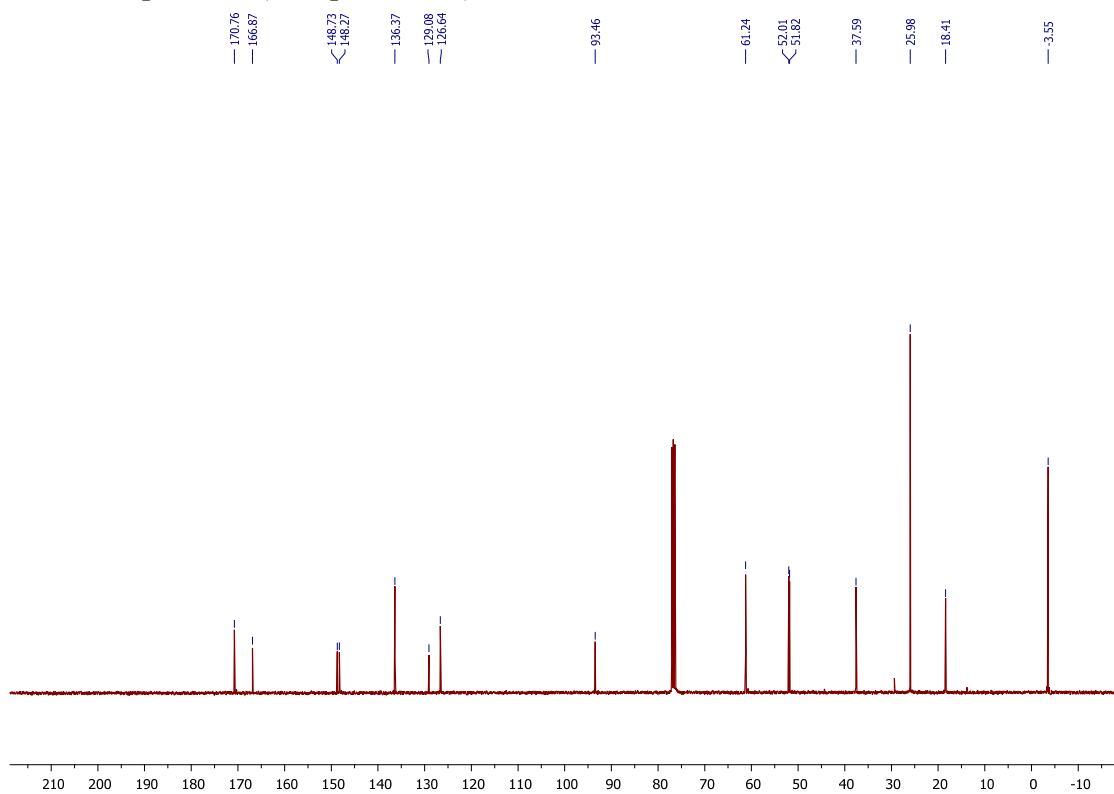
¹³C NMR Spectrum (Compound 309)



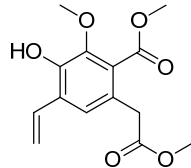
¹H NMR Spectrum (Compound 311)



¹³C NMR Spectrum (Compound 311)

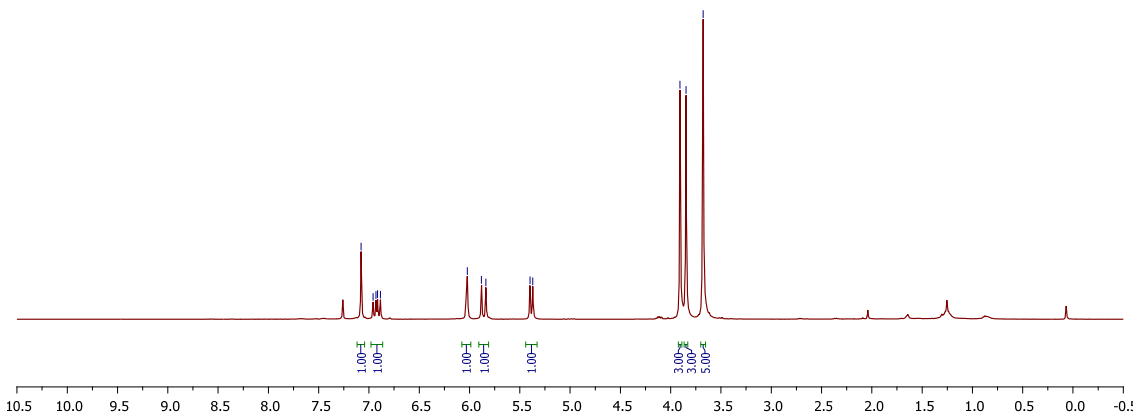


¹H NMR Spectrum (Compound 312)



7.08
6.96
6.91
6.89
6.02
5.88
5.84
5.40
5.37

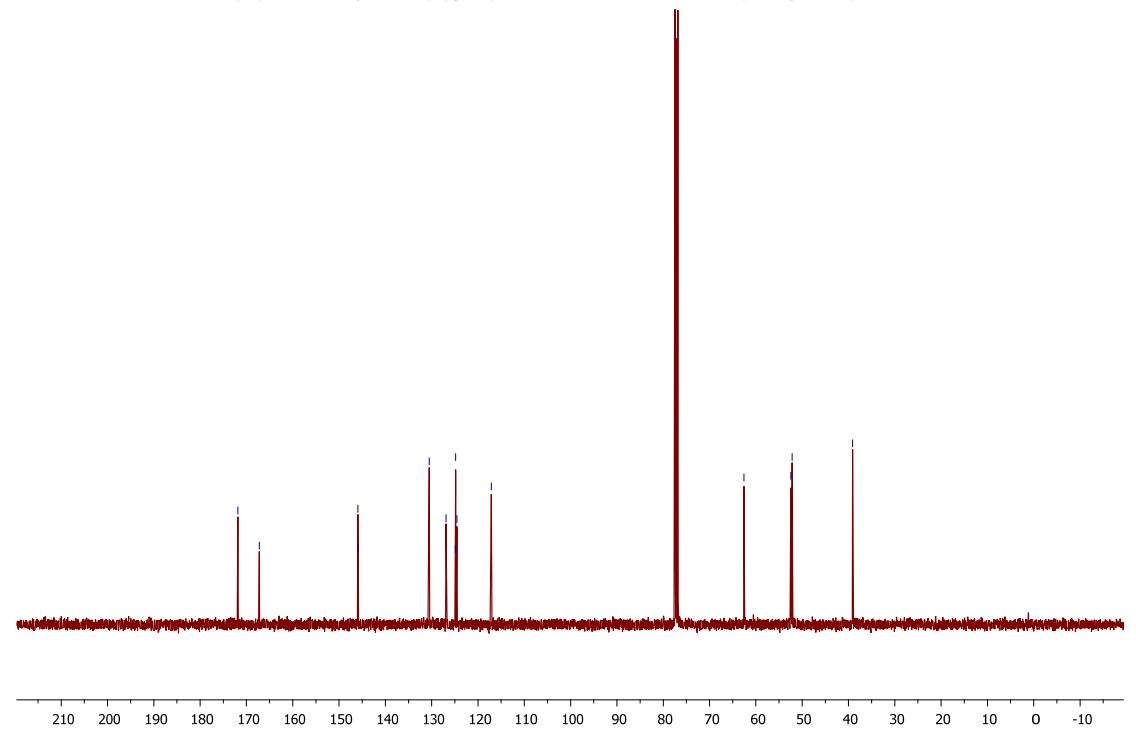
3.91
3.82
3.68



10.5 10.0 9.5 9.0 8.5 8.0 7.5 7.0 6.5 6.0 5.5 5.0 4.5 4.0 3.5 3.0 2.5 2.0 1.5 1.0 0.5 0.0 -0.5

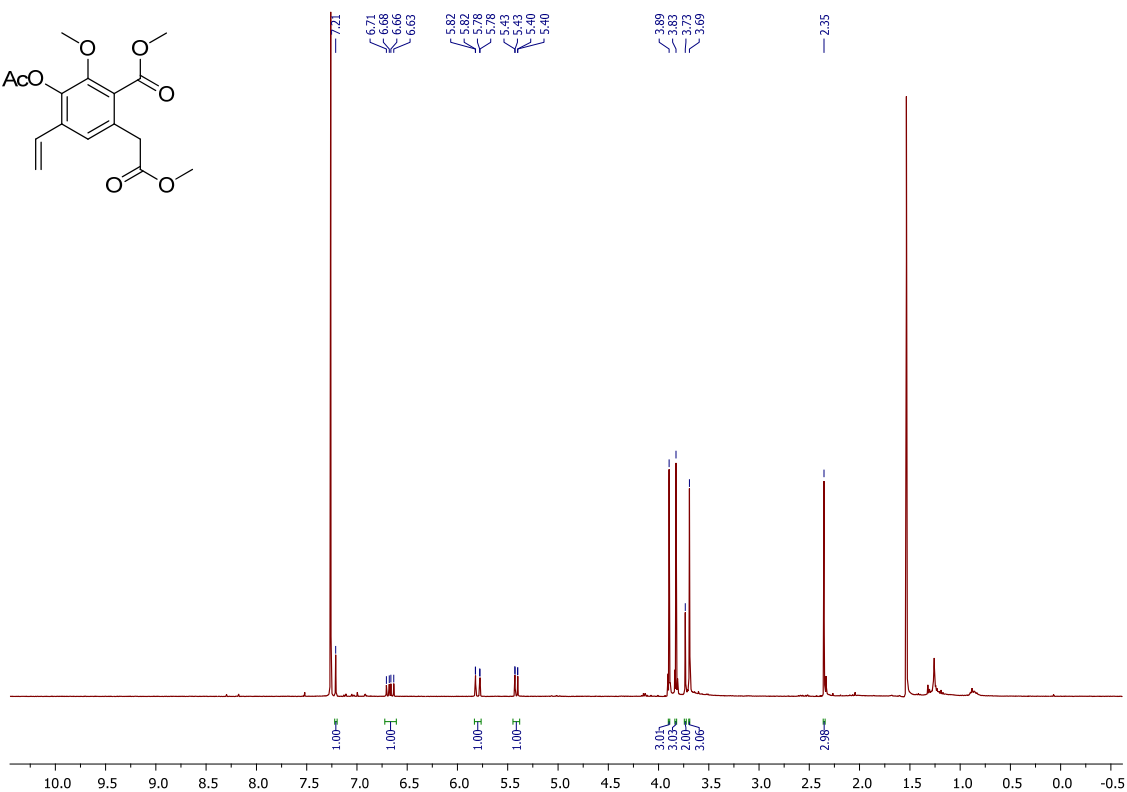
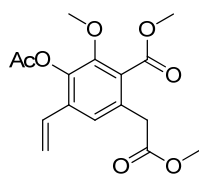
¹³C NMR Spectrum (Compound 312)

171.84
167.20
145.95
145.91
130.52
126.89
124.90
124.82
124.54
117.14
62.56
52.46
52.16
39.12

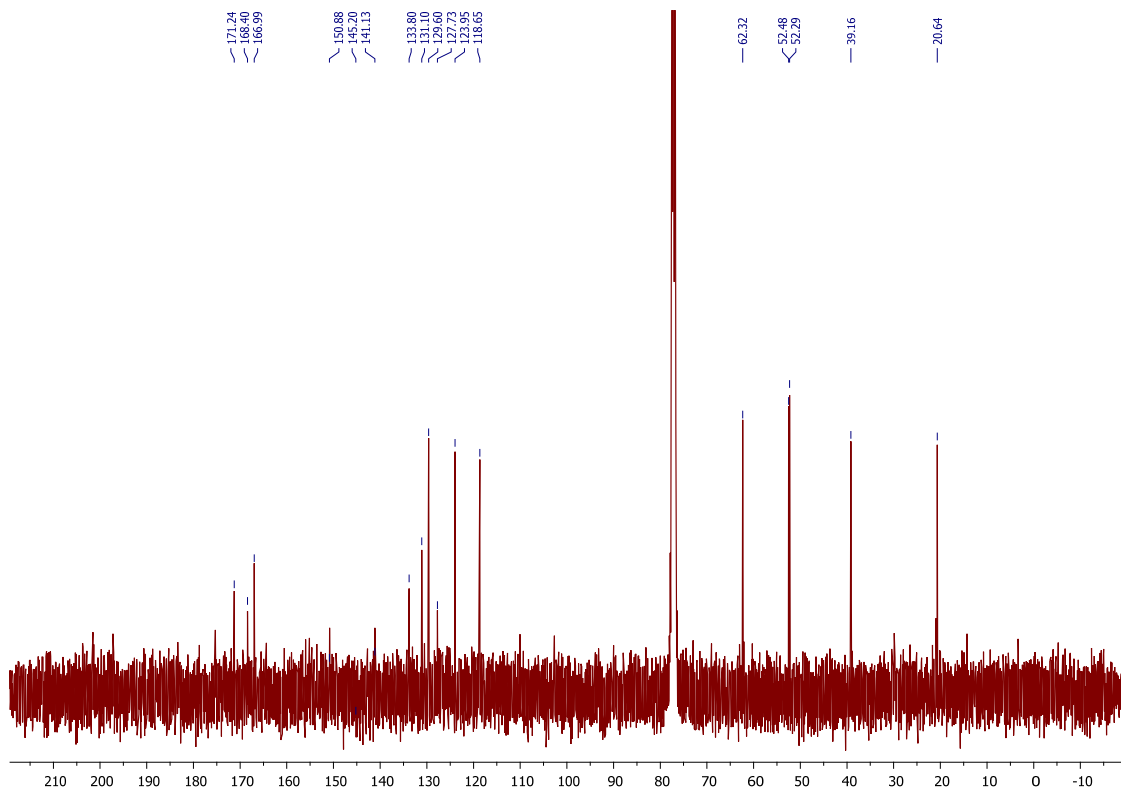


210 200 190 180 170 160 150 140 130 120 110 100 90 80 70 60 50 40 30 20 10 0 -10

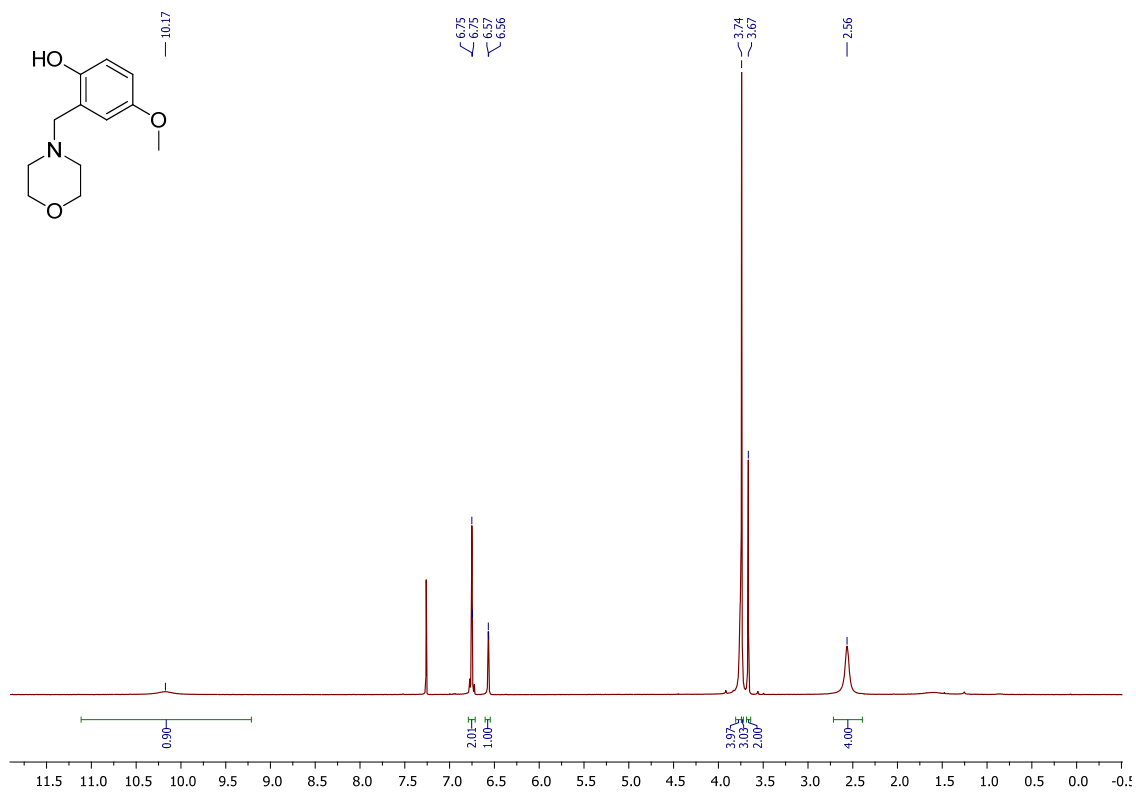
¹H NMR Spectrum (Compound 313)



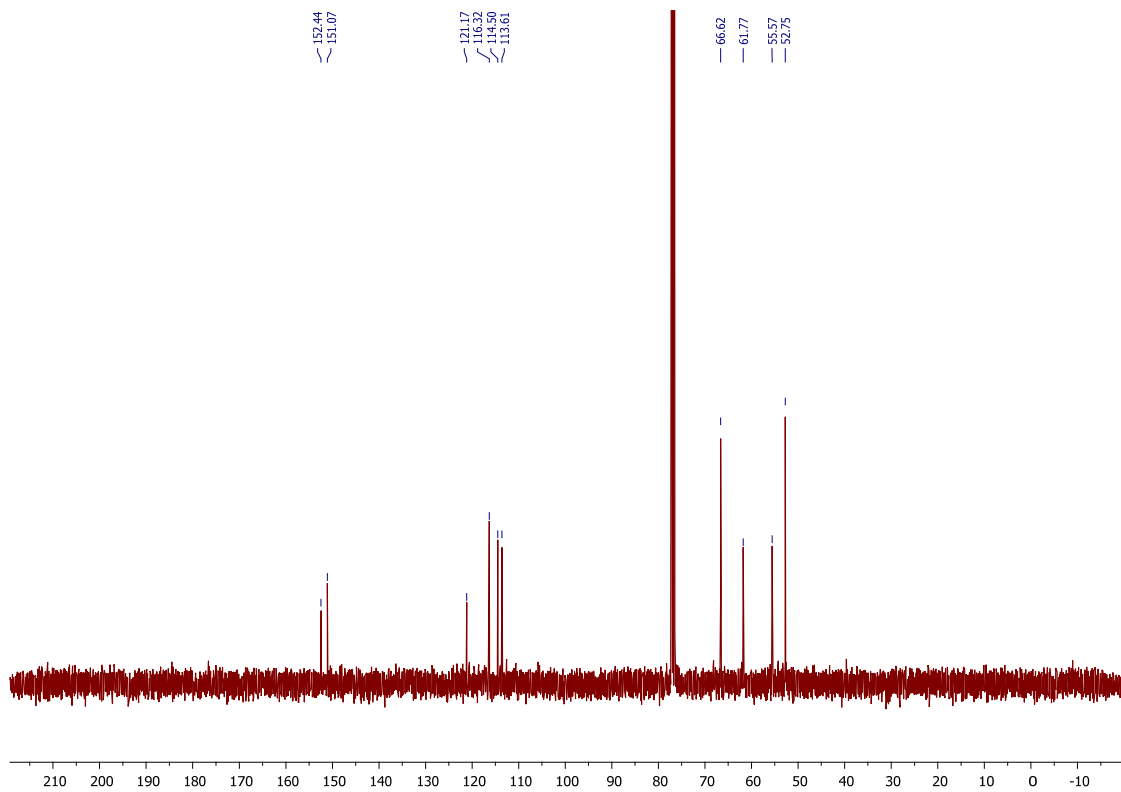
¹³C NMR Spectrum (Compound 313)



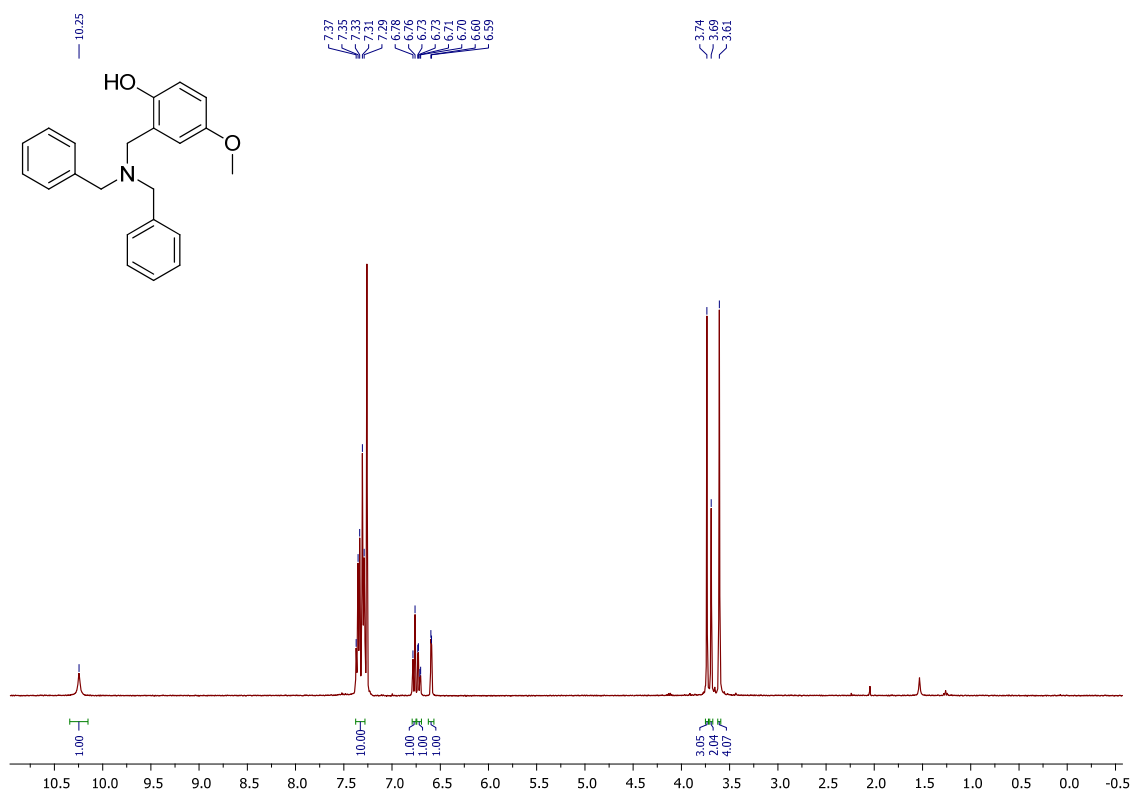
¹H NMR Spectrum (Compound 320)



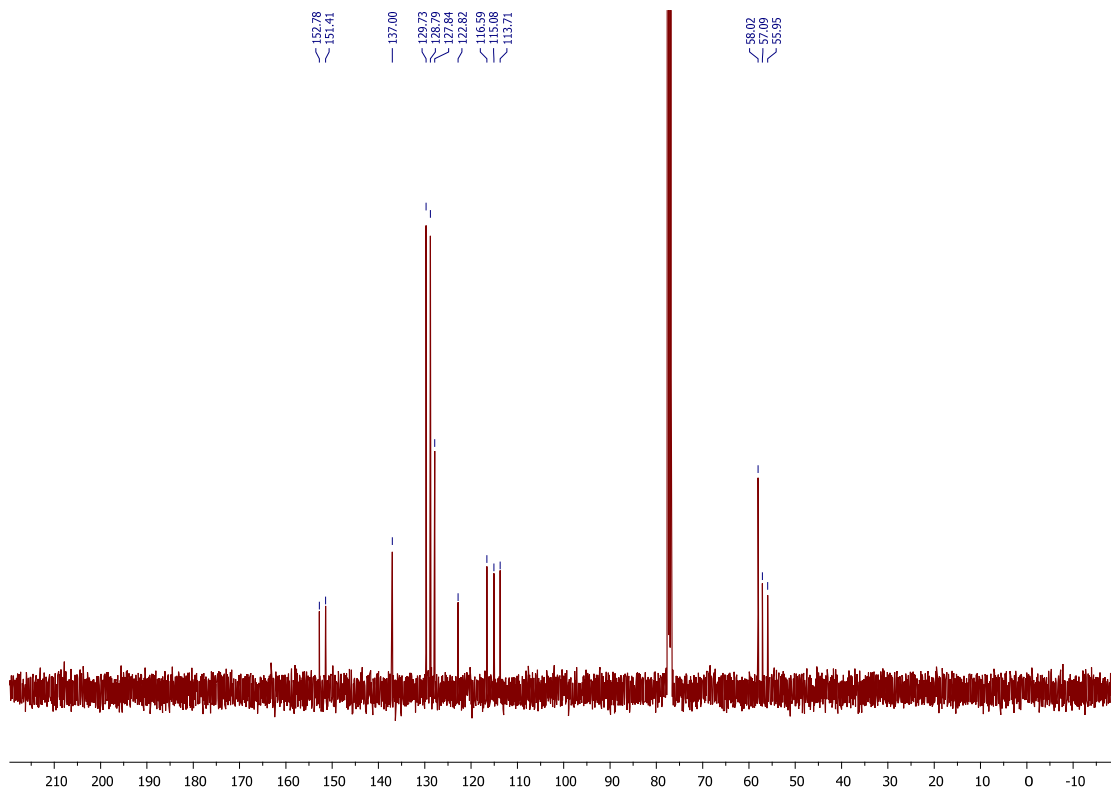
¹³C NMR Spectrum (Compound 320)



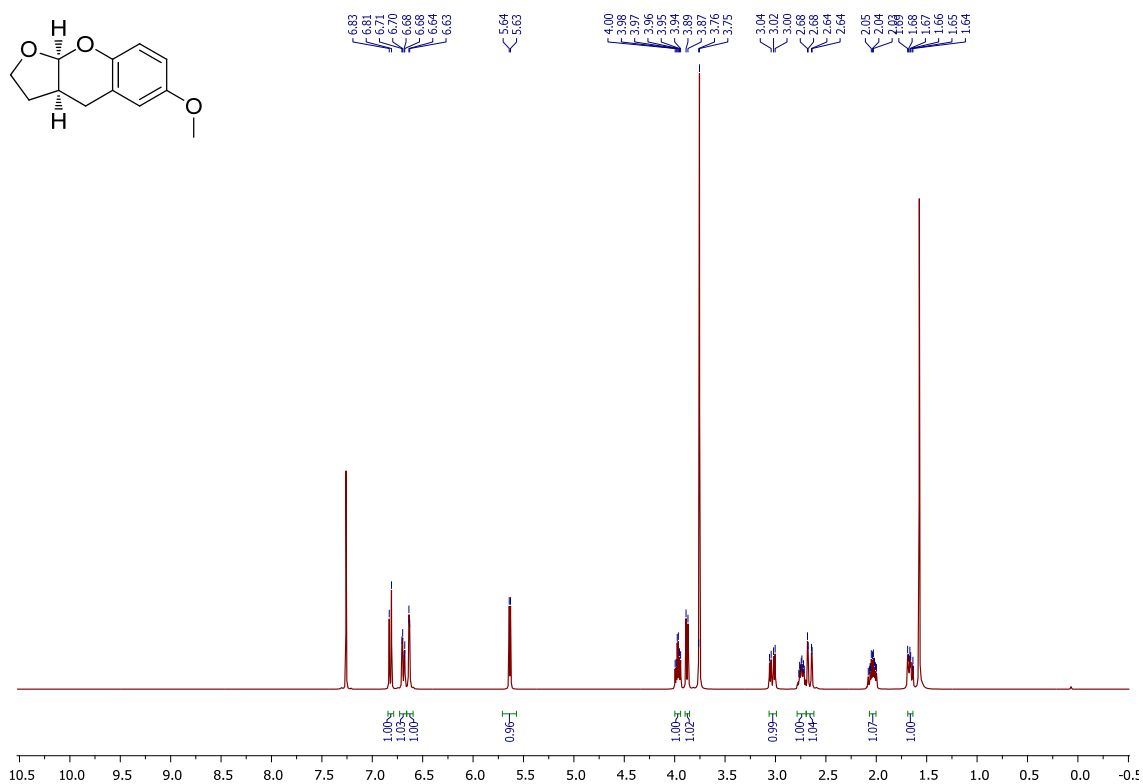
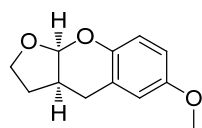
¹H NMR Spectrum (Compound 321)



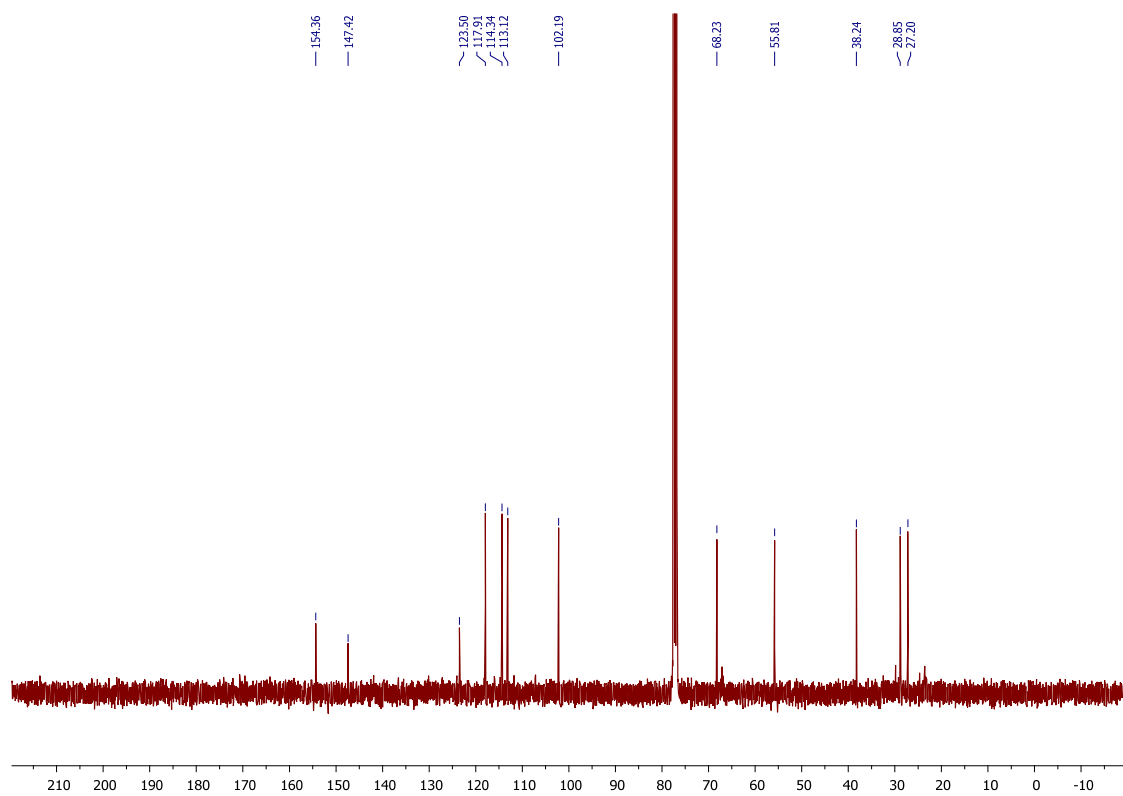
¹³C NMR Spectrum (Compound 321)



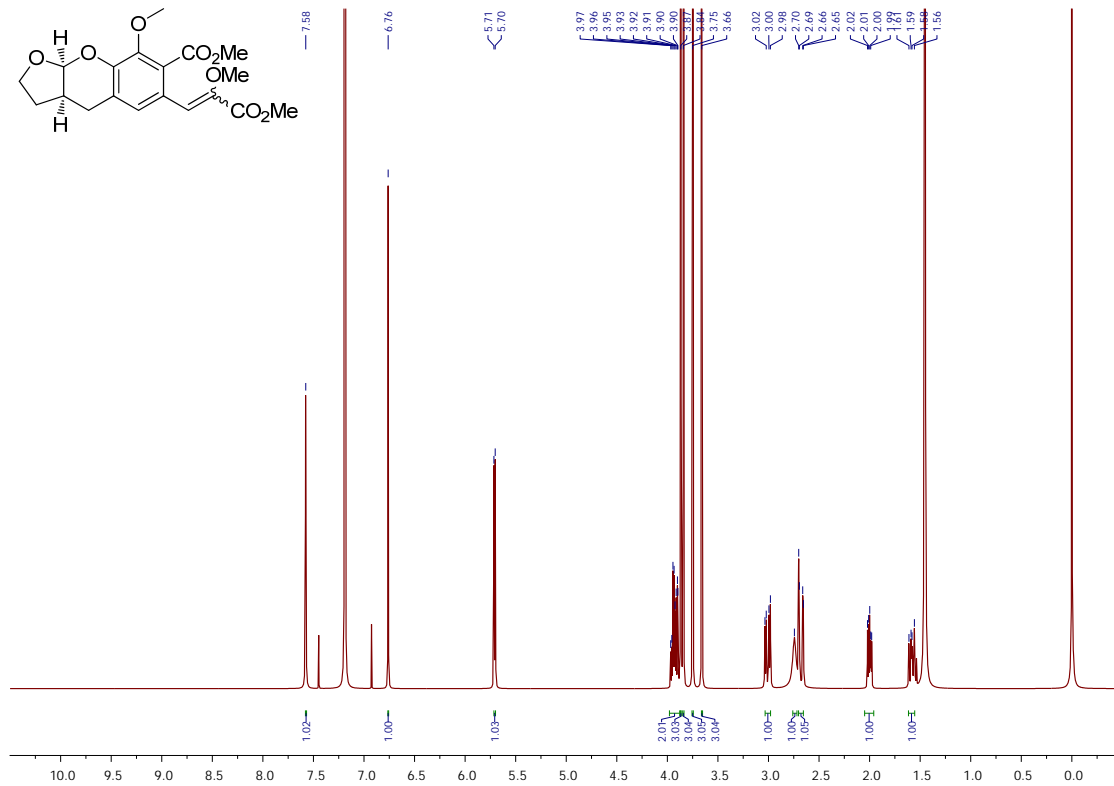
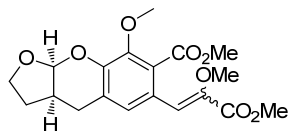
¹H NMR Spectrum (Compound 323)



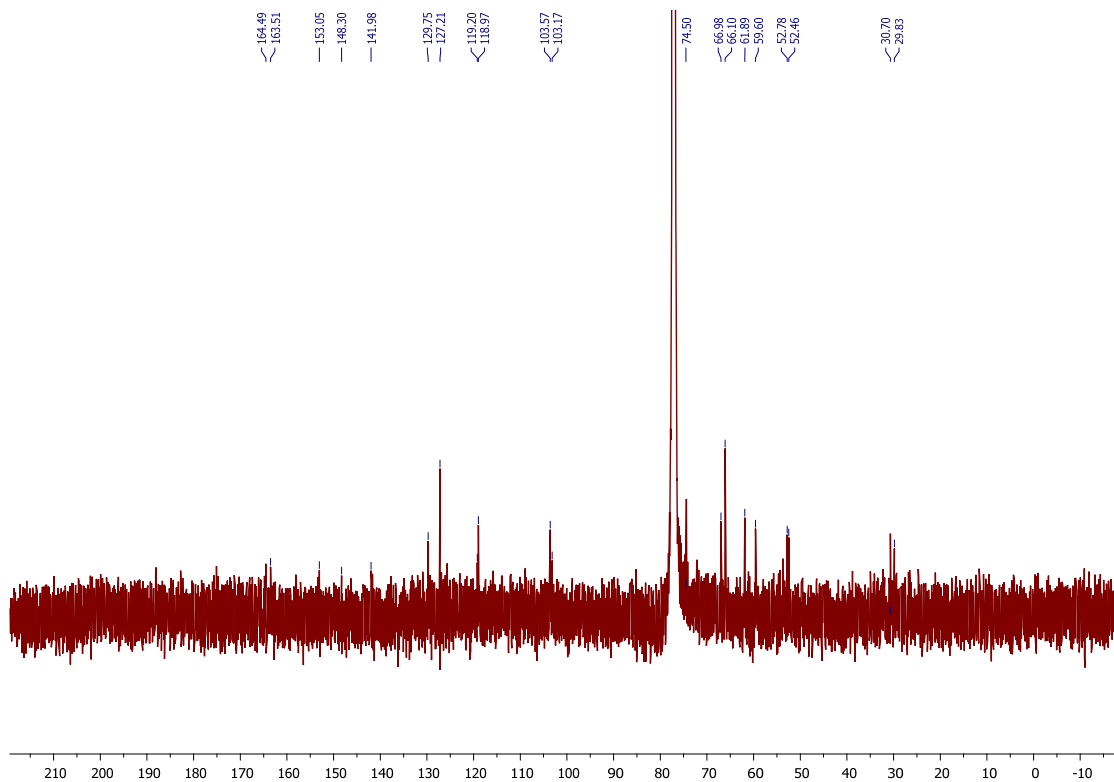
¹³C NMR Spectrum (Compound 323)



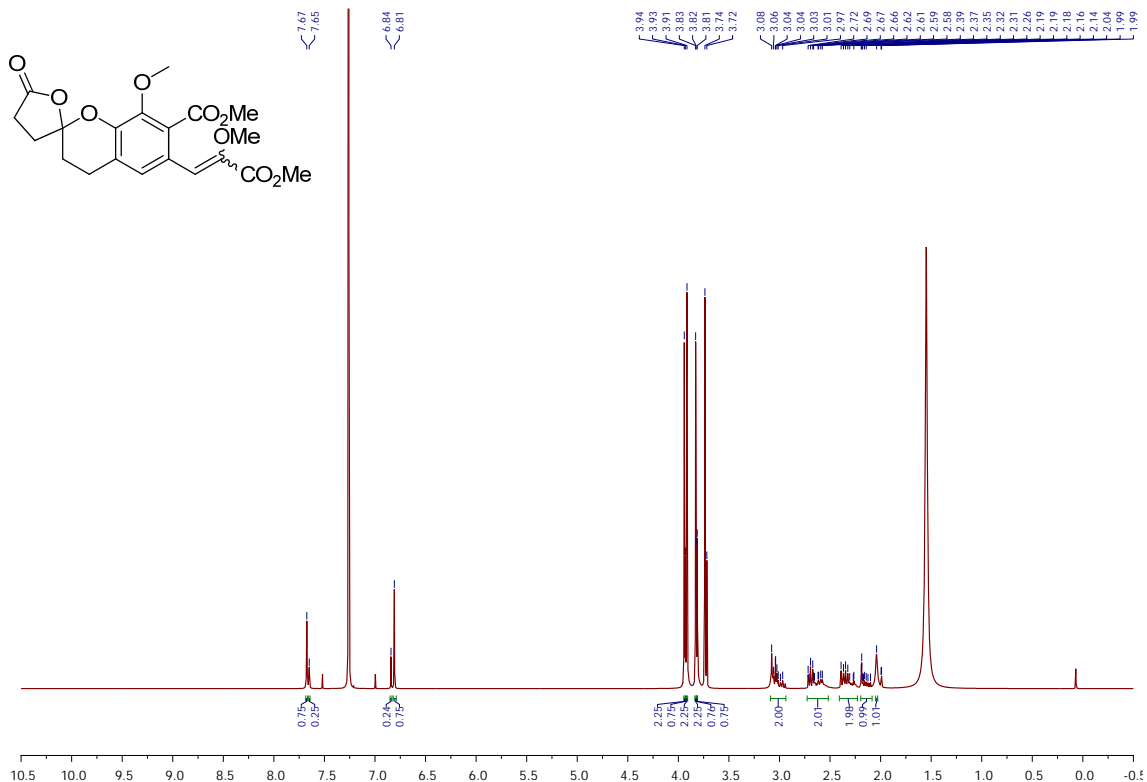
¹H NMR Spectrum (Compound 316)



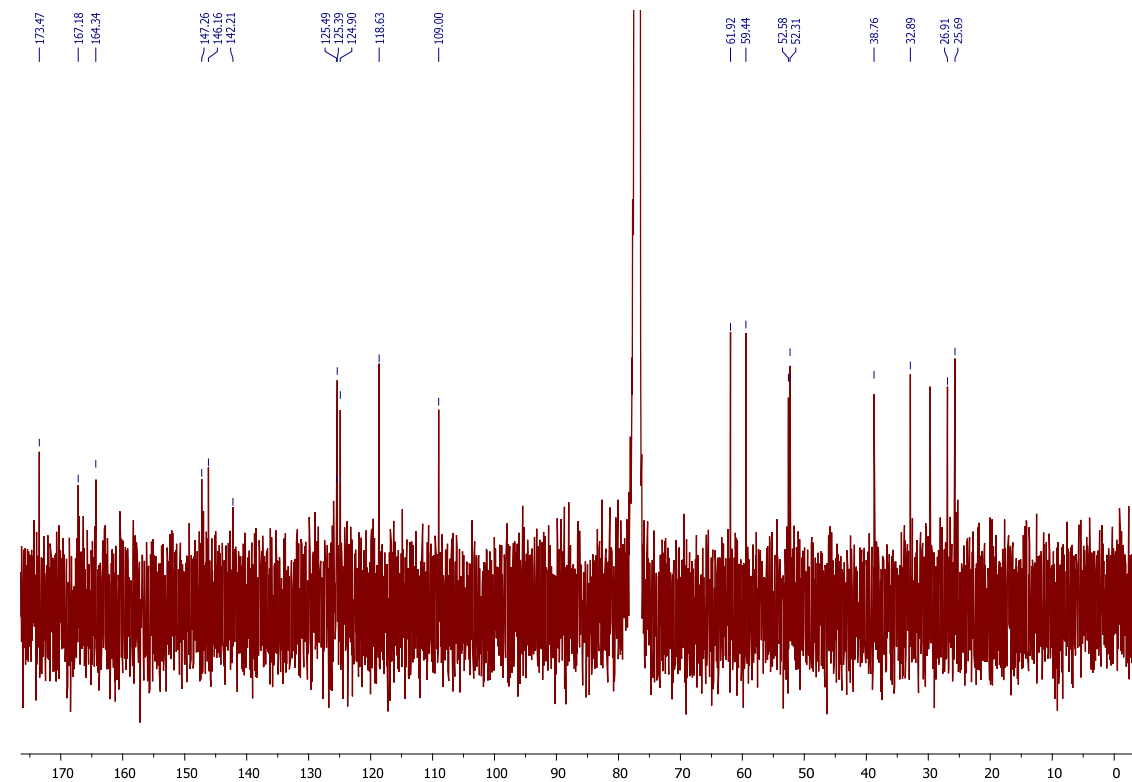
¹³C NMR Spectrum (Compound 316)



¹H NMR Spectrum (Compound 317)



¹³C NMR Spectrum (Compound 317)



References:

- 1 H. Brockmann and K. H. Renneberg, *Naturwissenschaften.*, 1953, **40**, 59–60.
- 2 H. Brockmann and K. H. Renneberg, *Naturwissenschaften.*, 1953, **40**, 166–167.
- 3 H. Brockmann, W. Lenk, G. Schwantje and A. Zeeck, *Tetrahedron Lett.*, 1966, **7**, 3525–3530.
- 4 C. Puder, S. Loya, A. Hizi and A. Zeeck, *Eur. J. Org. Chem.*, 2000, **5**, 729–735.
- 5 C. Coronelli, H. Pagani, M. R. Bardone and G. C. Lancini, *J. Antibiot.*, 1974, **27**, 161–168.
- 6 C. Coronelli, L. F. Zerilli, M. R. Bardone and E. Martinelli, *Tetrahedron.*, 1974, **30**, 2747–2754.
- 7 D. Tresselt, K. Eckardt and W. Ihn, *Tetrahedron.*, 1978, **34**, 2693–2699.
- 8 K. Eckardt, D. Tresselt and W. Ihn, *J. Antibiot.*, 1978, **31**, 970–973.
- 9 R. M. Stroshane, J. A. Chan, E. A. Rubalcaba, A. L. Garretson, A. A. Aszalos and P. P. Roller, *J. Antibiot.*, 1979, **32**, 197–204.
- 10 M. Chino, K. Nishikawa, M. Umekita, C. Hayashi, T. Yamazaki, T. Tsuchida, T. Sawa, M. Hamada and T. Takeuchi, *J. Antibiot.*, 1996, **49**, 752–757.
- 11 (a) Ref. 1; (b) Ref. 2; (c) The rubromycins exhibit activity against the reverse transcriptase of human immunodeficiency virus-1, M. E. Goldman, G. S. Salituro, J. A. Bowen, J. M. Williamson, L. Zink, W. A. Schleif and E. A. Emini, *Mol. Pharmacol.*, 1990, **38**, 20-25; (d) Purpuromycin is a potential topical agent for vaginal infections, A. Trani, C. Dallanoce, G. Panzone, R. Cdanhattista, F. Ripamonti, B. P. Goldstein and R. J. Ciabatti, *J. Med. Chem.*, 1997, **40**, 96-97; Heliquinomycin is an inhibitor of DNA helicase, (e) Ref.10,

-
- (f) M.Mhino, I. C. Nishikawa, T. Tsuchida, R. Sawa, H. Nakamura, K. T. Nakamura, Y. Muraoka, D. Ikeda, H. Naganawa, T. Sawa and T. Takeuchi, *J. Antibiot.*, 1997, **50**, 143-146.
- 12** T. Ueno, H. Takahashi, M. Oda, M. Mizunuma, A. Yokoyama, Y. Goto, Y. Mizushima, K. Sakaguchi and H. Hayashi, *Biochemistry.*, 2000, **39**, 5995-6002.
- 13** For an overview of the biological importance of benzannulated spiroketals see G. Liu, J. M. Wurst and D. S. Tan, *Org. Lett.*, 2009, **11**, 16, 3670–3673.
- 14** Image adapted and used under licence from <http://www.sciencephoto.com>.
- 15** J. D. Pata, W. G. Stirtan, S. W. Goldstein and T. A. Steitz, *Proc. Nat. Acad. Sci.*, 2004, **101**, 10548-10553.
- 16** (a) S. B. Cohen, M. E. Graham, G. O. Lovrecz, N. Bache, P. J. Robinson and R. R. Reddel, *Science*, 2007, **315**, 1850-1853; (b) A. J. Gillis, A. P. Schuller and E. Skordalakes, *Nature*, 2008, **455**, 633-638.
- 17** For a recent review of marketed HIV-RT inhibitors see F. Esposito, A. Corona and E. Tramonato, *Molecular Biology International*, 2012, Article ID 586401.
- 18** C. W. Greider and E. H. Blackburn, *Cell.*, 1987, **51**, 887-98.
- 19** T. L. Orr-Weaver, J. W. Szostak and R. J. Rothstein, *Proc. Nat. Acad. Sci.*, 1981, **78**, 6354-8.
- 20** J. W. Szostak and E. H. Blackburn, *Cell.*, 1982, **29**, 245-55.
- 21** J. Shampay, J. W. Szostak and E. H. Blackburn, *Nature.*, 1984, **310**, 154-7.
- 22** C. W. Greider and E. H. Blackburn, *Cell.*, 1985, **43**, 405-13.
- 23** L. Hayflick and P. S. Moorhead, *Exp. Cell. Res.*, 1961, **25**, 585-621.

-
- 24 N. W. Kim, M. A. Piatyszek, K. R. Prowse, C. B. Harley, M. D. West, P. L. Ho, G. M. Coviello, W. E. Wright, S. L. Weinrich and J. W. Shay, *Science*, 1994, **266**, 2011-2015.
- 25 S. A. Stewart and R. A. Weinberg, *Annu. Rev. Cell. Dev. Biol.*, 2006, **22**, 531-557.
- 26 For further information regarding TRAP see, M. A. Piatyszek, N. W. Kim, S. L. Weinrich, K. Hiyama, E. Hiyama, W. E. Wright and J. W. Shay, *Methods Cell Sci.* 1995, **17**, 1-15.
- 27 S. C. P Williams, *Nature Medicine*, 2013, **19**, 6.
- 28 L. Kelland, *Clin. Cancer Res.*, 2007, **13**, 4960-4963.
- 29 E. P. M. T. Cohn, K. L. Wu, T. R. R. Pettus, and N. O. Reich, *J. Med. Chem.*, 2012, **55**, 3678-86.
- 30 C. Hertweck, *Angew. Chem. Int. Ed.*, 2009, **48**, 4688-4716
- 31 C. Puder, S. Loya, A. Hizi and A. Zeeck, *Eur. J. Org. Chem.*, 2000, **5**, 729-735.
- 32 M. Chino, K. Nishikawa, R. Sawa, M. Hamada, H. Naganawa, T. Sawa and T. Takeuchi, *J. Antibiot.*, 1997, **50**, 781-784.
- 33 A. Li and J. Piel, *Chem. Biol.*, 2002, **9**, 1017-1026.
- 34 Z. Yunt, K. Reinhardt, A. Li, M. Engeser, H. Dahse, M. Gütschow, T. Bruhn, G. Bringmann and J. Piel, *J. Am. Chem. Soc.*, 2009, **131**, 2297-2305.
- 35 M. Brasholz, S. Sörgel, C. Azap and H. Reißig, *Eur. J. Org. Chem.*, 2007, 3801-3814.
- 36 E. Clemmensen, *Chemische Berichte.*, 1913, **46** 1837.

-
- 37 T. Capecchi, C. B. de Koning and J. P. Michael, *Tetrahedron Lett.*, 1998, **39**, 5429–5432.
- 38 T. Capecchi, C. B. de Koning, and J. P. Michael, *J. Chem. Soc., Perkin Trans. I*, 2000, 2681–2688.
- 39 R. S. Varma, R. Dahiya and S. Kumar, *Tetrahedron Lett.*, 1997, **38**, 5131–5134.
- 40 K. Y. Tsang, M. A. Brimble and J. B. Bremner, *Org. Lett.*, 2003, **5**, 4425–4427.
- 41 K. Sonogashira, Y. Tohda and N. Hagihara, *Tetrahedron Lett.*, 1975, **16**, 4467–4470.
- 42 K. Y. Tsang and M. A. Brimble, *Tetrahedron.*, 2007, **63**, 6015–6034.
- 43 S. Sörgel, C. Azap and H. Reißig, *Org. Lett.*, 2006, **8**, 4875–4878.
- 44 Y. Zhang, J. Xue, Z. Xin, Z. Xie and Y. Li, *Synlett.*, 2008, **6**, 940–944.
- 45 D. Qin, R. X. Ren, T. Siu, C. Zheng and S. J. Danishefsky, *Angew. Chem. Int. Ed.*, 2001, **40**, 4709–4713.
- 46 S. Akai, K. Kakiguchi, Y. Nakamura, I. Kuriwaki, T. Dohi, S. Harada, O. Kubo, N. Morita, and Y. Kita, *Angew. Chem. Int. Ed.*, 2007, **46**, 7458–7461.
- 47 C.C. Lindsey, K. L. Wu and T. R. R. Pettus, *J. Org. Lett.*, 2006, **8**, 2365–2367.
- 48 S. C. Roy and P. K. Mandal, *Tetrahedron*, 1996, **52**, 12495–12498.
- 49 For a comprehensive review of *hetero*-Diels-Alder chemistry see K. C. Nicolaou, S. A. Snyder, T. Montagnona and G. Vassilikogiannakis., *Angew. Chem. Int. Ed.*, 2002, **41**, 1668–1698.
- 50 O. Diels and K. Alder, *Liebigs. Ann. Chem.*, 1928, **460**, 98.

-
- 51** For a comprehensive review of Diels-Alder chemistry see; E. J. Corey. *Angew. Chem. Int. Ed.*, 2002, **41**, 1650-1667.
- 52** T. L. Gresham and T. R. Steadman, *J. Am. Chem. Soc.*, 1949, **71**, 737.
- 53** C. Timmons, A. Kattuboina, L. McPherson, J. Mills and G. Li., *Tetrahedron.*, 2005, **61**, 11837-11842.
- 54** R. K. Bansal, K. Karaghiosoff, N. Gupta, N. Gandhi and S. K. Kumawa, *Tetrahedron.* 2005, **61**, 10521-10528.
- 55** K. Fries, *Liebigs Ann. Chem.*, 1907, **353**, 350-356.
- 56** (a) H. Amouri, Y. Besace, J. Le Bras and J. Vaissermann, *J. Am. Chem. Soc.*, 1998, **120**, 6171-6172; (b) H. Amouri, J. Vaissermann, M. N. Rager and D. B. Grotjahn, *Organometallics*, 2000, **19**, 1740-1748; (c) H. Amouri, *J. Organometallics*, 2000, **19**, 5143-5148.
- 57** N. J. Willis and C. D. Bray, *Chem Eur. J.*, 2012, **18**, 9160-9173.
- 58** R. W. Van De Water and T. R. R. Pettus, *Tetrahedron*, 2002, **58**, 5367-5405.
- 59** S. B. Cavitt, H. Sarrafizadeh, P. D. Gardner, *J. Org. Chem.*, 1962, **27**, 1211-1216.
- 60** (a) Y. Herzig, L. Lerman, W. Goldenberg, D. Lerner, H. E. Gottlieb and A. Nudelman, *J. Org. Chem.*, 2006, **71**, 4130-4140; (b) G. Zhou, D. Zheng, S. Da, Z. Xie and Y. Li, *Tetrahedron Lett.*, 2006, **47**, 3349 – 3352; (c) G. Zhou, J. Zhu, Z. Xie and Y. Li, *J. Org. Lett.*, 2008, **10**, 721-724; K. Wojciechowski and K. Doatowska, *Tetrahedron*, 2005, **61**, 8419 – 8422; (d) C. Bray, *Synlett*, 2008, **16**, 2500-2502; (e) H. Zheng and D. G. Hall, *Tetrahedron Lett.*, 2010, **51**, 4256 – 4259.

-
- 61** (a) H. Yoshida, M. Watanabe, H. Fukushima, J. Oshita and A. Kunai, *Org. Lett.*, 2004, **6**, 4049 – 4051; (b) M. P. McCrane, E. E. Weinert, Y. Lin, E. P. Mazzola, Y. Lam, P. F. Scholl and S. E. Rokita, *Org. Lett.*, 2011, **13**, 1186–1189; (c) J. Tummatorn, S. Ruchirawat and P. Ploypradith, *Chem. Eur. J.*, 2010, **16**, 1445 – 1448; (d) T. B. Samarakoon, M. Y. Hur, R. D. Kurtz and P. R. Hanson, *Org. Lett.*, 2010, **12**, 2182–2185.
- 62** (a) R. M. Jones, C. Selenski and T. R. R. Pettus, *J. Org. Chem.*, 2002, **67**, 6911–6915; (b) A. S. Kiselyov, *Tetrahedron*, 2006, **62**, 543–548; (c) C. C. Lindsey and T. R. R. Pettus, *Tetrahedron. Lett.*, 2006, **47**, 201–204; (d) C. Bray, *Org. Biomol. Chem.*, 2008, **6**, 2815–3819.
- 63** (a) P. Batsomboon, W. Phakhodee, S. Ruchirawat and P. Ploypradith, *J. Org. Chem.*, 2009, **74**, 4009–4012; (b) S. Radomkita, P. Sarnpitaka, J. Tummatorn, P. Batsomboon, S. Ruchirawat and P. Ploypradith, *Tetrahedron*, 2011, **67**, 3904–3914.
- 64** (a) L. Jurd, *Tetrahedron*, 1977, **33**, 163 – 168; (b) L. Jurd and J. N. Roitman, *Tetrahedron*, 1978, **34**, 57 –62; (c) L. Jurd, *Aust. J. Chem.*, 1978, **31**, 347 – 352; (d) L. Jurd, J. N. Roitman and R. Y. Wong, *Tetrahedron*, 1979, **35**, 1041 – 1054; (e) L. Jurd and J. N. Roitman, *Tetrahedron*, 1979, **35**, 1567 – 1574; (f) L. Jurd and R. Y. Wong, *Aust. J. Chem.*, 1980, **33**, 137 – 154.
- 65** (a) K. Forest, P. Wan and C. M. Preston, *Photochem. Photobiol. Sci.*, 2004, **3**, 463–472; (b) M. K. Nayak and P. Wan, *Photochem. Photobiol. Sci.*, 2008, **7**, 1544–1554; (c) Y. Chen and M. G. Steinmetz, *J. Org. Chem.*, 2006, **71**, 6053–6060.
- 66** (a) F. Liebner, P. Schmid, C. Adelwöhrer and Thomas Rosenau, *Tetrahedron*, 2007, **63**, 11817–11821; (b) L. M. Bishop, M. Winkler, K. N. Houk, R. G. Bergman and D. Trauner, *Chem. Eur. J.*, 2008, **14**, 5405 – 5408; (c) A. Patel, T. Netscher and T. Rosenau, *Tetrahedron Lett.*, 2008, **49**, 2442–2445; (d)

-
- S. Böhmdorfera, A. Patela, T. Netscherb, L. Gillec and Thomas Rosenau, *Tetrahedron*, 2011, **67**, 4858-4861.
- 67** (a) J. Parrick, *Can. J. Chem.*, 1964, **42**, 190-191; (b) W. W. Sullivan, D. Ullman and H. Schechter, *Tetrahedron Lett.*, 1968, **10**, 457-461.
- 68** (a) L. E. Kaïm, L. Grimaud and J. Oble, *Org. Biomol. Chem.*, 2006, **4**, 3410–3413; (b) S. Jiménez-Alonso, A. Estévez-Braun, Á. G. Ravelo, R. Zárate and M. López, *Tetrahedron*, 2007, **63**, 3066 – 3074; (c) G. C. Nandi, S. Samai, R. Kumar and M. S. Singh, *Tetrahedron*, 2009, **65**, 7129 – 7134.
- 69** J. D. Pettigrew, R. P. Freeman and P. D. Wilson, *Can. J. Chem.*, 2004, **82**, 1640–1648.
- 70** R. Rodriguez, R. M. Adlington, J. E. Moses, A. Cowley and J. E. Baldwin, *Org. Lett.*, 2004, **6**, 3617-3619.
- 71** M. A. Marsini, Y. Huang, C. C. Lindsey, K. Wu and T. R. R. Pettus, *Org. Lett.*, 2008, **10**, 1477-1480.
- 72** Y. Huang and T. R. R. Pettus, *Synlett*, 2008, **9**, 1353-1356.
- 73** T. A. Wenderski, M. A. Marsini and T. R. R. Pettus, *Org. Lett.*, 2011, **13**, 118-121.
- 74** J. Sperry, Y. Liu, Z. E. Wilson, J. G. Hubert and M.A. Brimble, *Synthesis*, 2011, **9**, 1383-1398.
- 75** Z. Xin, Y. Zhang, H. Tao, J. Xue and Y. Li, *Synlett*, **2011**, 1579-1584.
- 76** W. Wei, L. Li, X. Lin, H. Li, J. Xue and Y. Li, *Org. Biomol. Chem.*, **2012**, **10**, 3494-3499.
- 77** X. Li, J. Xue, C. Huang and Y. Ling, *Chem. Asian J.*, 2012, **7**, 903-906.
- 78** K. C. Nicolaou, C. R. H. Hale, C. Nilewski and H. Ioannidou, *Chem. Soc. Rev.*, 2012, **41**, 5185-5238.

-
- 79 For a comprehensive review of the history of the rubromycins see; M. Brasholz, S. Sörgel, C. Azap and H. Reißig, *Eur. J. Org. Chem.*, 2007, 3801–3814.
- 80 T. Siu, D. Qin and S. J. Danishefsky, *Angew. Chem. Int. Ed.*, 2001, **40**, 4713–4716.
- 81 O. Mitsunobu, *Synthesis.*, 1981, **1**, 1-28.
- 82 C. Venkatesh and H. Reißig, *Synthesis*, 2008, **22**, 3605-3614.
- 83 S. Akai, K. Kakiguchi, Y. Nakamura, I. Kuriwaki, T. Dohi, S. Harada, O. Kubo, N. Morita and Y. Kita, *Angew. Chem. Int. Ed.*, 2007, **46**, 7458–7461.
- 84 M. K. Wong, C. W. Yu, W. H. Yuen and D. Yang, *J. Org. Chem.*, 2001, **66**, 3606–3609.
- 85 (a) E. J. Corey and X. M. Cheng, *The Logic of Chemical Synthesis*; John Wiley & Sons: New York, 1995; (b). J. B. Hendrickson, *Accounts Chem. Res.* **1986**, *19*, 274–281.
- 86 D. C. K. Rathwell, S. Yang, K. Y. Tsang and M. A. Brimble, *Angew. Chem. Int. Ed.*, 2009, **48**, 7996–8000.
- 87 P. J. Perry, V. H. Pavlidis and J. A. Hadfield, *Tetrahedron*, 1997, **53**, 3195-3204.
- 88 M. A. Rizzacasa and M. V. Sargent, *J. Chem. Soc. Perkin Trans 1*, 1988, **8**, 2425-2428.
- 89 T. Capecchi, C. B. De Koning and J. P. Michael, *Perkin Trans. 1*, 2000, **16**, 2681-2688.
- 90 A. Fürstner, F. Stelzer, A. Rumbo and H. Krause, *Chem. Eur. J.*, 2002, **8**, 1856-1871.
- 91 I. H. Sánchez and M. I. Larraza, *Tetrahedron*, 1985, **41**, 2355-2359.

-
- 92** J. Reichwagen, H. Hopf, A. Del Guerso, J. Desvergne and H. Bouas-Laurent, *Org. Lett.*, 2004, **12**, 1899 – 1902.
- 93** R. R. Fraser, T. S. Mansour and S. Savard, *Can. J. Chem.*, 1985, **63**, 3505-3509.
- 94** G. A. Molander, B. Canturk and L. E. Kennedy, *J. Org. Chem.*, 2009, **74**, 973-980.
- 95** G. A. Molander and I. N. Cavalcanti, *J. Org. Chem.*, 2011, **76**, 623-630.
- 96** S. H. Pine, R. Zahler, D. A. Evans and R. H. Grubbs, *J. Am. Chem. Soc.*, 1980, **102**, 3270–3272.
- 97** S. P. Waters and M. C. Kozlowski, *Tet. Lett.*, 2001, **42**, 3567–3570.
- 98** A. N. Lowell, P. D. Wall, S. P. Waters and M. C. Kozlowski, *Tetrahedron*, 2010, **66**, 5573-5582.
- 99** T. P Thrash, T. D. Welton and V. Behar, *Tetrahedron Lett.*, 2000, **41**, 29-31.
- 100** G. J. Keating and R. O’Kennedy, in *Coumarins Biology, Applications and Mode of Action*, ed R. O’Kennedy and R. D. Thornes, John Wiley & Sons, New York, 1997, ch. 2, pp 48-49.
- 101** J. N. Chatterjea, B. K. Banerjee and H. C. Jha, *Chem. Ber.* 1965, **98**, 3279-32285.
- 102** M. Brasholz and H. Reißig, *Synlett*, 2004, **15**, 2736 - 2738.
- 103** M. Brasholz, X. Luan and H. Reißig, *Synthesis*, 2005, **20**, 3571 – 3580.
- 104** T. W. Greene and P. G. M. Wuts, *Protective Groups in Organic Synthesis*, Third Edition, 1999 John Wiley & Sons, Inc.

-
- 105** T. Kametani, H. Kondoh, T. Honda, H. Ishizone, Y. Suzuki and W. Mori, *Chem. Lett.*, 1989, **5**, 901-904.
- 106** M. C. Carrigan, D. Sarapa, R. C. Smith, L. C. Wieland and R. S. Mohan, *J. Org. Chem.*, 2002, **67**, 1027–1030.
- 109** I. Fernández, J. R. Pedro and R. de la Salud. *Tetrahedron*, 1996, **52**, 12031-12038.
- 108** Reactions attempted using compounds (**267**), (**277**) and (**278**), on a 0.15 mmol scale according to the following literature procedures; (*ai.*) Ref. 99 (using both EtOH and AcOH as solvent; see **Schemes 103** and **105**); (*aii.*) Y. Suzuki and H. Takahashi, *Chem. Pharm. Bull.*, 1983, **31**, 1751-175; (*b*) K. C. Niocolaou, K. Koide, J. Xu and M. H. Izraelewicz, *Tetrahedron Lett.*, 1997, **38**, 3671-3674; (*c*) A. Bagno, W. Kantlehner, R. Kress, G. Saielli and E. Stoyanov, *J. Org. Chem.*, 2006, **71**, 9331–9340; (*d*) N. U. Hofsløkken and L. Skattebøl, *Acta Chem. Scand.*, 1999, **53**, 258-262; (*e*) C. W. Johannes, M. S. Visser, G. S. Weatherhead and A. H. Hoveyda, *J. Am. Chem. Soc.*, 1998, **120**, 8340-8347; (*g*). Q. Zhang, N. P. Botting and C. Kay, *Chem. Commun.*, 2011, **47**, 10596-10598.
- 109** N.B. Reactions in step **f** attempted using compounds (**268**), (**270**) and (**294**), on a 0.15 mmol scale according to the following literature procedures N. K. Kaiser, A. Hallberg and M. Larhed, *J. Comb. Chem.*, 2002, **4**, 109-111.
- 110** F. G. Bordwell, *Acc. Chem. Res.*, 1988, **21**, 456-463.
- 111** I. T. Ibrahim and A. Williams, *J. Chem. Soc., Perkin Trans. II*, 1982, **11**, 1459-1466.
- 112** *Eur. Pat.*, EP1445249A1, 2004.
- 113** Reactions carried out on 0.33 mmol scale according to the following procedures (*a*). A. Øyvind, T. Benneche, L. Gundersen and K. Undheim, *Acta*.

-
- Chemica Scandinavica*, 1992, **46**, 172 – 177; (bi) F. Babudri, A. Cardone, L. De Cola, G. M. Farinola, S. G. Kottas, C. Martinelli and F. Naso; *Synthesis*, 2008, **10**, 1580-1588; (bii.) Y. Hatanaka and T. Hiyama, *J. Org. Chem.*, 1988, **53**, 918-920; (c.) N. Murai, M. Yonaga and K. Tanaka, *Org. Lett.*, 2012, **14**, 1278 – 1281; (d.) *US Pat.* US2010048610A1, 2010.
- 114** V. VanRheenen, R. C. Kelly and D. Y. Cha, *Tetrahedron Lett.*, 1976, **23**, 1973–76.
- 115** G. Poli, *Tetrahedron Lett.*, 1989, **30**, 7385-7388.
- 116** B. M. Trost, G. Dong and J. A. Vance, *J. Am. Chem. Soc.*, 2007, **129**, 4540-4541.
- 117** S. Matsumoto, T. Asakawa, Y. Hamashima and T. Kan, *Synlett*, 2012, **23**, 1082-1084.
- 118** H. J. Günther, E. Guntrum and V. Jäger, *Liebigs Ann. Chem.*, 1984, **1**, 15-30.
- 119** A. R. Hajipour, M. Arbabian and A. E. Ruoho, *J. Org. Chem.*, 2002, **67**, 8622-8624.
- 120** S. Gagliardi, G. Nadler, E. Consolandi, C. Parini, M. Morvan, M. Legave, P. Belfiore, A. Zocchetti, G. D. Clarke, I. James, P. Nambi, M. Gowen and C. Farina, *J. Med. Chem.* 1998, **41**, 1568-1573.
- 121** V. Guay and P. Brassard, *Synthesis*, 1987, **3**, 294-297.
- 122** A. R. Hajipour, M. Arbabian and A. E. Ruoho, *J. Org. Chem.*, 2002, **67**, 8622-8624.
- 123** (a) H. Sliwa and D. Blondeau, *Heterocycles*, **1981**, **16**, 2159-2167; (b). R. Hernández-Altamirano, V. Y. Mena-Cervantes, S. Perez-Miranda, F. J. Fernández, C. A. Flores-Sandoval, V. Barba, H. I. Beltrán and L. S. Zamudio-Rivera, *Green Chem.*, **2010**, **12**, 1036-1048.

-
- 124** G. S. Hamilton, Y. Wu, D. C. Limburg, D. E. Wilkinson, M. J. Vaal, J. Li, C. Thomas, W. Huang, H. Sauer, D. T. Ross, R. Soni, Y. Chen, H. Guo, P. Howorth, H. Valentine, S. Liang, D. Spicer, M. Fuller and J. P. Steiner, *J. Med. Chem.* **2002**, *45*, 3549-3557.
- 125** S.S. Matsumoto, T. Asakawa, Y. Hamashima and T. Kan, *Synlett*, 2012, **23**, 1082– 1084.